Exploring *Leishmania* Biochemistry to Understand Effect of Spermidine Starvation and Identification of Novel Drug Candidates

A Thesis
Submitted in Partial
Fulfillment of the Requirements for the Degree of

DOCTOR OF PHILOSOPHY

By

Ms. Shalini Singh

Department of Biosciences and Bioengineering
Indian Institute of Technology Guwahati
Guwahati-781039, Assam, India

November 2015

Exploring *Leishmania* Biochemistry to Understand Effect of Spermidine Starvation and Identification of Novel Drug Candidates

A Thesis Submitted

By

Ms. Shalini Singh
11610628

In Partial Fulfillment of the Requirements for the Degree of

Doctor of Philosophy

Department of Biosciences and Bioengineering
Indian Institute of Technology Guwahati
Guwahati-781039, Assam, India

November 2015

Dedicated

To

My parents and mentor

INDIAN INSTITUTE OF TECHNOLOGY GUWAHATI

DEPARTMENT OF BIOSCIENCES AND BIOENGINEERING

CERTIFICATE

I hereby declare that the matter embodied in this thesis entitled "**Exploring *Leishmania* Biochemistry to Understand Effect of Spermidine Starvation and Identification of Novel Drug Candidates**" is the result of investigations carried out by me in the Department of Biosciences and Bioengineering, Indian Institute of Technology Guwahati, India under the supervision of **Prof. Vikash Kumar Dubey**.

In keeping with the general practice of reporting scientific observations, due acknowledgements have been made wherever the work of other investigators are referred.

Shalini Singh

November 2015

Roll No: 11610628

INDIAN INSTITUTE OF TECHNOLOGY GUWAHATI

DEPARTMENT OF BIOSCIENCES AND BIOENGINEERING

CERTIFICATE

It is certified that the work described in this thesis entitled "**Exploring *Leishmania* Biochemistry to Understand Effect of Spermidine Starvation and Identification of Novel Drug Candidates**" by **Ms. Shalini Singh (**Roll No: 11610628), submitted to Indian Institute of Technology Guwahati, India for the award of degree of Doctor of Philosophy, is an authentic record of results obtained from the research work carried out under my supervision at the Department of Biosciences and Bioengineering, Indian Institute of Technology Guwahati, India and this work has not been submitted elsewhere for a degree.

Prof. Vikash Kumar Dubey
(Supervisor)

Acknowledgement

I express my heartfelt thank to Indian Institute of Technology Guwahati, India and its Department of Biosciences and Bioengineering for providing me the best infrastructure to carry out my doctoral research. With immense pleasure I would like to express sincere and heartfelt gratitude to my Ph.D. supervisor Prof. Vikash Kumar Dubey for allowing me to carry out my research work under his esteemed guidance. His amiable nature helped me to clarify all my doubts at each step of my research progression. I sincerely thank him for his invaluable suggestions and moral support during my research work as well as the consistent encouragement and guidance to help me in my future career endeavors.

I would like to express deep reverence and sincere thank to the other members of my Doctoral Committee, Dr. Sanjukta Patra, Dr. Nitin Chaudhary, Dr. Anil Kr. Saikia for their valuable suggestions and advices which enabled me to improve my work at every step. I am grateful to Prof. Shyam Sundar, Banaras Hindu University for gifting us the strain of Leishmania donovani.I thank Dr. Keijiro Sameijima, Tokyo Metropolitan Kamagome Hospital, Tokyo, Japan for providing Decarboxylated S-adenosylmethionine which was used in enzymatic assay for spermidine synthase. I also thank Dr. Sigrid Roberts, Pacific University School of Pharmacy, Hillsboro, United State for gifting Spermidine synthase cDNA as a clone in pBluescript bacterial vector. I also acknowledge Dr. Jeremy Mottram, University of Glasgow, Glasgow, for providing us vector pGL1686 which was used to study autophagy. Support of mass spectrometry facility at Centre for Cellular and Molecular Platforms is also acknowledged for Proteomics related work. I also acknowledge various instrumentation facilities by Central Instrumentation Facility IIT Guwahati and Biotech Park Guwahati.I thank GE Healthcare for allowing me to use using GE Healthcare delta vision elite deconvolution microscope for fluorescence microscopy study.

I express special thanks to Dr. Shankar Prasad Kanaujia for helping me with some of the bioinformatics work. I also thank Dr. Manish Kumar for allowing me to use his laboratory facility which has helped me complete my research work.

I am grateful to the successive Heads of Department of Biosciences and Bioengineering, Indian Institute of Technology Guwahati, Prof. Arun Goyal and Prof. V. V. Dasu, for providing me the departmental facilities to carry out my research work. I would also like to thank the technical and non-technical staffs of the department for their help and assistance through the research tenure.

I am thankful to my present and previous lab members Ruchika, Kartikeya, Ritesh, Kamalesh, Adarsh, Gundappa, Ekta, Sona, Bijoy, Sudipta, Shyamli, Dr. Mousumi Das, Dr. Sushant Singh, Dr. Saudagar Prakash, Dr. Abhay N Singh, Dr. Anil Shukla, Manjeet, Vidyadhar, Ashish, Ankur, Prity and Robin for providing a conducive milieu and consistent support during the research tenure.

I owe my special thanks to my friends Aruna, Karukriti and S N Balaji for providing valuable suggestions, help and motivation. My other friends at IIT Guwahati deserve special mention for making my stay pleasant in the campus lively and enjoyable. Their love and affection has been a constant source of motivation that helped me sail through difficult times.

Finally, I owe my warm love and gratitude to my parents and family for encouraging me and providing me with moral support in difficult times. Their love and cooperation would remain indelible in my heart.

Shalini Singh

November, 2015

Abbreviations

ADME	:	Absorption, Distribution, Metabolism and Excretion
AMPK	:	AMP- activated protein kinase
ATP	:	Adenosine-5'-triphosphate
BLAST	:	Basic Local Alignment Search Tool
BSA	:	Bovine Serum Albumin
cDNA	:	Complementary Deoxyribonucleic Acid
dcSAM	:	Deacrboxylated S-adeenosyl Methionine
DMSO	:	Dimethyl Sulfoxide
DNA	:	Deoxyribonucleic Acid
DTT	:	Dithiothreitol
EDTA	:	Ethylene Diamine tetra Acetic Acid
eIF5A	:	Eukaryotic Initiation Factor 5A
GFP	:	Green Flourescence Protein
GSH	:	Glutathione
IPTG	:	Isopropyl β-D-1-thiogalactopyranoside
KCl	:	Potassium chloride
*Ld*SS	:	Spermidine synthase of *Leishmania donovani*
MDS	:	Molecular Dynamics Simulations
MDC	:	Monodansylcadaverine
$MgCl_2$	:	Magnesium chloride
mRNA	:	Messenger Ribonucleic Acid
MTA	:	3-Methyl Adenine
MTT	:	[(3-(4,5-Dimethylthiazol-2-yl)-2,5-Diphenyltetrazolium Bromide)]
NAC	:	N-acetylcysteine
NaCl	:	Sodium chloride
PBS	:	Phosphate Buffer Saline
PCR	:	Polymerase chain Reaction
PI	:	Propidium iodide
PMSF	:	Phenylmethanesulfonyl Fluoride
RMSD	:	Root Mean Square Deviation
RMSF	:	Root Mean Square Fluctuation

RNA	:	Ribonucleic Acid
ROS	:	Reactive Oxygen Species
SDS	:	Sodium Dodecyl Sulphate
SDS-PAGE	:	Sodium Dodecyl Sulfate Polyacrylamide Gel Electrophoresis
$T(SH)_2$	:	Trypanothione
TOR	:	Target of Rapamycin

List of Figures

List of Tables

Contents

CHAPTER I

Leishmaniasis: Introduction, Challenges and Scope of the Current Work*

1.1 Abstract:

Leishmaniasis is a vector borne disease caused by different species of *Leishmania*. *Leishmania* is an obligate parasite which is transmitted by vector sandfly. There are three clinical forms of leishmaniasis: visceral, mucocutaneous and cutaneous. Leishmaniasis is spread throughout the globe including major regions of Asia, Africa, South and Latin America. In India, the most commonly found form of the disease is visceral leishmaniasis. There is a wide arsenal of available drugs against leishmaniasis, but they suffer from certain disadvantages like high cost, toxicity, emergence of resistance, difficult route of administration etc. Several limitations of the existing drugs potentiate the need to develop new drug molecules with their specific drug targets. Till now the drug discovery is mainly focused on single target drug discovery approach, which means one compound for one target. However, many a times the organism is able to cope up the effect of inhibition of single target by modulating its biological system. Recently, there is a paradigm shift from single to multi target drug discovery approach where two or more different targets can be inhibited by single drug or by single formulation of different drugs. So, exploring the potential of two or more different targets for drug development could be a good strategy to bring more effective drug in the market.

* Part of review is likely to be submitted for publication

1.2 Introduction:

The most persistent and perilous challenge that world is addressing consists of maintaining and improving global health. However, solutions to the cure and prevention of several diseases have been achieved which have helped in overcoming different barriers to health improvement. Still there are certain neglected diseases which are underexplored and need attention to discover new tools and strategies to prevent, diagnose and treat them. According to World Health Organization (WHO), 17 diseases are classified as neglected tropical diseases which are affecting more than one billion people around the world. Neglected tropical diseases (NTDs) are known to be a group of diseases which affect the health of low-income population in developing countries. These NTDs coexist with poor people living in rural and urban slums where sanitation and access to clean water is very limited. Leishmaniasis is one among these neglected tropical diseases which is affecting health and livelihood of major portion of globe.

Leishmaniasis is a wide spread tropical disease caused by protozoan parasite *Leishmania* which belongs to order kinetoplastida and family trypanosomatidae. This parasite is transmitted by vector sandfly, of genus *Phlebotomous* and *Lutzomyia*. There are three forms of clinical manifestation of leishmaniasis depending on the type of infecting species, namely, cutaneous, mucocutaneous and visceral lieshmaniasis (*Shukla et al., 2009*). The most deadly form of the disease is visceral leishmaniasis, also known as kala azar, which is mainly caused by *Leishmania donovani* in India. As per WHO statistics, 350 million people in 88 countries are at the risk of developing the disease. Every year there are two million new cases of the disease and out of which half million new cases are of visceral leishmaniasis (*Murray et al., 2005; Stockdale and Newton, 2013*). The treatment of leishmaniasis relies mainly on chemotherapy as there are no vaccines available. Although there is a wide arsenal of available drugs in the market, they have several limitations (*Croft and Coombs, 2003; Croft et al., 2006*), which necessitates the need of novel drug candidates with specific drug targets.

Over the years, drug discovery have been advancing and transforming to generate more effective and efficient drugs. One such advancement includes switching from single target approach to multi target approach. In order to develop a better drug candidate, we chose to explore two different pathways of *Leishmania* namely redox metabolism and protein prenylation pathway.

1.2.1 ***Leishmaniasis:*** Leishmaniasis is a vector borne zoonotic disease caused by different species of protozoan parasite known as *Leishmania*. *Leishmania* is an obligatory intracellular parasite which is spread through the bite of infected female sandflies. There are three different forms of leishmaniasis: visceral leishmaniasis, cutaneous leishmaniasis and mucocutaneous leishmaniasis. It is widely spread all over the world affecting major regions of Asia, Africa and Latin America.

1.2.2 ***Leishmania*****:** *Leishmania* is an obligatory intracellular protozoan parasite. It was first described by Alexander Russell in 1756. It was named after William Boog Leishman, a doctor serving with British Army in India. He found ovoid shaped bodies in a soldier suffering from illness and experiencing fever, swollen spleen, muscular atrophy and anaemia. The illness was named as Dum-Dum fever and his findings were published in 1903. Few weeks after the publication, these symptoms were also recognized by Charles Donovan and the ovoid shaped bodies were then known as Leishman-Donovan bodies which were further given an scientific name as *Leishmania donovani*. *Leishmania* is a genus of family Trypanosomatidae and is characterized by the presence of a unique form of DNA known as kinetoplast.

1.2.3 ***Vectors of Leishmania*****:** *Leishmania* is transmitted via the bite of infected sandflies belonging to the genus *Phlebotomus* and *Lutzomyia*. *Phlebotomus* is known to spread the disease in the old world localities like Europe, Asia and Africa whereas *Lutzomyia* transmits *Leishmania* in the new world such as South and Central America. There are more than 700 known species of sandflies, of which only 10% are found to act as vectors of different diseases and 30 species are involved in transmission of *Leishmania*. The old world sandfly species, *Phlebotomus*, is found in desert or semi-arid ecosystem whereas new world sandfly, *Lutzomyia*, lives in forest dwelling (*Sharma and Singh, 2008; Claborn, 2010*). Figure 1.1 shows the Morphology of *Phlebotomus argentipes* and *Lutzomyia longipalpis*. The taxonomic classification of sandfly is as follows:

Phylum: Arthopoda
Family: Psychodidae
Class: Insecta
Order: Diptera

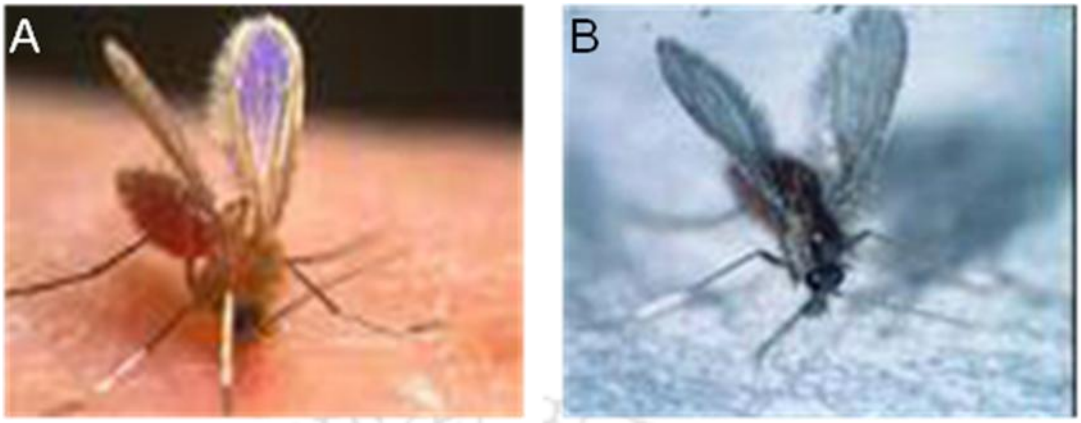

Figure 1.1: Morphology of vector sandfly: (A) *Phlebotomus argentipes* and (B) *Lutzomyia longipalpis*. Leishmania is transmitted by the bite of female sandfly of genus *Phlebotomus* in old world and *Lutzomyia* in new world countries. Sandfies belonging to both genera are morphologically similar but differ in their habitat. *Phelbotomus* are found in arid and semi arid regions whereas *Lutzomyia* are found in forest dwellings (Adopted with permission from Journal of Vector Borne Diseases, National Institute of Malaria Research (ICMR) *Ref:* J Vector Borne Dis 2008; 45, 255-272)

1.2.4 *Life cycle of Leishmania parasite*: *Leishmania* has digenetic life cycle which alternates between mammalian host and insect vectors i.e. sandflies. The metacyclic promastigotes which are infective forms are introduced into the mammalian host by the bite of infected sandfly. These promastigotes are then phagocytised by the macrophages where they are transformed into the intracellular amastigotes. These amastigotes multiply by binary fission in cell until the cell bursts and further infect other phagocytic cells of the body. This is a chronic stage which may last for months, years or lifetime depending upon the immune status of the host. When sand fly bites the infected mammalian host, the macrophages infected with amastigotes are ingested. These non-motile and round forms of parasite are released into the posterior part of alimentary tract of sand fly where they are metamorphosed into the motile, flagellated and elongated forms called promastigotes. These promastigotes then migrate to the anterior midgut of sand fly and multiply there. The promastigotes are converted into infectious metacylic promastigotes by undergoing metacyclogenesis within 7 days after feeding. These infective forms then move to the proboscis of the insect and are transferred to the mammalian host together with the saliva when the sand fly mutilate the skin (*Hide et al, 2007; MacMorris-Adix, 2008*). The life cycle of *Leishmania* is summarized in Figure 1.2.

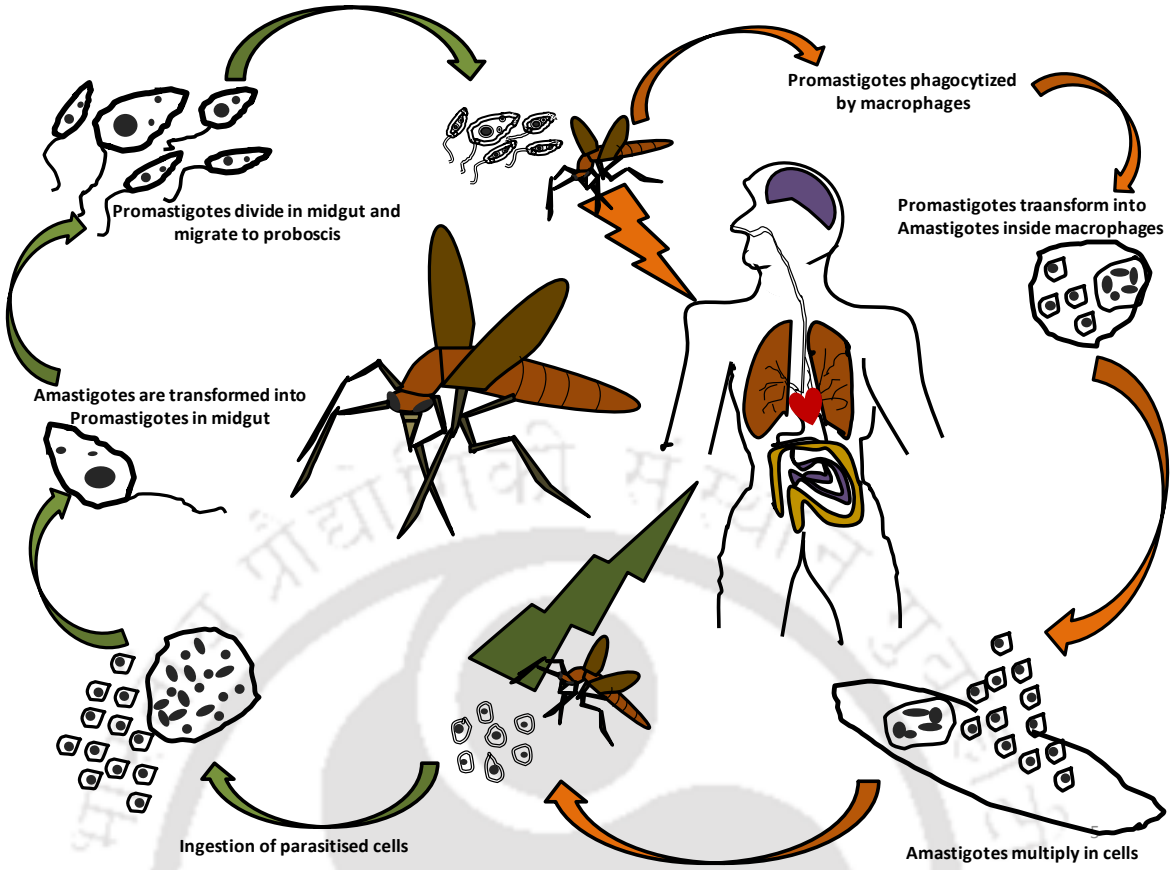

Figure 1.2: Life cycle of *Leishmania* parasite in mammalian and insect host. Leishmaniasis is transmitted by female sandfly which depends on the blood meal to produce eggs. The vector, sandflies are infected after feeding on the blood of infected host. The amastigotes present in the macrophages of the infected host are taken up with the blood and are released into the posterior midgut of the sandfly. In the midgut, the amastigotes are transformed into the promastigote form which further moves to the proboscis of the sandfly. After seven days of feeding, the promastigotes become metacyclic infectious promastigotes after undergoing metacyclogenesis. Further, these infective promastigotes are transferred to the host with the saliva of sandfly after laceration. These promastigotes are taken up by macrophages where they are transformed into amastigotes. These amastigotes increase their number by binary fission. Eventually, the cell bursts and the amastigotes are released into the blood to be taken up by sandfly and continue the life cycle (*Hide et al., 2007*)

1.2.5 ***Different forms of Leishmaniasis*:** Leishmaniasis has mainly three clinical manifestations depending on the type of *Leishmania* species infecting the host: visceral leishmaniasis, cutaneous leishmaniasis and mucocutaneous leishmaniasis. These different forms of leishmaniasis differ in symptoms and their consequences (*Hide et al, 2007*). Various clinical manifestations of the disease are shown in Figure 1.3. Visceral leishmaniasis, also known as kala azar is the most severe form leading to mortality if left untreated. It affects internal organs of the body and is usually caused by *Leishmania donovani*, *Leishmania infantum*, etc. It is characterized by fever, weight loss, hepatosplenomegaly, anaemia etc (*MacMorris-Adix, 2008; Stockdale and Newton, 2013*).

Figure 1.3: Different types of Leishmaniasis: (A) Visceral leishmaniasis, (B) Mucocutaneous leishmaniasis, (C) Cutaneous leishmaniasis. Leishmaniasis has three clinical forms: visceral, cutaneous and mucocutaneous leishmaniasis. Visceral leishmaniasis is the most fatal form of the disease as it affects the visceral organs of the body. Its causative organisms are *Leishmania donovani, Leishmania infantum* etc. Cutaneous leishmaniasis is the most commonly found form of the disease. It is characterized by the presence of painful lesions on the skin. It is caused by *Leishmania braziliansis, Leishmania amazonensis* etc. Mucocutaneous leishmaniasis is the severe form of cutaneous leishmaniasis. It mainly affects the mucus membranes of the body. It is caused *by Leishmania braziliansis, Leishmania panamensis* etc (*http://www.stanford.edu/class/humbio153/ImmuneEvasion/*).

Cutaneous leishmaniasis is the most common and widespread of all the three forms. It is characterized by painful skin lesions persisting for months or even years in some cases. Some of these lesions are self healing while some require antileishmanial treatment. These skin ulcers are localized to the site of sandfly bite, although some satellite lesions can also be observed in proximity to the original ulcers. Its etiologic agents include different *Leishmania* strains like *L. amazonensis, L. braziliansis, L. mexicana, L. shawi* etc in the New World and *L. major, L. tropica, L. arabica* etc in the Old World (*Bañuls et al, 2007; MacMorris-Adix, 2008*). The other form of the disease is mucocutaneous leishmaniasis, also called as *espundia.* This is a severe form of cutaneous leishmaniasis. It mainly affects mucous membranes of nose, mouth, throat and other body parts including arms, legs etc and ultimately lead to their disfiguration and destruction if untreated. It is usually caused by *L. braziliansi, L. guyanensis, L. panamensis* etc (*Hide et al, 2007; MacMorris-Adix, 2008*).

1.2.6 *Geographical distribution of leishmaniasis*: Leishmaniasis is widely spread all over the world including major portions of tropical and subtropical countries like Africa, Asia and Latin America. According to World Health Organization (WHO), leishmaniasis is endemic in 88 countries around the world of which 72 are developing countries. It is threatening life of approximately 350 million people with a reported 12 million new cases

annually. Visceral leishmaniasis is most prevalent in India, Bangladesh, Nepal, Sudan and Brazil. More than 90% of the cutaneous leishmaniasis cases are found in countries like Afghanistan, Iran, Syria, Peru, Brazil and Saudi Arabia. Mocucutaneous leishmaniasis is majorly concentrated in Brazil, Bolivia and Peru (*Hide et al, 2007*). Figure 1.4 shows the geographical distribution of leishmaniasis.

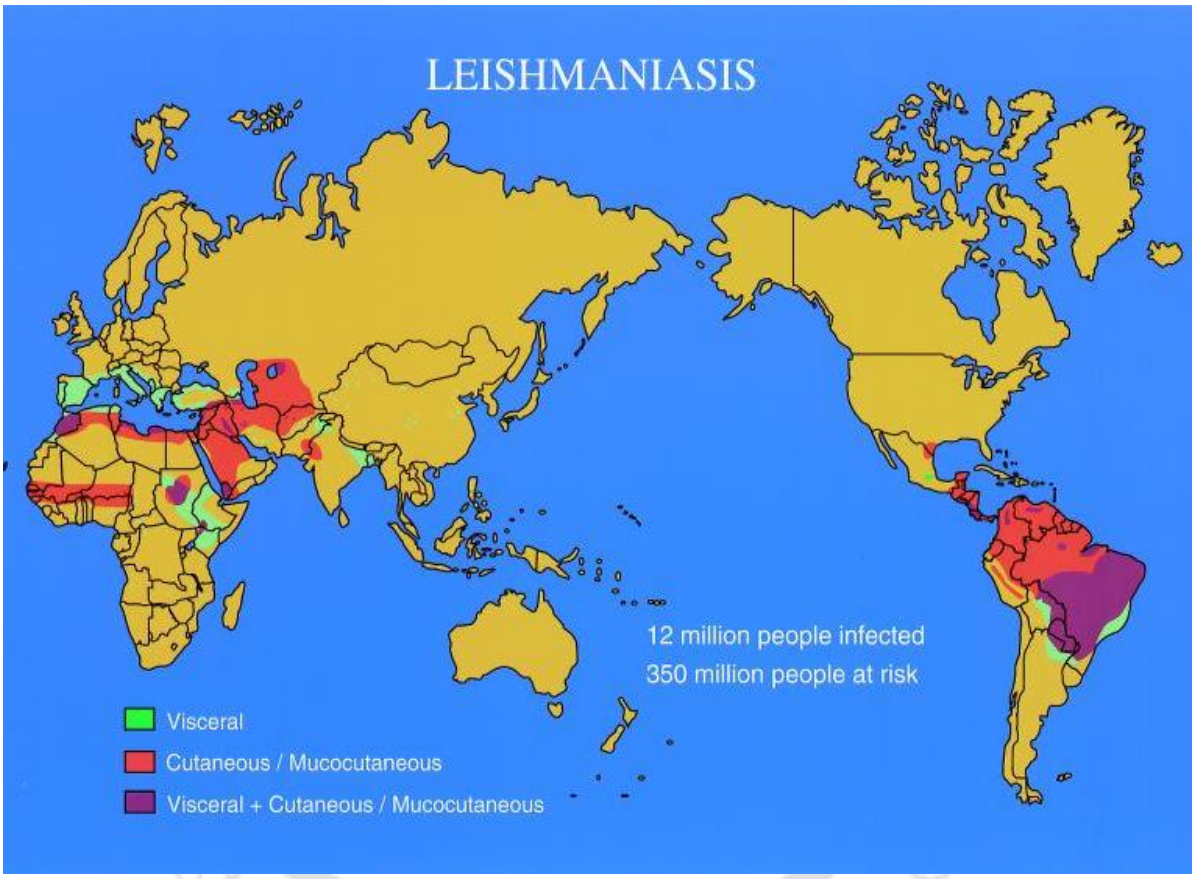

Figure 1.4: Geographical Distribution of visceral, cutaneous and mucocutaneous leishmaniasis. Leishmaniasis is endemic in many parts of the globe such as Africa, Latin and South America, Middle East and Southern Europe, and India. In India, the most commonly found form of the disease is visceral leishmaniasis (Adopted with permission from American Society for Microbiology *Ref: Clinical Microbiology Reviews.* 14: 229-243.)

1.2.7 *Antileishmanial drugs*: Currently, the treatment of leishmaniasis is based on chemotherapy with few available drugs. These drugs are known to have severe limitations like high cost, toxicity, emergence of resistance strains, lack of efficacy and difficult route of administration. The primary treatment of leishmaniasis involves the use of pentavalent antimonial compounds. Other commonly used drugs are amphotericin B, miltefosine, pentamidine and aminosidine. Pentavalent antimonials were developed way back in 1945 and are now used as first line antileishmanial drugs for both visceral and cutaneous leishmaniasis. Pentostam (sodium stibogluconate) was the first antimonial followed by glucantime and meglumine antimoniate which are used as antileishmanial drugs. Since the pentavalent antimonials are being used since many decades, the resistance of parasite to this class of drugs have increased which have limited its efficacy and use. In many areas where unresponsiveness to antimonials have increased, amphotericin B is being used as a first choice of drug especially in North Bihar, India. Amphotericin B is a macrolide polyene antifungal antibiotic compound obtained from *Streptomyces nodusus*. Although the cure rate with amphotericin B is very high, it is toxic and requires prolonged and close monitoring. These serious limitations of available drugs necessitate the discovery of novel drug targets against leishmaniasis (*Monzote, 2009; Mitropoulos, 2010; Kedzierski, 2012; Lindoso, 2012*). The structure of sodium stibogluconate, amphotericin B and miltefosine is shown in Figure 1.5.

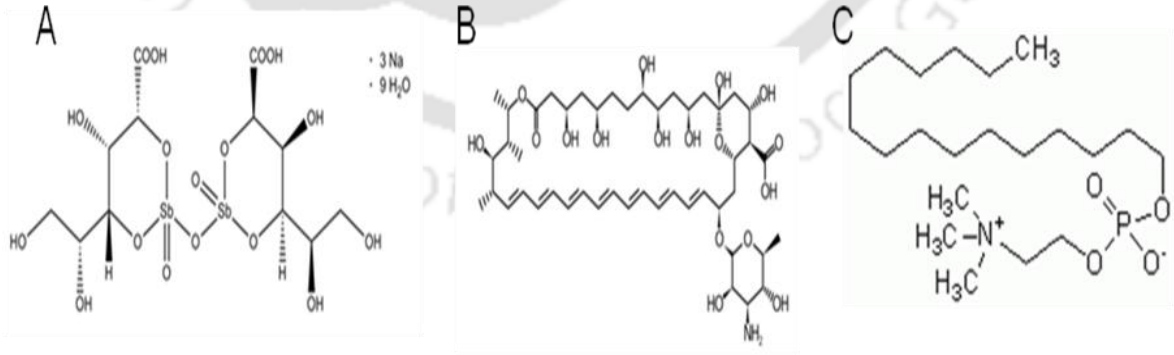

Figure 1.5: Chemical structure of drugs against leishmaniasis **(A)** Sodium stibogluconate **(B)** Amphotericin B and (**C**) Miltefosine. Pentavalent antimonials i.e. sodium stibogluconate, are used as the first line of treatment against leishmaniasis. Amphotericin B is obtained from *Strptomyces nodusus* and is used for cases unresponsive towards antimonials. Miltefosine is the only oral drug available in the market. Chemical structures were taken from web resources.

1.2.8 ***Discovering novel drug targets*****:** The identification and discovery of novel drug targets can be achieved by the use of comparative genomics. The search for a gene to be used as a potential drug target can be triggered by using comparative bioinformatics. The genes encoding a protein with known function or with known ability to act as a drug target in closely related organisms are identified using this comparative computational strategy. Simultaneously, the genes involved in different biochemical and signalling pathways which are crucial for the survival of the parasite can be identified and chosen as targets for drug discovery. The differences in biochemical setup between host and parasite are exploited as a basis to choose potential antileishmanial targets. The inhibitors against these targets can be predicted using *in silico* approach. This comparative analysis is then followed by functional genomics and biochemical analysis to validate the use of different candidate genes obtained through comparative analysis as potential drug targets (*Bañuls et al, 2007).*

1.2.9 ***The redox metabolism of Leishmania donovani:*** The redox metabolism of an organism plays an important role in regulation of cellular homeostasis and survival. Redox homeostasis is maintained by cells under normal physiological conditions by generating and eliminating reactive oxygen species. Any perturbation in the redox homeostasis generates oxidative stress and greatly affects the cell development and survival (*Trachootham et al., 2008*). The redox metabolism of protozoans of order kinetoplastida like trypanosomes and *Leishmania* is very unique since it is based on trypanothione in comparison to glutathione based redox metabolism of other eukaryotes (*Krauth-Siegel et al., 2003*). The redox metabolism pathway of trypanosomatids comprises of directly linked polyamine and thiol pathways (*Krauth-Siegel and Leroux, 2012*). Enzymes involve in redox metabolism has been proved to be potential drug targets against several pathogens (*Catalano-Dupuy et al., 2013*). The redox metabolism of trypanosomatids in general and *Leishmania* in specific is reviewed by Krauth-Siegel and Comini, 2008. The redox metabolism pathway with key metabolites and enzymes of the pathways of trypanosomatids is shown in Figure 1.6.

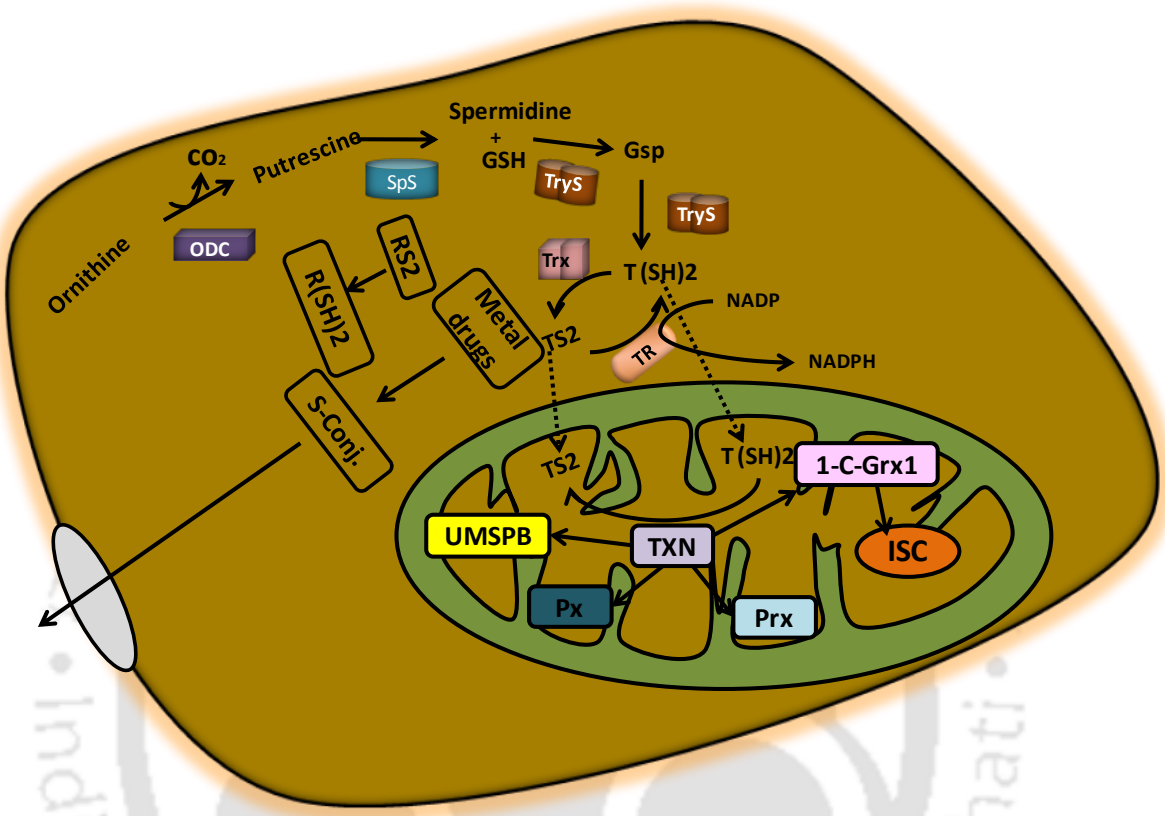

Figure 1.6: Trypanothione based redox metabolism pathway of *Leishmania donovani*. The first step of the pathway involves the formation of putrescine from ornithine in the presence of ornithine decarboxylase (ODC). Spermidine synthase (SpS) further catalyzes the conversion of putrescine to spermidine in presence of decarboxylated S-adenosylmethionine. Further, trypanothione synthetase catalyzes the conjugation of spermidine and glutathione (GSH) to form trypanothione (T(SH)2). Disulphides in proteins (RS2) like tryparedoxin (TXN) and thioredoxin (Trx) , are reduced by trypanothione (T(SH)2). Further, trypanothione reductase reduces the generated trypanothione disulphide (TS2) to dithiols. Trypanothine (T(SH)2) can also get conjugated to metal containing drugs (S-Conj) and is further extruded out of the cell through certain specific transporters. The reducing equivalents are transferred to peroxidises, the monothiol glutaredoxin (1-C-Grx1) and universal minicircle sequence binding protein (UMSBP), by tryparedoxin isoform in mitochondria. The monothiol glutaredoxin (1-C-Grx1) is reported to have role in biogenesis and metabolism of iron sulphur clusters (ISC). UMSBP are important to initiate the replication of kinetoplast DNA (Revised from Krauth-Siegel and Comini, 2008, Biochim Biophys Acta. 1780, 1236−1248)

1.2.10 ***Polyamines:*** Polyamines are small polycationic alkylamine molecules which are ubiquitous in nature. Different types of polyamines found in various organisms are ornithine, spermidine, putrescine, agmatine, spermine etc. Initially polyamines were considered to be the degradation products of cell, but later with advancement in polyamine research, they were found to have crucial role in different processes of life. The history of polyamine started long back in 1678 when Leeuwenhoek crystallized spermine from human sperm. Ladenburg and Abel named the base as spermine in 1888. Chemical nature of spermine was elucidated by Rosenheim and his fellows in 1920. They also discovered a base related to spermine which was named as spermidine. Other related bases like putrescine and cadaverine was discovered by Brieger in 1885 from the putrefying animal waste. Their chemical nature and structure was confirmed by Ladenburg in 1886 (*Heby, 1986*). Putrescine, spermidine and spermine contain two, three and four positive charges at physiological pH. Being polycationic in nature, polyamines bind to negatively charged molecules like DNA, RNA, lipids etc. Their potency to bind with such a variety of molecules make their importance indispensable in different cellular processes like cell growth, DNA stability etc (*Minois N, 2014*). Polyamine are also found to have important function in processes like transcription, translation, ion channel gating, post translational modifications, stability of membranes etc. They also play regulatory role in cell death processes like apoptosis, autophagy and are known to regulate differentiation, tumorigenesis and cell proliferation (*Mandal et al., 2013*). Several reports have shown that alteration in polyamine metabolism leads to different disease conditions. Therefore, enzymes involved in polyamine metabolism can be very good potential drug targets.

1.2.11 ***Spermidine:*** Spermidine is naturally occurring aliphatic polyamine which is a derivative of 1, 4-diaminobutane. Synthesis of spermidine is catalyzed by spermidine synthase from putrescine in presence of decarboxylated S-adenosylmethionine. Figure 1.7 is showing the various functions of spermidine.

1.2.12 ***Eukaryotic initiation factor 5A (eIF5A):*** eIF5A is an acidic protein found to be highly conserved and essential in organisms ranging from archaebacteria to mammals. However, the presence of eIF5A was not found in eubacteria. It undergoes a unique hypusine modification.

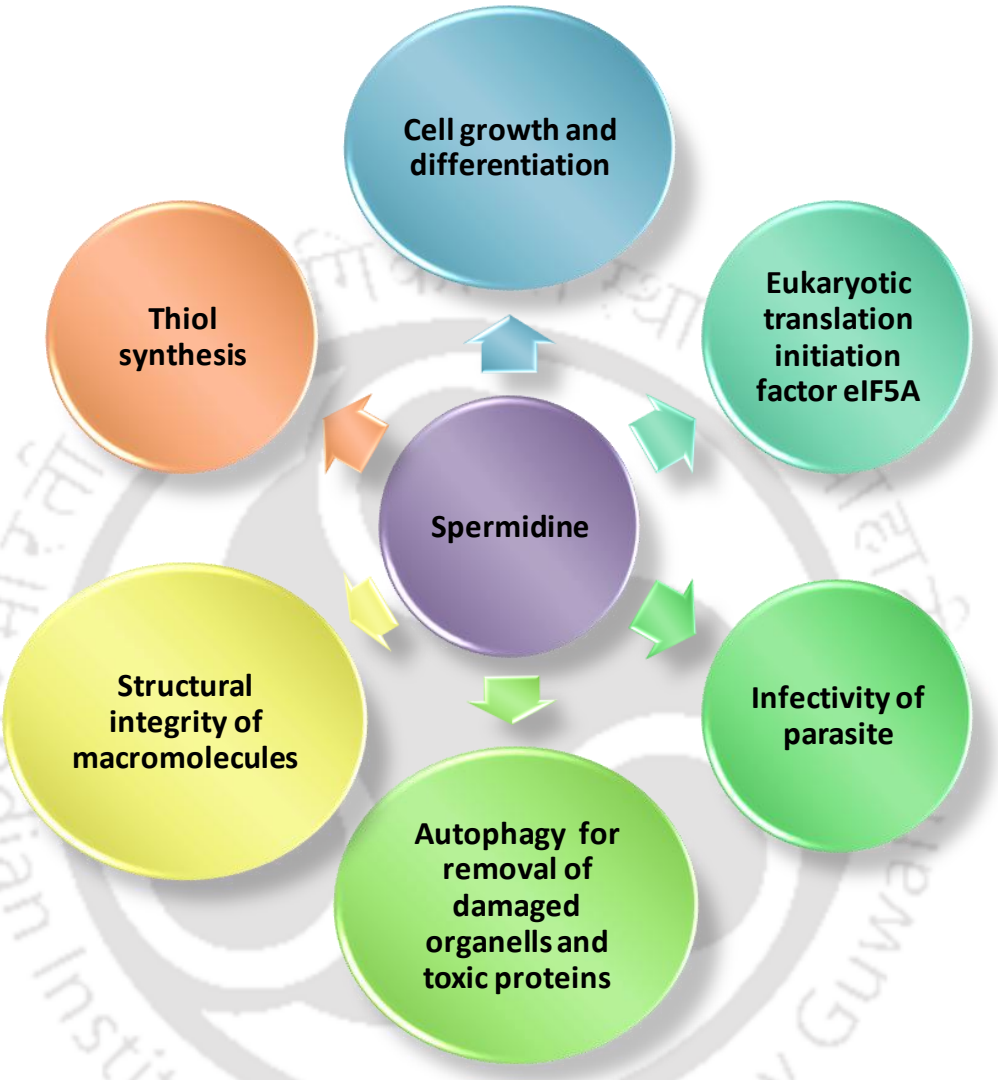

Figure 1.7: Various roles of spermidine in different organism. Spermidine was known to be involved in covalent modification of eukaryotic .initiation factor 5A of certain eukaryotes, generating an unusual amino acid called hypusine. Polyamines are also known to have regulatory role in cell death processes such as autophagy and apoptosis. They are also known to be involved in cell differentiation, tumerogenesis and proliferation in different organisms. Spermidine is also involved in thiol synthesis and in maintaining structural biosynthesis of various organisms (*Mandal et al., 2014*). In *Leishmania*, it is found to be crucial for the virulence of the parasite (*Gilroy et al., 2011*). However, its involvement in other processes in *Leishmania* is not yet explored.

The residues nearby the lysine residue, which is modified to hypusine, are found to be highly conserved in various organisms. Multiple sequence alignment of amino acid sequence of eIF5A revealed that N-terminal sequences are highly conserved among archaebacteria than eukaryotes, whereas C-terminal was found to be least conserved overall. Yeast and human eIF5A were found to show 64% of identity. This percentage identity is more or less same among other eukaryotes. However, yeast eIF5A shows only 35% identity with eIF5A of archaebacteria. This sequence identity difference is supported by the fact that fuction of yeast eIF5A can be substituted by human eIF5A but not with that of archaebacterial eIF5A (*Magdolen et al., 1994; Zanelli and Valentini, 2007*). More than one eIF5A has been reported in several eukaryotes. For example, in yeast and human, two eIF5A genes have been identified.

1.2.13 ***Hypusine modification of eIF5A:*** Eukaryotic initiation factor, eIF5A undergoes unique post translational modification called hypusination which is crucial for its activity. Hypusination includes the transfer of a 4- aminobutyl moiety of spermidine to a specific lysine residue of eIF5A (*Chattopadhyay et al., 2003*). Hypusine, [N epsilon-(4-amino-2-hydroxybutyl)lysine], was first discovered by Nakajima and his fellows. They have determined the structure of hypusine from the free form of this amino acid isolated from the bovine brain (*Park et al., 1981*). The hypusination of eIF5A is catalyzed in two enzymatic steps: (1) transfer of 4-aminobutyl group from spermidine to epsilon-amino group of a particular lysine of eIF5A by deoxyhypusine synthase (DHS) to form an intermediary molecule called deoxyhypusine (2) hydroxylation of deoxyhypusine by deoxyhypusine hydroxylase (DOHH) to form a mature eIF5A. Hypusine is found in most of the eukaryotes and archaebacteria, but is absent in eubacteria. The amino acid sequence of eIF5A surrounding hypusine is found to be highly conserved in different species affirming its importance throughout the evolutionary process (*Park et al., 1993; Maier et al., 2010*). Hypusine is found to be important for survival and growth of several organisms. eIF5A is known to be involved in translation initiation as evident by its activity in stimulating methionyl-puromycin synthesis. The eIF5A lacking hypusine was found to be inactive in methionyl-puromycin synthesis assay indicating the importance of hypusine for the activity of eIF5A (*Park et al., 1993*). Recently, the role of eIF5A has been elucidated in translation elongation in yeast (*Saini et al., 2009*). Figure 1.8 is showing cascade of enzymatic reaction responsible for hypusine modification.

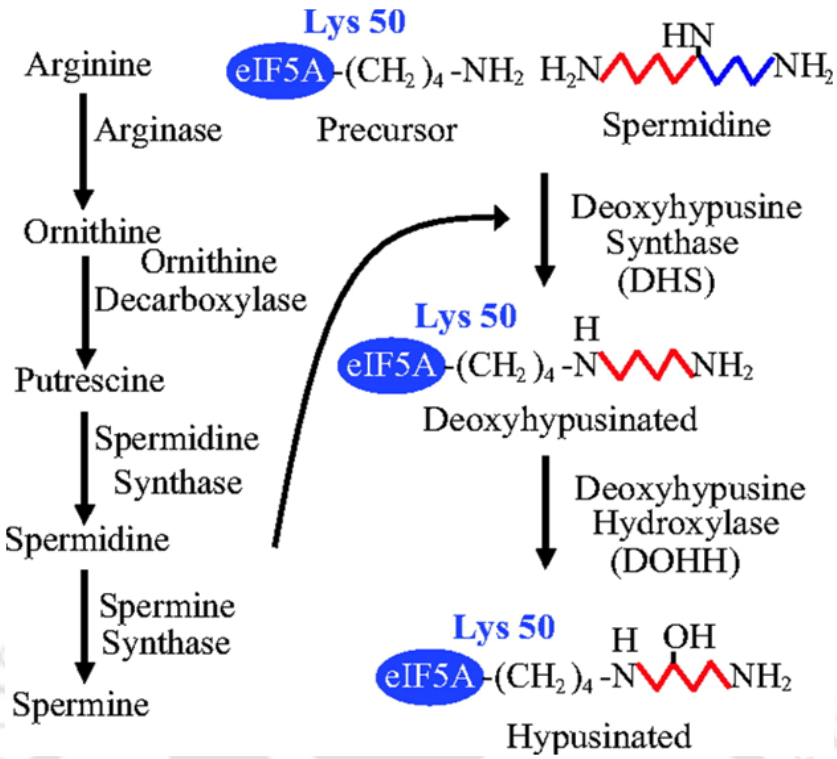

Figure 1.8: Different steps involved in hypusine modification of eIF5A. Hypusine modification involves the transfer of 4-aminobutyl moiety to a specific lysine of eIF5A by deoxyhypusine synthase to form an intermediate product called deoxyhypusinated eIF5A. Further, deoxyhypusine hydroxylase perform hydroxylation of deoxyhypusine to generate a mature and fully functional hypusinated eIF5A (Adopted with permission from Proceedings of the National Academy of Sciences of the United States of America *Ref:* PNAS. 2007, 104, 4194-4199). Copyright (2007) National Academy of Sciences, U.S.A.

1.2.14 *Autophagy*: About five decades ago, a phenomenon involving engulfment and degradation of cytoplasmic content within double membrane vesicles was puzzling scientists. In 1963, Christian de Duve described this phenomenon and coined the term 'autophagy'. The word 'autophagy' has Greek origin meaning 'eating one's self' (*Mizushima, 2007; Glick et al., 2010*). But the question arises, why a cell would eat itself and this lead to evolution of research in the area of autophagy. Autophagy has mainly three different forms: macroautophagy, microautophagy and chaperone mediated autophagy. In macroautophagy, cytoplasmic contents are delivered to lysosome through the formation of autophagosomes (double membrane vesicles) which forms autolysosomes after fusion with lysosome. In contrast, microautophagy involves the direct delivery of cytosolic material to the lysosome through lysosomal membrane invagination. Chaperone mediated autophagy utilizes chaperones to transfer the desired proteins across the lysosomal membrane. These proteins are further unfolded and

degraded after getting recognized by receptors of lysosomal membranes i.e. lysosomal associated membrane protein 2A (LAMP-2A) (*Glick et al., 2010*). Molecular mechanism and signalling pathway regulating autophagy is shown in Figure 1.9.

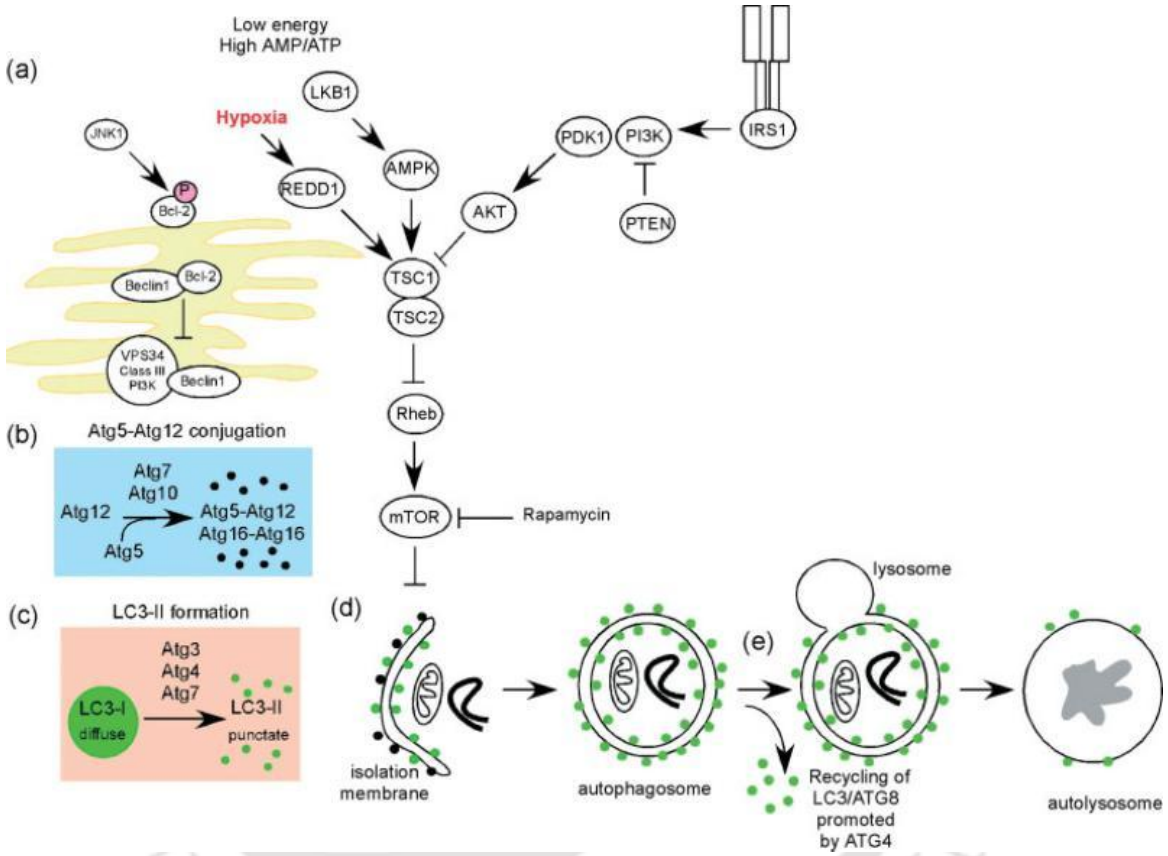

Figure 1.9: Molecular mechanism and signalling pathway regulating autophagy. Autophagy is called self degradation. It is a complex process which include five main steps (a) formation of phagophore which is controlled by Beclin-1/VPS34 at the endoplasmic reticulum and other membranes as a response towards stress signalling pathways; (b) Conjugation of Atg5 with Atg12 and the interaction of Atg5-Atg12 conjugate with Atg16L and further its multimerization at the phagophore; (c) Processing of LC3 and its insertion into the membrane of phagophore; (d) capture of targets for degradation and completion of autophagosome which is further followed by recycling of some LC3-II/ATG8 by ATG4; (e) fusion of lysosome with the formed autophagosome followed by degradation of engulfed molecule by proteases of lysosomes. There are several signalling pathways such as stress-signalling kinases like JNK-1 which regulates autophagy. JNK-1 promotes autophagy by phosphorylation of Bcl-2 which increases the interaction of Beclin-1 with VPS34. mTOR kinase is the most important signalling molecule involved in the autophagy. It regulates autophagy by inhibiting ATG1/Ulk-1/-2 complexes at the very early stages in formation of phagophore formation. Hypoxia and low cytosolic ATP levels induce autophagy through REDD1 and AMP-kinase which inhibits mTOR activity by reducing the activity of Rheb GTPase. Increase in growth factor signalling through the insulin receptor and its adaptor, IRS1, as well as other growth factor receptors inhibits autophagy by activating the PI3-kinases and Akt. Activation of PI3-kinase and Akt promotes the activity of mTOR kinase by inhibiting TSC1/TSC2 and increasing the activity of Rheb GTPase (Adopted with permission from John Wiley and Sons *Ref:* J Pathol. 2010, 221, 3–12).

The process of autophagy starts with the formation of phagophore. The phagophore are thought to be the components of trans-Golgi, endoplasmic reticulum or endosome. In mammalian cells, the origin of phagophore is not yet confirmed. The cargo, like ribosomes, protein aggregates and cellular organelles are engulfed by phagophore and further sequestered in autophagosomes. The autophagosome then fuses with lysosome allowing degradation of contents of autophagosome by the action of lysosomal proteases. The by-products of degradation like amino acids etc are exported back to the cytoplasm with the help of permeases and transporter proteins of the lysosome. Once back in the cytoplasm, these by-products can be reused for different processes like metabolism, building macromolecules etc. In addition to its role as 'recycle factory', autophagy also enhances ATP generation to increase energy efficiency and removes non functional organelles and proteins to negotiate cellular damage (*Glick et al., 2010*). The process of autophagy is divided into four main steps: induction, core recognition and selectivity, formation of autophagosomes and fusion of vesicles and breakdown of autophagosomes.

Induction: The most common inducer of autophagy is nutrient starvation. In yeast, starvation of some important components such as nitrogen, carbon, sulphate, nucleic acids and auxoptrophic amino acids are known to induce autophagy (*Takeshige et al*. 1992, *Mizushima 2007*). Regulation of autophagy in mammals is highly complicated. Amino acid starvation has also found to trigger autophagy in mammals, although the effect of amino acid starvation in regulation of autophagy has not yet been confirmed. Other amino acid signalling pathways like Beclin 1 and class 3 phosphatidylinositol 3- kinase are also reported to be involved in amino acid signalling towards autophagy (*Byfield et al. 2005; Nobukuni et al. 2005, Mizushima 2007*). Endocrine system is also found to regulate autophagy, for example, insulin was found to suppress liver autophagy whereas glucagon enhances it (*Mortimore and Pösö 1987*). Certain growth factors are also known to regulate autophagy such as interleukin-3 (IL-3) suppresses autophagy (*Lum et al. 2005b*). These signals directed by amino acids, hormones and growth factors, converge at mTOR signalling which is one of the main regulators of autophagy in nutrient starvation. Inhibitors of mTOR like rapamycin are found to induce autophagy in yeast and some animals (*Noda and Ohsumi 1998, Ravikumar et al. 2004, Mizushima 2007*). There are some other factors as well which play crucial role in regulation of autophagy such as, reactive oxygen species, AMP-activated protein kinase (AMPK), calcium, Bcl-2 etc (*Mizushima 2007*).

Cargo recognition and selectivity: The cargos engulfed by phagophore are recognized by certain receptor proteins. Clearance of aggregated proteins and ubiquitinated substrates by autophagy is a selective event mediated via p62/sequestosome 1 (SQSTM1) protein (*Bjørkøy et al.2005, Pohl and Jentsch 2009, He and Klionsky 2009*). p62 has ubiquitin binding domain which binds with ubiquitin via LC3 (microtubule-associated protein 1 light chain 3), a mammalian ATG8 homolog, and presents the ubiquitinated cargos to autophagic machinery for its further degradation (*Pankiv et al. 2007, Kim et al. 2008, He and Klionsky 2009*). C-terminal domain of p62 was found to share structural and functional similarity with ATG19 of yeast, suggesting that p62 in higher organisms is an analogue of ATG19 (*He and Klionsky 2009*).

Another example of selective autophagy is the degradation of P granules of *Caenorhabditis elegans* selectively in somatic cells by the process of autophagy. This degradation is mediated through a receptor protein, suppressor of ectopic P granule in autophagy mutants 1 (SEPA-1) which binds directly with P- granules and the homolog of ATG 8 in *C. elegans* i.e. LGG-1 (*He and Klionsky 2009, Zhang et al. 2009*).

Formation of autophagosomes: the formation of autophagosome starts by sequestration of organelles and cytoplasmic contents by phagophore. Phogophore, also called as isolation membrane, is flat in shape and appears like Golgi cisterna. The autophagosome is formed after complete sequestration by phagophore. The origin of autophagosomal membrane is thought be from different sources like Golgi, endoplasmic reticulum and mitochondria. In yeast, autophagosomes assemble at a site, called pre-autophagosomal structure (PAS). However, this structure was not found in mammalian cells (*Kim et al. 2001; Suzuki et al. 2001; Suzuki and Ohsumi 2007; Mizushima 2007*). The formation of autophagosome requires the recruitment of Atg (autophagy-related) proteins to the phagophore. There are 31 Atg proteins known in yeast, out of which 18 are found to be involved in the formation of autophagosomes and are called AP-Atg proteins. These Ap-Atg proteins are Atg1-10, Atg12-14, Atg16-18, Atg29 and Atg31. The recruitment of Ap-Atg proteins to PAS is a highly coordinated event. Atg17, Atg29 and Atg31 function together for organization of PAS. Atg12 and Atg8 are ubiquitin like proteins that have similar conjugation as ubiquitin. Atg12 is activated by Atg7 followed by its transfer to Atg10 leading to it covalent attachment to internal lysine residue of Atg5. Finally conjugated Atg12-Atg5 interacts with Atg16 which helps in its oligomerization and linking Atg12-Atg5-Atg16 tetramer to the phagophore (*Mizushima, 1999; Mizushima, 2003; Glick et al., 2010*). Atg8

conjugation involves its attachment with phosphatidylethanolamine (PE). The conjugation of Atg8 to PE starts with its processing by Atg4 which exposes its C-terminal glycine residue. Atg8 was then activated by Atg7 and transferred to Atg3 to finally get conjugated to PE through amide bond (*Hanada 2007*; *Mizushima 2007*; *He and Klionsky 2009*). Under normal condition, Atg8 is mainly found in cytoplasm whereas under autophagic conditions, it gets conjugated to lipid and gets localized to the both sides of the phagophore. This lipidation of Atg8 is used to monitor autophagy (*Kirisako, 1999; Kabeya, 2000; He and Klionsky, 2009*).

Fusion of vesicles and breakdown of autophagosomes: Next step of autophagy process involves the fusion of autophagosome and lysosome to form autolysosome. Autophagosome fuses with endosomes prior to lysosome to form amphisomes. It is believed that fusion of autophagosome with lysosome provides nascent autophagosome, a machinery to mediate its fusion with lysosome. Amphisomes were believed to deliver cargo and a component of machinery related to membrane fusion and further lowers the pH of autophagic vesicles before entry of acid proteases of lysosome (*Eskelinen, 2005; Mizushima, 2007*). Once autophagomes are formed, PE from Atg8-PE conjugate is cleaved by Atg4 releasing Atg8 back to cytoplasm. In yeast, the fusion of lysosome to autophagosome is mediated by several proteins like GTPase Ypt7 of rab family, N-ethylmaleimide sensitive fusion (NSF) proteins homolog Sec18, the class C Vps/HOPS complex proteins, SNARE Vam3, Vam7, Vti1, and Ykt6 etc (*Klionsky, 2005; He and Klionsky, 2009*). However, in mammals, the fusion of lysosome with autophagosome requires the small GTPase Rab7 and LAMP-2 (Lysosomal membrane protein). In yeast, inner vesicles are degraded by acid hydrolases of lysosomes like proteinase A and B and lipase Atg15 (*Teter et al., 2001; Epple et al., 2001*). In mammals, degradation of vesicles involves cathepsin B, D and L. The degradation product such as amino acids are effluxed back to the cytoplasm and are ready to be reused for cellular processes under starvation conditions (*Tanida et al., 2005, He and Klionsky, 2009*).

1.2.15 *mTor signalling:* Target of rapamycin (TOR) was first identified as a target for rapamycin showing antifungal properties and hence inhibiting the growth of *Saccharomyces cerevisiae* (*Heitman et al., 1991* ; *Alers et al., 2012*). It was later found to be one of the key components among several that regulate autophagy and growth of an organism under starvation and stress conditions. TOR belongs to phosphatidylinositol kinase-related kinase family and is a serine/threonine protein kinase. In yeast and other

higher eukaryotic organisms, TOR was found to be involved in regulating translation, transcription and metabolism in response to growth factors and nutrients. Several factors has been identified which are involved in the regulation of TOR activity. In yeast, availability of nitrogen and carbon are found to regulate TOR activity, whereas in mammals, levels of amino acids and glucose were found to regulate mTOR (mammalian target of rapamycin) activity (*Hara et al., 1998*; *Inoki et al., 2003; Wullschleger et al., 2006; Jung et al., 2010*). In yeast, TOR is present as two different complexes, TORC1 (TOR complex 1) and TORC2 (TOR complex 2), of which rapamycin was found to bind with TORC1 only. Common binding partners of yeast TORC1 and TORC2 complex are KOG1, LST8, and TCO89 whereas TORC2 also binds with BIT61, LST8, Avo1, Avo2, and Avo3 to form a complex different from TORC1 (*Wullschleger et al., 2006; Jung et al., 2010*). In mammals, mTORC1 binds with raptor (regulatory associated protein of TOR) which is a KOG1 ortholog, PRAS40, DEPTOR and GβL/mLst8. mTORC2 binds with GβL/mLst8, DEPTOR, Sin1 (ortholog of Avo1), PRR5/protor and rictor (*Hara et al., 2002; Sarbassov et al., 2004; Jacinto et al., 2006; Haar et al., 2007; Jung et al., 2007*). The KOG1 of yeast TORC1 and raptor of mTORC1 are known to play role in induction of autophagy under starvation condition and are also known as important regulators of ribosome biogenesis and translation. The mTORC2, however known to be insensitive, but likely to be target of rapamycin, has regulatory role in activation and phosphorylation of Akt/PKB, protein kinase C, serum- and glucocorticoid-induced protein kinase (*Sarbassov et al., 2005; Jung et al., 2010*). Figure 1.10 is showing the composition of mTORC1 and mTORC2.

1.2.16 ***Upstream regulators of mTOR:*** There are a variety of factors regulating TOR signalling network. These factors are stress, nutrients, growth factors and energy. The upstream regulators of mTOR is shown in Figure 1.11.

1.2.16.1 *Nutrients:* Nutrients like amino acids regulate mTOR signalling pathway. The activation of mTORC1 by amino acids has been proposed to be through stimulation of GTPase Rheb or inhibition of tuberous sclerosis complex TSC1-TSC2 (*Gao et al., 2002; Wullschleger et al., 2006; Russell et al., 2011*). Amino acid availability was found to regulate binding of Rheb to mTOR and not GTP charging of Rheb (*Long et al., 2005*). It was also found that hVPS34, a class III Phosphoinositide 3-kinase (PI3K), regulate mTOR in a manner independent of TSC1-TSC2 and Rheb (*Byfield et al., 2005; Nobukuni et al., 2005; Wullschleger et al., 2006*).

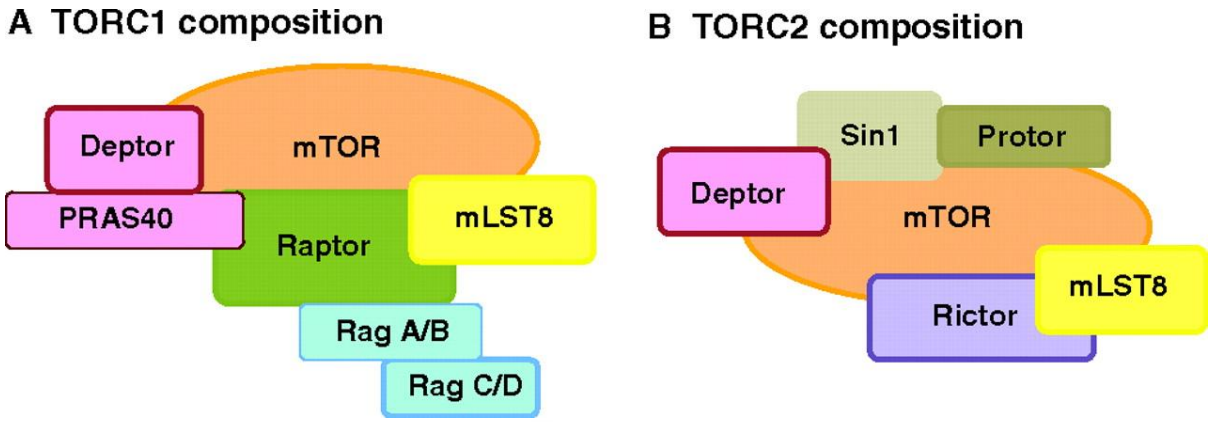

Figure 1.10: Composition of mTORC1 and mTORC2. **A**) Monomer subunit of target of rapamycin complex 1 (TORC1) contains of mammalian TOR (mTOR), raptor (regulatory associated protein of mTOR), PRAS40 (proline-rich AKT substrate 40 KDa), Deptor (DEP domain TOR-binding protein) and mLST8 (mammalian lethal with Sec-13 protein 8). Raptor promotes the formation of dimmers of TORC1 complexes. Binding of PRAS40 to TORC1 exhibits inhibitory effect and this binding is thought to be mediated by the direct interaction of PRAS40 with either raptor or mTOR. Deptor inhibits both TORC1 and TORC2 after binding with FAT (FRAP, ATM and TTRAP) domain of mTOR. mLST8 binds with the kinase region of mTOR through its multiple WD40 repeats. Binding of Rag A/B and Rag C/D to TORC1 is linked to its direct interaction with raptor. (**B**) Monomer complex of TORC2 complex consists of mTOR kinase, Sin 1 (stress-activated protein kinase-interacting protein 1), Rictor (rapamycin-insensitive companion of mTOR), Deptor, mLST8, and protor i.e protein-binding Rictor. Rictor contains certain domains which are conserved and are hypothesized to be involved in recruitment of substrate and formation of TORC2 complex. Sin1 is important for promoting Rictor-mTOR binding and regulating the substrate specificity. Function of Protor is still elusive, although it is known to bind with Rictor. mLST8 is thought to be important required for the functioning of TORC2 and binds wit TOR (Russell et al., 2011). (Adopted with permission from Company of Biologists *Ref:* Development. 2011, 138, 3343–3356).

1.2.16.2 *Stress:* TOR signalling has been known to play important role in response to cellular stress such as hypoxia, DNA damage etc. Hypoxia was found to inhibit TOR signalling in mammals and drosophila, further decreasing the cellular protein synthesis of the organism. Hypoxia signalling to mTORC1 is mediated through REDD1 and REDD2 proteins. Hypoxia induces up regulation of REDD proteins through transcription factor HIF1. REDD acts downstream of Akt and upstream of TSC1-TSC2. Increased expression of REDD protein inhibits the mTORC1 signalling pathway (*Brugarolas et al., 2004*). Increased hypoxia was found to cause ATP depletion and further AMPK activation. Other stress such as DNA damage inhibits mTOR via p53 activation and AMPK-TSC2 signalling (*Feng et al., 2005*; *Wullschleger et al., 2006*).

1.2.16.3 *Growth factor:* mTOR regulation through growth factor is regulated via PI3K pathway.PI3K binds to insulin receptor substrate (IRS) once it is phosphorylated after binding of insulin or insulin like growth factors to their receptors. After binding to IRS,

PI3K converts phosphatidylinositol-4, 5-phosphate (PIP2) to phosphatidylinositol-3, 4, 5-phosphate (PIP3). PIP3 further recruits Akt and PDK1 to the cell membrane. PDK1 phosphorylates and activates Akt1. mTOR is linked to PI3K pathway through TSC1 and TSC2 proteins which negatively regulates mTOR (*Manning, 2004*; *Wullschleger et al., 2006*).

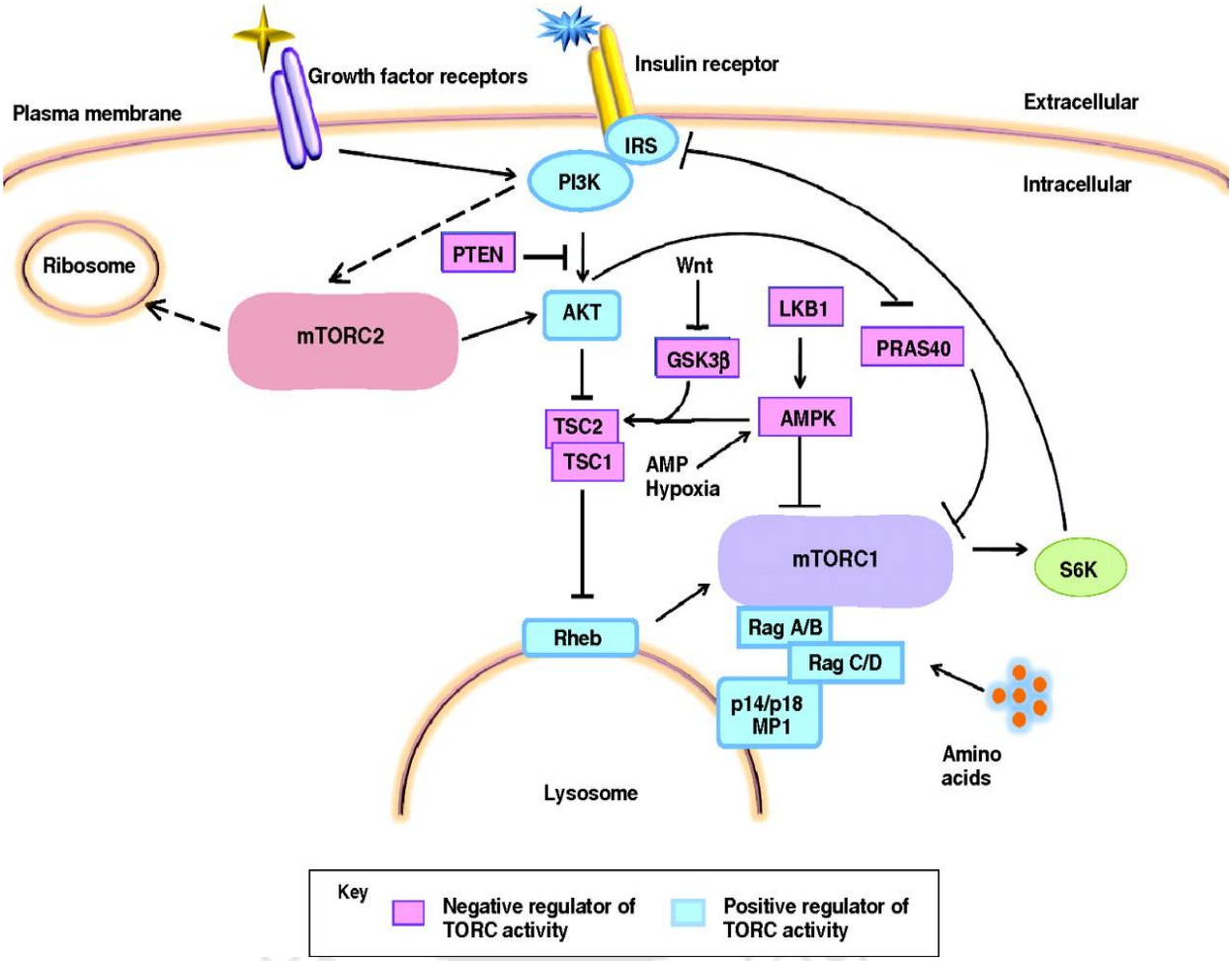

Figure 1.11: Upstream regulation of mTOR. There are a number of positive (shown in blue) and negative (shown in pink) regulators of mammalian target of rapamycin complex (mTORC). Certain growth factors and insulin signalling pathways activate mTORC1 by activating phosphatidylinositol 3-kinase (PI3K) and AKT (a serine/threonine protein kinase). This activation of PI3K and AKT inhibits the tuberous sclerosis complex (TSC) 1/2 complex which further cause repression of Rheb. Low ATP levels and hypoxia activates AMP kinase which in turn inhibits mTORC1 via phosphorylation of TSC2 and through inhibition of raptor. Certain amino acids at the lysosomal membrane can also activate mTORC1 via the Rag proteins and the Ragulator complex (containing p14, p18 and MP1). Certain growth factors (through PI3K) and undetermined effectors (indicated by the broken arrow) can activate mTORC2. In response to this, mTORC2 can regulate AKT, thereby acting as upstream regulator of TORC1. Association of ribosomes can also activate mTORC2. Abbreviations: MP1, MEK partner 1; IRS, insulin receptor substrate; LKB1, liver kinase B1; GSK3β, glycogen synthase 3β; PRAS40, proline-rich AKT substrate 40 KDa; S6K, ribosomal S6 kinase; PTEN, phosphatase and tensin homolog protein (Adopted with permission from Company of Biologists *Ref: Development* 2011, 138, 3343-3356)

1.2.16.4 *Energy:* AMP-activated protein kinase mediates mTOR sensing towards cell energy levels. High AMP/ATP level induces activation of AMPK which in turn inhibits mTORC1 by phosphorylating TSC2 (*Inoki et al., 2003*).

1.2.16.5 *mTOR regulation of autophagy:* Under starvation condition, cells degrade their cytosolic contents and organelles by a catabolic process called autophagy and recycle them back to the cytoplasm to be reused by improvised cells. mTOR was found to negatively regulate autophagy. In the autophagy pathway, Atg1 is the first molecule downstream of TOR and is involved in the early stages to autophagy induction like nucleation and PAS formation. The importance of Atg1 in induction of autophagy has been established in several eukaryotes like *S. cerevisiae, C. elegans, Drosophila melanogaster* and *Dictyostelium discoideum* (*Meléndez et al., 2003; Scott et al., 2004*). In yeast, Atg1 was found to interact with other autophagy related proteins like Atg13, Atg17, Atg 29 and Atg31. This interaction is dependent on the nutrient availability to organism and activity of TOR. Sometimes even under nutrient rich conditions, Atg1 get localized to PAS. This may be because of the presence of cytoplasm to vacuole targeting (Cvt) which involves the formation of Cvt vesicles (small double membrane vesicle). These Cvt vesicles are similar to autophagosomes. Atg13 is important for Atg1 activity whereas Atg17 is required for localization of Atg1 and other autophagy related proteins like Atg9 to PAS (*Kamada et al., 2000; Suzuki et al., 2007; Jung et al, 2011*).

1.2.17 ***Exploring the protein prenylation pathway to identify genes as potential drug candidates:*** The post-translational modifications of biological molecules are known to be crucial for their functional activation, regulation and localization. Prenylation is one such modification which is involved in post-translational modification of various important proteins like proteins of Ras superfamily which are involved in a variety of regulatory and signalling events in eukaryotes. Prenylation is attachment of isoprenoid group (15C farnesyl or 20C geranylgaranyl group) to a cysteine residue in a thioether linkage. These prenylated proteins are found in different cellular compartments including nucleus, cytosol and membrane bound organelles. Most of the prenylated proteins belong to the Ras superfamily which are involved in a variety of cellular functions like cytokinesis, membrane trafficking, control of cell growth, differentiation etc. Different types of prenylated proteins are shown in Figure 1.12. The targets for post-translational prenylation are the small GTP-binding proteins containing CAAX motif at or near its carboxyl terminus. These types of proteins undergo three different prenyl dependent

processing for their ultimate maturation and localization (*Casey, 1992; Zhang and Casey 1996*).

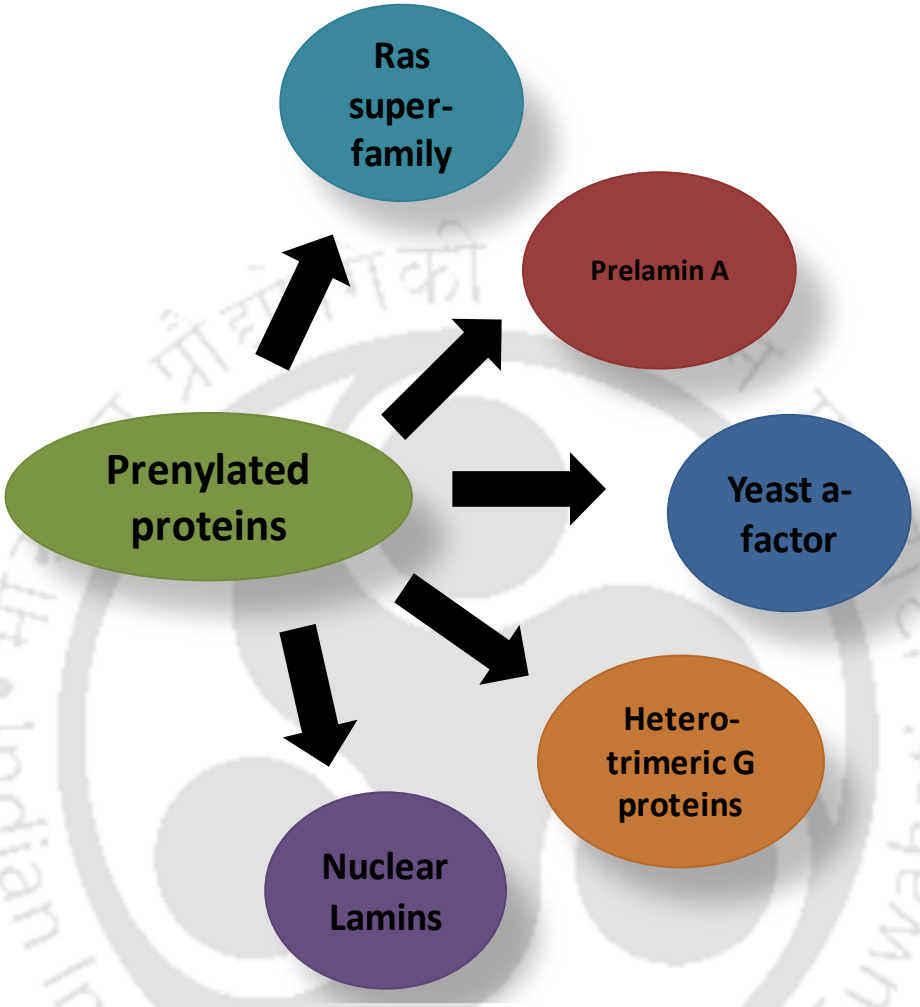

Figure 1.12: Different types of prenylated proteins. There are different types prenylated proteins which include nuclear lamins, gamma subunit of heterotrimeric G proteins, proteins belonging to Ras superfamily, prelamin A etc (*Casey, 1992; Sinensky and Lutz, 1992; Sinensky et al., 1994*).

1.2.18 *The CAAX motif*: The presence of a CAAX motif at the carboxyl terminus is an essential requirement for the prenyl dependent post-translational processing of a protein. 'C' in the CAAX motif stands for cysteine, 'A' denotes aliphatic amino acids and 'X' can be any amino acid residues and determines the specificity of enzyme. The amino acid present at 'X' position determines whether the cysteine residue is to be farnesylated (15C) or geranylgeranylated (20C) (*Wright and Philips, 2006*). Figure 1.13 shows the CAAX motif representing its different residues.

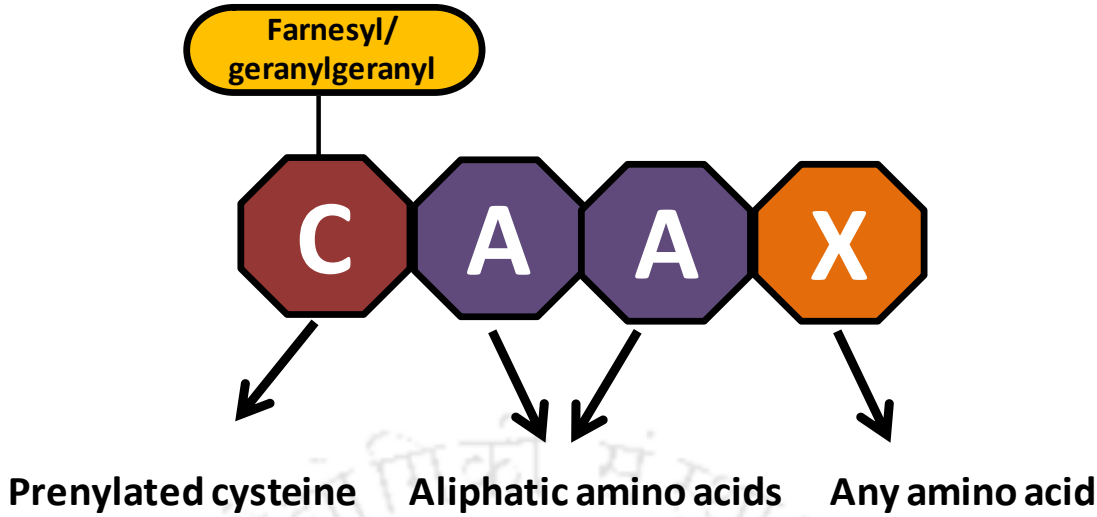

Figure 1.13: The CAAX motif representing its different residues. The presence of a CAAX motif at the carboxyl terminal is indispensable for prenylation and its further processing. Here in CAAX motif, C represents cysteine, A stands for aliphatic amino acids and X can be any amino acid. The amino acid at X position determines the specificity of enzyme as it decides whether the protein is going to be farnesylated or geranygeranylated (*Wright and Philips, 2006*).

1.2.19 ***Processing of proteins containing CAAX motif*:** The consensus sequence CAAX is known to direct a series of post-translational processing initiated by addition of lipid moiety with a polyisoprene, which is followed by endoproteolysis and further carboxyl methylation of proteolysed proteins. Addition of isoprenoid group is done by a pair of cytosolic prenyl transferases which attaches isoprenoid moiety to the cysteine residue of CAAX motif via thioether linkage. These prenyl transferases can be either farnesyl transferase (FTase) or geranylgeranyl transferase (GGTase) depending on whether a 15C farnesyl or a 20C geranylgeranyl group is to be attached. These prenylated sequences then act as substrates for CAAX prenyl proteases (CAAX prenyl proteases I & CAAX prenyl proteases II) to initiate endoproteolysis and remove –AAX amino acids from the CAAX motif. The newly exposed prenylated C-terminal prenylcysteine is attacked by carboxyl methyltransferase (Icmt) which methyl esterifies α-carboxyl group of prenylated cysteine (*Wright and Philips, 2006*).

1.2.20 ***The CAAX prenyl proteases:*** There are two types of CAAX prenyl proteases: type I & type II. The type I CAAX prenyl proteases are named as alpha-factor converting enzyme (AFC1). They are known to be metalloproteases with HEXXH conserved motif (where H is histidine, E is glutamate and X is any amino acid) in it (*Boyartchuk et al, 1997; Schmidt et al, 2000; Tam et al, 2001*). Type II CAAX prenyl proteases are called

Ras and a-factor converting enzyme (RCE1). They lack the conserved motif present in type I CAAX prenyl proteases and their catalytic nature is still a topic of debate. However, they were suggested to be cysteine proteases based on the some inhibition studies and activity of cysteine, histidine and glutamate mutations. This was supported by the study that reveals the presence of cysteine residue near the active site of yeast Rce1p and it was found that upon mutation of this cysteine residue or by using cysteine protease inhibitors, the enzyme gets deactivated (*Dolence et al*, 2000; *Pei et al, 2011*). Few literatures suggest them to be metalloproteases (*Pei et al, 2001; Pei et al, 2011*). It has been reported that yeast type I CAAX prenyl protease (Afc1p) and yeast type II CAAX prenyl protease have distinct but overlapping substrate specificity (Figure 1.14). Although Afc1p and Rce1p lack sequence similarity, both were found to proteolyse the a-factor CAAX sequence, CVIA. However, the a-factor CAAX sequence substituted by CAMQ & CTLM was found to be processed only by Afc1p and Rce1p respectively. Also, the yeast Ras2 protein (CIIS) was found to be catalysed by Rce1p but apparently not by yeast Afc1p. (*Boyartchuk et al, 1997; Trueblood et al, 2000*). In addition to its CAAX proteolysis activity, Ste24p, a type I CAAX prenyl protease of yeast, is found to have NH_2-terminal proteolysis activity for processing yeast a-factor precursor (*Tam et al, 2001*). Figure 1.15 shows the prenylation and processing of prenylated proteins in eukaryotes.

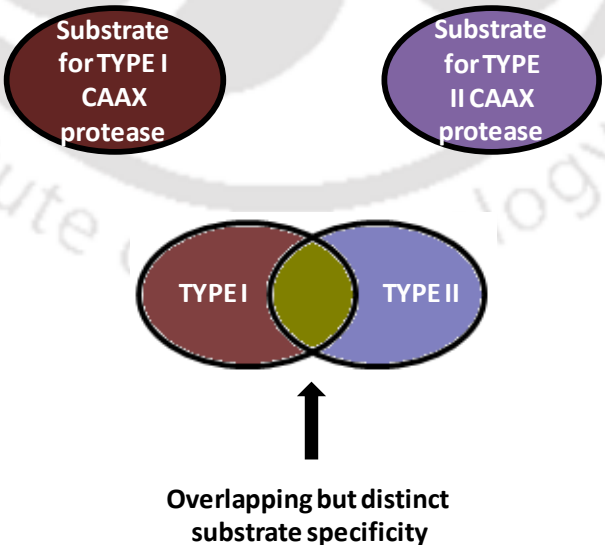

Figure 1.14: Diagram showing distinct but overlapping substrate specificity of CAAX prenyl protease I and II. In yeast, type I CAAX prenyl protease (Afc1p) and type II CAAA prenyl protease (Rce1p) both proteolyse the a factor CAAX sequence i.e. CVIA. However, if this sequence is substituted by CAMQ the a factor is processed by only Afc1p and after substitution with CTLM it is only processed by Rce1p (*Boyartchuk et al, 1997; Trueblood et al, 2000*).

1.2.21 ***Role of post prenylation processing*****:** The role of CAAX processing has been demonstrated in various protein functions and trafficking by mutating cysteine of CAAX to another amino acid so as to prevent prenylation of protein (*Wright and Philips, 2006*). However, this cannot figure out the importance of CAAX prenyl proteases and methyl transferase since prenylation is a prerequisite for their activity. Their physiological importance were assessed when mouse embryonic fibroblast lacking Rce1 (CAAX prenyl protease II required for endoproteolysis) or Icmt (carboxyl methyl transferase required for carboxyl methylation of isoprenylcysteine) showed mislocalization of farnesylated Ras proteins (*Michaelson et al, 2005*). Rce1 deficiency was found to be lethal in late embryonic development in mouse which also affirms the physiological significance of CAAX prenyl proteases (*Kim et al, 1999*). It was also found that knock out of Rce1 results in pronounced impairment of growth in *Trypanosoma brucei* (*Gillespiea et al, 2007*). Recently, the type I yeast CAAX prenyl protease, Ste24 is found to have play role in chitin synthesis (*Meissner et al, 2010*). It was found that variants of type I CAAX prenyl proteases (Afc1) in yeast showed reduction in a-factor production below detectable limit even in presence of type II CAAX prenyl protease, Rce1 (a-factor can also be processed by Rce1). This could be because of the loss of N-terminal processing of a-factor by Afc1p in combination with partial defect in prenylation (*Trueblood et al, 2000*). Human Afc1 has been found to process farnesylated prelamin A by removing –AAX from the –CAAX sequence of prelamin A and also cleaving at sites 15 residues upstream of farnesylated cysteine. It was observed that accumulation of farnesylated prelamin A due to mutation in human Afc1 enzyme or prelamin A cleavage site was found in genetic diseases like Huchinson-Gilford progeria and Mandibuloacral dysplasia (*Gillespiea et al, 2007*). The discussion mentioned here concluded that both type I and type II CAAX prenyl proteases are involved in processing of various physiologically important proteins in different organisms and their role and significance in others is yet to be explored.

1.2.22 ***CAAX prenyl proteases as antileishmanial drug target*****:** The prenyl transferases and carboxyl methyltransferases involved in prenylation and processing of prenylated proteins have been well explored, characterized and studied in different organisms. However, the CAAX prenyl proteases responsible for endoproteolysis of prenylated proteins are still underexplored and hence these proteases can be chosen to study their role in *Leishmania* and further ensure their validity as a potential drug targets against leishmaniasis.

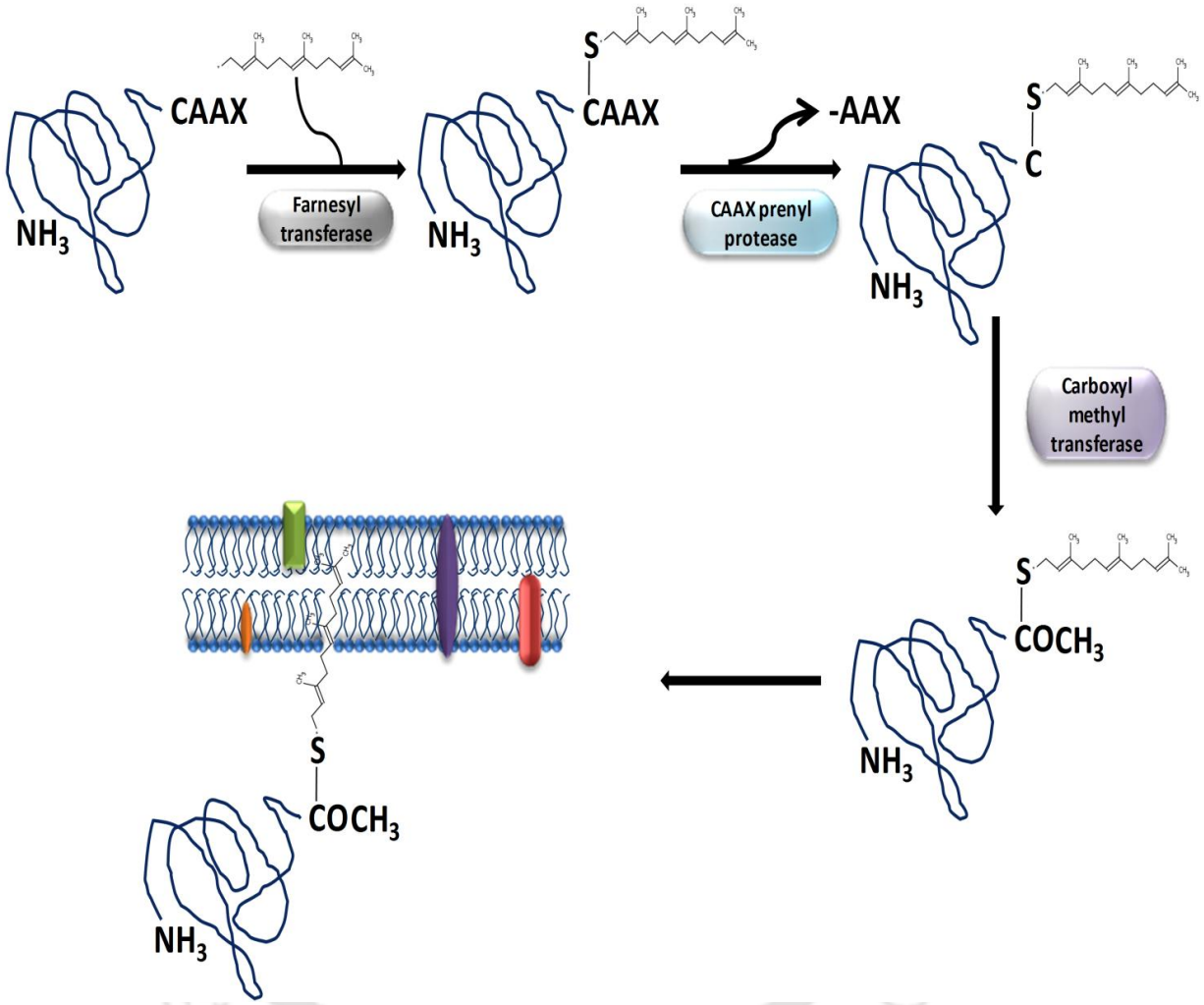

Figure 1.15: Prenylation and processing of prenylated eukaryotic proteins showing the role of CAAX prenyl protease. The presence of CAAX motif directs the addition of isoprenoid group to by prenyl transferases such as farnesyl transferase (FTase) etc. These prenylated proteins are proteolysed by CAAX prenyl proteases (Type I and Type II) which remove –AAX amino acids from the prenylated CAAX motif leaving a free prenylated cysteine. This free prenyl cysteine acts as substrate for carboxyl methyltransferase which methylates α-carboxyl group generating a mature protein (*Al-Quadan et al, 2011*).

To verify the physiological role and significance of CAAX prenyl proteases I in *Leishmania*, we look forward to model these proteases and identify inhibitors against them.

1.2.23 ***Multi target drug discovery approach:*** Past decade has witnessed advances in several high throughput techniques and efforts towards drug development. However, with increasing developments in drug discovery, the number of successful drugs against leishmaniasis has not increased significantly. Many available drugs till now focus on inhibiting single target. Increasing biological knowledge has revealed that inhibiting single target does not show desirable effect on the entire targeted system even though it is successfully inhibiting its specific target. The reason could be the compensatory effect of the organism in response to the drug by which it is able to cope up the effect of inhibition of single target generating resistance against the drug (*Lu et al., 2012*). Recently, there has been a paradigm shift from single to multi target drug discovery approach to cope up the resistance problem and discover a more effective drug molecule. Single formulation of drugs inhibiting two different targets could also be employed as an efficient strategy to kill the parasite and control the spread of the disease.

1.2.24 ***Significance of the work:*** Owing to the disadvantages of several available drugs against leishmaniasis, the need to develop new and effective drug candidates is continued. Continuing the search, we have identified hypericin as a potential drug candidate against leishmaniasis. We have identified spermidine synthase as a potential drug target for the development for novel, specific and effective drug candidates against leishmaniasis. Searching the mechanism of action of hypericin, we have observed that spermidine might have potential role in processes other than redox metabolism of the parasite. Further, we have identified the pathways being affected by the inhibition of spermidine synthase of *Leishmania donovani*. We have observed that the expression of genes involved in redox metabolism, hypusination of eIF5A, DNA repair pathway and autophagy are being altered. We have found that spermidine is a crucial player in hypusine modification of eIF5A. We have also analyzed the induction and effects of autophagy as a cytoprotective mechanism after hypericin treatment. Finally, we have analyzed that the hypericin induced death of the parasite is due to altered hypusine modification of eIF5A and the death is necrosis with autophagy. Multitarget approach is a new paradigm in science towards development of more potent and effective drugs against diseases. In an attempt to

develop a more effective drug circumpassing the limitations and disadvantages of available drugs, we have identified CAAX prenyl protease I and II as another good targets. We have also identified the potential inhibitors of CAAX prenyl protease I and II using *in silico* studies. These inhibitors can be further taken up for further validation of their drug candidature.

The work presented here is divided into following experimental chapters:

Probing the molecular mechanism of hypericin-induced parasite death: A novel inhibitor, hypericin, against spermidine synthase of *Leishmania donovani* has been identified by using *in silico* analysis. The *in silico* identified drug was further validated by using biochemical approach and its antileishmanial effects were also checked. The specificity of the inhibitor was further confirmed by measuring the intracellular glutathione and trypanothione levels. Hypericin was found to cause necrosis like death of the parasite with induction of ROS generation. Trypanothione, a key redox molecule, has reverted back the ROS level but death of the parasite was not reverted back. Whereas, spermidine supplementation has reverted back the ROS as well as the death of the parasite. So, we have concluded that the death of the parasite was completely independent of ROS generation and spermidine has potential role in pathways other than redox metabolism of the parasite.

Molecular events leading to death of *Leishmania donovani* under spermidine starvation: Differential expression of genes of different pathways was analyzed after hypericin treatment. Genes involved in redox metabolism, hypusination, autophagy and DNA repair pathways were found to show altered expression after hypericin treatment. Hypericin was found to induce ROS dependent autophagy as a cytoprotective mechanism towards DNA damage. There was a significant decrease in the expression level of histone deacetylase, SIR2RP, but an increase in intracellular NAD^+ level of the parasite indicating the need to identify molecules required for the exposure of sirtuins to NAD^+. The increase in NAD^+ level can be correlated to increased AMPK expression. We have observed the altered hypusine modification of eIF5A which was reverted back by spermidine supplementation but not by trypanothione supplementation. So, here we have concluded that the death of the parasite after hypericin treatment is mainly due to decreased hypusine modification and is termed as necrosis with autophagy.

Proteome analysis of *Leishmania donovani* under spermidine starvation: Proteome profiling is now a day emerging as a powerful tool for answering various biological questions. Hypericin has shown to alter the expression of genes related to various pathways like autophagy, hypusination, DNA repair and redox metabolism. In order to further explore the mechanism of hypericin mediated cell death, we have used label free quantitation approach to analyze proteome profile of *Leishmania donovani*. The protein identified to be altered after hypericin treatment has been classified into nine major categories. Relative distribution of total altered proteins, up regulated and down regulated proteins were identified and shown as pie chart. Overall, the results are showing good correlation with our previous result showing death due to altered translation and cytoprotective mechanism against DNA damage. These modulations also led to the altered cellular metabolism as well as signaling pathways of the parasite after hypericin treatment.

Molecular docking and structure based virtual screening studies of CAAX prenyl protease I &II of *Leishmania donovani*: CAAX prenyl proteases are involved in modification of several signaling proteins. Working on a paradigm shift from single to multitarget drug discovery, we have identified CAAX prenyl protease I and II as potential drug targets. We have modeled the structure of CAAX prenyl protease I and II using homology modeling approach. The predicted structures were further validated using Ramachandran plot, SAVES and ProSA. Active site prediction of both CAAX prenyl protease I and I was done which has shown presence of different residues at the active site of both the proteases. Electrostatic surface potential was also analyzed for both CAAX prenyl protease I and II. Reported bisubstrate analogue inhibitors of protein farnesyl transferase and peptidyl (acyloxy) methyl ketones were used for molecular docking with CAAX prenyl protease I and II. Structure based virtual screening was also used to find out the new and potent inhibitors of both CAAX prenyl protease I and II. Best docked conformations of protein ligand complexes were found to be stable throughout 20ns of molecular dynamics simulations. Also, the best docked compounds were found to follow Lipinski's rule of druglikliness. Overall, we have identified novel potential drug candidates against CAAX prenyl protease I and II of *Leishmania donovani*.

CHAPTER II

Probing the Molecular Mechanism of Hypericin Induced Parasite Death*

2.1 Abstract:

Hypericin, a natural compound from *Hypericum perforatum*, has been identified as a specific inhibitor of *Leishmania donovani* spermidine synthase (*Ld*SS). Hypericin showed *in vitro* inhibition of recombinant *Ld*SS enzyme activity. The *in vivo* estimation of spermidine levels in *Leishmania* promastigotes after hypericin treatment showed significant decreases in the spermidine pools of the parasites, indicating target specificity of the inhibitor molecule. The inhibitor, hypericin, showed significant antileishmanial activity, and the mode of death showed necrosis-like features. Further, decreased trypanothione levels and increased glutathione levels with elevated reactive oxygen species levels were observed after hypericin treatment. Supplementation with trypanothione in the medium with hypericin treatment restored *in vivo* trypanothione levels and ROS levels but could not prevent necrosis-like death of the parasites. However, supplementation with spermidine in the medium with hypericin treatment restored *in vivo* spermidine levels and parasite death was prevented to a large extent. The data overall suggest that the parasite death due to spermidine starvation as a result of *Ld*SS inhibition. Moreover, the work provides a novel antileishmanial chemical scaffold, i.e., hypericin.

**** Published in Antimicrobial Agents and Chemotherapy, 2015; 59:15-24***

2.2 Introduction:

Leishmaniasis is a widespread tropical disease caused by the protozoan parasite *Leishmania*, which belongs to the order *Kinetoplastida* and the family Trypanosomatidae. This parasite is transmitted by the vector sandfly, of the genera *Phlebotomus* and *Lutzomyia*. There are three forms of clinical manifestations of leishmaniasis, depending on the type of infecting species, namely, cutaneous, mucocutaneous, and visceral leishmaniasis (*Shukla et al., 2010*). The most deadly form of the disease is visceral leishmaniasis, also known as kala-azar, which is caused mainly by *Leishmania donovani* in India. According to WHO statistics, 350 million people in 88 countries are at risk of developing the disease. Every year there are 2 million new cases of the disease, of which 0.5 million are cases of visceral leishmaniasis (*Murray et al., 2005; Stockdale and Newton, 2013*). The treatment of leishmaniasis relies mainly on chemotherapy, as there are no vaccines available. Although many drugs are available on the market, they have several limitations (*Croft and Coombs, 2003; Croft et al., 2006*), indicating a need for novel drug candidates with specific drug targets. All aerobic organisms are exposed to oxidative stress and generate toxic reactive oxygen species (ROS) that can degrade DNA, modify proteins, and adversely affect survival of the organism. The amastigote form of the parasite resides and multiplies inside macrophages, which produce large amounts of hydrogen peroxide. *Leishmania* parasites are reported to be very sensitive to oxidative stress if the functions of trypanothione metabolism enzymes are disrupted (*Krauth-Siegel and Comini, 2008*). The trypanothione system responsible for removal of oxidative stress in *Leishmania* parasites is unique but is analogous to mammalian host glutathione systems. Trypanothione, bis(glutathionyl)spermidine, is exclusively found in parasitic protozoa of the order *Kinetoplastida*, such as trypanosomes and *Leishmania*. Spermidine synthase, a key enzyme for the second step of trypanothione synthesis, catalyzes the formation of spermidine. Glutathione and spermidine are used by trypanothione synthetase for trypanothione synthesis. Thus, inhibition of spermidine synthase is likely to starve the parasite with respect to spermidine for trypanothione synthesis. There are reports showing that the enzyme spermidine synthase is necessary for the survival and virulence of the parasite and shows only 56% amino acid identity with its human counterpart (*Gilroy et al., 2011*). However, it remains unclear whether the death of parasites is because of increased levels of reactive oxygen species due to decreases in the production of spermidine leading to low levels of trypanothione, because of other

possible roles of spermidine in parasite survival, or both. It is worth mentioning that spermidine is essential for hypusine modification of the translation factor eIF5A in some organisms. Spermidine performs diverse cellular functions in various other organisms (*Pichiah et al., 2011*). In the case of mammals, spermidine is involved in inhibition of neuronal nitric oxide synthase and transcription of RNA through stimulation of T4 polynucleotide kinase and T7 RNA polymerase activity (*Hu et al., 1994; Wan and Wilkin 1993*). Spermidine is also reported to be involved in autophagy, a process essential for removal of damaged organelles and potentially toxic protein aggregates, in the case of *Caenorhabditis elegans* (*Morselli et al., 2011*). Thus, spermidine starvation in parasites, leading to parasite death, may be due to other factors completely unrelated to ROS generation. Thus, inhibiting *Leishmania donovani* spermidine synthase (*Ld*SS) could adversely affect survival of the parasite, making this a potent and effective drug target for leishmaniasis. We have designed a novel specific inhibitor of *Ld*SS and investigated the effects of the inhibitor on *Leishmania* promastigotes. Overall, the study provides conclusive evidence that the inhibition of spermidine synthase results in spermidine starvation, increases in ROS levels, and necrosis-like death. However, the necrotic death due to spermidine starvation is not linked to elevated ROS levels in the pathogen.

2.3 Materials and methods:

2.3.1 ***Parasites, cell lines and chemicals:*** The *Leishmania donovani* (MHOM/IN/2010/BHU1081) was obtained from Prof. Shyam Sundar, Banaras Hindu University, India. Macrophage cell line J774A.1 used in the study was taken from "National Centre for Cell Science" (NCCS), Pune. The procedures for *Leishmania donovani* and Macrophage cell line J774A.1 are optimized and reported in our previous publications (*Shukla et al., 2011; Shukla et al., 2012; Saudagar et al, 2013; Das et al., 2013*). Decarboxylated S-adenosylmethionine was gifted by Dr. Keijiro Sameijima, Tokyo Metropolitan Kamagome Hospital, Tokyo, Japan. Spermidine synthase cDNA was obtained as a clone in pBluescript bacterial vector from Dr. Sigrid Roberts, Pacific University School of Pharmacy, Hillsboro, United State. CM-H_2DCFDA dye and apoptosis kit were obtained from Life Technologies. Hypericin and all other chemicals used in the experiments were of the highest grade procured from Sigma-Aldrich or Merck. Protein molecular weight markers and DNA markers were purchased from New England Biolabs.

2.3.2 ***Cloning, expression and purification of spermidine synthase*****:** The spermidine synthase cDNA (900 bp) obtained as a clone in pBluescript bacterial vector was used as a template to amplify the cDNA. The cDNA was amplified using forward and reverse primers whose sequence is mentioned in Table 1. The spermidine synthase cDNA was then cloned in *Nhe*I and *Bam*HI restriction sites of pET-28a(+) vector. This fusion vector was further transformed into BL21(DE3) for overexpression of recombinant spermidine synthase. The transformed colonies were picked and allowed to grow at 37 °C till absorbance of 0.5- 0.6 at 600 nm was obtained. The cells were induced with 1 mM IPTG at 25 °C for 8 h and then harvested by centrifugation at 7,000 rpm for 10 min at 4 °C. The pellet was dissolved in lysis buffer (50 mM sodium phosphate buffer, 0.1 mM EDTA, 0.1 mM DTT, 200 mM sodium chloride) having pH 7.4. The cells were lysed by sonication and cell debris was separated by centrifugation at 12,000 rpm for 40 minutes. The supernatant was collected and protein was purified using Ni-NTA affinity chromatography. Concentration of enzyme was determined using Bradford assay.

2.3.3 ***Enzymatic assay and Inhibition studies*****:** The spermidine synthase assay mixture (40 µl) contains 5 µg *Ld*SS, substrates of spermidine synthase i.e putrescine and decarboxylated S-adenosylmethionine and 0.1 mM DTT in 100 mM sodium phosphate buffer (pH 7.4). The enzymatic assay was carried out at 37 °C for 2 h. The product formed, spermidine, was estimated using method reported earlier (*Enomoto et al., 2006; Porta et al., 1981*). In brief, 40 µl of the assay mixture was taken and derivatized by adding 40 µl of saturated sodium carbonate and 120 µl of 75 mM dansyl chloride. The reaction mixture was incubated at 60°C for 2 h in dark. After incubation, the mixture was centrifuged and 20 µl of the supernatant was separated on C18 column and analyzed using HPLC (Dionex Ultimate 3000). The dansylated polyamines were detected with excitation and emission wavelength of 360 nm and 510 nm, respectively. The separation was done using gradient of mobile phase A (50 mM ammonium formate (pH 5.0): acetonitrile; 90: 10) and mobile phase B (50 mM ammonium formate (pH 5.0): acetonitrile; 10 : 90) where mobile phase B was varied from 55% to 100 % for 20 minutes to separate the polyamines (*Enomoto et al., 2006; Porta et al., 1981*). Determination of K_m and V_{max} of substrate was done by varying concentration of that substrate while keeping saturating concentration of other substrate. The concentration of dcSAM was varied from 30 µM to 70 µM and that of putrescine was varied from 0.1 mM to 2 mM.

In silico identified inhibitor, hypericin was assessed against recombinant spermidine synthase. For inhibition studies, the enzyme was incubated with hypericin (100 µM), keeping saturating concentration of one substrate while varying the concentration of other substrate in the assay buffer. The data was plotted in double reciprocal plot for calculation of inhibitory constant (K_i).

2.3.4 *Cell viability assay*: The effect of hypericin on the survival of the *Leishmania* promastigotes was analyzed by using MTT assay (*Mosmann, 1983*) as reported in our earlier publications (*Das et al., 2013; Saudagar et al., 2013*). In brief, 200 µl of *Leishmania* promastigotes (2.5 x 10^6 cells/ml) were treated with varying doses (10 µM, 20 µM, 40 µM, 80 µM and 100 µM) of hypericin for 24 h at 25°C. Promastigotes were then centrifuged to remove the media. Subsequently, 200 µl of 0.5 mg/ml MTT [(3-(4,5-Dimethylthiazol-2-yl)-2,5-Diphenyltetrazolium Bromide)] was added to the promastigotes and incubated for 4 h. After the incubation period, MTT was removed from the promastigotes and the formed formazan was dissolved in Dimethyl sulfoxide (DMSO). Appropriate blanks were taken for each concentration of hypericin treated and untreated promastigotes.

2.3.5 *Reactive oxygen species (ROS) detection*: The endogenous ROS levels were detected using chloromethyl derivative of H_2DCFDA which is a cell permeable fluorescent probe. Untreated *Leishmania* promastigotes (2.5 x 10^6 cells/ml) were incubated with 20 µM of CM- H_2DCFDA at 25°C for 45 minutes. Similarly, reactive oxygen species level was detected in *Leishmania* promastigotes treated with hypericin (18 µM) for different time intervals (1.5 h, 3 h, 6 h, 12 h and 24 h). Promastigotes were also pretreated with N-acetylcysteine (NAC) before hypericin treatment to check the attenuation of ROS developed due to hypericin. NAC pretreatment includes treatment with 20 mM NAC for 30 minutes. ROS production was also monitored in *Leishmania* promastigotes with trypanothione (0.5 µM) or spermidine (100 µM) supplementation followed by treatment with hypericin (18 µM). The fluorescence of the probe indicating the ROS level was assessed and analyzed by using BD FACSCalibur flow cytometer and CellQuestPro software (*Shukla et al., 2011; Shukla et al., 2012; Saudagar et al, 2013; Das et al., 2013*).

2.3.6 *Analysis of apoptosis/necrosis of Leishmania promastigotes*: Analysis of apoptotic/necrotic features was done as reported in our earlier publications using annexin V-FITC apoptosis kit from Life Technologies (*Saudagar et al, 2013; Das et al., 2013*).

Untreated promastigotes of *Leishmania donovani* were taken at a cell density of 2.5 X 10^6 cells/ml and staining with annexin-V FITC and propidium iodide (PI) was done according to the instructions given by the manufacturer. The fluorescence of the stained promastigotes was detected by BD FACSCalibur flow cytometer and the results were analyzed using CellQuestPro software (*Saudagar et al, 2013*). Similarly, hypericin (18 µM) treated promastigotes with or without trypanothione (0.5 µM) or spermidine (100 µM) supplementation were analyzed for apoptosis/necrosis. *Leishmania* promastigotes treated with miltefosine (50 µM) for 24 h were used as positive control for apoptosis. Promastigotes pretreated with NAC followed by hypericin treatment were also analyzed to determine the mode of cell death.

2.3.7 *Intracellular thiols detection*: The *in vivo* thiols, trypanothione and glutathione, levels of *Leishmania donovani* promastigotes were measured using HPLC using method reported earlier (*Saudagar et al, 2013; Mukhopadhyay et al., 1996; Bhattacharya et al., 2009*). In brief, 10 ml of *Leishmania* promastigotes (2.5 x 10^6 cells/ml) were taken and treated with hypericin (18 µM) for 12 h or 24 h. These promastigotes were collected and washed twice with phosphate buffer saline (PBS). Equal number of untreated or treated promastigotes (1 X 10^7 cells) were re-suspended in 50 µl of 50 mM HEPES (pH 8.0) containing 5 mM EDTA followed by the addition of 0.1 ml of 2 mM monobromobimane (dissolved in 100% ethanol). The suspension was then incubated at 70°C for 3 minutes. After incubation, 0.2 ml of 25 % ice cold solution of trichloroacetic acid was added to it and incubated on ice for 20 min. Finally, the volume of derivatized lysate was 350 µl. Therefore, the intracellular thiol indicates concentration of the same in cell lysate of 1 x 10^7 *Leishmania* promastigotes diluted to 350 µl in process of derivatization. Cell debris and denatured proteins were separated by centrifugation and acid soluble thiols were separated using HPLC (Dionex Ultimate 3000) on C18 column with linear gradient of 50-100% methanol in 0.25% acetic acid (pH 3.5). The fluorescence of bimane with emission and excitation wavelength of 360 nm and 450 nm, respectively, was used to identify the thiols. The retention time was compared with standard thiols after same treatment. To verify intake of thiol after supplementation, *Leishmania* promastigotes were supplemented with trypanothione (0.5 µM) and treated with hypericin (18 µM) for above mentioned time intervals and thiol levels were estimated using same procedure. Untreated *Leishmania* promastigotes thiol levels were also determined for comparison.

2.3.8 *Intracellular spermidine detection*: *In vivo* spermidine concentration was assessed after hypericin treatment (18 µM). Shortly, 1 ml of *Leishmania* promastigotes (2.5 x 10^6 cells/ml) were taken and treated with hypericin for 12 h and 24 h. Equal numbers of untreated and treated promastigotes (1 X 10^6 cells) were taken to compare the spermidine pool. Promastigotes were washed with PBS and centrifuged to collected cells. Subsequently, promastigotes were lysed in 40 µl phosphate buffer and spermidine level was estimated using methods reported earlier (*Porta et al., 1981; Enomoto et al., 2006*). In brief, lysed promastigotes (40 µl) were used to derivatize polyamines by adding 120 µl of 75 mM dansyl chloride and 40 µl of saturated sodium carbonate. This makes the final volume of the derivatized lysate to 200 µl. Therefore, the spermidine level indicates concentration of the same in cell lysate of 1 x 10^6 *Leishmania* promastigotes diluted to 200 µl in process of derivatization. To verify intake of spermidine as well as change in spermidine pool of the parasite after spermidine (100 µM) or trypanothione (0.5 µM) supplementation followed by hypericin (18 µM) treatment, the *in vivo* spermidine was determined using same procedure in all these conditions. *In vivo* spermidine concentration of untreated promastigotes was also estimated for comparison. Higher concentration of spermidine (100 µM) was used for supplementation as less efficient spermidine transporter is not able to recover decreased spermidine level at low concentration in the time frame used in the study.

2.3.9 *Statistical analysis*: The statistical significance of differences between two groups was analyzed by unpaired Student's t test using SigmaPlot software. Differences were considered significant with p values < 0.05 and < 0.01.

2.4 Results:

2.4.1 *Preparation of recombinant spermidine synthase from Leishmania donovani:* Complete cDNA for Spermidine synthase of *Leishmania donovani* obtained as a clone in pBluescript vector was subcloned in pET-28a(+) vector. Amplified cDNA band of *Ld*SS is shown in figure 2.1A. Figure 2.1B and 2.1C represents the clone confirmation result of *Ld*SS cDNA cloned in pET-28a(+) vector by PCR and restriction digestion, respectively. Double digestion of clone with *NheI* and *BamH1* shows a release of DNA band of size 900 bp confirming the insertion of *Ld*SS cDNA into pET-28a(+) vector. The clone was further confirmed by sequencing using primers for T7 promoter and T7 terminator. This

*Ld*SS clone was transformed into BL21(DE3) expression strain of *E. coli* and protein overexpression was induced using 1mM IPTG at 25 °C for 8 h. The overexpressed recombinant protein was then purified using Ni-NTA affinity chromatography. Purified band of spermidine synthase is shown in Figure 2.1D lane 3.

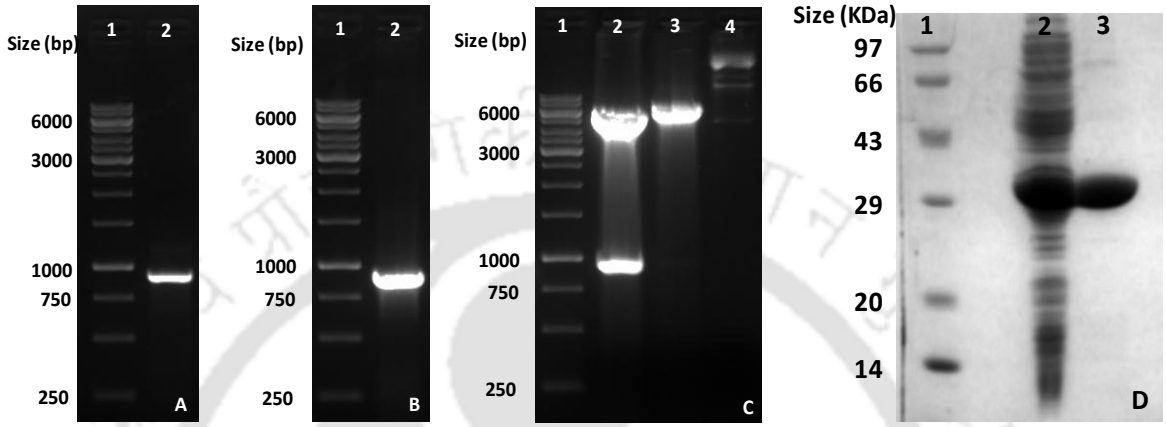

Figure 2.1: Cloning and Overexpression of *Ld*SS in pET28a(+) vector. **(A)** PCR amplification of *Ld*SS cDNA. Lane 1: 1kb DNA ladder, Lane 2: amplified band of *Ld*SS showing size of around 900bp. **(B)** Clone confirmation of *Ld*SS in pET28a(+) vector by PCR. Lane 1: 1Kb ladder, Lane 2: amplified band of size 900 bp from *Ld*SS clone in pET28a(+) vector. **(C)** Clone confirmation of *Ld*SS in pET28a(+) vector by restriction digestion. Lane 1: 1Kb ladder, Lane 2: Restriction digestion of clone with *NheI* & *BamHI* showing release of insert of size 900bp, Lane 3: Restriction digestion of clone with *NheI* only, Lane 4: Undigested *Ld*SS clone in pET28a(+) vector. **(D)** SDS-PAGE analysis of purified *Ld*SS protein. Lane 1: Protein molecular weight marker, Lane 2: crude supernatant**,** Lane 3: purified recombinant *LdSS* protein.

2.4.2 *Hypericin shows in vitro inhibition of spermidine synthase*: In order to find the optimum condition for enzyme assay, the pH (2-12) and temperature (20 °C -90 °C) were varied over a range and the optimal values (pH- 8.0, temperature- 37 °C) found were used for further experiments. The K_m and V_{max} values were also calculated by varying the substrate concentration. The K_m with respect to putrescine (K_m^P) was 1.23 mM and V_{max}^P was 8.85 mM min^{-1} (Figure 2.2A). The K_m and V_{max} with respect to dcSAM, K_m^S and V_{max}^S, was calculated to be 90.34 µM, 97.09 µM min^{-1}, respectively (Figure 2.2B).

Hypericin was found to inhibit spermidine synthase activity. The mode of inhibition was assessed by Lineweaver Burk plot (Figure 2.2). Hypericin shows competitive mode of inhibition with respect to putrescine since there is no change in V_{max} although there is increment in K_m value with respect to control (Figure 2.2A). The inhibitory constant, K_i, with respect putrescine (K_i^P) was calculated to be 201.6 µM. Hypericin shows linear

mixed inhibition with respect to dcSAM which is evident from decrease in V_{max} and increase in K_m values of inhibited enzymatic reaction as compared to uninhibited reaction (Figure 2.2B). The inhibition constant, K_i with respect to dcSAM (K_i^S) was 3.68 µM. (Figure 2.2B).

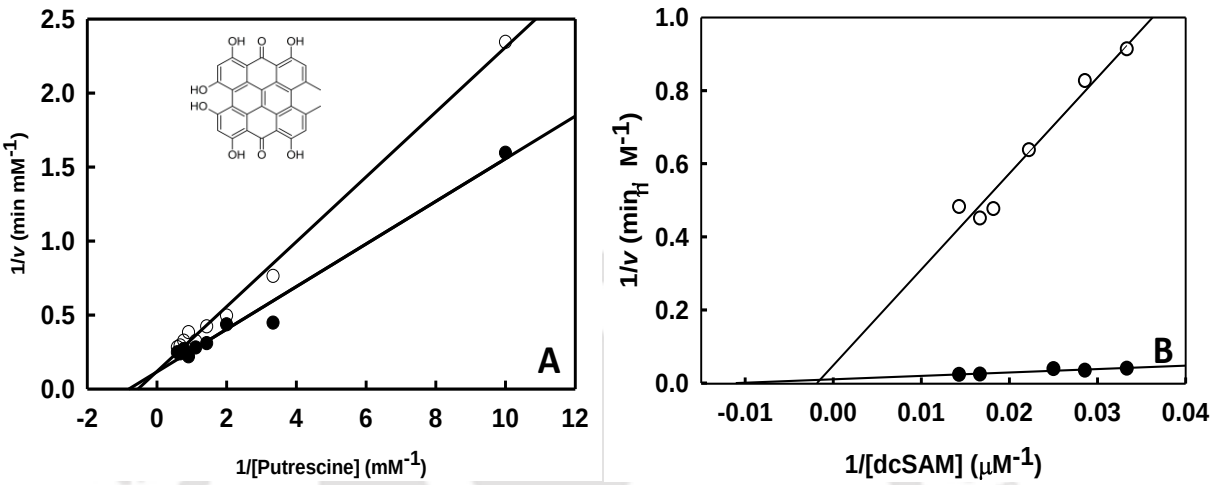

Figure 2.2: Inhibition of spermidine synthase by hypericin at varying concentrations of different substrates (putrescine and dcSAM). **(A)** Hypericin shows competitive inhibition of spermidine synthase with respect to putrescine having K_m^P = 1.23 mM, V_{max}^P = 8.59 mM min^{-1} and K_i^P = 201.6 mM. Inset shows the structure of hypericin **(B)** Hypericin shows linear mixed inhibition of spermidine synthase with respect to dcSAM with K_m^S = 90.9 µM, V_{max}^S = 97.087 µM min^{-1} and K_i^S = 3.68 µM. Solid circles (●) represents Lineweaver Burk plot of enzyme assay without inhibitor and hollow circle (o) represents enzyme assay in presence of inhibitor i.e. hypericin. The data is plotted as an average of three independent experiments.

2.4.3 ***Hypericin shows antileishmanial activity but no effect on macrophage cells*:** Hypericin was assessed to exhibit antileishmanial effect after 24 h treatment of promastigotes (2.5 X 10^6 cells/ml) with varying doses (10 µM - 100 µM). Hypericin was found to display significant antileishmanial activity with IC_{50} of 18 µM (Figure 2.3A). It is the first evaluation of antileishmanial effect of the compound. The novel scaffold may be used for development of future and better antileishmanial compounds of the class. For a molecule to be an effective and potent drug candidate, it is important to have high specificity with least adversity on patients. With this view, hypericin was evaluated to exhibit death of the macrophages, but found to have no significant effect on macrophages even at a concentration 4 times higher than IC_{50} doses (Figure 2.3B). This asserts the high specificity of hypericin towards *Ld*SS.

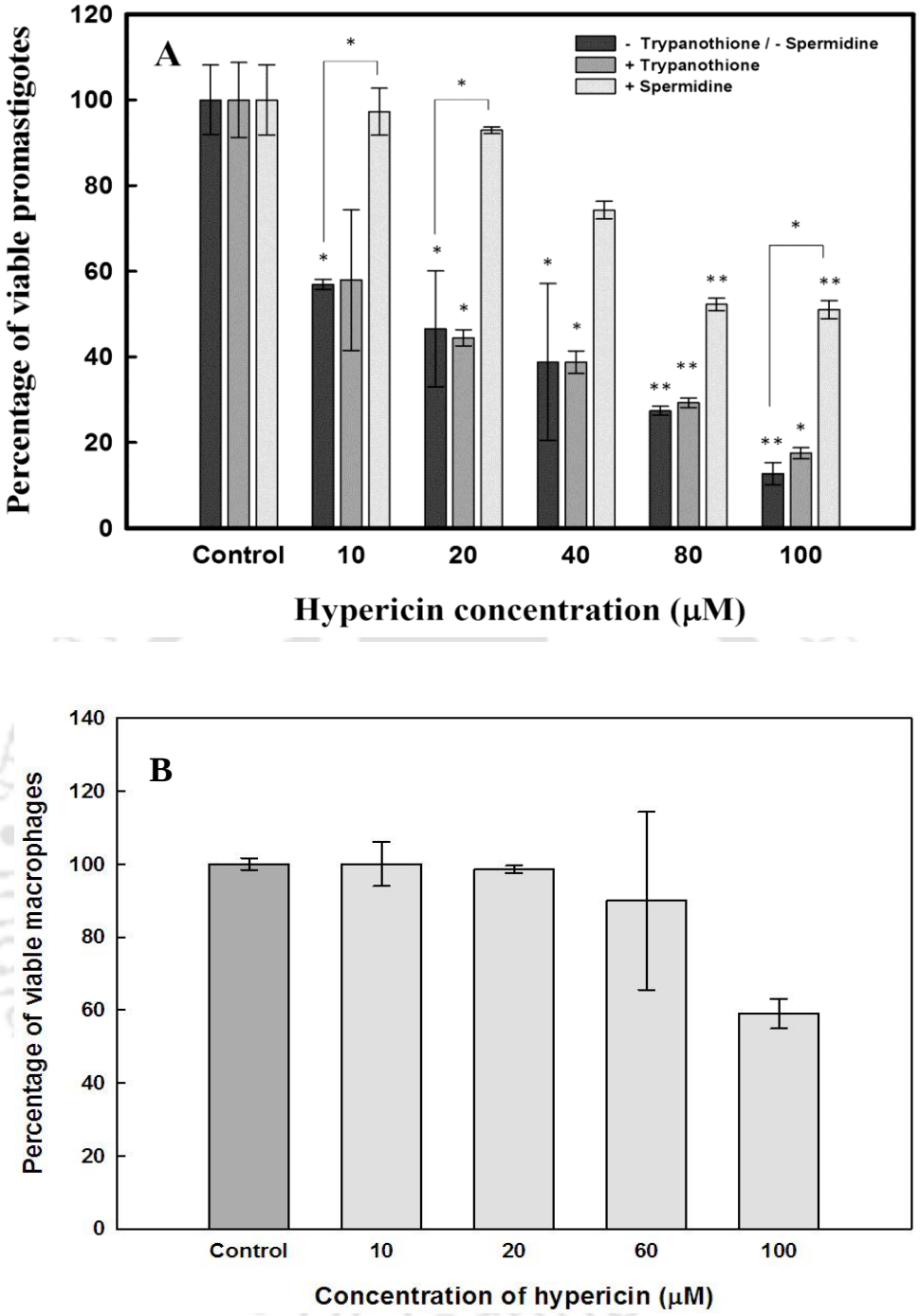

Figure 2.3: Cell viability assay on *Leishmania* promastigotes and macrophages after hypericin treatment (A) Cell viability assay on *Leishmania donovani* promastigotes. *Leishmania* promastigotes (2.5 X 10^6 cells/ml) were taken to check the antileishmanial effect of hypericin. Promastigotes were treated with varying concentrations of hypericin for 24 h and cell viability was checked by using MTT assay. The IC_{50} value obtained for hypericin was 18.00 µM. Promastigotes were also supplemented with trypanothione (0.5 µM) and spermidine (100 µM) and then treated with hypericin. Promastigotes supplemented with trypanothione showed IC_{50} value of 17.42 µM which is comparable to treated promastigotes without any supplementation. However, promastigotes supplemented with spermidine showed survival of ~90% of promastigotes at IC_{50} value of hypericin. Data having *P* values <0.05 (*) and < 0.01 (**) were considered to have statistically significant difference. (B) Cell viability assay on macrophages. Macrophages (2 X 10^6 cells/ml) were taken and treated with varying concentrations of hypericin. Hypericin is found to be not very effective in killing the macrophages even with higher doses.

2.4.4 *Spermidine pool was depleted after treatment with hypericin showing target specificity of inhibitor*: *Leishmania* promastigotes culture (2 ml) with cell density (2.5 X 10^6 cells/ml) was treated with IC_{50} dose (18 µM) of hypericin for 12 h and 24 h. Intracellular spermidine level was checked as described in method section. Hypericin treated promastigotes showed diminished levels of spermidine as compared to untreated promastigotes. The amount of spermidine calculated in untreated promastigotes was 34 ± 1 µM whereas promastigotes treated with hypericin for 12 h and 24 h showed spermidine level of 3 ± 1 µM and 1 ± 0.1 µM, respectively (Table 2.1). Promastigotes were also supplemented with trypanothione (0.5 µM) followed by treatment with hypericin. Trypanothione supplementation did not rescue the spermidine level in promastigotes. Concentration of spermidine after trypanothione supplementation followed by hypericin treatment for 12 h and 24 h were 3 ± 0.5 µM and 2 ± 0.2 µM respectively. Spermidine level in untreated, treated promastigotes and promastigotes treated after trypanothione supplementation is mentioned in Table 2. However, spermidine supplementation resulted in revival of intracellular spermidine pool after 24 h. Spermidine concentration measured in *Leishmania* promastigotes supplemented with spermidine (100 µM) and treated with IC_{50} value of hypericin after 12 h and 24 h was 7 ± 1 µM and 38 ± 8 µM, respectively (Table 2.1).

2.4.5 *Hypericin alters the intracellular thiol level in Leishmania promastigotes*: Since spermidine is conjugated with glutathione to form trypanothione in presence of trypanothione synthetase, so decrease in *in vivo* spermidine level should result in non utilization of glutathione for trypanothione synthesis. This should result in diminished levels of trypanothione and elevated levels of glutathione inside the parasite. So, in order to check the alteration of thiol pool of the parasite after hypericin treatment, *Leishmania* promastigotes culture (10 ml) of cell density 2.5 X 10^6 cells/ml were treated with IC_{50} dose of hypericin for 12 h and 24 h. Intracellular thiol level was measured by derivatizing thiols as explained in method section. The level of trypanothione [$T(SH)_2$] was found to decrease significantly after 12 h and 24 h of treatment as compared to the untreated promastigotes. Trypanothione level in untreated, 12 h and 24 h treated promastigotes are 317 ± 54 µM, 43 ± 2 µM, and 39 ± 9 µM, respectively. This further suggests that low spermidine level due to inhibition of *Ld*SS in hypericin treated promastigotes causes low *in vivo* concentration of trypanothione (Table 2.1). However, a remarkable increase in the intracellular glutathione (GSH) level was contemplated after 12 h and 24 h of treatment in

contrast to the untreated promastigotes. Glutathione level in untreated, 12 h and 24 h treated promastigotes was 206 ± 17 µM, 739 ± 149 µM, and 549 ± 21 µM, respectively. Thiol levels for untreated and treated promastigotes for different time points are summarized in Table 2.2.

Since existence of trypanothione transporter is evident from the literature (*Basselin et al., 2000*), so trypanothione supplementation can provide deep insight to the mode of cell death opted by *Leishmania* promastigotes after hypericin treatment. Supplementing parasite with trypanothione before hypericin treatment should result in reversal of altered thiol levels of the parasite. In order to check the effect of trypanothione on the *in vivo* thiol pool of the parasite, 10 ml culture of *Leishmania donovani* (2.5 X 10^6 cells/ml) was supplemented with 0.5 µM of trypanothione followed by treatment with IC_{50} dose of hypericin for 12 h and 24 h. As compared to unsupplemented promastigotes treated with hypericin, $T(SH)_2$ level was regained after trypanothione supplementation whereas reduction in the level of GSH was observed. $T(SH)_2$ level in promastigotes supplemented with trypanothione and treated with hypericin was 235 ± 88 µM and 478 ± 212 µM for 12 h and 24 h respectively. Intracellular level of GSH in trypanothione supplementation was calculated to be 208 ± 114 µM and 395 ± 123 µM for 12 h and 24 h respectively. Table 2.1 is showing the thiol levels after supplementation with trypanothione.

Table 2.1: Intracellular trypanothione [$T(SH)_2$], glutathione (GSH) and spermidine levels in *Leishmania* promastigotes The intracellular thiol represents concentration of the same in final volume of 350 µl containing cell lysate of 1 x 10^7 *Leishmania* promastigotes. The intracellular spermidine indicates concentration of spermidine in final volume of 200 µl containing cell lysate of 1 x 10^6 *Leishmania* promastigotes. The control shows concentration without any treatment. Other data shows concentration with or without supplementation with treatment of hypericin (18 µM).

<table>
<tr><th colspan="2" rowspan="3">Metabolites</th><th rowspan="3">Control</th><th colspan="4">Hypericin (18 µM)</th></tr>
<tr><th colspan="2">Without supplementation</th><th colspan="2">With trypanothione supplementation</th></tr>
<tr><th>12h</th><th>24 h</th><th>12 h</th><th>24 h</th></tr>
<tr><td rowspan="2">Thiols (µM)</td><td>$T(SH)_2$</td><td>317±54</td><td>43±2</td><td>39±14</td><td>235±88</td><td>478±212</td></tr>
<tr><td>GSH</td><td>206±17</td><td>739±149</td><td>549±21</td><td>208±114</td><td>395±123</td></tr>
<tr><td colspan="2" rowspan="3">Spermidine (µM)</td><td rowspan="3">34±1</td><td rowspan="3">3±1</td><td rowspan="3">1±0.1</td><td>3±0.5</td><td>2±0.2</td></tr>
<tr><td colspan="2">With spermidine supplementation</td></tr>
<tr><td>7±1</td><td>38±8</td></tr>
</table>

2.4.6 ***Trypanothione supplementation was a futile attempt to reduce cell death; however spermidine supplementation displays survival of the parasite*****:** Promastigotes were supplemented with 0.5 µM of trypanothione, and assessed for antileishmanial activity of hypericin. The trypanothione supplementation did not prevent death of the parasite since IC_{50} value was found to be consistent with the one without supplementation (Figure 2.3A). Viability of *Leishmania* promastigotes was also assessed after 100 µM of spermidine supplementation followed by treatment with hypericin. Interestingly, spermidine supplementation has significantly improved parasite survival and ~90% of *Leishmania* promastigotes survived at IC_{50} value of hypericin (Figure 2.3A). The statistical significance of difference of untreated promastigotes were analyzed individually with hypericin treated, trypanothione supplemented, spermidine supplemented promastigotes. Another group used for analysis of statistical significance was hypericin treated & spermidine supplemented promastigotes.

2.4.7 ***Production of reactive oxygen species was triggered in the Leishmania promastigotes after treatment with hypericin*****:** Promastigotes of *Leishmania donovani* were treated with IC_{50} dose of hypericin (18 µM) for varying time periods (1.5 h, 3 h, 6 h, 12 h and 24 h). As compared to untreated *Leishmania* promastigotes, an increase in ROS was observed in 1.5 h post treatment with slight increase after 3 h and maximum at 6 h. However, the lower level of reactive oxygen species was seen in the parasite treated for 24 h (Figure 2.4A). This may be due to membrane damage of the parasite and subsequent leakage of generated ROS in the media. The N-acetylcysteine (NAC), a scavenger of ROS, pretreated promastigotes before hypericin treatment for 6 h, display a significant reduction in the level of reactive oxygen species as compared to the NAC untreated promastigotes. The change in level of reactive oxygen species at different time points is shown in Figure 2.4A.

Trypanothione or spermidine supplementation exhibits reversal of increased ROS pool in promastigotes treated with hypericin: *Leishmania* promastigotes were supplemented with 0.5 µM of trypanothione or 100 µM of spermidine in the media. The supplemented promastigotes were then treated with IC_{50} dose of hypericin for 6 h. The level of ROS reduced significantly after trypanothione or spermidine supplementation as compared to the un-supplemented promastigotes treated with hypericin for same time point. The comparison of ROS level in un-supplemented and supplemented promastigotes is shown in Figure 2.4B.

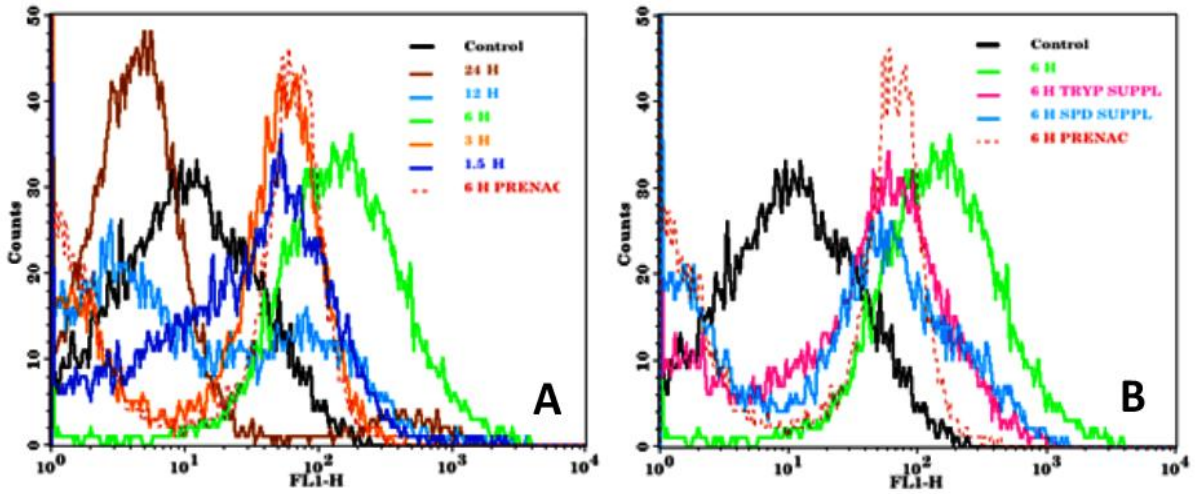

Figure 2.4: Flow cytometric analysis for the production of reactive oxygen species in promastigotes treated with IC_{50} dose of hypericin for varying time points i.e. 1.5 h, 3 h, 6 h, 12 h and 24 h. Untreated sample was taken as control and pretreated samples were given NAC (20 mM) treatment for 30 minutes before treating with IC_{50} dose of hypericin for 6 h. Also, the promastigotes were supplemented with trypanothione (0.5 µM) and spermidine (100 µM) and then treated with IC_{50} dose of hypericin for 6 h. The samples were stained with H_2DCFDA for 45 minutes to 1 h and then analyzed by using flow cytometry. (**A**) Comparison of production of reactive oxygen species in untreated, NAC pretreated, and treated promastigotes for different time points. (**B**) Comparison of production of reactive oxygen species in promastigotes NAC pretreated, un-supplemented, supplemented with trypanothione and spermidine separately followed by treatment with hypericin for 6 h.

2.4.8 ***Hypericin stimulates necrosis like death in parasite*:** In order to check the mode of cell death after hypericin treatment, flow cytometric analysis of *Leishmania donovani* was done after staining with annexin V-FITC and propidium iodide in various conditions. The negative control (promastigotes without any treatment) did not show staining either with annexin V-FITC or propidium iodide. The control for apoptosis with miltefosine (50 □M) treatment showed both annexin V-FITC and propidium iodide binding indicating apoptosis. *Leishmania donovani* promastigotes treated with IC_{50} dose of hypericin for 6 h and 24 h were not stained with annexin V-FITC but showed positive staining for PI, indicating that promastigotes after hypericin treatment are opting for necrosis like death. NAC pretreatment before hypericin treatment did not prevent necrotic death (Figure 2.5).

Leishmania donovani promastigotes supplemented with 0.5 µM of trypanothione in the media were treated with IC_{50} dose of hypericin for 6 h and 24 h. Flow cytometric assessment reveals that the trypanothione could not prevent parasite death and the percentages of promastigotes undergoing necrosis like death after trypanothione supplementation were comparable to the promastigotes without supplementation for

respective time points (Figure 2.5). Interestingly, spermidine (100 µM) supplementation in the media before hypericin treatment prevented parasite death to large extent. Promastigotes supplemented with spermidine showed survival of ~90% of promastigotes at IC_{50} value of hypericin. However, at many fold higher IC_{50} value of hypericin growth inhibition was restored only 50-60 %, suggesting some off-target effects of hypericin at higher concentration.

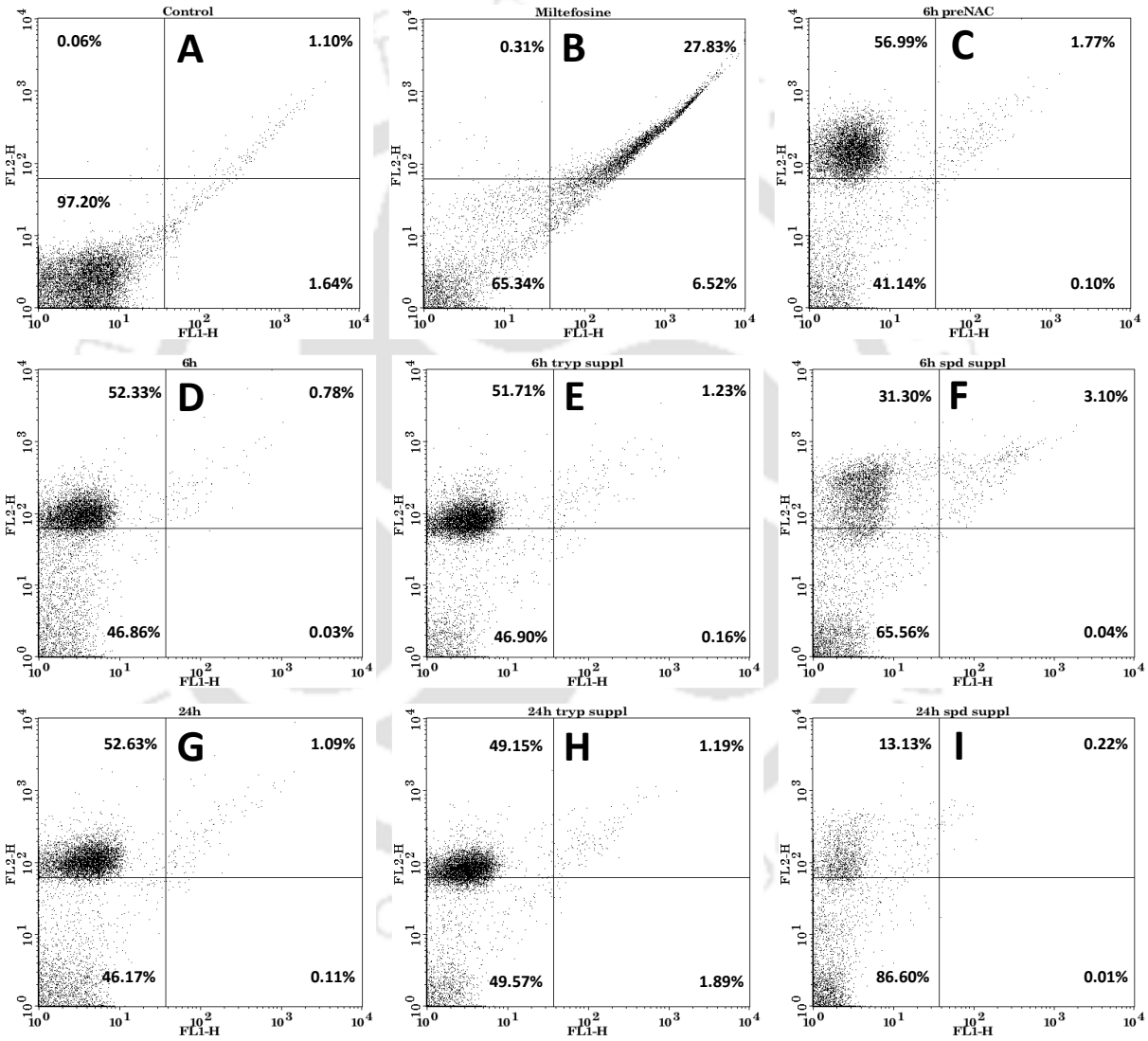

Figure 2.5: Analysis of mode of cell death of *Leishmania* promastigotes. Promastigotes (A) without any treatment (B) treated with miltefosine (50 µM) for 24 h (C) N-acetylcysteine (20 mM) pretreated before hypericin (18 µM) treatment for 6 h. (D) treated with hypericin (18 µM) for 6 h (G) treated with hypericin (18 µM) for 24 h (E) Promastigotes supplemented with trypanothione (0.5 µM) before hypericin (18 µM) treatment for 6 h and (H) 24 h. (F) Promastigotes supplemented with spermidine (100 µM) before hypericin (18 µM) treatment for 6 h and (I) 24 h. Samples were stained with annexin V-FITC and propidium iodide and analyzed by using flow cytometry. Promastigotes are shown to undergo necrosis after treatment with hypericin.

2.5 Discussion:

Inhibiting key redox metabolism enzymes has been a good approach towards discovering new drug candidate against leishmaniasis. Here, we have shown the adverse effects of inhibition of one such enzyme, spermidine synthase, on the survival of the *Leishmania*. Hypericin is a naturally occurring anthraquinone derivative obtained from *Hypericum perforatum* (*Basselin et el., 2000*). We have identified it as a strong inhibitor of spermidine synthase of *Leishmania donovani* using computational approach. This *in silico* analysis was supported by biochemical assessment which also affirms the inhibition of spermidine synthase by hypericin. Further, the effects of hypericin were examined on *Leishmania donovani* promastigotes, since promastigotes are the infective stage of *Leishmania*. Antileishmanial assay with hypericin suggests that it inhibits the survival of the parasite. Interestingly, target specificity of hypericin was evident from insignificant toxicity of hypericin towards macrophages and decrease in spermidine pool of the parasite after hypericin treatment.

Spermidine together with glutathione form trypanothione in presence of trypanothione synthetase. Trypanothione is indispensable for maintaining the redox metabolism and hence is crucial for the survival of the parasite (*Krauth-Siegel RL and Comini, 2008; Kubin et al., 2005*). Since trypanothione synthesis is directly related to the presence of spermidine, so inhibition of spermidine synthesis should result in decreased levels of trypanothione and increased glutathione inside the parasite leading to the redox imbalance and ultimate death of the parasite. The *in vivo* trypanothione estimation also shows decreased level of trypanothione after hypericin treatment. This alteration in thiol pool of the parasite after hypericin treatment was reverted back with trypanothione supplementation. Elevated ROS was observed in the parasite treated with hypericin which could be assigned to decreased trypanothione level of parasite. If the ROS generation is because of decreased trypanothione level after hypericin treatment, supplementing the promastigotes with excess of trypanothione should revert back the effects caused by oxidative stress inside the *Leishmania*. We have observed that supplementation with trypanothione has resulted in reduced levels of reactive oxygen species produced after hypericin treatment. However, trypanothione supplementation does not increase the survival of the parasite suggesting that oxidative stress produced due to decrease in trypanothione was not a cause of parasitic death. Moreover, the cell death due to reactive oxygen species is directed through apoptotic pathway (*Krauth-*

Siegel and Leroux, 2012). Our result displays necrotic like death of the parasite after treatment with hypericin. This reasserts that ROS generated due to trypanothione depletion was insufficient to kill the parasite. Further, the specificity of hypericin was also assessed by measuring the intracellular thiol and spermidine pool of the parasite.

Supplementation of spermidine in media recovered the survival of the parasite after hypericin treatment affirming that death of the parasite is solely dependent on the spermidine starvation due to hypericin. Overall we have analyzed that although hypericin specifically target spermidine synthase (a redox metabolism enzyme); the death of the parasite due to spermidine starvation is not related to redox imbalance inside the parasite. This suggests the involvement of spermidine in pathway other than redox metabolism thereby opening door for the novel investigation of correlation of spermidine with its potential interacting molecules.

Promastigotes and axenic amastigotes are capable of transporting spermidine (*Simon et al., 2000*). The question of polyamine salvage by parasites in infected macrophages is certainly crucial for the validation of the *Ld*SS as therapeutic targets. However, when mice were infected with a spermidine synthase knockout strain, infectivity was significantly reduced compared to wild type parasites (*Gilroy et al., 2011*). This suggests that although parasites are able to transport spermidine, there is not enough spermidine present in the phagolysosome for salvage.

Overall, the results suggest hypericin as a potent antileishmanial molecule that inhibits *Ld*SS resulting in spermidine starvation. As there is no effect on macrophage cells even at 4 times of IC_{50} values, the effect of hypericin seems to be specific to *Leishmania*. The data indicates that a cellular process other than trypanothione production may be affected by spermidine depletion. Spermidine is essential in all tested eukaryotes for the hypusine modification of the translation factor eIF5A, the only known essential function of spermidine in all eukaryotes. In fact, the enzyme that transfers the aminobutyl group from spermidine to eIF5A to form deoxyhypusine (deoxyhypusine synthase) is an essential enzyme in *Leishmania donovani* (*Chawla et al., 2010*) and, as mentioned, in all tested eukaryotes. The hypusine modified eIF5A translation factor is required for translation of mRNAs encoding proteins containing polyproline tracts (*Gutierrez et al., 2013*). It is not surprising therefore, that the depletion of spermidine leads to parasitic death via altered hypusine modification of the translation factor eIF5A. However, further studies required to confirm the hypothesis. Our study also suggests that spermidine is crucial for the

survival of parasite and this cruciality is not only linked with the involvement of spermidine in redox metabolism but also its importance in processes critical for the parasite survival. The previous reports hit toward suitability of hypericin for therapeutic uses (*Basselin et al., 2000*). Taken together, the work provides fundamental insights into molecular mechanism of antileishmanial effect of hypericin that may be used for development of novel drug against this neglected topical disease.

CHAPTER III

Molecular Events Leading to Death of *Leishmania donovani* Under Spermidine Starvation*

3.1 Abstract:

Role of spermidine in *Leishmania donovani* is explored under spermidine starvation by treatment of hypericin, an inhibitor of spermidine synthase. Quantitative gene expression analysis has shown altered expression of several genes involved in redox metabolism, hypusine modification of eIF5A, DNA repair pathway and autophagy. Further, spermidine starvation has resulted in significant defect in translation initiation but very less alteration in translation elongation of the parasite. Western blot analysis revealed decrease in hypusine modification which has reverted back with spermidine but not with trypanothione supplementation. Hypericin treatment has revealed ROS induced increase in HAT expression and decreased SIR2RP expression which has reverted back by trypanothione or spermidine supplementation. Hypericin induces autophagy via AMPK activation in response to ROS induced DNA damage. This was further confirmed by increased intracellular ATP pool of the parasite after hypericin treatment which was reverted back by trypanothione or spermidine supplementation and 3-methyladenine pretreatment. This suggests that autophagy induces ATP surge as a cytoprotective mechanism towards ROS induced DNA lesions. Overall, the data suggests that the death of the parasite is mainly due to translational defects induced by lowered hypusine modification due to spermidine starvation.

**Part of the work is submitted for publication*

3.2 Introduction:

Spermidine has been known for its various functions in several eukaryotes. Spermidine has been reported to be involved in hypusination of translation initiation factor eIF5A in some organisms including *Saccharomyces cerevisiae* (*Wolff et. al., 1989*). Hypusination of translation initiation factor, eIF5A, has been proved essential for the survival of *Saccharomyces cerevisiae* (*Schnier et. al., 1991*). The presence of a hypusine pathway has been elucidated in *Leishmania donovani* (*Chawla* et. al., *2012*). However, it remains unclear if spermidine also have role in hypusination of translation initiation factor eIF5A of protozoan parasite *Leishmania.*

Autophagy is considered a programmed cell death which involves the formation of autophagosomes, double membrane vesicles. Autophagy is generally triggered during starvation conditions (*Eisenberg et al, 2009*). Spermidine has shown to induce autophagy in *Saccharomyces cerevisiae*, *Caenorhabditis elegans* and *Drosophila melanogaster (Madeo et al., 2010).* The induction in autophagy has been reported to be induced by deacetylation of histone H3. This deacetylation was trigerred through inhibition of histone acetyl transferase (HAT), thereby increasing longevity by suppressing oxidative stress and necrosis (*Eisenberg et al, 2009*). Nutrient restrictions have found to show anti-ageing effects in several organisms ranging from yeast to primates. This anti-ageing effect is modulated by inhibition of TOR (Target of rapamycin) kinases of TOR signalling pathway. TOR signalling pathway inhibits autophagy, so repressing TOR signalling should increase the longevity in a similar fashion as spermidine by inducing autophagy. However, the role of spermidine as mimetic to nutrient restrictions has not been explored yet (*Kaerberlein, 2009*). Kinases like AMPK (AMP- activated protein kinase) are also one among the prominent regulators of autophagy (*Morselli et al, 2009*). Interestingly, most of the studies about relationship of autophagy and spermidine have not considered effect of spermidine starvation.

Our previous studies have shown that inhibition of spermidine synthase by hypericin results in spermidine starvation, subsequent decrease in trypanothione level, generation of ROS and parasitic death. It is worth mentioning that spermidine required for synthesis of trypanothione, a key redox molecule of *Leishmania* (*Krauth-Siegel and Comini, 2008*). Further, we have observed that spermidine supplementation but not trypanothione supplementation is able to revival the death of the parasite after hypericin treatment indicating that the generated ROS is not primary cause of parasitic death. The study

related to inhibition of spermidine synthase of *Leishmania donovani* has highlighted the putative role of spermidine in processes other than redox metabolism of *Leishmania donovani* (*Singh et al., 2015*). Additionally, hypericin treatment and subsequent spermidine starvation shows parasitic death with some necrotic feature (*Singh et al., 2015*). In the current report we have further investigated mode of death and other biochemical effect on *Leishmania* parasite under spermidine starvation. Furthermore, ROS generated after hypericin treatment may cause oxidative damage to the DNA. We investigated response of *Leishmania* parasite with respect to regulation of genes involved in DNA repair pathway as an attempt by parasite to heal the damaged DNA.

Mode of cell death in protozoan parasites like *Leishmania* is a matter of controversy. There are several reports about regulated cell death pathways. However, a recent opinion by Proto et al suggest cell death pathways in protozoan parasite as incidental death with mixed features of regulated and unregulated death (*Proto et al., 2013*). In the current studies, we have checked cell death pathways of *Leishmania* under effect of spermidine starvation. The data indicates that the cell death of *Leishmania* in spermidine starvation condition has mixed features of necrosis and autophagy. Further effect on hypusine modification of eIF5A translation initiation factor and expression of DNA repair pathways genes under spermidine starvation after hypericin treatment provided fundamental insights into role of spermidine in *Leishmania* biochemistry.

3.3 Materials and Methods:

3.3.1 *Chemicals and cell lines*: *Leishmania donovani* (MHOM/IN/2010/BHU1081) strain was gifted by Prof. Shyam Sundar, Banaras Hindu University, India. Hypericin, 3-methyl adenine, monodansylcadaverine, propidium iodide etc. were procured from Sigma Aldrich. ATP determination kit and power sybr green PCR master mix were obtained from Life Technologies. AMV first strand cDNA synthesis kit and DNase I were purchased from New England Biolabs. RNeasy Mini Kit was obtained from Qiagen.

3.3.2 *Treatment and supplementation of Leishmania promastigotes*: *Leishmania* promastigotes ($1X10^6$ cells/ml) were treated with 18 µM of hypericin for 24 h. The concentration of hypericin used is IC_{50} against *Leishmania* promastigote on same strain (*Singh et al., 2015*). For the supplementation studies, *Leishmania* promastigotes were supplemented with 0.5 µM of trypanothione and 100 µM of spermidine, respectively, for

1 hr followed by treatment with 18 µM of hypericin for 24 h as reported in our previous studies (*Singh et. al., 2015*). For autophagy assay, *Leishmania* promastigotes ($1X10^6$ cells/ml) were also treated with 10 mM 3-methyl adenine, an autophagy inhibitor (*Seglen and Gordon, 1982; McFarland et al., 2012*) for 2 h followed by treatment with hypericin (18 µM) for 24 h.

3.3.3 *RNA extraction and cDNA synthesis*: *Leishmania* promastigotes with cell density of $1X10^6$ cells/ml were taken and total RNA was extracted using RNeasy mini kit from Qiagen using manufacturer's instruction and procedure reported earlier (*Tavares et al., 2011*). Total RNA extracted was quantified using nanodrop. cDNA was synthesized using AMV first strand synthesis kit from New England Biolabs using manufacturer's instructions. For cDNA synthesis, 500 µg RNA from each sample was taken. Reaction mixture was prepared by adding 2 µl of random primers and nuclease free water was added to make up the final volume to 8 µl. This reaction mixture was heated at 70 ºC for 5 min to denature RNA. After this, PCR tube was spin briefly and placed promptly on ice. To each tube 10 µl of AMV reaction mix and 2 µl of AMV enzyme mix were added. The cDNA synthesis reaction was then incubated at 25 ºC for 5 min followed by incubation at 42 ºC for 1 h. Further, enzyme was inactivated by incubating the reaction at 80 ºC for 5 min. Finally, each reaction was diluted to 50 µl by adding 30 µl of nuclease free water (*Liao and Gong, 1997*).

3.3.4 *Quantitative real time polymerase chain reaction*: For quantitative analysis of gene expression, the real time polymerase chain reaction was carried out using power sybr green. PCR was carried out using 0.5 pmoles of gene specific forward and reverse primers, equal volume of cDNA for each reaction dissolved in 1X power sybr green reaction mixture. Real time monitoring was done using applied biosystems 7500 real-time pcr system. All quantitative assays were performed with housekeeping alpha-tubulin and dihydrofolate reductase gene as endogenous controls as reported in literature (*Carter et al., 2006*).

3.3.5 *Polysome profiling and mRNA extraction from polysomes*: *Leishmania* promastigotes ($2X10^6$ cells/ml) were treated with hypericin for 24 h. Untreated promastigotes were taken as control. To check defects in translation initiation, promastigotes were treated with 100 µg/ml of cycloheximide for 10 min to block the translation elongation and termination (*Cloutier et. al., 2012*). Defects in translation elongation were checked in absence of cycloheximide. Further, promastigotes were

harvested by centrifugation and washed twice with phosphate buffer saline (PBS). Promastigotes were then re-suspended in lysis buffer (10 mM Tris-HCl, 150 mM NaCl, 10 mM $MgCl_2$, 1mM DTT, 100 µg/ml cycloheximide (only for monitoring translation initiation defects), 15 µl/ml protease cocktail inhibitor, pH 7.4) and lysed using sonication (cycle of 2 sec ON & 5 sec OFF). Lysate was then centrifuged at 13,000 rpm for 20 min to remove cell debris. Absorbance of lysate was measured at 260 nm and equal optical density of treated and untreated promastigotes were loaded on sucrose gradient (15% - 45%) prepared in gradient buffer (50 mM Tris-HCl, 50 mM KCl, 10 mM $MgCl_2$, 1mM DTT, pH 7.4). Ultracentrifugation was then performed at 35,000 rpm for 2 h. After centrifugation, the fractions were manually collected from the top of the ultracentrifuge tube and absorbance of each fraction was measured at 254 nm (*Cloutier et. al., 2012*). Polysome to monosome ratio was calculated by calculating area under the curve for polysomes and 80S ribosomes. RNA from polysomes was extracted using trizol method (*Rio et al., 2010*). Briefly, polysome fractions were dissolved in trizol followed by addition of 0.2 ml chloroform per ml of trizol reagent. Mixture was vortexed vigorously for 15 sec and incubated at room temperature for 2-3 min. It was further centrifuged at 12,000xg at 4 ºC for 15 min. Upper aqueous phase was transferred into fresh microcentrifuge tubes and RNA was precipitated by mixing 0.5 ml isopropanol per ml of trizol reagent. Samples were incubated at 25 ºC for 10 min and centrifuged at 12,000xg for 10 min at 4 ºC *(Rio et al., 2010*). Precipitated RNA was further purified using Qiagen RNeasy mini kit.

3.3.6 *Western blot analysis*: *Leishmania* promastigotes treated with IC_{50} dose of hypericin (18 µM) for 24 h, supplemented with trypanothione or spermidine and then treated with hypericin for 24 h and without any treatment were used for western blot analysis. After treatment, promastigotes were harvested and washed four times with cold PBS. Promastigotes were then lysed using sonication in lysis buffer (10 mM Tris-HCl, 150 mM NaCl, 10 mM $MgCl_2$, 1mM DTT, 15 µl/ml protease cocktail inhibitor, pH 7.4). After lysis, cell debris was removed by centrifugation at 12,000 rpm for 20 min at 4 ºC. Supernatant was collected and total protein concentration was estimated using Bradford method (*Bradford, 1976*). Equal amount of protein (250 µg) from cell lysate of untreated and treated promastigotes were separated on SDS PAGE gel (12 % running and 5 % stacking) and transferred on polyvinylidene fluoride membrane. After transfer, the membrane was incubated with antibodies against alphatubulin (Thermo Scientific) and

hypusine (Merck Millipore) followed by immunodetection using ECL chemiluminescent substrate for horse radish peroxidase. Here, anti-alphatubulin was taken as loading control (*Mahmood and Yang, 2012*).

3.3.7 *NAD^+ estimation*: *Leishmania* promastigotes were lysed using sonication in lysis buffer. Total protein concentration of cell lysate was determined. Cell lysate containing equal amount of protein each from untreated, hypericin (18 µM) treated, hypericin (18 µM) treated with trypanothione or spermidine supplemented promastigotes were processed for pyridine extraction. Equal volume of Phenol:Chloroform:Isoamyl (25:24:1) was added to each lysate. It was further mixed vigorously and centrifuged at 12,000 rpm for 10 min. Aqueous phase was collected and an equal volume of chloroform was added to it. Solution was again centrifuged at 12,000 rpm for 10 min. Upper aqueous phase containing pyridines was collected in fresh microcentrifuge tubes. The extract contains both oxidized and reduced forms (NAD^+/NADH). Oxidized form (NAD^+) is stable in acidic conditions whereas reduced form (NADH) is stable in alkaline condition. So, to degrade the reduced form of pyridine nucleotides we have exploited the difference in the stability of oxidized and reduced forms. Reduced form of pyridine nucleotides (NADH) was degraded by adding 2 µl of 0.1 M HCl to 18 µl of pyridine extract. The extract was incubated at 65 ºC for 30 min. After incubation, the solution was neutralized before performing recycling assay by adding 2 µl of 0.1 M NaOH. The reaction mixture for NAD^+ assay contains 0.1 M HEPES, 0.6 M ethanol, 50 mM EDTA, 2 mM PES (phenazine ehtosulpahte) and 0.5 mM MTT ((3-(4,5-Dimethylthiazol-2-yl)-2,5-Diphenyltetrazolium Bromide)). Equal volume of extract was added for each untreated, treated and supplemented samples. Reaction was started by adding alcohol dehydrogenase to a final concentration of 0.2 mg/ml. NAD^+ standard curve was plotted by taking varying concentrations of NAD^+ ranging from 1 nM to 400 nM. The absorbance was taken at 570 nm (*Zhu and Rand, 2012*).

3.3.8 *Staining with monodansylcadaverine*: Presence of autophagic vacuoles was detected by treating *Leishmania* promastigotes with monodansylcadaverine. All studies related to cellular staining for autophagy was done after 12 h incubation with IC_{50} value of hypericin as 24 h treatment shows lower fluorescence possibly due to 50% death of parasite. *Leishmania* promastigotes were washed four times and re-suspended in cold PBS (pH 7.4). Monodansylcadaverine (MDC) was added to the promastigotes at a final concentration of 0.05 mM followed by incubation at 37 °C for 10 min. After incubation,

promastigotes were washed with cold PBS (pH 7.4) excitation wavelength of 360 nm and emission wavelength of 525 nm using GE Healthcare delta vision elite deconvolution microscope (*Bera et. al., 2003*).

3.3.9 *Staining with acridine orange*: *Leishmania* promastigotes ($1X10^6$ cells/ml) were washed twice with PBS (pH 7.4). Acridine orange was added to the promastigotes at a final concentration of 1 µg/ml. Promastigotes were then incubated at 25 °C for 15 min. Further, promastigotes were washed with PBS (pH 7.4) and analyzed using BD FACSCalibur flow cytometer (*Wang et. al., 2008).* Flow cytometeric analysis was done using 488nm laser. The two detectors used for analysis are FL1 (530/30) and FL2 (585/42).

3.3.10 *Transfection and localization of GFP-ATG8*: Vector pGL1686 (gift from Dr. Jeremy Mottram, University of Glasgow, Glasgow) containing GFP-ATG8 of *Leishmania major* was transfected in promastigotes of *Leishmania donovani* using low voltage electroporation method. Transfected promastigotes were selected on 25 µg/ml of G418 (*Williams et al., 2012*). These transfected promastigotes were then treated with IC_{50} dose of hypericin (18 µM) for 12 h and analyzed for localization of ATG8 using confocal laser scanning microscope with excitation and emission wavelength of 488 and 525 nm respectively. Similar experiment was performed after hypericin treatment in trypanothione or spermidine supplemented promastigotes. As mentioned earlier also, all studies related to cellular staining for autophagy were done after 12 h incubation with IC_{50} value of hypericin as 24 h treatment shows lower fluorescence possibly due to 50% death of parasite.

3.3.11 *ATP determination*: ATP estimation was done by using ATP determination kit provided by Life Technologies using manufacturer's instructions and procedure available in literature (*Leach, 1981*). Briefly, standard reaction solution was made by adding 0.1mM DTT, 0.5 mM D-luciferin and 0.25 µg firefly luciferase to 1X reaction buffer. The tube was gently inverted to mix. Varying concentration of ATP (5 pmoles to 50 pmoles) was used as standard. *Leishmania* promastigote culture (1 ml) with cell density of $1X10^6$ cells/ml was harvested and washed with PBS (pH 7.4). Equal number of promastigotes were taken for all reactions containing untreated, treated, trypanothione or spermidine supplemented and 3-methyladenine pretreated promastigotes. After washing, the promastigotes were re-suspended in 10 µl of PBS and added in a microtitre well.

Standard reaction solution was then added to it and luminescence was monitored at emission wavelength of 560 nm (*Leach, 1981*).

3.4 Results:

3.4.1 *Change in expression of gene after hypericin treatment*: Spermidine starvation of *Leishmania donovani* by hypericin treatment generated reactive oxygen species (ROS). However, detailed experimental analysis hits towards parasitic death due to other possible role of spermidine in the parasite (*Singh et al., 2015*). In order to evaluate other possible roles of spermidine and also to get insight into response of parasite against developed ROS, we have checked the differential expression of several genes after hypericin treatment. Quantitative gene expression analysis after hypericin treatment has revealed altered levels of expression of genes related to autophagy, hypusination, DNA repair and redox metabolism (Figure 3.1, Figure 3.2, Figure 3.3, Figure 3.4, Figure 3.5 and Figure 3.6). We have observed that, most of the genes involved in autophagy, hypusination pathway and redox metabolism are being altered after hypericin treatment. Further, there was increased expression of 5'-AMP-activated protein kinase (AMPK), which induces autophagy by inhibiting mTOR signalling (*Kim et al, 2011*). In line with this, we have also observed decreased expression of kinases involved in mTOR signalling such as phosphatidylinositol 3-kinase (tor2)-like protein (TOR2) and phosphatidylinositol 3-kinase-like protein (TOR3). The results also show decreased expression of genes involved in hypusine modification of eIF5A such as deoxyhypusine hydroxylase (DOHH) and deoxyhypusine synthase (DHS).

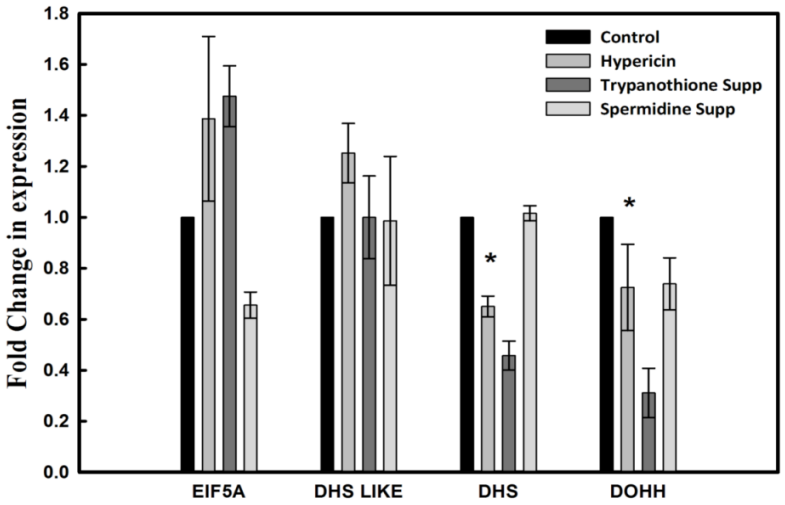

Figure 3.1: Quantitative gene expression profiling of genes related to hypusination of eIF5A. DOHH: Deoxyhypusine hydroxylase; EIF5A: Eukaryotic initiation factor 5A (eIF5A); DHS LIKE: Deoxyhypusine synthase like; DHS: Deoxyhypusine synthase. Here, * represents P value ≤0.05 respectively.

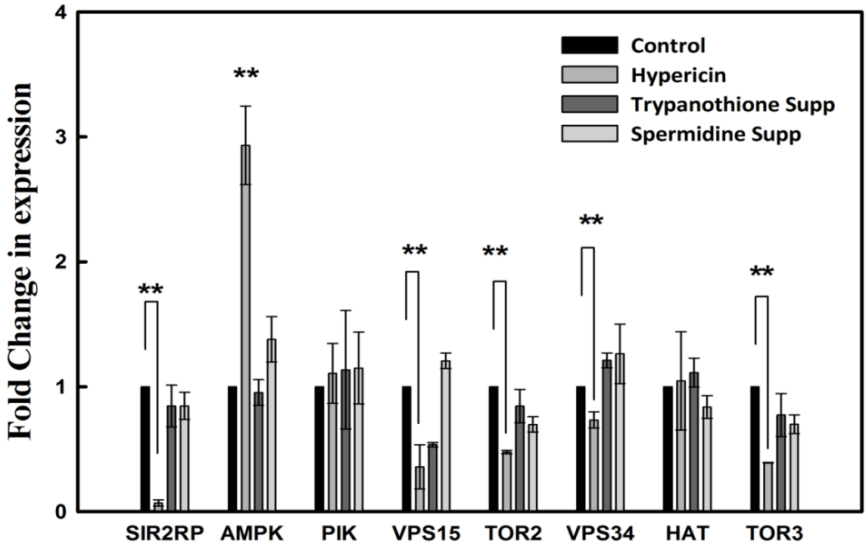

Figure 3.2: Quantitative gene expression profiling of genes responsible for autophagy induction, histone acetyltransferase and histone deacetylase. SIR2RP: NAD-dependent histone deacetylase SIR2; AMPK: 5'-AMP-activated protein kinase; PIK: phosphatidylinositol 3 kinase, putative; VPS15: phosphoinositide-3-kinase, regulatory subunit 4; VPS34: phosphatidylinositol 3-kinase; TOR2: phosphatidylinositol 3-kinase (tor2)-like protein; HAT: Histone acetyltransferase; TOR3: phosphatidylinositol 3-kinase-like protein. Here, ** represents P value ≤0.005 respectively.

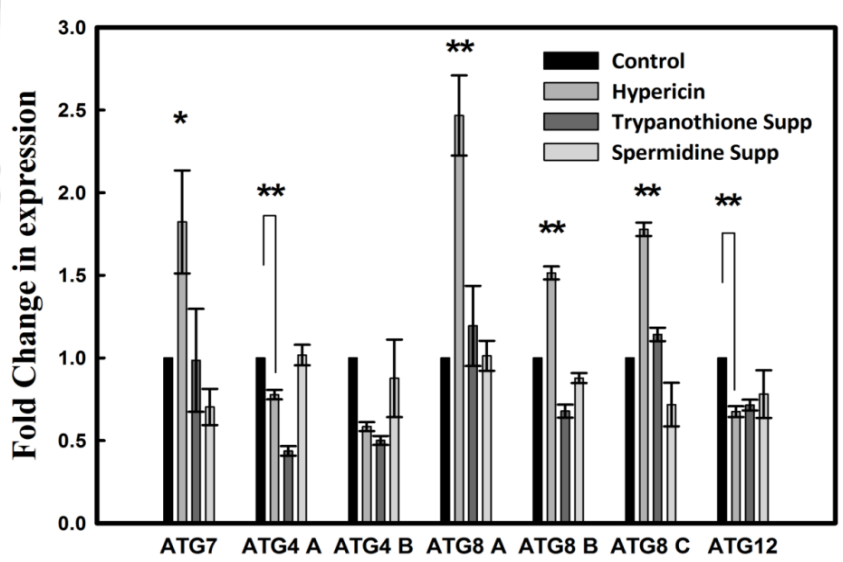

Figure 3.3: Quantitative gene expression profile of genes related to autophagic vacuole formation. ATG7: ubiquitin-like modifier-activating enzyme; ATG4 A: ATG4- Ld300270; ATG4 B: ATG4 - Ld324040; ATG8 A: ATG8 LD190840; ATG8 B: ATG8 LD191660; ATG8 C: ATG8 LD190850; ATG12: LD221120. Here, * and ** represents P value ≤0.05 and ≤0.005 respectively.

List of primers used in this study is mentioned in Table 3.1. Our previous work has shown the generation of ROS in *Leishmania donovani* after hypericin treatment. ROS generation causes oxidative DNA damage (*Cooke et al., 2003*). We have also checked the change in expression of genes involve in DNA repair machinery. Majority of the genes involved in DNA repair pathway are being up-regulated with few being down-regulated and other remaining unaffected after hypericin treatment. Altered levels of expression of autophagy, DNA repair and redox metabolism related genes was reverted back by trypanothione or spermidine supplementation. However hypericin induced alteration in expression of genes involved in hypusination was gained back by spermidine supplementation and not by trypanothione supplementation. Further, we have also checked alteration in histone acetylase (HAT) and type III histone deacetylase *i.e.* SIR2RP of *Leishmania donovani*. Expression of HAT was found to be increased whereas SIR2RP expression was decreased after hypericin treatment. Altered levels of HAT and SIR2RP were reverted back by either trypanothione or spermidine supplementation. Statistical significance of difference was calculated between untreated and hypericin treated *Leishmania* promastigotes individually for each gene.

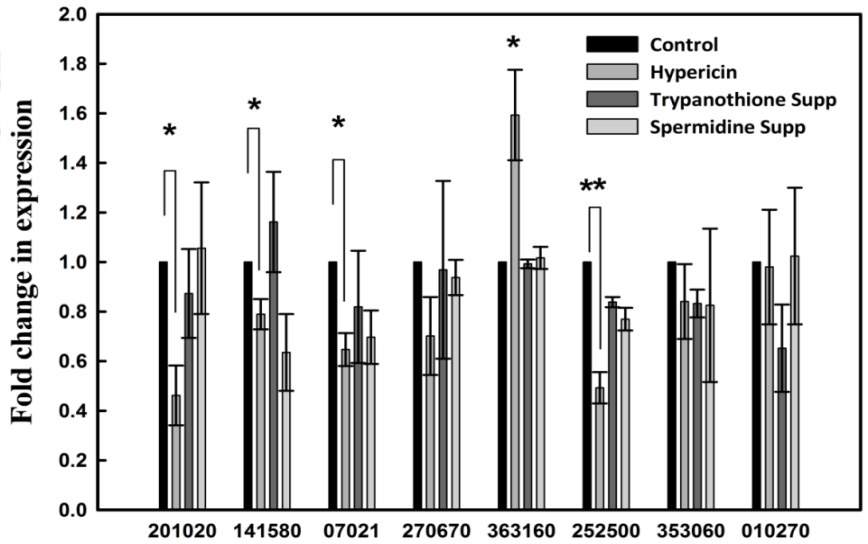

Figure 3.4: Quantitative gene expression profile of gene related to redox metabolism of *Leishmania donovani*. 201020: Glutaredoxin putative; 141580: Glutathione – S-transferase/ Glutaredoxin putative; 07021: Cytochrome c1 heme protein; 270670: Glutaredoxin like protein; 363160: Glutathione peroxidase putative; 252500: Glutathionyl spermidine synthase; 353060; Glyoxylase I trypanothione-dependent glyoxylase I; 010270: Tryparedoxin putative. Here, * and ** represents P value ≤0.05 and ≤0.005 respectively.

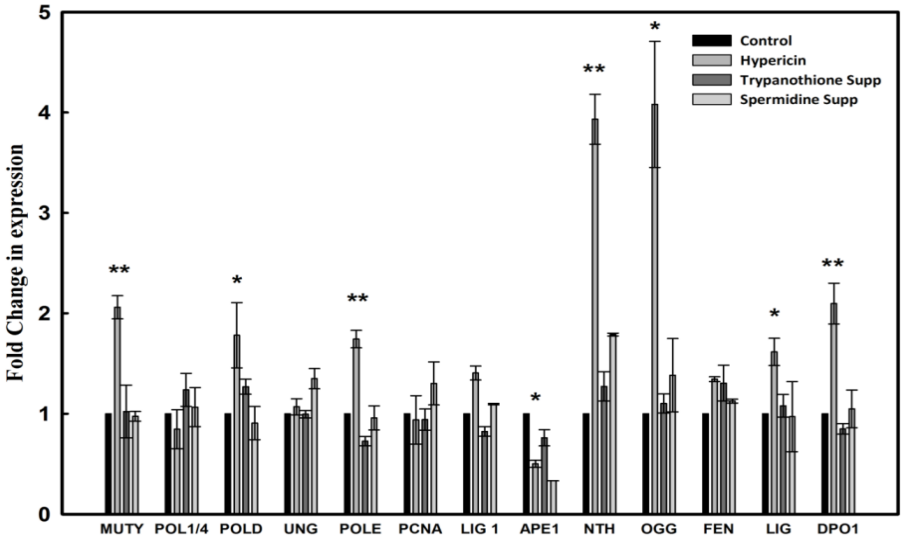

Figure 3.5: Quantitative gene expression profile of genes related to DNA repair pathway. NTH: endonuclease III, APE1: putative; apurinic/apyrimidinic endonuclease-redox protein; DPO1: mitochondrial DNA polymerase I protein B, putative; POL1/4: mitochondrial DNA polymerase beta; LIG: DNA ligase, putative; UNG: uracil-DNA-glycosylase, putative; MUTY: A/G-specific adenine glycosylase, putative; PCNA: proliferative cell nuclear antigen, putative; POLD: DNA polymerase delta subunit 2, putative; POLE: DNA polymerase epsilon subunit b; FEN1: flap endonuclease-1; LIG1: DNA ligase I; OGG: 8-oxoguanine DNA glycosylase, putative. Here, * and ** represents P value ≤0.05 and ≤0.005 respectively.

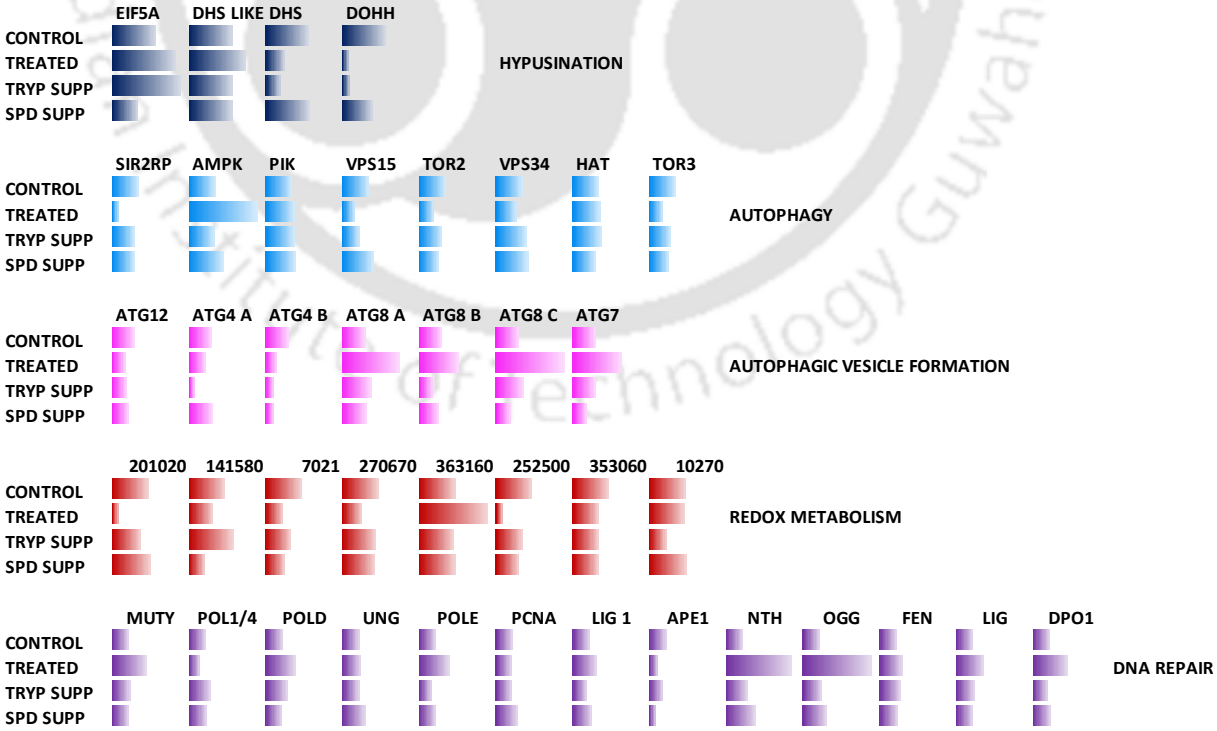

Figure 3.6: Summary of quantitative gene expression profile of genes related to hypusination, autophagy, autophagic vesicle formation, redox metabolism and DNA repair pathway. Here, the length of the bars is indicative of quantitative values of fold change in gene expression.

Table 3.1: Various primers used for real time PCR

Name Of Gene	Abbreviation	Primer Sequence
Histone acetyltransferase-LDBPK_140140 (HAT)	HAT F	CAGAGCAGCAGAATGCAGAG
	HAT R	CAGAGCAGCAGAATGCAGAG
5'-AMP-activated protein kinase-LDBPK_292140 (AMPK)	AMPK F	AGTCAGCACATGCGATTGAG
	AMPK R	AATAACGACAGGATTTGCCG
Phosphoinositide-3-kinase, regulatory subunit 4 -LDBPK_281880 (VPS15)	VPS15 F	CTTTTCAAGCCATGCCAAAT
	VPS15 R	TCGAAGTTGACGTTGCTCAC
Phosphatidylinositol 3-kinase-LDBPK_201140 (VPS34)	VPS34 F	GTGATCCACAAGACGGTGTG
	VPS34 R	GCCTTACTCCACCAGCAGAG
Phosphatidylinositol 3-kinase (tor2)-like protein- LDBPK_344160	TOR2 F	TCAACGAACAGCGTCTCATC
	TOR2 R	GTGTCTTGCACAAACTGCGT
Phosphatidylinositol 3-kinase-like protein- LDBPK_343750 (tor 3)	TOR3 F	AACACCACTCCGACTTCCAC
	TOR3 R	CACAGACTCCTCCTCTTCCG
Phosphatidylinositol 3 kinase, putative- LDBPK_366580 (PIK)	PIK F	TTCTACGACATCAACGAGCG
	PIK R	TCAAGGTGGTGACGGATGTA
Ubiquitin-like modifier-activating enzyme ATG7- LDBPK_070010	ATG7 F	ATAAGCCTGCTCCGTCAGAA
	ATG7 R	TCGAACAAGCAGACGACAAC
NAD-dependent histone deacetylase SIR2- LDBPK_260200 (SIR2RP)	SIR2RP1 F	CTACTCTATCGCACGGGAGC
	SIR2RP1 R	TTCTGCTCAATGCTGAATGG
8-oxoguanine DNA glycosylase, putative (OGG)- LDBPK_341930	OGG F	ACAAGTTGCGGTGGAGTACC
	OGG R	CTTCCTCTATCGCCTTCACG
Endonuclease III, putative (NTH)-LDBPK_090070	NTH F	TGCAAAGTTGGGTTTCACAA
	NTH R	AACATGTGTATCGACGCCAA
Apurinic/apyrimidinic endonuclease-redox protein (APE1)-LDBPK_160680	APE1 F	TTCAAGTCGATGCAGGAGTG
	APE1 R	CGACCAGAAGGAGTAGACCG
Mitochondrial DNA polymerase I protein B, putative (DpoI)-LDBPK_130080	DpoI F	CCACATCACAAACGCTATGG
	DpoI R	TGAGTCGCAAAACAGAATGC
Mitochondrial DNA polymerase beta (POL1/4)- LDBPK_080830	POL1/4 F	AGGGCTACTTGCTGAACGAA
	POL1/4 R	TAGGGCATCCCAAGTACGTC
DNA ligase, putative (Lig)-LDBPK_110450	Lig F	TCGGCTGTCTTCTACGGACT
	Lig R	TCTTCATAGTGGCAGATGCG
LDBPK_180480- uracil-DNA-glycosylase, putative (UNG)	UNG F	GGAGTCGACATTCCCACCTA
	UNG R	TCTCTCCACTCGAGGTTCGT
A/G-specific adenine glycosylase, putative (MUTY)- LDBPK_282290	MUTY F	CATTGTCATGGATGTGGAGG
	MUTY R	TCCGACATTAGGAAGATCCG
Proliferative cell nuclear antigen (PCNA), putative (PCNA)-LDBPK_151500	PCNA F	CGCAACATTATTCTTGGCCT
	PCNA R	AGTGCTGCGGTAGTCCATCT
DNA polymerase delta subunit 2, putative (POLD)- LDBPK_251450	POLD F	GACTCGTCTCGAATCCGTTC
	POLD R	ACGTCGTTTATGTTCTGCCC
DNA polymerase epsilon subunit b (polE)- LDBPK_251450-	POLE F	CTTGATTGGGGAACAATGCT
	POLE R	TAGCGTTGATTGAGGCACTG
LDBPK_270260- flap endonuclease-	FEN1F	GATATGGACGCCTTGACGTT

1 (FEN-1), putative (FEN1)		
	FEN1R	AGCCGAGAAGAATGCAAAGA
LDBPK_303490- DNA ligase I (Lig1)	Lig1 F	TCTTCTACGAGGTGCCGAGT
	Lig1 R	GAACTTCTTGCCCTGCAGAC
Deoxyhypusine hydroxylase (DOHH)	DOHH F	GGATAACGTCTCGGCACTGT
	DOHH R	AGCTCTCTAGCACTGGCAGC
Eukaryotic initiation factor 5A (eIF5a) - LDBPK_250750	eIF5a F	TCAAAGACGTATCCCTTGCC
	eIF5a R	GCGGTTTCCAGTGAAAATGT
Deoxyhypusine synthase like (DHSlike)- LdBPK_200270	DHSlike F	TACAGGCTACCCAGATTGGC
	DHSlike R	TACGTAAACGTGTCGCGAAG
Deoxyhypusine synthase (DHS)- LdBPK_340350	DHS F	CCTGTTCATGGGTGTGACTG
	DHS R	CGTACTCCCTCTTGAGTCGC
ATG12 (LdBPK 221120.1)	ATG12 F	AGCTGCCAGTCGTTGTTTCT
	ATG12 R	TTCCAGCAAGTAGCCAAGGT
ATG4 -Ld324040, ATG4 B	ATG4 B F	CATCCAAAACGCCTACACCT
	ATG4 B R	ATTAGTGGAAACGCCACGAG
ATG4- Ld300270, ATG4 A	ATG4 A F	AGCACACTTTCAAACAGGGG
	ATG4 A R	GGCTGCTCCATCAGTTTTTC
ATG8 LdBPK 190840, ATG8 A	ATG8 A F	ACGACAAACAAGAAGGTGGC
	ATG8 A R	GTTGCCAAAACAGCAAAAG
ATG8 LdBPK 190850, ATG8 C	ATG8 C F	CACTTCTCTCTGCCGCGAC
	ATG8 C R	CGCAGAATGTGTGTAGTCGG
ATG8 LdBPK 191660, ATG8 B	ATG8 B F	GAAAACTCACCCGTTCCTG
	ATG8 B R	GTAGCGATTGAAGAGGTCGC
Alphatubulin	Alphatubulin F	CTACGGCAAGAAGTCCAAGC
	Alphatubulin R	CAATGTCGAGAGAACGACGA
Dihydrofolatereductase-thymidylated (DHFR)	060890_F	CCTTTCAACATCGCCTCCTA
	060890_R	AACTGACGCTCCTCCTTGAA
Tryparedoxin putative	010270_F	GTGGACGCAGACAACAACAC
	010270_R	CGCCTCCTCTCGTATCTTTG
Glyoxylase I trypanothione-dependent glyoxylase I	353060_F	CATATTGCTATCGGGGTGGA
	353060_R	GTGCCCTGCTCCTTCATATC
Glutathione – S-transferase/ Glutaredoxin putative	141580_F	CGTAGAGGTGGAGCCAATGT
	141580_R	GACAAAGCGGACGAGAGAAC
Glutaredoxin putative	201020_F	CTCATCTCCGCCACCTACTG
	201020_R	GTCGTATCCGCCAAGGTACT
Glutaredoxin like protein	270670_F	AAGTGGTGGTTTTCTCGTGG
	270670_R	CATCTGGTCGCACTCGTAAA
Glutathione peroxidase putative	363160_F	CTATGCGACGCTTATCGTGA
	363160_R	CACCCGTAGCATCTGAAACA
Glutathionyl spermidine synthase	252500_F	TAGTTGACAGTGACGGCGAC
	252500_R	ATGTCAGAGAGCGTCGGACT
Cytochrome c1 heme protein	070210_F	GCGTGATTGGTATTGGAACC
	070210_R	GTAAGGGGTGGGTAGGGTGT

3.4.2 ***Polysome profiling of Leishmania promastigotes showed translational arrest after hypericin treatment*****:** eIF5A has well established role in protein synthesis. Alteration in hypusine modification of eIF5A renders it inactive which should ultimately affects the global translation state of an organism. In order to evaluate role of spermidine starvation in hypusine modification of eIF5A, it is important to first check if there is any change in translation state of parasite after hypericin treatment. Further, the effect of spermidine starvation on translation, polysome profile was analyzed after treating promastigotes with IC_{50} dose of hypericin for 24 h. To analyze defect in translation initiation, promastigotes were treated with cycloheximide to block translation elongation. Polysome profiling of promastigotes treated with hypericin showed increased number of free ribosomes as compared to untreated promastigotes (Figure 3.7A). Polysome to monosome ratio in untreated and hypericin treated *Leishmania* was 2.01 and 1.10 respectively. This decrease in polysome to monosome ratio indicates the alteration in translation initiation due to spermidine starvation after hypericin treatment. To analyze post initiation defects due to spermidine starvation, polysome analysis was done in absence of cycloheximide. Any defect in elongation or termination would result in retention of polysomes due to slower run off of ribosomes. This post initiation defect is indicated by increase in polysome to monosome ratio (*Saini et. al., 2009*). Here, we have observed that increase in polysome to monosome ratio is not significant after hypericin treatment as compared to untreated promastigotes. Polysome to monosome ratio for untreated and hypericin treated promastigotes in absence of cycloheximide were 1.15 and 1.37 respectively (Figure 3.7B). Ribosome binding of eIF5A was checked by isolating RNA from polysome fractions of untreated and hypericin treated *Leishmania* promastigotes. The ribosome bound eIF5A was analyzed by quantitative real time PCR of eIF5A from RNA isolated form polysomes. We have observed that binding of eIF5A mRNA to polysomes was greatly decreased after hypericin treatment (Figure 3.8). The eIF5A mRNA binding to polysome in hypericin treated promastigotes with respect to untreated promastigotes was 22.47% considering 100 % binding in untreated promastigotes.

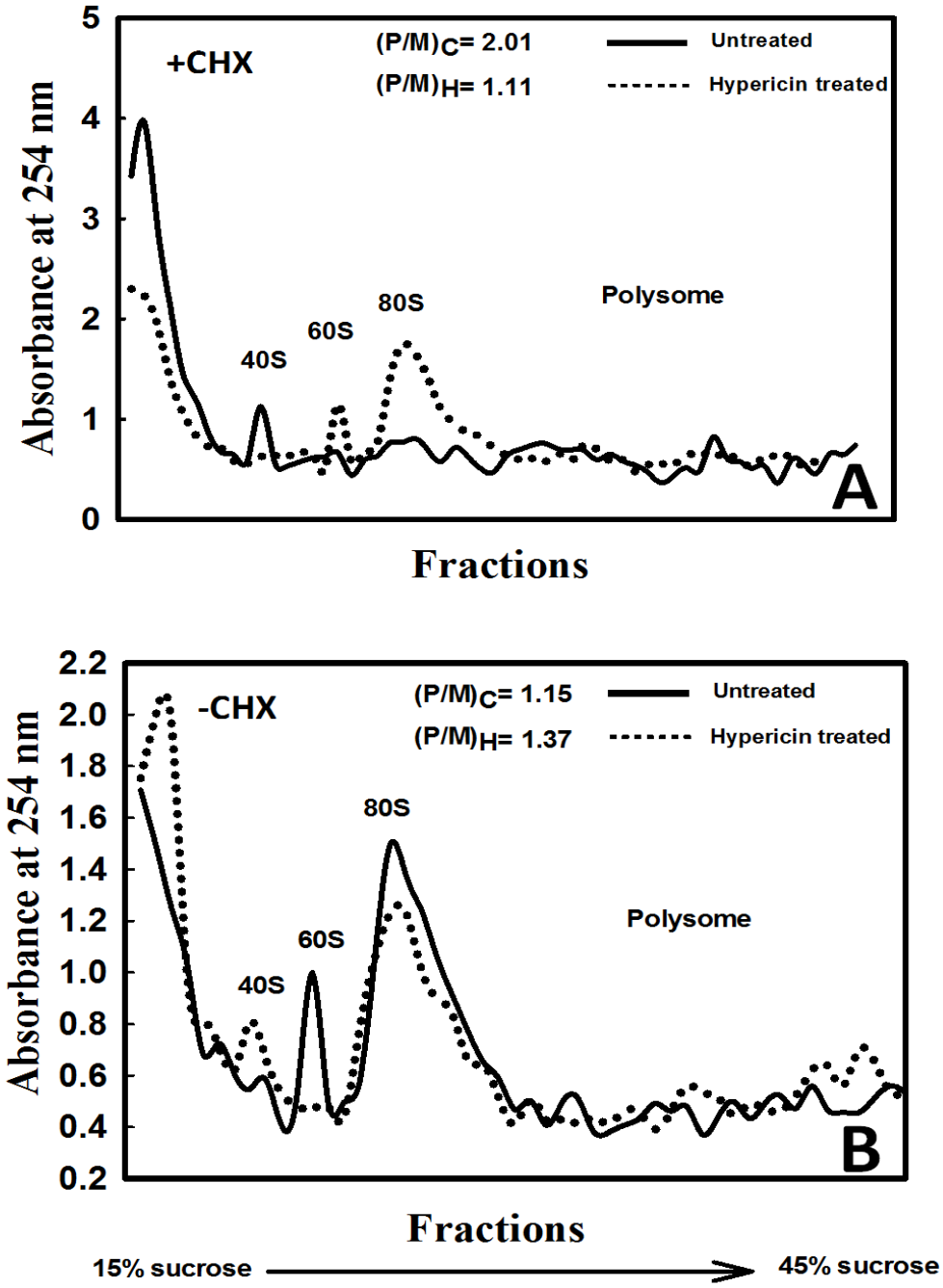

Figure 3.7: Analysis of defects in translation and hypusine modification of eIF5A of *Leishmania donovani* after hypericin treatment. **(A)** Polysome profile analysis of *Leishmania* promastigotes to monitor defects in translation initiation. Polysome profile of promastigotes treated with hypericin shows increased levels of free ribosome as compared to untreated promastigotes indicating translational defects due to spermidine starvation. Polysome to monosome (P/M) ratio was calculated by analyzing area under the curve. To check initiation defects, polysome profiling was done in presence of cycloheximide (+CHX). Polysome to monosome ratio for untreated promastigotes $(P/M)_C$ was 2.01, whereas polysome to monosome ratio for hypericin treated promastigotes $(P/M)_H$ was 1.10. **(B)** Polysome profile analysis of *Leishmania* promastigotes to check elongation defects was done in absence of cycloheximide (-CHX). Polysome to monosome ratio for untreated promastigotes $(P/M)_C$ was 1.15, whereas polysome to monosome ratio for hypericin treated promastigotes $(P/M)_H$ was 1.37.

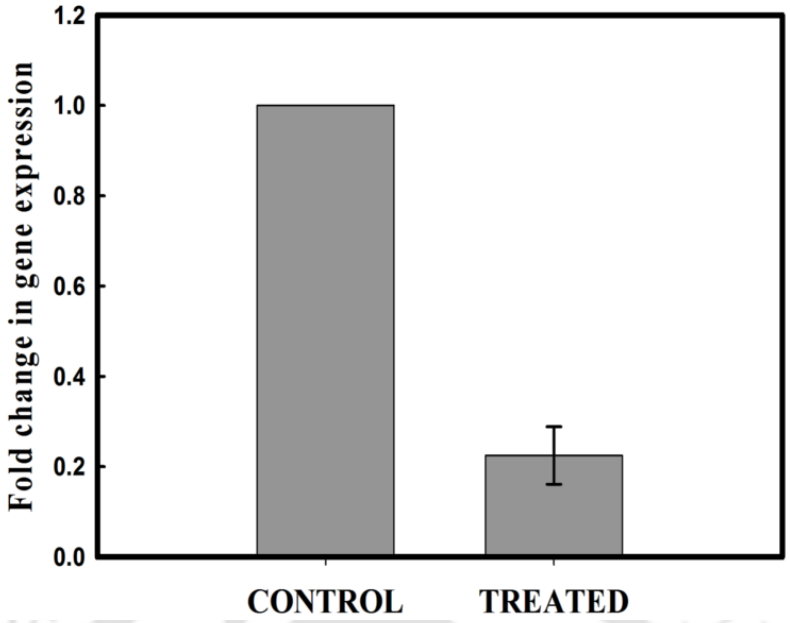

Figure 3.8: mRNA abundance of eIF5A in polysomes. RNA was isolated from polysomes of control and hypericin treated promastigotes. RNA was converted into cDNA and gene expression of eIF5A was monitored. eIF5A showed lower expression in polysomes of hypericin treated promastigotes.

3.4.3 ***Spermidine starvation shows defects in hypusination of eIF5A*****:** Hypusine modification of eIF5A is important for its activity. As our studies has shown altered global translational state under spermidine starvation, it is important to check whether there is any change in hypusine modification of eIF5A. *Leishmania* promastigotes were treated with IC_{50} dose of hypericin for 24 h. Equal amount of protein from lysate of untreated and treated promastigotes were analyzed for the presence of hypusine by using anti-hypusine antibody. *Leishmania* promastigotes treated with hypericin showed decrease in hypusination as compared to untreated *Leishmania* promastigote (Figure 3.9). Here, alphatubulin is taken as reference. Interestingly, trypanothione supplementation has not reverted back the altered hypusination whereas spermidine supplementation has shown reversal of altered hypusination due to hypericin treatment. Densitometry analysis of the bands also reveals significant decrease in hypusine modification after hypericin treatment. Fold change was calculated after normalizing loading control i.e. alphatubulin.

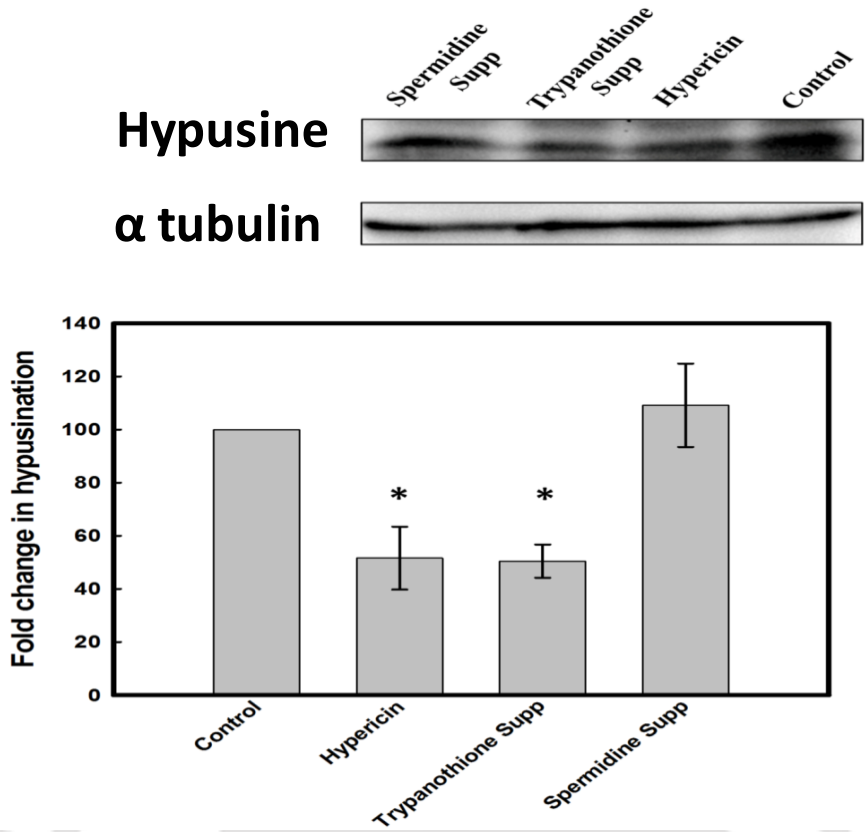

Figure 3.9: Densitometry analysis of western blot for the differential hypusination of eIF5A in untreated and hypericin treated promastigotes. Here, alphatubulin is taken as reference control. Hypericin treatment shows decrease in hypusination of eIF5A. Spermidine supplementation has reverted back the altered hypusination of eIF5A, whereas trypanothione supplementation does not show reversal of hypusination after hypericin supplementation. Inset of the figure represents the bands of western blot using anti- hypusine and anti-alphatubulin antibody. Here * represents P <0.007.

3.4.4 ***Hypericin treatment shows increase in intracellular NAD$^+$ of the parasite*****:** Spermidine has found to be involved in histone acetylation by inhibiting histone acetyltransferase in yeast (*Eisenberg et al, 2009*). SIR2RP is a NAD$^+$ dependent histone deacetylase. Quantitative gene expression analysis has revealed decrease in expression of SIR2RP after hypericin treatment. It has been reported that activity of sirtuins are regulated by NAD$^+$ availability (*Lu and Lin, 2010*). Here, we have observed decrease in SIR2RP expression but increase in intracellular levels of NAD$^+$. Intracellular NAD$^+$ concentration of the promastigotes was measured after hypericin treatment. Intracellular pool of NAD$^+$ was observed to be increased after hypericin treatment. Intracellular NAD$^+$ levels in untreated and hypericin treated promastigotes were 123±5 nM and 522±64 nM respectively. However, either trypanothione or spermidine supplementation have reverted back the NAD$^+$ levels (Table 3.2). NAD$^+$ levels in trypanothione and spermidine supplementation were 243±26 nM and 295±46 nM respectively. The increase in NAD$^+$

level could also be correlated to AMPK activation and possibly due to increase transcription of NAD^+ biosynthetic enzymes or reduced glycolysis (*Lin et al., 2001;Guan and Xiong, 2011*).

Table 3.2: NAD^+ estimation (in nanoM) of *Leishmania* promastigotes. *Leishmania* promastigotes were treated with IC_{50} dose of hypericin. Promastigotes were also supplemented with trypanothione and spermidine individually followed by hypericin treatment. Here the NAD^+ concentration refers to the concentration of 10 µl of NAD^+ extracted from 841.5 µg of protein from cell lysate containing 5 mg/ml protein concentration in a reaction volume of 200 µl.

Control	Hypericin (18 µM) treatment		
	Without Supplementation	Trypanothione Supplementation	Spermidine Supplementation
123±5	522±64	243±26	295±46

3.4.5 ***Acridine orange staining to check autophagy after hypericin treatment*:** Quantitative gene expression of autophagy related gene has indicated the presence of autophagy after hypericin treatment. In order to confirm the occurrence of autophagy after hypericin treatment, we have done acridine orange staining of parasite. Autophagy includes formation of acidic vacuoles. Acridine orange fluoresce green at neutral pH, whereas, it tend to accumulate at sites having acidic pH and fluoresce red. Flow cytometry analysis revealed that number of cells showing red fluorescence has increased after hypericin treatment indicating the acidic cellular environment. However, trypanothione or spermidine supplementation or 3-methyladenine pretreatment has shown increased green fluorescence indicating lesser acidic environment inside promastigotes. The percentage of promastigotes showing low green and higher red fluorescence (top left quadrant) is very low (>1%) in control untreated promastigotes and promastigotes treated with 3-methyladenine (Figure 3.10 A; Figure 3.10 B) indicating no acidic vacuolar organelles. As shown in figure 3C, after treatment with hyericin, 56.10% of promastigotes showing low green and higher red fluorescence (top left quadrant) indicating increase in acidic vacuolar organelles characteristic of autophagy. However, supplementation of trypanothione or spermidine followed by hypericin treatment, numbers of promastigotes in top left quadrant is significantly decreased showing reversal of autophagy (Figure 3.10

D; Figure 3.10 E). Promastigotes pre-treated with 3-methyl adenine, an inhibitor of autophagy, before hypercin treatment shows number of cells in top left quadrant close to control indicating complete reversal of autophagy (Figure 3.10F). Although, acridine orange labelling is a poor marker for autophagy since acridine orange labels acidocalcisome organelles in *Leishmania*, however here we have shown comparative analysis of untreated and treated promastigotes which could be a reliable way to observe induction of autophagy.

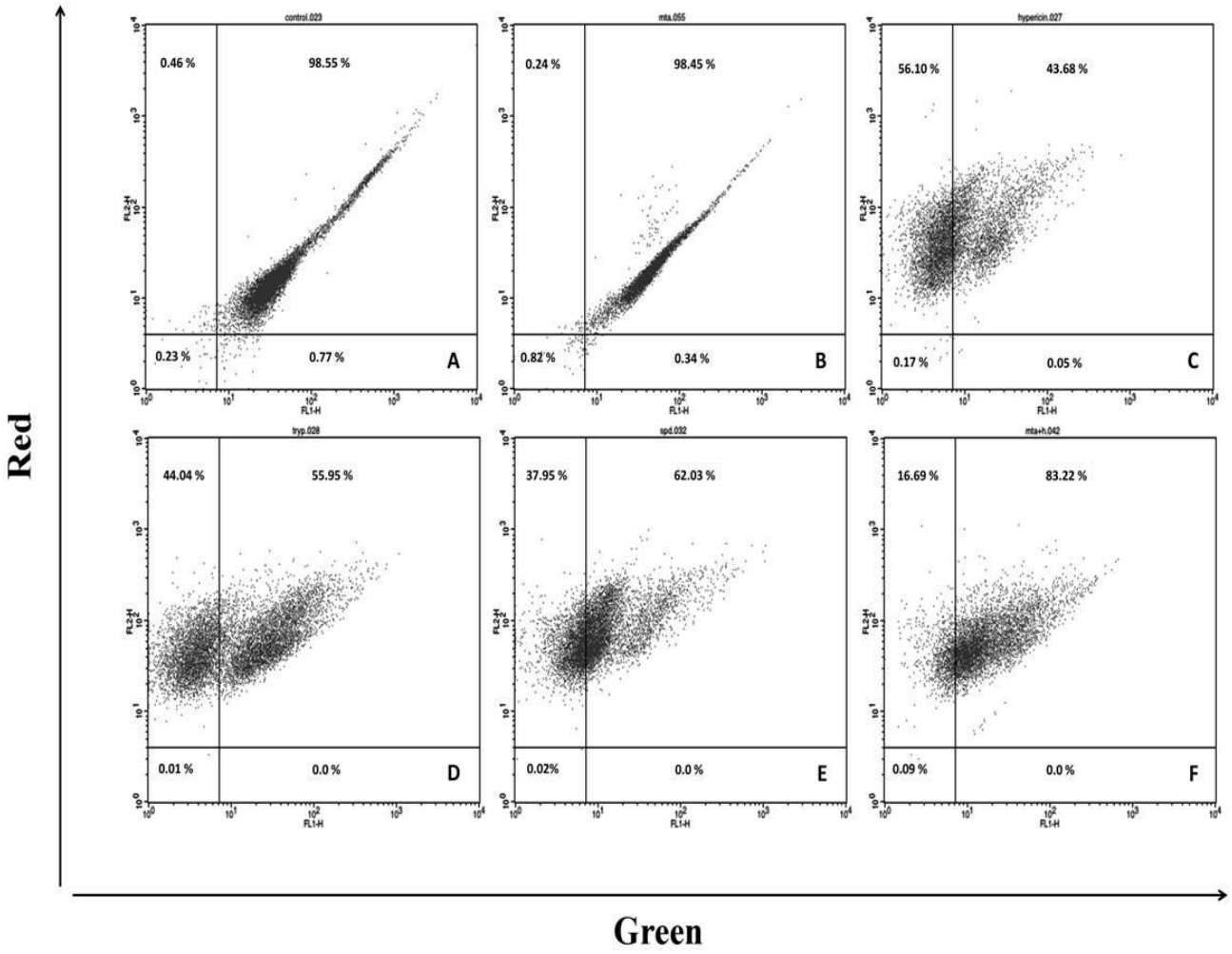

Figure 3.10: Analysis of *Leishmania* promastigotes for autophagy by using acridine orange staining. *Leishmania* promastigotes were analyzed by flow cytometry to detect acidic vacuolar organelles by acridine orange staining. *Leishmania* promastigotes were stained with 1 µg/ml of acridine orange at 25 ºC for 15 min. After staining, promastigotes were analyzed using flow cytometry. *Leishmania* promastigotes showed increased acidic vacuolar organelles after treatment with hypericin, however spermidine supplementation has reverted back the increased number of acidic vacuolar organelles after hypericin treatment. **(A)** Untreated promastigotes **(B)** promastigotes treated with 3-methyladenine **(C)** Promastigotes treated with hypericin for 12 h **(D)** promastigotes supplemented with trypanothione followed by hypericin treatment **(E)** promastigotes supplemented with spermidine followed by hypericin treatment **(F)** promastigotes pretreated with 3-methyl adenine followed by treatment with hypericin.

Although the acridine orange staining did not show significant and conclusive evidence about reversal of autophagy after trypanothione treatment, the results were supplemented by other methods (staining with monodansylcadaverine and ATG8 puncta formation) to monitor autophagy showing clear reversal of autophagy after trypanothione supplementation.

3.4.6 ***Leishmania promastigotes are stained by monodansylcadaverine after 12 h of hypericin treatment*****:** In order to further confirm the formation of autophagic vacuoles, we have used staining with monodansylcadaverine, a fluorescent dye, which labels autophagic vacuoles. *Leishmania* promastigotes showed positive labeling with monodansylcadaverine after 12 h treatment with hypericin. However, there was no fluorescence observed in untreated promastigotes and promastigotes supplemented with trypanothione or spermidine after hypericin treatment or pre-treatment of 3–methyl adenine (Figure 3.11). The results indicate that hypericin induces autophagy in *Leishmania* promastigotes. Both, trypanothione or spermidine supplementation has reverted back the autophagy induced by hypericin treatment.

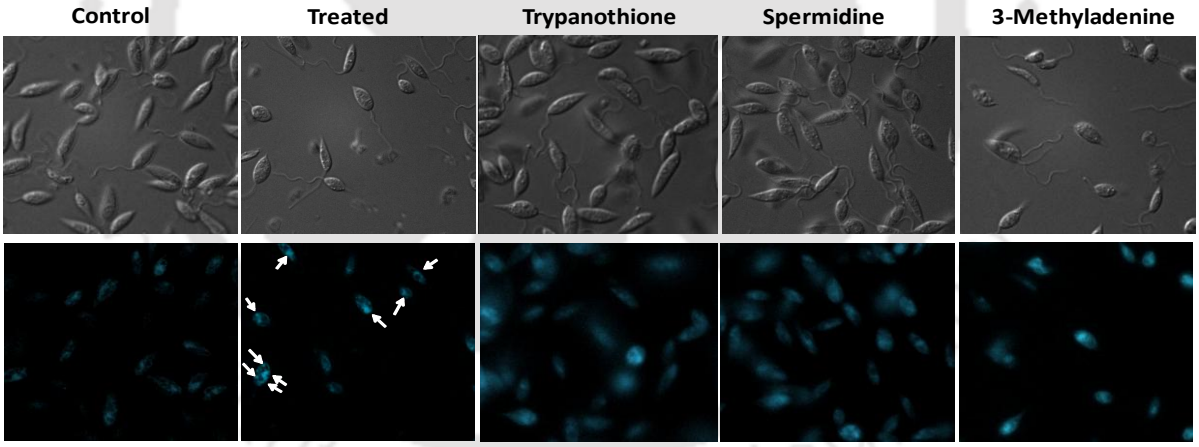

Figure 3.11: Analysis of autophagic vacuoles by staining with monodansylcadaverine. Staining with monodansylcadaverine was analyzed in untreated promastigotes as control, promastigotes treated with hypericin for 12 h**,** promastigotes supplemented with trypanothione followed by treatment with hypericin for 12 h, promastigotes supplemented with spermidine followed by treatment with hypericin for 12 h and promastigotes pre-treated with 3-methyladenine and treated by hypericin treatment for 12 h. However, trypanothione as well as spermidine supplementation has decreased the formation of autophagic vacuoles after hypericin treatment. Here, promastigotes pretreated with 3-methyladenine (autophagy inhibitor) followed by hypericin treatment, were taken as control to show autophagy reversal.

3.4.7 ***Formation of ATG8 labeled puncta was observed in Leishmania promastigotes after hypericin treatment*****:** In order to confirm the formation of auotophagic vacuoles, *Leishmania* promastigotes containing GFP-ATG8 were treated with hypericin and

analyzed using confocal laser scanning microscope. *Leishmania* promastigotes has shown increase in number of ATG8 puncta after hypericin treatment as compared to untreated promastigotes. Interestingly, number of ATG8 puncta has decreased after each trypanothione and spermidine supplementation (Figure 3.12).

3.4.8 ***ATP determination after hypericin treatment has shown increase in intracellular ATP pool of Leishmania parasite*:** Intracellular ATP estimation was done in order to identify the overall change in ATP due to spermidine starvation (Table 3.3). Equal number promastigotes were treated with hypericin, supplemented with spermidine or trypanothione after treatment with IC_{50} dose of hypericin for 24 h. Promastigotes were also pre-treated with 3-methyl adenine before treatment with IC_{50} dose of hypericin for 24 h. ATP estimation showed an increase in intracellular ATP pool of the parasite after hypericin treatment. ATP concentration of the untreated and hypericin treated promastigotes were 27±8 pM and 74±7 pM respectively. However, this increase in ATP pool is reverted back after supplementation with trypanothione or spermidine or in case of pre-treatment with 3-methyl adenine before hypericin treatment. Intracellular ATP pool of parasite supplemented with trypanothione, spermidine, or 3-methyladenine followed by hypericin treatment were 33±2 pM, 36±4 pM and 27±6 pM respectively. Untreated and only 3-methyl adenine treated promastigotes were taken as controls. Promastigotes treated with only 3-methyladenine showed 29±2 pM of intracellular ATP levels. DNA damaging agents has shown to induce autophagy associated ATP production which could be blocked by pretreatment with 3-methyl adenine (*Katayama et al., 2007*). The increase in ATP after hypericin treatment also appears to be autophagy associated.

Table 3.3: ATP estimation (in picoM) of *Leishmania* promastigotes. *Leishmania* promastigotes were treated with IC_{50} dose of hypericin. Promastigotes were also supplemented with trypanothione, spermidine and 3-methyladenine individually followed by hypericin treatment. Here, the concentration of ATP represents its concentration in $1X10^6$ cells dissolved in 10 µl of PBS.

Control	3-Methyl Adenine	Hypericin (18 µM) treatment			
		Without Supplementation	Trypanothione Supplementation	Spermidine Supplementation	3-Methyl Adenine pre-treatment
27±8	29±2	74±7	33±2	36±4	27±6

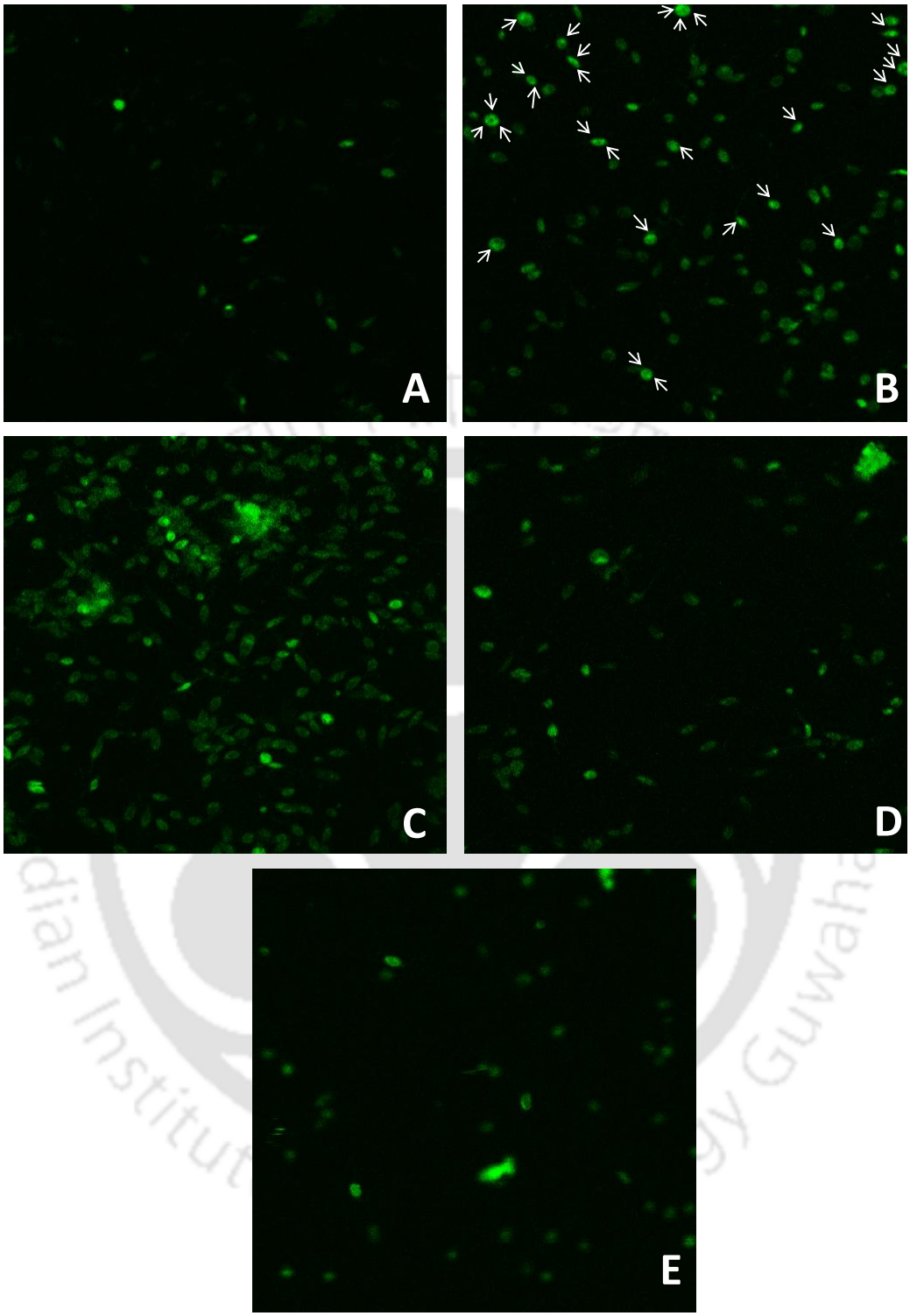

Figure 3.12: Analysis of ATG8 puncta formation. *Leishmania* promastigotes transfected with pGL1686 containing GFP-ATG8. ATG8 puncta formation was analysed in **(A)** untreated **(B)** hypericin treated for 12 h **(C)** trypanothione supplemented and hypericin treated **(D)** spermidine supplemented and hypericin treated and **(E)** 3-methyladenine pretreated and hypericin treated *Leishmania* promastigotes. Hypericin treatment shows ATG8 puncta formation which is reverted back by either trypanothione or spermidine supplementation or 3-metyhladenine pretreatment. Although, the images are not of the best possible quality, conclusions are supported by many other experiments

3.5 Discussion:

Our previous study has indicated the role of spermidine in pathways other than redox metabolism of *Leishmania donovani*. We have demonstrated that the spermidine starvation results in increased ROS and necrosis like death but the necrotic death due to spermidine starvation is not linked to elevated ROS in the pathogen (*Singh et al., 2015*). In the current report, we have further explored the potential role of spermidine and the cause of death of parasite due to spermidine starvation. In order to decipher the pathways linked to the involvement of spermidine, we have analyzed the differential gene expression profile of the parasite after spermidine starvation that has given us clue about possible alteration in redox metabolism pathway, DNA damage repair, hypusination of eIF5A pathways and autophagy.

To get further insight into the cause of parasite death after hypericin treatment and subsequent spermidine starvation in *Leishmania donovani*, we have checked the expression profile of genes involved in hypusination of eIF5A. We have observed global translational defect and decreased hypusination of eIF5A after hypericin treatment. We have observed altered translation initiation after hypericin treatment. Alteration of hypusine modification of eIF5A by spermidine is also reported in *Saccharomyces cerevisiae* (*Chattopadhyay et. al., 2008*). Recently, role of eIF5A in translation elongation has also been reported in some organisms (*Saini et. al., 2009*). However, we have not observed significant change in translation elongation after hypericin treatment. This may be an indication of involvement of eIF5A of *Leishmania donovani* mainly in initiation of translation than its involvement in elongation. Also, spermidine starvation has resulted in decreased mRNA distribution of eIF5A in polysome fractions. Altered hypusination of eIF5A was reverted back to large extent by spermidine supplementation whereas trypanothione supplementation has shown no reversal of the defective hypusination due to hypericin treatment. This affirms that defects in translation state and hypusination of eIF5A are solely due to spermidine starvation of the parasite and it is completely independent of redox imbalance due to hypericin treatment. As our data shows that hypusine containing eIF5A is involved in translation initiation in the parasite, altered hypusination due to spermidine could alter the translation of several important proteins, thereby inhibiting growth and survival of the parasite (*Dever et al., 2014*).

Moreover, spermidine also inhibits activity of histone acetyltransferase (HAT) in yeast (*Eisenberg et al., 2009*). If spermidine is involved in inhibition of HAT in *Leishmania*

parasite as well, spermidine starvation of the parasite should relieve the inhibition of HAT. Histone acetylation and deacetylation play important role in chromatin condensation. Although, role of spermidine in inhibiting histone acetyltransferase in yeast is known, histone deacetylase, SIR2, has shown no correlation with spermidine (*Eisenberg et al, 2009*). It has been reported that increasing the cellular acetylation by histone deacetylase (HDAC) inhibitors can promote autophagy in nutrient rich conditions (*Yi and Yu, 2012*). Interestingly, in our studies, we have observed increase in HAT expression and decrease in SIR2RP (a type III histone deacetylase) expression of parasite after spermidine starvation. SIR2RP is NAD^+ dependent histone deacetylase whose activity is dependent on the availability of NAD^+. Surprisingly, we have observed increase in NAD^+ after hypericin treatment. This statistically significant increase in NAD^+ points to difficulty in linking intracellular NAD^+ pool directly to the SIR2RP activity and points towards the importance of identifying factors involved in regulating exposure of sirtuins to NAD^+ (*Guan and Xiong, 2011*). We have observed the increase in NAD^+ levels after hypericin treatment which was reverted back by trypanothione or spermidine supplementation. This suggests that trypanothione, a key regulator of redox metabolism, is sufficient to revert back the altered levels of SIR2RP in hypericin treated *Leishmania* parasite, indicating the ROS induced alteration of SIR2RP. Here, we have observed that ROS has induced AMPK activation in hypericin treated promastigotes. It has been reported that glucose starvation result in defective differentiation of skeletal muscles which is linked with AMPK activation and increased transcription of NAD^+ biosynthesis enzyme leading to increased intracellular NAD^+/NADH ratio (*Lin et al., 2001; Guan and Xiong, 2011*). So, in our study the increase in NAD^+ level could also be correlated to AMPK activation and possibly due to increase transcription of NAD^+ biosynthetic enzymes or reduced glycolysis. Since histone deacetylase (HDAC), induces chromatin condensation, so decrease in SIR2RP, a type III HDAC, should result in chromatin relaxation, allowing more access of DNA repair protein to repair the ROS induced DNA damage (*Gong and Miller, 2013*).

Spermidine has been known for its ability to induce autophagy and increase life span in yeast (*Eisenberg et al, 2009*). However, in *Leishmania*, no such role of spermidine is reported till date. Moreover, effect of spermidine starvation is not studied in *Leishmania*. In order to know the role of spermidine in autophagy, we have analyzed the expression of several autophagy related genes after spermidine starvation. We found altered expression

of several important genes involved in induction of autophagy and vesicle formation. Here we have seen increased expression of 5'-AMP-activated protein kinase (AMPK) after hypericin treatment. AMPK activation induces autophagy by inhibiting mTOR signalling pathway. It has been reported that the generation of reactive oxygen species (ROS) causes DNA damage and lead to the activation of AMPK (*Li, 2013; Sanli, 2014*). In our previous study, we have also reported the generation of ROS after hypericin treatment, which was reverted back by both trypanothione and spermidine supplementation (*Singh et al., 2015*). So, if the AMPK activation is induced due to generation of ROS after hypericin treatment, it should be reverted back individually by trypanothione as well as spermidine supplementation. Affirming this hypothesis, we have observed reversal of increased AMPK expression after trypanothione as well as spermidine supplementation. Moreover, the presence of autophagic vacuoles was also observed after hypericin treatment and number of autophagic vacuoles decreases with trypanothione as well as spermidine supplementation. Although, acridine orange staining does not provide conclusive evidence about reversal of autophagy in trypanothione supplementation, other experiments such as staining with monodansylcadaverine and ATG8 puncta formation show significant reversal of autophagy with either trypanothione, spermidine supplementation following hypericin treatment or 3-methyladenine pretreatment followed by hypericin treatment. This indicates that hypericin induced ROS generation leads to the induction of autophagy via AMPK activation. Our previous work showed that trypanothione supplementation is not rescuing the death of the parasite after hypericin treatment. Surprisingly, trypanothione is reverting back the autophagy induced due to hypericin treatment. This indicates that although there is autophagy, however death of the parasite is not due to autophagy.

We have observed that hypericin induced autophagy was a result of DNA damage response towards ROS generation. This was further confirmed by monitoring intracellular ATP level of parasite after hypericin treatment. It has been reported that DNA damaging agents that induces autophagy also induce ATP surge that act as cytoprotective mechanism and may lead to drug resistance in malignant glioma cells (*Katayama et al., 2007*). In our study, we have observed an increase in intracellular ATP pool of the parasite after hypericin treatment. Interestingly, altered ATP levels due to hypericin were rescued with trypanothione or spermidine supplementation and 3- methyl adenine pretreatment. In our studies we have also observed that trypanothione or spermidine

supplementation and pretreatment with 3-methyl adenine has reverted back the autophagy. Thus, it appears that the ATP surge was induced due to autophagy. This suggests that autophagy induction after hypericin treatment is a cyotoprotective mechanism to protect itself from DNA lesions caused due to ROS generation. Increase in ATP pool is also reported

The data reported in the manuscript indicates that the indication of autophagy and impaired deacetylation are not the cause of death of the parasite under spermidine starvation. The death of the parasite is mainly due to the defects in hypusination pathways of eIF5A leading to translational defects and hence defective translation of several crucial genes of the parasite. Thus, the hypericin induced parasite death may be explained as "death with autophagy" and not "death by autophagy".

CHAPTER IV

Proteome Analysis of *Leishmania donovani* Under Spermidine Starvation *

4.1 Abstract:

Hypericin has been found to cause death of *Leishmania donovani* mainly by spermidine starvation that results altered translation initiation by lowering hypusine modification of eukaryotic initiation factor 5A. *Leishmania* promastigotes have also shown to exert a cytoprotective mechanism in response to DNA damage induced by ROS generation due to hypericin. We have used label free proteome quantitation approach to identify differentially modulated proteins after hypericin treatment. Although, we could not map entire proteome of the parasite due to limitation of technique, significant numbers of proteins with altered expression were identified. Differentially modulated proteins have been broadly classified under nine major categories. Increase in Ribosomal protein S7 protein suggests the repression of translation. Inhibition of proteins related to ubiquitin proteasome system, RNA binding protein and translation initiation factor also further confirms altered translation. These alterations in translation could be a direct or indirect effect of lowered hypusine modification of eIF5A. We have also observed altered expression stress of related proteins. These data was rigorously analyzed to get more insight into effect of spermidine starvation in *Leishmania* parasite

**** Accepted for publication in Plos One, 2016, doi: 10.1371/journal.pone.0154262.***

4.2 Introduction:

Leishmaniasis is a vector borne disease caused by a digenetic parasite of genus *Leishmania*. There are several drugs available in the market against leishmaniasis, but they have many limitations, like drug resistance, toxicity, high cost etc. These limitations of available drugs emphasize the need of new and better drug candidates. In search of this, we have identified a novel drug candidate, hypericin, against leishmaniasis.

Hypericin was found to be an inhibitor of spermidine synthase of *Leishmania donovani* causing necrotic death of the parasite. Spermidine was found to play important role in various organisms. In addition to its role in redox metabolism, spermidine was also found to play important role in autophagy and hypusine modification of eukaryotic initiation factor 5A (*Singh et al., 2015*). Analyzing proteome profile of *Leishmania* promastigotes will help us in understanding the global picture of mechanism of hypericin induced cell death. Quantitative proteomics is an important tool for analyzing differential expression of proteins of organisms in different conditions. This further helps in exploring and identifying different mechanisms and new pathways of an organism. Here we have used label free quantification approach for proteome profiling of *Leishmania donovani*. Label free quantification relies on separation of peptides of digested protein through liquid chromatography followed by introduction of ionized peptides into mass spectrometer (*Wong and Cagney, 2009*). Quantitation is based on two methods: one includes measurement in differences of ion intensities like peak area, peak height of the peptide and second is based on the spectral counting of the proteins identifies after LC/MS/MS (*Zhu et al., 2010*).

Hypericin has shown to cause defect in translation by lowering hypusine modification of eukaryotic initiation factor 5A. Hypericin treatment has resulted in altered levels of genes involved in autophagy, redox metabolism, hypusine modification, histone deacetylase and DNA repair pathway. It was also found that hypericin treatment has resulted in induction of autophagy as a result of cytoprotective mechanism against DNA damage induced by ROS generation. However, to know the overall mechanism of hypericin induced death of *Leishmania donovani*, it is important to know the global picture of proteome modulation after hypericin treatment. Here we have analyzed proteome of untreated and hypericin treated *Leishmania donovani*. Although, we could not map entire proteome of the parasite due to limitation of technique, significant numbers of proteins with altered expression were identified and analyzed.

4.3 Materials and Methods:

4.3.1 *Chemicals and cell lines*: *Leishmania donovani* (MHOM/IN/2010/BHU1081) strain a kind gift from Prof. Shyam Sundar, Banaras Hindu University, India. Hypericin and Protease inhibitor cocktail was procured from Sigma Aldrich. Tris-Cl, NaCl etc were of high quality obtained from Himedia.

4.3.2 *Treatment of Leishmania promastigotes*: *Leishmania* promastigotes with a cell density of ($1X10^6$ cells/ml) were treated with IC_{50} dose of hypericin (18 µM) for 24 h (*Singh et al., 2015*).

4.3.3 *Sample preparation for mass spectrometry analysis*: Untreated and hypericin treated *Leishmania* promastigotes were analyzed by mass spectrometry. *Leishmania* promastigotes ($1X10^6$ cells/ml) were harvested and dissolved in lysis buffer (50 mM tris-Cl, 150 mM NaCl, and protease inhibitor cocktail). Promastigotes were lysed using ultrasonication with pulse cycle of 2 sec ON and 10 sec OFF for 5 min in lysis buffer. After lysis, promastigotes were centrifuged at 12,000 rpm for 20 min to remove the cell debris. Supernatant was collected and again centrifuged at 12,000 rpm for 20 min. Protein was precipitated from lysate of *Leishmania* promastigotes by using acetone precipitation. Further, protein concentration was measured using bicinchoninic acid (BCA) analysis. Equal amount (30 µg) of each sample was subjected to digestion by trypsin which was then followed by alkylation and reduction. After this, samples were dissolved in 15 µl of 2% acetonitrile and 0.1 % formic acid. Each sample (1 µl) is subjected to reverse phase liquid chromatography for 180 min which is then followed by acquisition of data on LTQ-Orbitrap-MS (*Haqqani et al., 2008; Gundry et al., 2009*).The experiment was done in triplicate.

4.4.4 Analysis of mass spectrometry data: The data obtained from mass spectrometry was analyzed by using Progenesis QI for proteomics. The software identifies the peak and creates peak models retaining important information of quantification and position. Further, the reproducibility of the experiment was increased by aligning the results of different runs by identifying a best reference run. Aligned runs were analyzed to create a data set containing the information about all the peaks identified in all sample runs. After quantification of ion abundance from each run, the data was normalized to compare the results from different runs. Statistical analysis was done by using ANOVA. Peptide ions

were further identified by using MASCOT MS/MS ion search tool. Unique peptides were considered for protein quantification (*Progenesis QI for proteomics, Bao et al., 2015*).

4.3.5 Protein protein interaction analysis: Differentially up regulated proteins above 1.5 fold and down regulated protein below 0.9 fold were taken to analyze the interaction between them. Protein-protein interaction was analyzed by using STRING database. STRING (Search Tool for the Retrieval of Interacting Genes) is a database containing known and predicted associations between proteins. Protein interactions in STRING are not only based on direct and physical association of proteins but also on their genetic interactions and their involvement in subsequent catalysis steps in metabolic processes (*Szklarczyk et al., 2011, Islam et al., 2015*).

4.4 Results:

4.4.1 *Distribution of proteins being altered after hypericin treatment into major classes*: Differentially modulated proteins are categorised into nine major classes. These classes are: Protein synthesis, stress and protein folding, metabolic processes, protein turnover and modification, cytoskeleton and cell motility, fatty acids, signalling, transporters and membrane proteins, nucleic acid and hypothetical proteins. Relative distribution among different classes of total proteins being altered after hypericin treatment is shown by plotting a pie chart (Figure 4.1A). Out of total altered protein, 15 % are in the category of protein synthesis, 5 % in stress and protein folding, 17 % under metabolic processes, 2 % in protein turnover and modification, 3 % in cytoskeleton and cell motility, 2 % related to fatty acids, 13 % related to signalling, transporters and membrane proteins, 3 % in nucleic acids and 40 % hypothetical proteins (Figure 4.1A). The relative distribution of up regulated proteins (up regulated above 1.5 fold with ANOVA value less than 0.05) is also checked by plotting pie chart (Figure 4.1B). The percentage of up regulated proteins out of total up regulated proteins are: 17 % protein synthesis, 5 % stress and protein folding, 26 % metabolic processes, 0 % protein turnover and modification, 2 % cytoskeleton and motility, 4 % fatty acids, 9 % signalling, transporters and membrane proteins, 2 % nucleic acids and 35 % hypothetical proteins (Figure 4.1B). Out of total proteins being down regulated (down regulated below 0.9 fold with ANOVA value less than 0.05), 11 % belong to the category of protein synthesis, 3 % stress and folding, 3 % metabolic processes, 6 % protein turnover and modification, 5 % cytoskeleton and cell motility, 0 %

fatty acids, 19 % signalling, transporters and membrane proteins, 6 % nucleic acids and 47 % hypothetical proteins (Figure 4.1C).

4.4.2 ***Differential regulation of proteins related to translation*****:** There was 2.96 fold and 1.68 fold increase in elongation factor 1 alpha and eukaryotic translation initiation factor respectively. Ribosomal protein S7 and ribosomal protein L15 has shown 5.26 and 1.99 fold increase in expression after hypericin treatment. There is an increased expression of poly(A)-binding protein and threonyl-tRNA synthetase after hypericin treatment (Table 4.1). Proteins showing decreased expression after hypericin treatment are 60S ribosomal protein L12 (0.83 fold), splicing factor ptsr1-like protein (0.73 fold), RNA-binding protein (0.63 fold) and translation initiation factor (0.75 fold) (Table 4.2).

4.4.3 ***Differential modulation of proteins related to stress and protein folding:*** Increase in expression level of some heat shock proteins was observed. There was 3.27 fold increase in expression of heat shock protein 83-1 and 3.72 fold increase in heat shock protein 83 after hypericin treatment. Other stress related protein such as stress-inducible protein STI1 homolog was also found to show increased expression (2.43 fold) after hypericin treatment (Table 4.1). However, cyclophilin (0.46 fold) expression was significantly decreased after hypericin treatment (Table 4.2).

4.4.4. ***Differential modulation of proteins involved in metabolic processes*****:** Expression of several proteins involved in carbohydrate metabolism, amino acid metabolism and pyruvate metabolism was found to be altered due to hypericin. Several enzymes involved in glucose metabolism were shown to have increase expression after hypericin treatment. Several enzymes like NADH-dependent fumarate reductase (1.51 fold), malate dehydrogenase (1.60 fold), cytochrome c oxidase subunit IV (1.96 fold), 2-oxoglutarate dehydrogenase E1 component (1.67 fold) and 2-oxoglutarate dehydrogenase, E2 component, dihydrolipoamide succinyltransferase (1.55 fold) shows altered expression (Table 4.1). However 2-hydroxy-3-oxopropionate reductase was found to show decreased expression in hypericin treated *Leishmania* promastigotes. Several enzymes involved in mitochondrial biogenesis were also found to increase. Mitochondrial processing peptidase, beta subunit was increased by 1.71 fold and mitochondrial processing peptidase alpha subunit was increased by 1.78 fold in promastigotes treated with IC_{50} value of hypericin for 24 h. Certain enzymes of amino acid biosynthesis and metabolism were also found to be up regulated. Phenylalanine-4-hydroxylase (1.69 fold) and 5-methyltetrahydropteroyltriglutamate-homocysteine S-methyltransferase (1.52 fold) were

shown increased expression after hypericin treatment. Decreased expression of 2-hydroxy-3-oxopropionate reductase (0.73 fold) was found to be decreased in hypericin treated Leishmania promastigotes (Table 4.2).

4.4.5 ***Differential expression of enzymes involved in protein turnover, processing and modification was observed after hypericin treatment*****:** The enzymes involved in protein turnover and modification were found to be altered in promastigotes treated with hypericin for 24 h. Proteasome alpha 7 has shown 0.76 fold decrease expression after hypericin treatment. Also, proteasome alpha 1 subunit expression was decreased to some extent (0.87 fold) (Table 4.2).

4.4.6 ***Differential expression of proteins involved in cytoskeleton and cell motility*****:** Some of the protein involved in cytoskeleton formation and cell motility were altered. Expression of beta tubulin was increased 2.16 fold in promastigotes treated with hypericin for 24 h (Table 4.1). However, proteins involved in cellular motility were found to show decreased expression after hypericin treatment. C-terminal motor kinesin and flagellar radial spoke protein has shown significant decrease of 0.50 fold and 0.70 fold respectively (Table 4.2).

4.4.7 ***Differential modulation of proteins involved in fatty acid biosynthesis*****:** Proteins involved in fatty acid synthesis shows increased expression after hypericin treatment. Fatty acid elongase expression was increased 14.86 fold in promastigotes treated with hypericin for 24 h. Also, the expression of farnesyl pyrophosphate was found to be higher (2.07 fold) after hypericin treatment (Table 4.1).

4.4.8 ***Alteration in expression of proteins involved in signalling, transport and membrane proteins*****:** There was alteration in expression of signalling proteins, transporters, and membrane proteins in promastigotes treated with IC_{50} dose of hypericin for 24 h. Few proteins show up regulation. Pteridine transporter FT3 (1.62 fold), vacuolar proton translocating ATPase subunit A (1.58 fold), ADP/ATP mitochondrial carrier-like protein (1.64 fold), ATPase alpha subunit (1.57 fold) were found to be up regulated after hypericin treatment of promastigotes for 24 h (Table 4.1). Many signalling proteins and transporters show decreased expression after hypericin treatment. The down regulation of vesicule-associated membrane protein (0.55 fold), leishmanolysin (0.65 fold), ADP-ribosylation factor (0.79 fold), ATP synthase, epsilon chain (0.90 fold), protein kinase (Accession number: 322500321) (0.76 fold), protein kinase (Accession number:

322501646) (0.70 fold) and HASPB1 protein (0.87 fold) was observed in promastigotes treated with hypericin for 24 h (Table 4.2).

4.4.9 *Differential modulation of proteins involved in nucleic acid synthesis and metabolism*: Altered expression of proteins involved in nucleic acid biosynthesis and metabolism was observed. Adenylosuccinate synthetase and dihydrofolate reductase-thymidylate synthase were up regulated by 1.79 fold and 2.14 fold after hypericin treatment (Table 4.1). Some of the proteins were also down regulated such as universal minicircle sequence binding protein (UMSBP) (0.72 fold) and aspartate carbamoyltransferase (0.87 fold) (Table 4.2).

4.4.10 Protein-protein interaction of differentially modulated proteins: Differentially up regulated protein above 1.5 fold and down regulated proteins below 0.9 fold were taken as input to analyze the protein-protein interaction. The differentially altered proteins were found to be interconnected with each other forming a network shown in Figure 4.2. list of input proteins with their accession numbers and list of predicted functional partners of input proteins are mentioned in Table 4.3 and Table 4.4 respectively.

Table 4.1: Distribution of up regulated proteins after hypericin treatment into major categories. Here ◐ represents the up regulated proteins after hypericin treatment with ANOVA value less than 0.05.

Accession	Anova (P*)	Folds	Peptides (Peptides in quantitation)	Score	Tags	Description	Average Normalized Abundance	
							Treated	Control
Transcription/Translation/Protein synthesis								
15788964	1.08e-003	2.96	29 (6)	702.34	◐	elongation factor 1-alpha, partial	5.42e+007	1.83e+007
322496059	6.23e-003	5.26	10 (1)	230.03	◐	ribosomal protein S7, putative	3.47e+006	6.59e+005
322502154	0.01	1.45	16 (4)	395.57	◐	40S ribosomal protein S3, putative	9.68e+006	6.68e+006
322497920	0.01	1.38	14 (2)	177.76	◐	eukaryotic translation initiation factor 1A, putative	2.08e+006	1.51e+006
322501313	0.02	1.99	11 (4)	151.09	◐	ribosomal protein L15, putative	4.21e+006	2.12e+006
322498799	0.04	1.26	13 (3)	387.10	◐	la RNA binding protein, putative	3.17e+006	2.52e+006
322498921	8.95e-003	1.48	23 (6)	322.74	◐	RNA helicase, putative	7.19e+006	4.88e+006
322499565	1.17e-003	1.64	18 (4)	309.36	◐	poly(A)-binding protein, putative	3.10e+006	1.89e+006
322502963	0.05	1.52	17 (7)	345.52	◐	threonyl-tRNA synthetase, putative	5.28e+006	3.47e+006
322500575	0.04	1.68	10 (4)	295.75	◐	eukaryotic translation initiation	4.08e+006	2.43e+006

Accession	Anova (P*)	Folds	Peptides (Peptides in quantitation)	Score	Tags	Description	Average Normalized Abundance	
							Treated	Control
						factor, putative		
322497525	0.03	1.39	26 (8)	571.80		leucyl-tRNA synthetase, putative	6.28e+006	4.53e+006
322497888	0.04	1.34	16 (3)	133.77		glutaminyl-tRNA synthetase, putative	6.58e+006	4.93e+006
322502866	8.01e-004	1.31	15 (5)	318.63		ATP-dependent DEAD-box RNA helicase, putative	1.29e+007	9.82e+006
322496663	0.04	1.56	13 (2)	201.10		ATP-dependent DEAD/H RNA helicase, putative	4.39e+006	2.82e+06
68235787	3.18e-004	5.06	9 (2)	197.04		histone H2B protein	1.07e+07	2.11e+06
322498355	0.04	1.54	7 (1)	197.38		prolyl-tRNA synthetase, putative, partial	7.46e+05	4.83e+05
322503349	0.03	1.25	19 (4)	212.95		polyadenylate-binding protein 1, putative	3.00e+007	2.39e+007
322503415	8.95e-003	1.45	22 (2)	234.71		Mitochondrial elongation factor G, putative	4.33e+006	2.99e+006
322503916	0.03	1.32	8 (2)	105.09		branch point binding protein, putative	2.37e+006	1.79e+006
Stress and protein folding								
322502093	0.02	3.27	54 (3)	1817.23		heat shock protein 83-1	1.74e+007	5.32e+006
12232034	0.04	1.24	32 (1)	319.92		chaperonin TCP20	2.16e+006	1.73e+006
123669	0.03	3.72	33 (2)	908.40		RecName: Full=Heat shock protein 83; Short=HSP 83; AltName: Full=HSP 90	3.88e+006	1.04e+006
322497565	0.03	1.10	26 (5)	405.24		chaperonin TCP20, putative	1.44e+007	1.32e+007
322503363	0.04	2.43	11 (2)	289.24		stress-inducible protein STI1 homolog	4.15e+006	1.71e+006
322504075	0.03	1.28	24 (8)	729.49		protein disulfide isomerase	4.07e+007	3.17e+007
145411494	0.02	1.07	11 (2)	215.58		cytoplasmic tryparedoxin peroxidase	1.08e+007	1.00e+007
Metabolic processes								
16797868	0.03	1.48	39 (9)	1033.69		glucose-regulated protein 78, partial	2.76e+007	1.87e+007
322502940	0.03	1.51	53 (18)	961.31		NADH-dependent fumarate reductase, putative	3.00e+007	1.99e+007
322502306	0.04	1.44	28 (2)	645.87		succinyl-coA:3-ketoacid-coenzyme A transferase, mitochondrial precursor, putative	2.13e+006	1.47e+006
322500910	0.04	1.15	24 (9)	562.03		ATP-dependent phosphofructokinase	1.15e+007	9.96e+006
322500647	1.13e-003	1.41	4 (2)	90.64		glucose 6-phosphate N-acetyltransferase, putative	4.98e+006	3.52e+006
322503662	0.02	1.23	17 (3)	552.53		succinyl-CoA ligase [GDP-forming] beta-chain, putative	5.32e+006	4.34e+006

Accession	Anova (P*)	Folds	Peptides (Peptides in quantitation)	Score	Tags	Description	Average Normalized Abundance	
							Treated	Control
322503492	2.88e-03	1.74	19 (2)	186.23		N-acetyltransferase subunit Nat1, putative	5.97e+06	3.43e+06
148913117	0.04	1.62	15 (3)	181.43		glycogen synthase kinase 3 short	4.71e+06	2.91e+06
322497288	4.36e-003	1.27	37 (9)	657.91		pyruvate phosphate dikinase, putative	1.02e+007	8.04e+006
322502415	9.44e-004	1.60	13 (1)	331.12		malate dehydrogenase	5.72e+006	3.57e+006
322497392	1.55e-003	1.96	9 (3)	158.65		cytochrome c oxidase subunit IV	9.15e+006	4.66e+006
322502326	0.02	1.35	14 (6)	300.21		isocitrate dehydrogenase, putative	7.32e+006	5.40e+006
322498469	6.07e-003	1.21	14 (4)	232.64		glycosomal malate dehydrogenase	4.17e+006	3.45e+006
190335775	0.04	1.33	33 (8)	1021.25		enolase	1.05e+007	7.86e+006
322502960	5.32e-003	1.71	17 (4)	394.15		mitochondrial processing peptidase, beta subunit, putative	1.06e+007	6.18e+006
322503715	0.02	1.67	22 (12)	382.32		2-oxoglutarate dehydrogenase E1 component, putative	6.41e+006	3.85e+006
322497501	0.04	1.26	19 (5)	311.09		mitochondrial processing peptidase alpha subunit, putative	6.13e+007	4.85e+007
322500587	9.51e-003	1.55	9 (3)	127.36		2-oxoglutarate dehydrogenase, E2 component, dihydrolipoamide succinyltransferase, putative	3.64e+006	2.35e+006
322496602	0.02	2.14	5 (1)	60.63		dihydrofolate reductase-thymidylate synthase	7.01e+005	3.28e+005
322500467	0.02	1.69	7 (2)	119.16		phenylalanine-4-hydroxylase, putative	2.50e+006	1.48e+006
322498779	0.02	1.78	8 (2)	109.23		mitochondrial processing peptidase alpha subunit, putative	1.87e+006	1.05e+006
322502201	0.03	1.56	6 (2)	105.24		cysteine conjugate beta-lyase, aminotransferase-like protein (pyruvate metabolism)	7.29e+006	4.69e+006
322501324	0.02	1.52	22 (5)	491.49		5-methyltetrahydropteroyltriglutamate-homocysteine S-methyltransferase, putative (Methionine metabolism)	8.51e+006	5.61e+006
322502231	4.73e-003	1.16	6 (2)	173.98		peptidase M20/M25/M40, putative	3.98e+006	3.42e+006
322499163	0.04	1.66	14 (2)	199.28		(H+)-ATPase G subunit, putative	2.23e+006	1.35e+006
Protein turnover and modification								
322502952	0.03	1.27	9 (2)	426.04		ubiquitin-conjugating enzyme e2, putative	1.14e+007	8.93e+006

Accession	Anova (P*)	Folds	Peptides (Peptides in quantitation)	Score	Tags	Description	Average Normalized Abundance	
							Treated	Control
322503495	7.69e-003	1.22	40 (15)	898.84		Transitional endoplasmic reticulum ATPase, putative	3.49e+007	2.87e+007
322500536	0.03	1.30	9 (6)	115.89		X-pro, dipeptidyl-peptidase,serine peptidase, Clan SC, family S15, putative	4.21e+006	3.25e+006
478212838	0.01	1.26	10 (5)	84.48		cysteine protease b	1.01e+007	8.01e+006
322497214	0.03	1.19	12 (6)	198.50		proteasome alpha 7 subunit, putative	9.22e+007	7.77e+007
322497557	0.04	1.46	10 (4)	198.12		ubiquitin-conjugating enzyme-like protein	6.97e+06	4.76e+06
Cytoskeleton and cell motility								
322497027	5.37e-003	1.40	23 (6)	295.01		paraflagellar rod component, putative	2.84e+006	2.03e+006
299829504	0.01	2.16	42 (10)	1952.49		beta tubulin	1.57e+008	7.27e+007
6708172	0.03	1.43	8 (4)	300.18		ADP-ribosylation factor-like protein 3A	2.60e+006	1.82e+006
322496512	5.60e-03	1.62	16 (4)	184.04		prefoldin subunit, putative	1.03e+07	6.38e+06
Fatty acids								
322499210	0.05	1.47	28 (9)	710.85		3-ketoacyl-CoA thiolase-like protein	1.39e+007	9.48e+006
322497652	1.85e-003	14.86	4 (1)	109.81		fatty acid elongase, putative	8.63e+005	5.80e+004
322499741	0.02	1.47	7 (2)	104.12		3-oxo-5-alpha-steroid 4-dehydrogenase, putative	4.25e+006	2.89e+006
322499090	2.68e-003	2.07	6 (2)	93.29		farnesyl pyrophosphate synthase	2.07e+006	9.96e+005
Signalling, Transporters and membrane proteins								
151413555	7.83e-003	1.46	21 (5)	392.70		adenylate nucleotide translocase	1.33e+007	9.11e+006
5813867	0.04	1.62	12 (1)	300.51		putative pteridine transporter FT3	1.48e+007	9.10e+006
322503191	0.01	1.20	15 (5)	406.76		Gim5A protein, putative	1.54e+007	1.28e+007
322499307	0.01	1.58	8 (1)	112.93		vacuolar proton translocating ATPase subunit A, putative	2.86e+006	1.80e+006
322497687	0.04	1.64	6 (1)	62.86		ADP/ATP mitochondrial carrier-like protein	4.80e+005	2.92e+005
322497170	0.01	1.25	5 (3)	78.82		rab1 small GTP-binding protein, putative	2.59e+006	2.07e+006
322502740	0.03	1.47	23 (4)	312.96		vacuolar ATP synthase catalytic subunit A, putative	2.01e+006	1.37e+006
322501447	0.04	1.30	10 (2)	237.88		vacuolar-type proton translocating pyrophosphatase 1, putative	1.14e+007	8.76e+006
322496444	5.23e-003	1.57	17 (4)	466.13		ATPase alpha subunit	1.63e+007	1.04e+007
322498413	0.02	1.26	11 (4)	189.73		protein kinase, putative	2.55e+06	2.02e+06
Nucleic acid								

Accession	Anova (P*)	Folds	Peptides (Peptides in quantitation)	Score	Tags	Description	Average Normalized Abundance	
							Treated	Control
322498952	9.58e-003	1.12	17 (5)	326.04		centromere/microtubule binding protein cbf5, putative	3.45e+006	3.09e+006
322498624	0.02	1.24	15 (4)	201.35		cytidine triphosphate synthase, putative	4.05e+006	3.26e+006
322497534	0.03	1.79	17 (3)	272.86		adenylosuccinate synthetase, putative (purine metabolism)	1.30e+007	7.29e+006
Hypothetical proteins								
322502830	0.05	1.41	5 (3)	60.28		unnamed protein product, partial	2.58e+006	1.82e+006
322497208	0.04	1.53	5 (2)	58.37		hypothetical protein, conserved	2.25e+006	1.47e+006
322501229	0.04	1.31	4 (2)	54.47		hypothetical protein, conserved	2.78e+006	2.12e+006
322501847	0.02	2.62	6 (2)	27.39		hypothetical protein, unknown function	2.71e+006	1.03e+006
322498448	0.01	4.65	4 (1)	26.88		hypothetical protein, conserved	4.00e+005	8.60e+004
322502714	0.04	1.33	6 (1)	75.50		hypothetical protein, conserved	1.68e+006	1.27e+006
322497611	1.45e-003	1.57	3 (1)	77.89		hypothetical protein, conserved	4.82e+006	3.07e+006
322497181	0.02	1.62	6 (1)	73.13		hypothetical protein, conserved	7.13e+006	4.39e+006
322499167	0.01	1.53	4 (1)	72.42		hypothetical protein, conserved	2.47e+006	1.61e+006
322498140	4.14e-003	1.27	5 (2)	85.40		hypothetical protein, conserved	4.58e+006	3.62e+006
322502559	8.21e-003	1.29	8 (5)	96.53		hypothetical protein, conserved	1.62e+007	1.26e+007
322500809	4.22e-004	2.53	8 (1)	106.38		hypothetical protein, conserved	1.33e+006	5.25e+005
322502778	0.04	1.63	5 (2)	113.50		hypothetical protein, conserved	5.08e+006	3.11e+006
322503307	3.70e-005	2.31	10 (4)	117.83		hypothetical protein, conserved	1.12e+007	4.84e+006
322500012	0.01	1.57	5 (2)	123.32		hypothetical protein, conserved	2.54e+006	1.62e+006
322503312	2.62e-003	2.78	12 (1)	126.28		hypothetical protein, conserved	1.64e+006	5.92e+005
322498829	0.03	1.31	15 (2)	130.64		hypothetical protein, conserved	4.36e+007	3.32e+007
322498659	0.03	1.41	10 (4)	129.48		hypothetical protein, conserved	6.22e+006	4.42e+006
322501903	0.03	1.89	14 (1)	151.47		hypothetical protein, conserved	4.06e+006	2.14e+006
322502401	0.01	1.96	16 (4)	163.46		hypothetical protein, conserved	2.57e+006	1.31e+006
322496063	0.04	1.33	21 (8)	212.80		hypothetical protein, conserved	9.06e+006	6.82e+006
322497523	0.03	1.20	25 (7)	207.01		hypothetical protein, unknown function	2.06e+007	1.71e+007
322502955	0.02	1.75	11 (4)	229.44		hypothetical protein, conserved	2.20e+007	1.26e+007
322496696	0.05	1.16	20 (5)	228.43		hypothetical protein, conserved	5.87e+006	5.05e+006
322499284	0.02	2.30	8 (1)	254.93		hypothetical protein, conserved	7.81e+005	3.40e+005
322503433	0.01	4.20	16 (5)	240.22		hypothetical protein, conserved	1.25e+007	2.97e+006
322501739	0.01	1.30	11 (4)	374.99		hypothetical protein, conserved	1.26e+007	9.70e+006
322496809	0.03	1.58	49 (12)	379.88		hypothetical protein, conserved	2.48e+007	1.57e+007

Accession	Anova (P*)	Folds	Peptides (Peptides in quantitation)	Score	Tags	Description	Average Normalized Abundance	
							Treated	Control
322496585	1.58e-003	1.75	38 (6)	312.42		hypothetical protein, conserved	1.00e+007	5.73e+006
322496901	0.04	1.35	28 (4)	395.31		hypothetical protein, conserved	4.16e+007	3.07e+007
322496996	0.04	1.44	20 (6)	555.79		hypothetical protein, conserved	1.72e+007	1.20e+007
322500235	0.04	1.21	27 (5)	193.20		hypothetical protein, conserved	7.68e+006	6.36e+006
322502308	0.02	1.51	13 (1)	186.52		hypothetical protein, conserved	2.30e+06	1.52e+06

Table 4.2: Distribution of down regulated proteins after hypericin treatment into major categories. Here represents the down regulated proteins after hypericin treatment with ANOVA value of less than 0.05.

Accession	Anova (P*)	Folds	Peptides (Peptides in quantitation)	Score	Tags	Description	Average Normalized Abundance	
							Treated	Control
Transcription/Translation/Protein synthesis								
322500439	0.05	0.95	12 (3)	337.51		ribosomal protein S20, putative	3.23e+006	3.39e+006
322498212	0.05	0.75	13 (6)	160.66		translation initiation factor, putative	3.54e+006	4.72e+006
322500281	0.04	0.63	8 (1)	104.82		RNA-binding protein, putative	4.72e+005	7.47e+005
322503038	0.01	0.83	7 (4)	78.94		60S ribosomal protein L12, putative	7.11e+006	8.54e+006
322496746	2.71e-003	0.73	23 (6)	366.99		splicing factor ptsr1-like protein	6.50e+006	8.89e+006
Stress and protein folding								
322501328	0.02	0.46	2 (1)	33.66		cyclophilin, putative	1.57e+006	3.39e+006
Metabolic processes								
322500964	4.77e-003	0.73	10 (3)	155.73		2-hydroxy-3-oxopropionate reductase, putative	7.86e+006	1.08e+007
Protein turnover and modification								
322500105	0.01	0.76	7 (3)	283.01		proteasome alpha 7 subunit, putative	3.38e+006	4.44e+006
322503519	0.02	0.87	9 (3)	415.66		proteasome alpha 1 subunit, putative	6.10e+006	7.01e+006
Cytoskeleton and cell motility								
322497455	4.71e-003	0.70	11 (3)	105.39		flagellar radial spoke protein, putative	1.93e+006	2.76e+006
322498424	0.04	0.50	19 (6)	224.79		C-terminal motor kinesin, putative	1.43e+007	2.86e+007
Signalling, Transporters and membrane proteins								
322498892	0.02	0.55	10 (2)	95.98		vesicule-associated membrane protein, putative	1.42e+006	2.57e+006

Accession	Anova (P*)	Folds	Peptides (Peptides in quantitation)	Score	Tags	Description	Average Normalized Abundance	
							Treated	Control
325973870	9.88e-003	0.65	14 (1)	453.56		leishmanolysin, partial	9.56e+005	1.47e+006
322501606	0.02	0.79	5 (2)	115.91		ADP-ribosylation factor, putative	6.56e+006	8.30e+006
322501308	0.02	0.90	5 (3)	262.66		ATP synthase, epsilon chain, putative	1.00e+007	1.11e+007
322500321	0.04	0.76	8 (3)	71.71		protein kinase, putative	3.66e+006	4.83e+006
322501646	2.03e-004	0.70	4 (2)	55.93		protein kinase, putative	6.65e+007	9.50e+007
3724134	2.84e-003	0.87	5 (1)	178.77		HASPB1 protein	9.59e+006	1.10e+007
322497143	0.03	0.67	8 (3)	193.43		small GTP-binding protein Rab11, putative	4.62e+06	6.81e+06
Nucleic acid								
322503524	0.04	0.72	8 (5)	155.97		universal minicircle sequence binding protein (UMSBP), putative	1.80e+007	2.51e+007
322497959	0.03	0.87	9 (3)	125.16		aspartate carbamoyltransferase, putative	2.86e+006	3.28e+006
Hypothetical proteins								
322503652	7.08e-003	0.67	3 (1)	60.32		hypothetical protein, conserved	9.11e+005	1.36e+006
322499442	0.04	0.84	11 (4)	74.57		hypothetical protein, conserved	1.80e+006	2.14e+006
322502261	0.01	0.64	8 (3)	72.20		hypothetical protein, conserved	2.12e+006	3.32e+006
322501879	5.33e-003	0.82	6 (2)	91.16		hypothetical protein, conserved	4.66e+007	5.69e+007
322496451	1.66e-004	0.66	6 (3)	90.96		hypothetical protein, conserved	1.98e+008	2.98e+008
322502124	0.01	0.88	5 (4)	188.65		hypothetical protein, conserved	1.96e+07	2.21e+07
322502229	0.03	0.36	9 (1)	187.25		hypothetical protein, conserved	2.88e+05	7.96e+05
322501950	0.04	0.71	11 (3)	96.42		hypothetical protein, conserved	2.55e+006	3.60e+006
322496438	0.01	0.74	4 (1)	110.62		hypothetical protein, conserved	1.44e+007	1.95e+007
322498397	0.01	0.73	6 (2)	109.81		hypothetical protein, conserved	8.78e+006	1.20e+007
322503852	5.53e-003	0.83	11 (7)	113.24		hypothetical protein, conserved	8.56e+006	1.03e+007
322498975	1.17e-003	0.81	7 (3)	123.07		hypothetical protein, conserved	1.17e+006	1.45e+006
322501425	0.05	0.57	13 (4)	159.34		hypothetical protein, conserved	1.48e+006	2.61e+006
322498169	1.02e-003	0.61	12 (4)	172.14		hypothetical protein, conserved	5.79e+006	9.47e+006
322499746	0.03	0.47	15 (2)	214.38		hypothetical protein, conserved	5.84e+005	1.23e+006
322503960	0.04	0.79	18 (4)	226.67		hypothetical protein, conserved	1.61e+007	2.03e+007
322502578	0.03	0.91	31 (12)	256.67		hypothetical protein, conserved	5.50e+007	6.05e+007
322501429	9.67e-003	0.74	18 (7)	353.79		hypothetical protein, unknown function	1.21e+007	1.64e+007

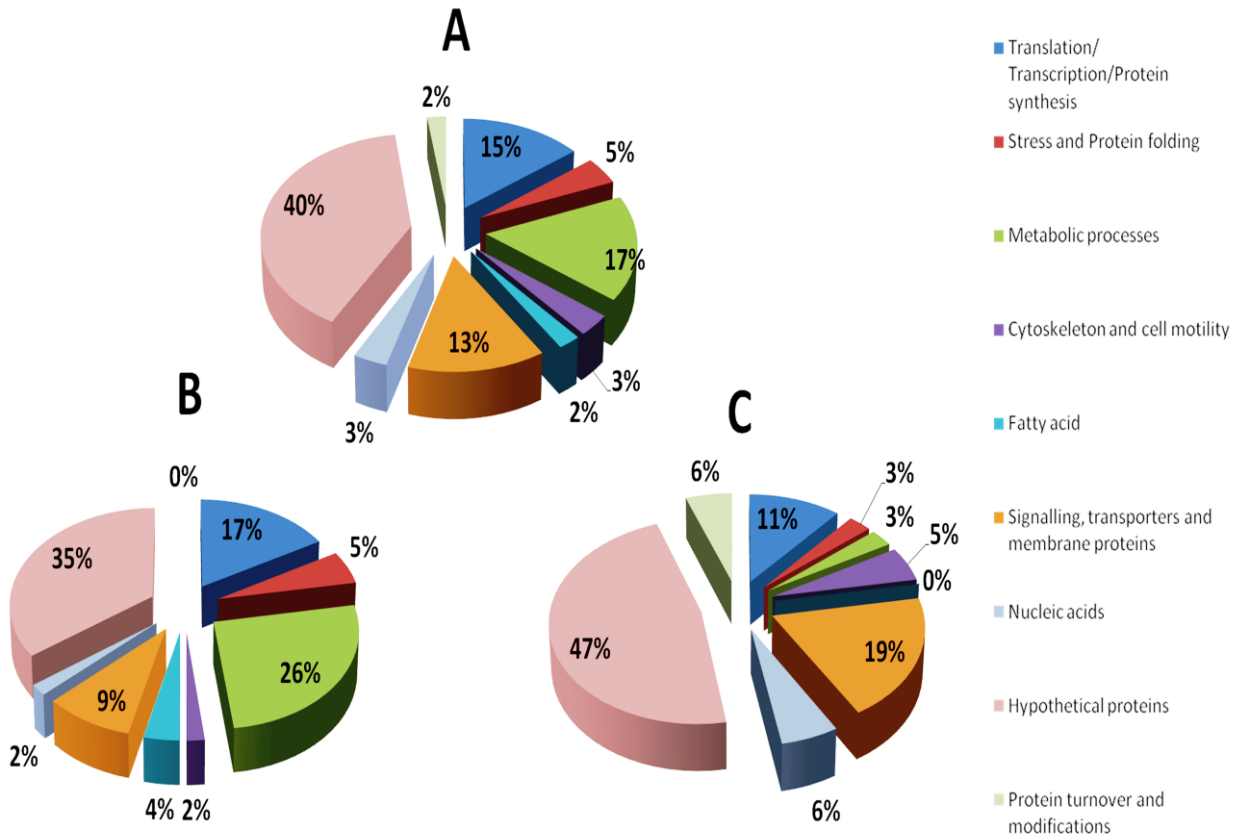

Figure 4.1: Pie chart showing relative distribution of differentially modulated proteins (up regulated above 1.5 fold and down regulated below 0.9 fold with ANOVA value less than 0.05) of *Leishmania donovani* after hypericin treatment. (A) Pie chart of total proteins being altered after hypericin treatment showing their relative distribution among 9 major categories. (B) Pie chart of up regulated proteins after hypericin treatment showing their relative distribution. (C) Pie chart of down regulated proteins after hypericin treatment showing their relative distribution.

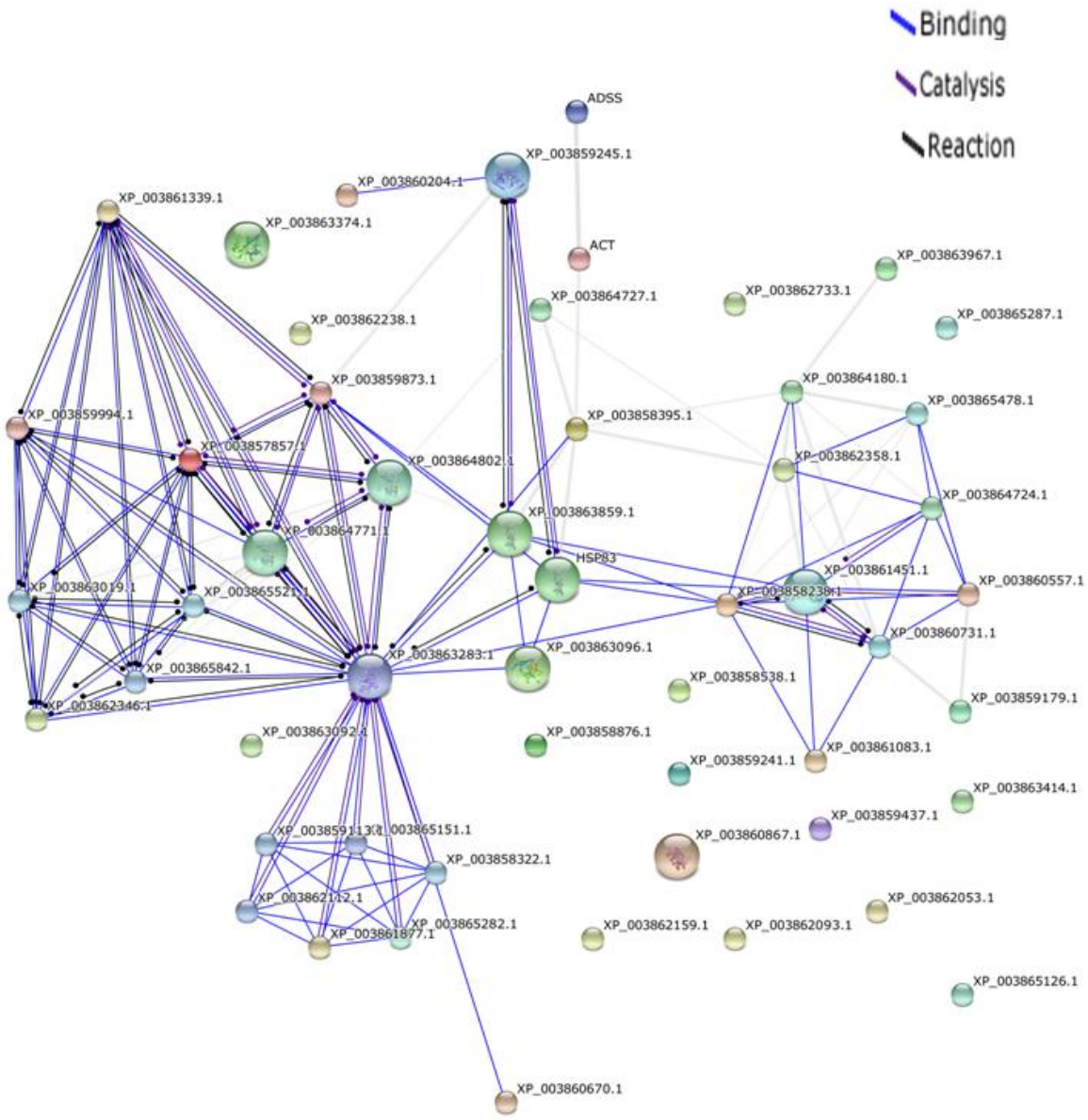

Figure 4.2: Protein protein interaction diagram of proteins up regulated above 1.5 fold and down regulated below 0.9 fold with ANOVA value less than 0.05. Protein-protein interactions between the proteins were analyzed by using STRING database. Here the thickness of the lines represents the strength of the association between two proteins.

Table 4.3: List of input protein list for protein interaction analysis with their accession numbers.

Accession Number	Name of Protein
XP_003857857.1	ribosomal protein S7, putative (200 aa)
XP_003858238.1	ATPase alpha subunit; Produces ATP from ADP in the presence of a proton gradient across the membrane (By similarity) (574 aa)
XP_003858395.1	dihydrofolate reductase-thymidylate synthase; Bifunctional enzyme. Involved in de novo dTMP biosynthesis. Key enzyme in folate metabolism (By similarity) (520 aa)
XP_003858538.1	splicing factor ptsr1-like protein (375 aa)
XP_003858876.1	folate/biopterin transporter, putative (691 aa)
XP_003859179.1	cytochrome c oxidase subunit IV (343 aa)
XP_003859241.1	flagellar radial spoke protein, putative (600 aa)
XP_003859245.1	alpha tubulin; Tubulin is the major constituent of microtubules. It binds two moles of GTP, one at an exchangeable site on the beta chain and one at a non-exchangeable site on the alpha chain (By similarity) (451 aa)
ADSS	adenylosuccinate synthetase, putative; Plays an important role in the salvage pathway for purine nucleotide biosynthesis. Catalyzes the first committed step in the biosynthesis of AMP from IMP (By similarity) (710 aa)
XP_003859437.1	fatty acid elongase, putative (280 aa)
ACT	aspartate carbamoyltransferase, putative (327 aa)
XP_003859873.1	elongation factor 1-alpha; This protein promotes the GTP-dependent binding of aminoacyl-tRNA to the A-site of ribosomes during protein biosynthesis (By similarity) (449 aa)
XP_003859994.1	translation initiation factor, putative (709 aa)
XP_003860204.1	C-terminal motor kinesin, putative (841 aa)
XP_003860557.1	mitochondrial processing peptidase alpha subunit, putative (467 aa)
XP_003860670.1	vesicule-associated membrane protein, putative (257 aa)
XP_003860867.1	farnesyl pyrophosphate synthase (362 aa)
XP_003861083.1	vacuolar proton translocating ATPase subunit A, putative (775 aa)
XP_003861339.1	poly(A)-binding protein, putative (544 aa)
XP_003861877.1	proteasome alpha 7 subunit, putative (238 aa)
XP_003862053.1	RNA-binding protein, putative (403 aa)
XP_003862093.1	protein kinase, putative (560 aa)
XP_003862159.1	major surface protease gp63, putative (566 aa)
XP_003862238.1	phenylalanine-4-hydroxylase, putative (452 aa)
XP_003862346.1	eukaryotic translation initiation factor, putative; Component of the eukaryotic translation initiation factor 3 (eIF-3) complex, which is involved in protein synthesis and, together with other initiation factors, stimulates binding of mRNA and methionyl-tRNAi to the 40S ribosome (By similarity) (405 aa)
XP_003862358.1	2-oxoglutarate dehydrogenase, E2 component, dihydrolipoamide succinyltransferase, putative (389 aa)

XP_003862733.1	2-hydroxy-3-oxopropionate reductase, putative (299 aa)
XP_003863092.1	5-methyltetrahydropteroyltriglutamate-homocysteine S-methyltransferase, putative (770 aa)
XP_003863096.1	cyclophilin, putative; PPIases accelerate the folding of proteins (By similarity) (229 aa)
XP_003863374.1	ADP-ribosylation factor, putative (178 aa)
XP_003863414.1	protein kinase, putative (429 aa)
XP_003863859.1	heat shock protein 83-1 (700 aa)
HSP83	heat shock protein 83-1; Molecular chaperone that promotes the maturation, structural maintenance and proper regulation of specific target proteins involved for instance in cell cycle control and signal transduction. Undergoes a functional cycle that is linked to its ATPase activity. This cycle probably induces conformational changes in the client proteins, thereby causing their activation. Interacts dynamically with various co-chaperones that modulate its substrate recognition, ATPase cycle and chaperone function (By similarity) (700 aa)
XP_003863967.1	cysteine conjugate beta-lyase, aminotransferase-like protein (414 aa)
XP_003864180.1	malate dehydrogenase (317 aa)
XP_003864724.1	mitochondrial processing peptidase, beta subunit, putative (490 aa)
XP_003864727.1	threonyl-tRNA synthetase, putative (788 aa)
XP_003864771.1	ribosomal protein L15, putative (204 aa)
XP_003864802.1	60S ribosomal protein L12, putative (164 aa)
XP_003865126.1	stress-inducible protein STI1 homolog (255 aa)
XP_003865282.1	proteasome alpha 1 subunit, putative; The proteasome is a multicatalytic proteinase complex which is characterized by its ability to cleave peptides with Arg, Phe, Tyr, Leu, and Glu adjacent to the leaving group at neutral or slightly basic pH. The proteasome has an ATP-dependent proteolytic activity (By similarity) (264 aa)

Table 4.4: List of predicted functional partners of input protein list used for protein protein interaction analysis.

Accession Number	Name of Protein
XP_003861451.1	hypothetical protein; (525 aa)
XP_003860731.1	ATP synthase F1 subunit gamma protein, putative (303 aa)
XP_003865521.1	eukaryotic translation initiation factor 3 subunit, putative (356 aa)
XP_003863019.1	eukaryotic translation initiation factor 3 subunit 7-like protein (531 aa)
XP_003858322.1	proteasome beta 6 subunit, putative (247 aa)
XP_003865842.1	eukaryotic translation initiation factor 3 subunit 8, putative (731 aa)
XP_003859113.1	hypothetical protein; (283 aa)
XP_003862112.1	proteasome beta 3 subunit, putative (205 aa)
XP_003865151.1	proteasome beta 2 subunit, putative (206 aa)
XP_003863283.1	ubiquitin-fusion protein (128 aa)

4.5 Discussion:

Previously we have analyzed that the hypericin induced death of the parasite is mainly because of altered hypusine modification due to spermidine starvation. Our studies reported in chapter III have revealed that the parasite also showed features of cytoprotective autophagy in response to DNA damage induced by reactive oxygen species. Here, we have analyzed the complete proteome of the *Leishmania donovani* after hypericin treatment. We have performed quantitative proteome analysis to analyze differentially modulated proteins after hypericin treatment. We have observed differential expression of proteins involved in several pathways.

We have observed increase in expression of Ribosomal protein S7 after hypericin treatment. Ribosomal protein S7 is encoded by str operon. It is reported that ribosomal protein S7 act as repressor of translation. In bacteria, the overexpression of ribosomal protein S7 results in translation repression by binding to str operon and causing ultimate reduction in bacterial growth. This repression would result in imbalance between transcription of rRNA and translation of various ribosomal proteins (*Robert and Brakier-Gingras, 2001*). Here, a significant increase in expression of ribosomal protein S7 could be a result altered hypusine modification. Significant decrease in RNA binding protein and translation initiation factor could be a direct result of defective hypusine modification of eIF5A. In addition to its role in transcription, RNA binding proteins are also known as regulators of translation (*Glisovic et al., 2008*). There has been decrease in proteasome alpha 7 subunit and proteasome alpha 1 subunit after hypericin treatment. Inhibition of ubiquitin proteasome system leads to the inhibition of hypusine modification and accumulation of unmodified eIF5A (*Jin et al., 2003*).

There was altered expression of stress related proteins like heat shock protein 90 and heat shock protein 83-1, stress inducible protein 1 and cyclophilin. It is reported that inhibition of HSP 90 decreases cellular response towards DNA damage due to radiation (*Sharma et al., 2012*). Here we have observed increased expression of HSP 90 after hypericin treatment suggesting response towards DNA damage induced by ROS generation. There was an increase in expression of stress inducible protein 1 (STI1) which is reported to be a cochaperone of HSP 90 after hypericin treatment. Hypericin treatment has decreased the expression of cyclophilin in *Leishmania* promastigotes. It is reported that mice lacking Ppif gene (forming cyclophilin D) was protected from cell death induced by oxidative

stress (*Baines et al., 2005*). This is in line with our previous studies which suggest that hypericin induced death of the parasite is independent of ROS generation.

All these alterations have led to the disturbed metabolism of the parasite as evident by altered expression of several genes involved in different metabolic pathways and biosynthesis. Overall, we have analyzed cascade of proteins involved in translational arrest leading to death of the parasite and those involved as a cytoprotective mechanism towards ROS induced DNA damage.

CHAPTER V

Molecular Docking and Structure Based Virtual Screening Studies of CAAX Prenyl Protease I and II of *Leishmania donovani*

5.1 Abstract:

In a search for developing drug molecules specifically targeting CAAX prenyl proteases of *Leishmania donovani*, we have modelled the structure of CAAX prenyl protease I and II by using homology modelling approach. The structures were further validated by using Ramachandran plot and ProSA. Active site prediction and electrostatic surface map of CAAX prenyl protease I and CAAX prenyl protease II have suggested significant difference in their activity. Molecular docking with known bisubstrate analogue inhibitors of protein farnesyl transferase and peptidyl (acyloxy) methyl ketones reveals significant binding of these molecules with CAAX prenyl protease I but comparatively less binding with CAAX prenyl protease II. New and potent inhibitors were also found by using structure based virtual screening. The best docked compounds obtained from virtual screening were subjected to induced fit docking to get best docked configurations. Prediction of drug like characteristics has revealed that the best docked compounds are in line with Lipinski's rule. Moreover, best docked protein-ligand complexes of CAAX prenyl protease I and II are found to be stable throughout 20 ns simulation. Overall, the study has identified potent drug molecules targeting CAAX prenyl protease I and II of *Leishmania donovani* whose drug candidature can be verified further by using biochemical and cellular studies.

**** Accepted for publication in Journal of Biomolecular Structure and Dynamics, 2016, 1-20.***

5.2 Introduction:

Despite of huge disease burden, leishmaniasis is one of the most neglected diseases since decades primarily because of its association with poverty. Although there is a wide arsenal of available drugs in the market, they suffer from serious limitations which include unacceptable host toxicity, lack of target specificity, poor efficacy, high cost and acquired parasite drug resistance (*Stuart et al., 2008*). In addition, the co-infection of leishmaniasis and Human immunodeficiency virus (HIV) infections is being emerging as a serious worldwide concern. Therefore, the development of vaccines, effective drugs for treatment and improved approaches of the disease diagnosis are now a matter of urgency. We have earlier targeted redox metabolism of the parasite for discovery of novel drug candidates with promising results (*Singh et al., 2008; Saudagar et al., 2013; Das et al., 2013; Singh et al., 2015*)

The post-translational modifications of biological molecules are known to be crucial for their functional activation, regulation and localization. Prenylation is one such modification which is involved in post-translational modification of various important proteins like proteins of Ras superfamily which are involved in a variety of regulatory and signalling events in eukaryotes. Prenylation is attachment of isoprenoid group (15C farnesyl or 20C geranylgaranyl group) to a cysteine residue in a thioether linkage. These prenylated proteins are found in different cellular compartments including nucleus, cytosol and membrane bound organelles. Most of the prenylated proteins belong to the Ras superfamily which are involved in a variety of cellular functions like cytokinesis, membrane trafficking, control of cell growth and differentiation etc. The targets for post-translational prenylation are the small GTP-binding proteins containing CAAX motif at or near its carboxyl terminus. These types of proteins undergo three different prenyl dependent processing for their ultimate maturation and localization (*Casey, 1992; Zhang and Casey, 1996*).

There are two types of CAAX prenyl proteases: type I and type II. The type I CAAX prenyl proteases are named as alpha-factor converting enzyme (AFC1). They are known to be metalloproteases with HEXXH conserved motif (where H is histidine, E is glutamate and X is any amino acid) in it (*Boyartchuk et al., 1997; Schmidt et al., 2000; Tam et al., 2001*). Type II CAAX prenyl proteases are called Ras and a-factor converting enzyme (RCE1). They lack the conserved motif present in type I CAAX prenyl proteases and their catalytic nature is still a topic of debate. However, they were suggested to

cysteine proteases based on the some inhibition studies and activity of cysteine, histidine and glutamate mutations. This is supported by the study that reveals the presence of cysteine residue near the active site of yeast RCE1P and it was found that upon mutation of this cysteine residue or by using cysteine protease inhibitors, the enzyme gets deactivated (*Dolence et al., 2000; Pei et al., 2011*). Few literatures suggest them to be metalloproteases (*Pei and Grishin, 2001; Pei et al., 2011*). It has been reported that yeast type I CAAX prenyl protease (AFC1p) and yeast type II CAAX prenyl protease have distinct but overlapping substrate specificity (Boyartchuk , Ashby, & Rine, 1997). Although Afc1p and RCE1P lack sequence similarity, both were found to proteolyse the a-factor CAAX sequence, CVIA. However, the a-factor CAAX sequence substituted by CAMQ and CTLM was found to be processed only by AFC1P and RCE1P respectively. Also, the yeast Ras2 protein (CIIS) was found to be catalysed by RCE1P but apparently not by yeast AFC1P. (*Boyartchuk et al., 1997; Trueblood et al., 2000*). In addition to its CAAX proteolysis activity, Ste24p, a type I CAAX prenyl protease of yeast, is found to have NH_2-terminal proteolysis activity for processing yeast a-factor precursor (*Tam et al., 2001*).

The role of CAAX processing has been demonstrated in various protein functions and trafficking by mutating cysteine of CAAX to another amino acid so as to prevent prenylation of protein (*Wright and Philips, 2006*). However, this cannot figure out the importance of CAAX prenyl proteases and methyl transferase since prenylation is a prerequisite for their activity. Their physiological importance were assessed when mouse embryonic fibroblast lacking RCE1 (CAAX prenyl protease II required for endoproteolysis) or ICMT (carboxyl methyl transferase required for carboxyl methylation of isoprenylcysteine) showed mislocalization of farnesylated Ras proteins (*Michaelson et al., 2005*). RCE1 deficiency was found to be lethal in late embryonic development in mouse which also affirms the physiological significance of CAAX prenyl proteases (*Kim et al., 1999*). It was also found that knock out of RCE1 results in pronounced impairment of growth in *Trypanosoma brucei* (*Gillespiea et al., 2007*). Recently, the type I yeast CAAX prenyl protease, STE24 is found to have play role in chitin synthesis (*Meissner et al., 2010*). It was found that variants of type I CAAX prenyl proteases (AFC1) in yeast showed reduction in a-factor production below detectable limit even in presence of type II CAAX prenyl protease, RCE1 (a-factor can also be processed by Rce1). This could be because of the loss of N-terminal processing of a-factor by AFC1P in combination with

partial defect in prenylation (*Trueblood et al., 2000*). Human AFC1 has been found to process farnesylated prelamin A by removing –AAX from the –CAAX sequence of prelamin A and also cleaving at sites 15 residues upstream of farnesylated cysteine. It was observed that accumulation of farnesylated prelamin A due to mutation in human AFC1 enzyme or prelamin A cleavage site was found in genetic diseases like Huchinson-Gilford progeria and Mandibuloacral dysplasia (*Gillespiea et al., 2007*).

From the above discussion, it is evident that both type I and type II CAAX prenyl proteases are involved in processing of various physiologically important proteins in different organisms. CAAX prenyl proteases of *Leishmania* have unique active site environment and low sequence similarity with CAAX prenyl proteases of human host. The sequence identity and query coverage with CAAX prenyl proteases I was 34% and 93%, respectively. Similarly, identity and query coverage with CAAX prenyl proteases II was 24% and 67%, respectively. It is possible to make structure based rational drug which can target these CAAX prenyl proteases of pathogen without interfering with the function of human counterparts. Recently, inhibitors against gBP21 protein essential for RNA editing in *Leishmania donovani* has been identified by using computational approach (*Sahoo et al., 2013*). Also, imidazole analogues have been identified as potential inhibitors of trypanothione reductase of *Leishmania donovani* by using molecular docking and virtual screening approach (*Pandey et al., 2015*). In this study, we have performed Homology modeling, Active site prediction, structure based virtual screening, ADME prediction and molecular dynamics simulations to find new and potent inhibitors for CAAX prenyl proteases I and II of *Leishmania donovani*. The current study will help in discovering new drug like molecules which could be possible inhibitors of CAAX prenyl proteases of *Leishmania donovani*.

5.3 Materials and Methods:

5.3.1 ***Sequence alignment and protein modelling*****:** The protein sequence of CAAX prenyl protease I (Accession No.: E9BTI9) and CAAX prenyl protease II (Accession No.: E9BIT3) were retrieved from UniProtKB database**.** The amino acid sequence was aligned by using Clustal Omega software. Three dimensional structure of CAAX prenyl protease I and CAAX prenyl protease II of *Leishmania donovani* were modelled using homology modelling. The homology modeling was done using Robetta. Robetta is a protein

structure prediction server. It uses a template based homology domain prediction method, Rosetta, to yield a high quality 3D structure of the target protein (*Kim et al., 2004*). The template used for the homology modeling of CAAX prenyl protease I is human nuclear membrane zinc metalloprotease ZMPSTE24 (PDB ID: 4AW6) and that for CAAX prenyl protease II is *Methanococcus maripaludis* homologue of RCE1 (PDB ID: 4CAD). At the initial stage of structure prediction, Ginzu, a domain prediction method was used to screen the query sequence for regions homologous to the experimentally characterized structure by using BLAST, PSI-BLAST, and Pcons2 (*Kim et al., 2004; Mount, 2007*). In second stage, sequences are fragmented into putative domains based on matches, known families and structures, multiple sequence information and secondary structure information. After domain parsing, each putative domain it follows, it assigns protocol track to generate the structure of the target protein.

5.3.2 *Validation*: The modelled structures of both CAAX prenyl protease I and II of *Leishmania donovani* were validated by using Structural Analysis and Verification Server (SAVES) (*Lakhlili et al., 2015; Baglo et al., 2013*). The PROSA tools were used to check the energy criteria against the potential mean force (*Wiederstei and Sippl, 2007*). Other parameters like ERRAT and Verify 3D were also checked using SAVES (*Yadav et al., 2014*). Other methods like ERRAT and Verify 3D were also employed from the SAVES server (Yadav et al., 2014).

5.3.3 *Protein preparation*: The coordinates of protein were further prepared using protein preparation wizard (Protein preparation wizard, Schrodinger, 2014) in Glide. Bond orders were assigned and hydrogen atoms were added to the modeled structure. Model was subjected to energy minimization using Optimized Potential for Liquid Simulations (OPLS-2005) and implicit solvation. The minimization was terminated when root mean square deviation (RMSD) of heavy atoms in the minimized structure executed 0.3 Å relative to the model structure.

5.3.4 *Active site prediction*: The ligand binding site of the receptor can be predicted through SiteMap available in Schrödinger Suite (SiteMap, version 3.0, 2014). SiteMap clusters all the regions of the site map based on the site score. A white color spheres was picked using Vander Waal's radius scaling factor of 1.0 and partial charge cutoff of 0.25. Here the position of the grid box was set on xyz axes with the measurements of x-value: 87.94, y-value: 55.59, and z-value: 54.43 with the radius of 2.0.

5.3.5 ***Electrostatic potential surface map*****:** The electrostatic potential surface of the protein was generated using create surface tool available in Maestro in order to find the electropositive as well as the electronegative regions of the protein surface. Here the blue color indicated the electropositive regions and the red color indicates the electronegative regions which are involved in the electron transfer activity of the protein and the ligands.

5.3.6 ***Ligand preparation*****:** A group of 16 compounds of bi substrate analogue, farnesyl transferase inhibitors (*Schlitzer et al., 2001*) and three compounds of peptidyl (acyloxy) methyl ketones (*Porter et al., 2007*) were collected from the literature and were prepared by using Ligprep module of Schrödinger suite (*LigPrep, version 2.9, 2014*). It can generate number of structures with various ionization states, tautomers, stereoisomers and ring conformations to eliminate molecules using various criteria including molecular weight or the specified numbers and types of functional groups present with the correct chiralities for each processed successful structure.

5.3.7 ***Molecular docking studies*****:** To test the docking parameters for the compounds under consideration, the compounds were docked into the predicted binding site of the modeled proteins using Grid-Based Ligand Docking with Energetics (Glide) module from Schrödinger(*Glide, version 6.2, 2014*). To soften the potential for non-polar parts of the receptor, we scaled Van der Waal radii of the receptor atoms by 1.00 with a partial atomic charge 0.25. A grid box with coordinates X = 24.391, Y = 26.441, Z = 29.382 was generated at the centroid of the active site. The ligands were docked with the active site using the extra precision glide docking (Glide XP). Glide generates the conformations internally and passes through the series of filters. The final best docked compounds were chosen using values of Glide score, Glide energy and Glide emodel (*Friesner et al., 2004; Friesner et al., 2006*).

5.3.8 ***Structure based virtual screening*****:** To find the novel inhibitor for CAAX prenyl protease I, Glide program was used to run high throughput virtual screening (HTVS), standard precision (SP) and extra precision (XP) protocols. Semi flexible docking protocols were used in docking simulations. The ligands being docked were kept in flexible, in order to examine the arbitrary number of torsional degrees of freedom spanned by the transitional and rotational parameters. The generated ligand poses were elapse through series of hierarchical filters that evaluated ligand interaction with its receptor. The best docked compounds were chosen based on Glide score (*Sastry et al., 2013; Reddy and Singh, 2014; Reddy et al., 2014*).

5.3.9 *Binding free energy calculations*: The top docked poses are subjected to binding free energy calculations using Prime/MM-GBSA approach (*Glide, version 6.2, Schrodinger, 2014*). This method is used to predict the binding free energy for a set of ligands to the receptor. Minimization of the docked poses using local optimization feature in Prime and the energies of the complex were calculated using OPLS-AA (2005) force field and generalized Born/surface area (GB/SA) continuum solvent model. Prime uses a surface generalized Born (SGB) model employing a Gaussian surface instead of Van der Waals surface for better representation of a solvent accessible surface area (*Suryanarayanan and Singh, 2014; Lyne et al., 2006*).

5.3.10 *Induced fit docking*: After identification of a set of compounds, their binding mode was further examined by Induced Fit Docking method (*Induced Fit Docking, Schrodinger, 2014*). Initially, Glide XP docking of chosen hits to the rigid receptor was performed. Prime was used to generate maximum 20 poses for each ligand and the residues within 5 Å of 20 poses. Receptor side chain flexibility was introduced while the coordinates of other residues and the backbone remain fixed. Finally, the ligands were rigorously redocked in Glide XP mode into the lowest energy induced fit receptor structure with no scaling (vdW scaling of 1) and their final scores were obtained (*Sherman et al., 2006; Suryanarayanan and Singh, 2014*).

5.3.11 *ADME properties*: The newly identified best compounds were studied for their absorption, distribution, metabolism and excretion (ADME) properties prior by using Qikprop. The required principle and physiochemical properties of drug compounds can be predicted by this module. It gives the detailed analysis of the log P (octanol/water), QP% (human oral absorption). It also evaluates the acceptability of the entire known and screened compounds on the basis of Lipinski's rule of 5, which is significant for rational drug design (*Suryanarayanan and Singh, 2014; Reddy et al., 2014*).

5.3.12 *Molecular dynamics simulations*: Molecular dynamics simulations (MD) were performed for the modelled as well as three best docked complexes of CAAX prenyl proteases I and II using Desmond module of Schrödinger and the OPLS –AA 2005 (Optimized Potential for Liquid Simulations- All Atom) force field for minimization of the system. CAAX prenyl proteases are reported to be membrane proteins (Seabra, 1998; Pie & Grishin, 2001), so we have performed molecular dynamics simulations of these proteins in DPPC lipid membrane with water solvent. The Desmond system builder was used at a 10 Å buffered orthorhombic system and periodic boundary conditions were

constructed using a DPPC lipid membrane and a TIP3P explicit water solvent. Salt concentration of 0.15M NaCl was added to the system. NPT ensemble was used to perform simulations. The pressure of 1.013 bar and temperature of 325K were kept constant coupling to a system to a Berendsen thermostat and barostat. Default membrane protein relaxation protocol was applied and each simulation was performed for 20 ns of time period (*Guo et al., 2010; Selvaraj et al., 2014; Tripathi et al., 2012; Mori and Okumura, 2013*).

5.4 Results:

5.4.1 ***Sequence alignment, protein modelling and validation*****:** The sequence of CAAX prenyl protease I and II were aligned with respect to their human counterparts and the alignment is represented in Figure 5.1C and Figure 5.1D respectively. The percent sequence identity between CAAX prenyl protease I of Human and *Leishmania donovani* is 35.24%. The percent sequence identity between CAAX prenyl protease II of human and *Leishmania donovani* is 24.12%. The predicted 3D structures of CAAX prenyl proteases I and II are shown in Figure 5.1A and 5.1B respectively. The model was further validated using Structural Analysis and Verification Server (SAVES) and PROtein Structure Analysis server (PROSA) server. Ramachandran plot, verify 3D, Errat and overall model quality were predicted. The results of structure validation of both CAAX prenyl protease I and CAAX prenyl protease II are given in Table 1 and 2. The realistic 3D structural qualities were evident for both the models from the validation parameters. Ramachandran plot of CAAX prenyl protease I shows that 96.1 % of amino acid residues lie in most favored regions, 3.4 % in additionally allowed regions, 0.5 % in generously allowed regions and G-score of 0.29 (Figure 5.2A and Table 5.1). Validation of CAAX prenyl protease II structure by Ramachandran plot shows 93 % residues in most favoured regions, 5.5 % in additionally allowed regions, 0 % in generously allowed regions and G-score of 0.19 (Figure 5.2B and Table 5.1).ERRAT plot for CAAX prenyl protease I and II show overall quality factor of 97.613 and 93.056 (Table 5.2). Verify 3D profile suggests that 81.5 % and 79.02 % residues of CAAX prenyl protease I and II respectively possess score over 0.2 (residues having a score of more than 0.2 are reliable) (Table 5.2). The Z-score is indicative of the overall quality of a model and verifies whether the predicted structure has a score within the range of z-scores of other native proteins of similar size (*Azam et al., 2014*). The Z scores of CAAX prenyl protease I and II are -7.52 and -4.45

respectively (Table 5.2). The PROSA plot for CAAX prenyl protease I is shown in Figure 5.2C and for CAAX prenyl protease II is shown in Figure 5.2D. Validation of the predicted models reveals their quality and allows the structure can be carried for further structure based studies.

5.4.2 *Active site prediction*: The active site of the protein was predicted through SiteMap which clusters the top ranked sites on the basis of site score. The site score and druggability score (D-score) of CAAX prenyl protease I are 1.083 and 1.124 respectively whereas the residues involved in the active site are His 409, Leu 385, Ile 388, Ser 389, Pro 410, Pro 411, Ile 280, Val 412,Leu 413, Val 283, Arg415, Leu 284, His 286, Asn 392, Glu 287, Ala 394 and Ser 395. The site score and druggability score for CAAX prenyl protease II are 0.817 and 0.827 respectively whereas the residues involved in the active site are Ala 11, Arg 22, Phe 12, Gln 23, Arg 79, Ala 15, Thr 8, Ile 72, Val 20, Glu 75, Gln 21 and Leu 76. Predicted active sites of both proteins are shown in Figure 5.3. It was also found that the predicted active sites are same as provide in literature (Pryor et. al., 2013). The contact score is a measure of interaction of receptors with the average site points. The contact score for CAAX prenyl protease I and II are 0.899 and 0.818 respectively, where average contact score for tight binding site is considered to be 1.0 (Table 5.3). The relative hydrophobicity and hydrophilicity of the site is measured by phobic and philic scores. The balance score refers to the ratio of phobic to philic scores. The average philic and phobic score for tight binding site is 1.0 whereas the average balance score is 1.6. The phobic, philic and balance score for CAAX prenyl protease I are 0.883, 0.848 and 1.041 respectively (Table 5.3). The phobic, philic and balance score for CAAX prenyl protease I are 1.214, 0.670 and 1.811 respectively (Table 5.3). The donor/acceptor property measures the ability with which a ligand can donate hydrogen bonds. The donor/acceptor score for CAAX prenyl protease I is 0.847 whereas for CAAX prenyl protease II is 0.750 (Table 5.3).

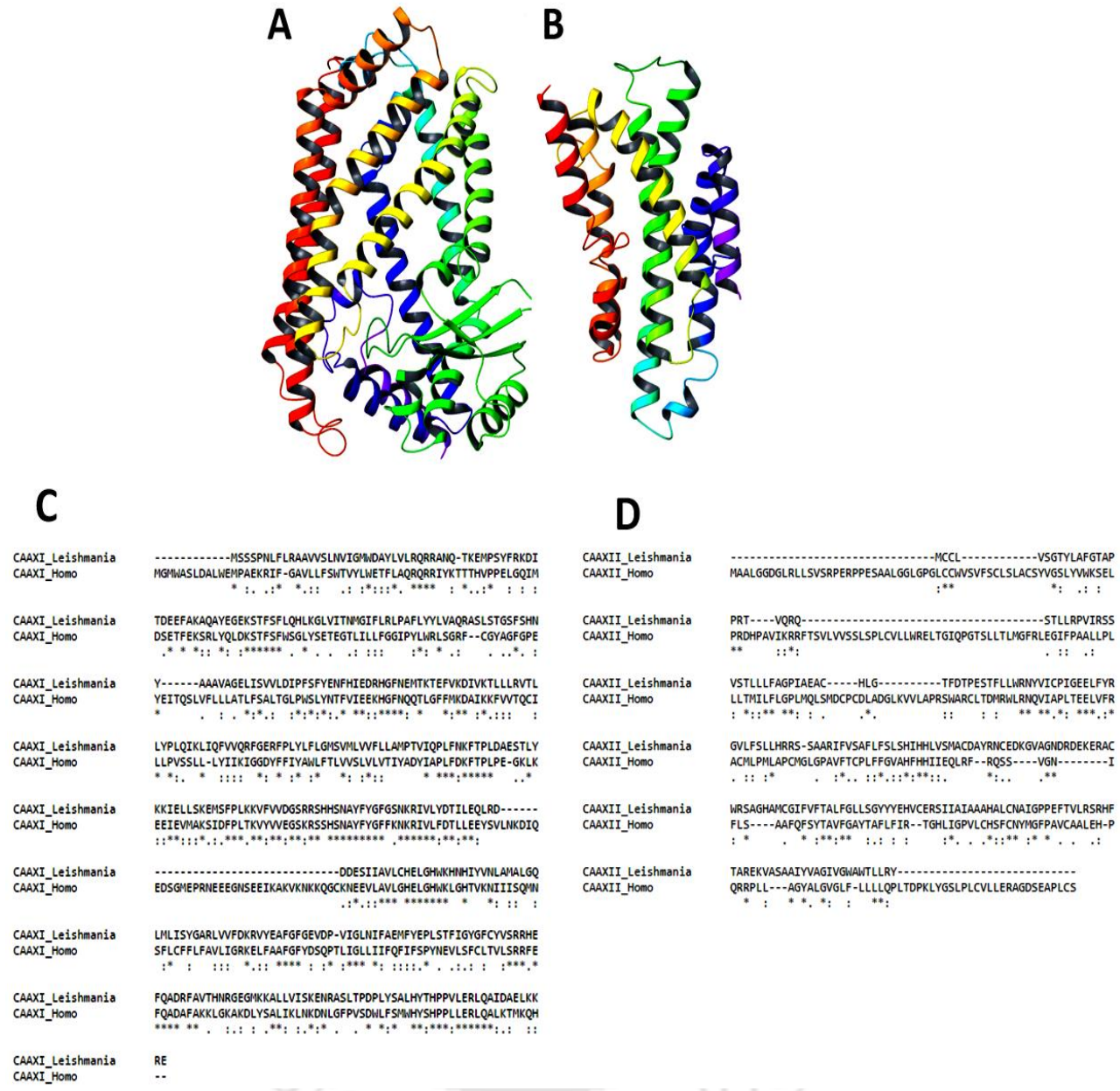

Figure 5.1: Sequence alignment and three dimensional structure of modeled proteins.The structure was modelled using homology modelling by using Robetta software. (A) The modelled structure of CAAX prenyl protease I usinghuman nuclear membrane zinc metalloprotease ZMPSTE24 (PDB ID: 4AW6) as template and (B) the modelled structure of CAAX prenyl protease II using *Methanococcus maripaludis* homologue of RCE1 (PDB ID: 4CAD) as template (C) Sequence alignment of CAAX prenyl protease I of *Leishmania donovani* and *Homo sapiens* (D) Sequence alignment of CAAX prenyl protease II of *Leishmania donovani* and *Homo sapiens*.

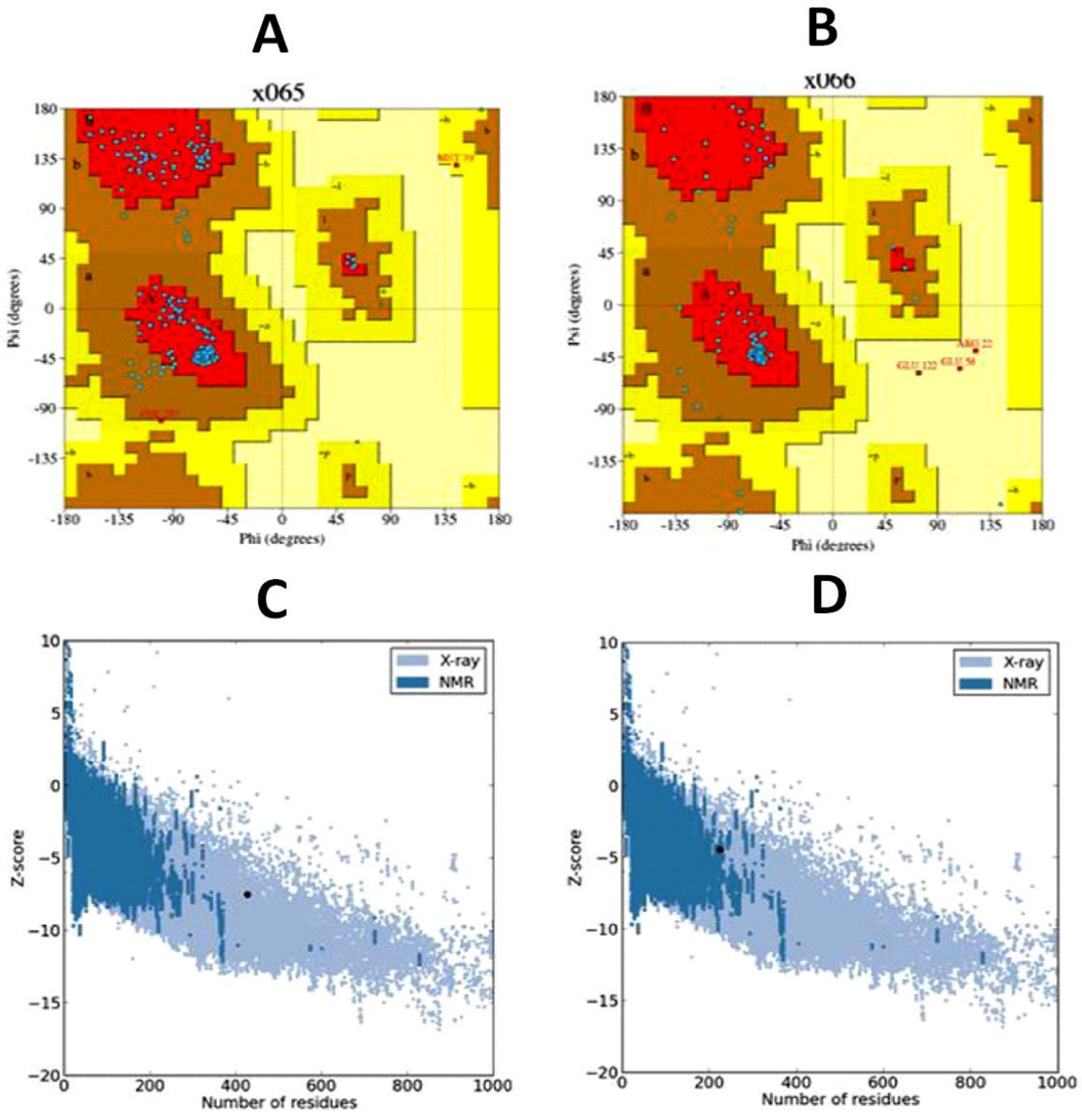

Figure 5.2: Validation of modelled structure of CAAX prenyl protease I and II using Ramachandran plot and ProSA. (A) Ramachandran plot for modelled CAAX prenyl protease I, (B) Ramachandran plot for modelled CAAX prenyl protease II, (C) Protein structure analysis (ProSA) for CAAX prenyl protease I and (D) Protein structure analysis (ProSA) for CAAX prenyl protease II. The red, brown, and yellow regions in A & B, represent the favored, allowed, and "generously allowed" regions respectively where the circles and squares represents the amino acids of protein.

Table 5.1: Validation of CAAX prenyl protease I and II by Ramachandran plot showing percentage of residues in most favoured regions, additional allowed regions, generously allowed regions, disallowed regions and G score.

Target Name	Most favoured regions	Additional allowed regions	Generously allowed regions	Disallowed regions	G Score
CAAX prenyl protease I	96.1	3.4	0.5	0.0	0.29
CAAX prenyl protease II	93.0	5.5	0.0	1.5	0.19

Table 5.2: Analysis of modelled structures of CAAX prenyl protease I and II by using SAVES (Structure Analysis Verification Server) and ProSA (protein structure analysis). ERRAT, Verify 3D and Z-score for both CAAX prenyl protease I and CAAX prenyl protease II are tabulated.

Target Name	ERRAT	Verify 3D	Z-Score
CAAX prenyl protease I	97.613	81.50	-7.52
CAAX prenyl protease II	93.056	79.02	-4.45

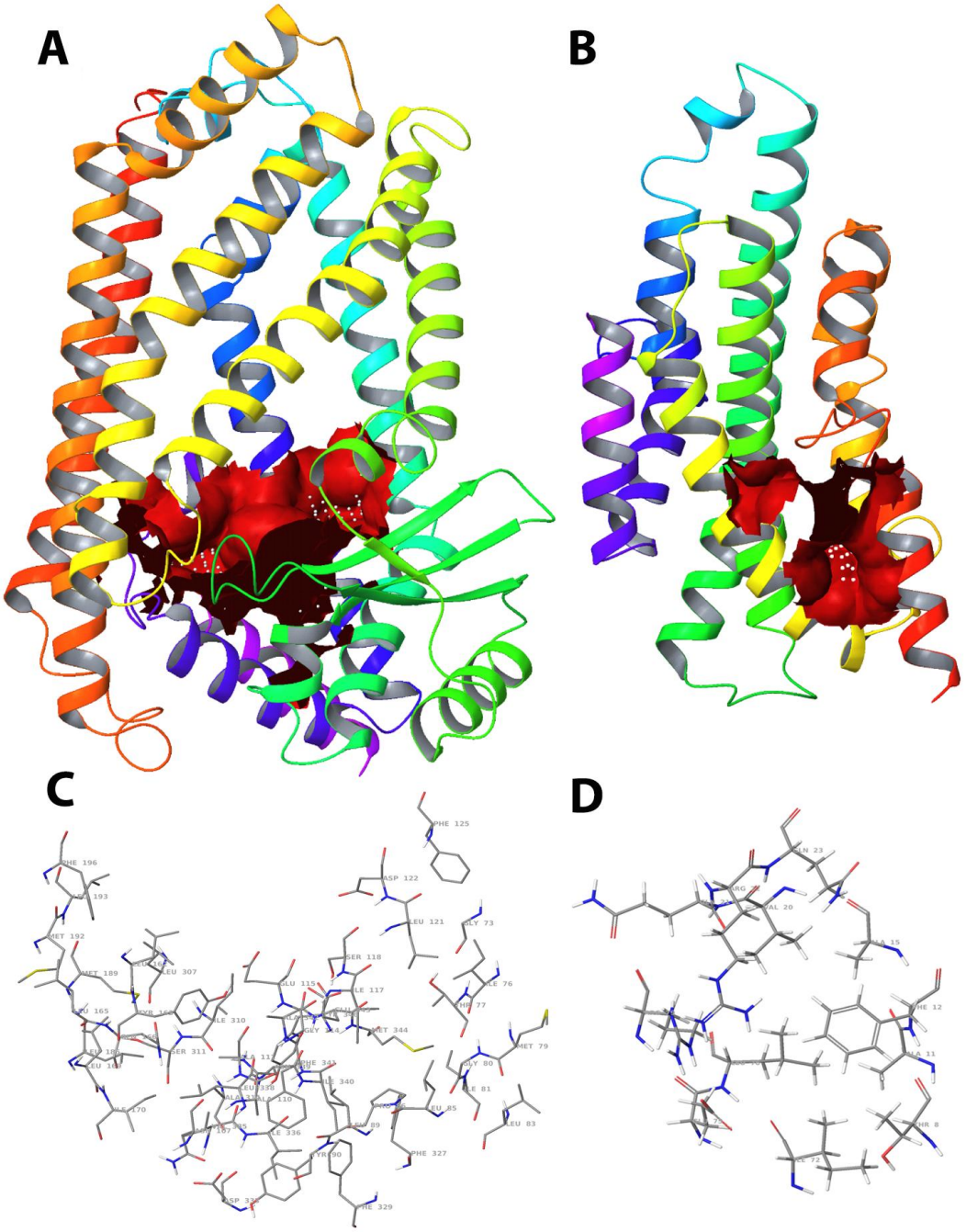

Figure 5.3: Active site regions of CAAX prenyl protease I (A) and II (B).The active sites of modelled CAAX prenyl protease I and II were predicted by using SiteMap software of Schrödinger Suite where the red contour surface with small white spheres represent the active site regions.

Table 5.3: Results of active site prediction of CAAX prenyl protease I and CAAX prenyl protease II by using SiteMap.

Target name	CAAX prenyl protease I	CAAX prenyl protease II
Site score	1.083	0.817
D score	1.124	0.827
Volume	527.191	90.895
Contacts	0.899	0.818
Phobic	0.883	1.214
Philic	0.848	0.67
Balance	1.041	1.811
Donor/Acceptor	0.847	0.75
Residues	His 409, Leu 385, Ile 388, Ser 389, Pro 410, Pro 411, Ile 280, Val 412, Leu 413, Val 283, Arg 415, Leu 284, His 286, Asn 392, Glu 287, Ala 394, Ser 395	Ala 11, Arg 22, Phe 12, Gln 23, Arg 79, Ala 15, Thr 8, Ile 72, Val 20, Glu 75, Gln 21, Leu 76

5.4.3 ***Electrostatic potential Surface of protein*****:** The electrostatic potential surface of the protein was generated using molecular mechanics method which reveals the electropositive and electronegative potential regions of the protein. The predicted electrostatic surface contour for CAAX prenyl protease I is shown in figure 5.4A and for CAAX prenyl protease is shown in Figure 5.4B. Here, the blue color indicates the electropositive regions and the red color indicates the electronegative regions. Figure 5.4 reveals that CAAX prenyl protease I has more electropositive regions whereas electronegative regions were more in active site of CAAX prenyl protease II. This result reflects the difference in activity of both proteins.

5.4.4 ***Molecular docking studies*****:** To carry out the docking studies we have taken two sets of inhibitors namely, bi substrate analogue inhibitors of protein farnesyl transferase of 16 derivative compounds and peptidyl (acyloxy) methyl ketones of three compounds. Bi substrate analogue inhibitors are substrate mimetics containing both peptidomimetic and farnesylmimetic (Porter et al., 2007). The IUPAC name of bisubstrate analogue inhibitors and Peptidyl (acyloxy) methyl ketones are mentioned in Table 5.4 and Table 5.5 respectively. Extra precision docking was carried out by glide module in the Schrödinger software package. The results of docking of known inhibitors with CAAX prenyl protease

I were represented in Table 5.6 and the docking results of CAAX prenyl protease II were given in Table 5.7.

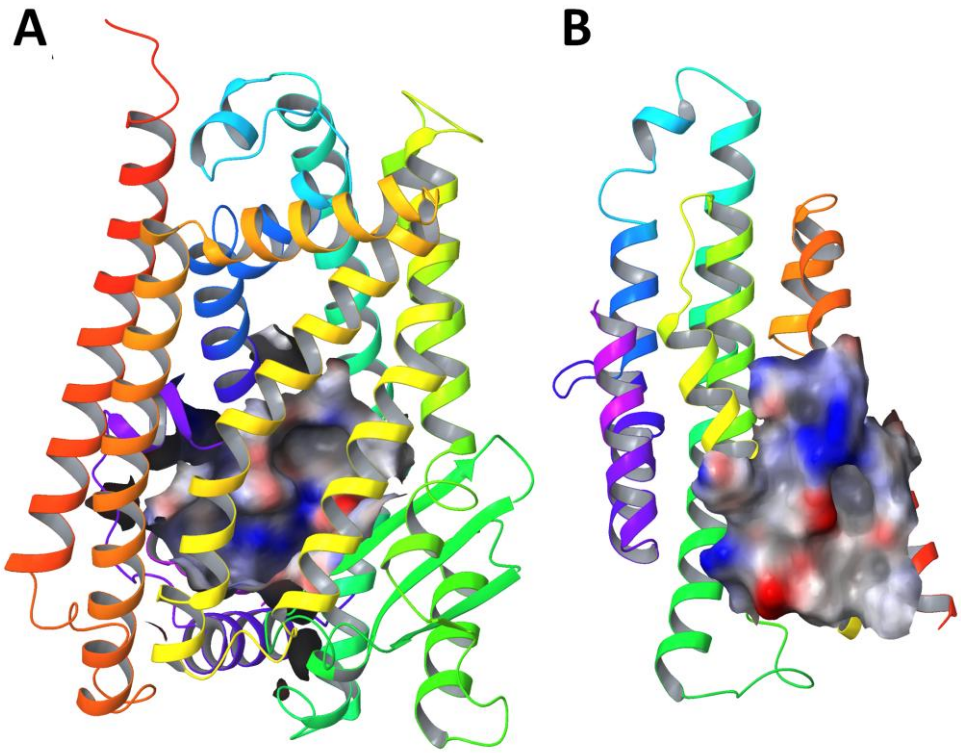

Figure 5.4: Electrostatic potential surface map of active site of (A) CAAX prenyl protease I (B) CAAX prenyl protease II. Here the blue colour is indicative of electropositive regions whereas the red colour represents electronegative regions of the proteins.

In order to assess the interference with the function of analogous enzyme of human, all the inhibitors were docked to the active site of human CAAX prenyl protease I and the results are provided in Table 5.8. The docking results of human and *Leishmania* CAAX proteins reveals that there will be no interference in function as the interacting residues, docking scores and binding energy values have no similarity. Among bi substrate analogue inhibitors, compound 8 (**IUPAC name:** N-{2-[(3-{[2-(1H-indol-3-yl)ethyl]sulfamoyl}phenyl)carbamoyl]ethyl}hexadecanamide) has shown the lowest docking score of -9.811 indicating its best binding with CAAX prenyl protease I. However, among all the screened peptidyl(acyloxy)methyl ketones, Y(FGBK(CH3)2 has shown lowest docking score of -10.391. It was found from the docking result that the known compound taken for the study are having good binding with CAAX prenyl

protease I whereas CAAX prenyl protease II have very low docking scores with all the known compounds. It reflects the difference in active site between both proteins. It was also found that Zn metal ion was playing important role in binding in case of CAAX prenyl protease I. Binding energy calculated for the all protein ligand complexes support the docking results.

Table 5.4: IUPAC name of non-peptidic, non-prenylic inhibitors (bisubstrate analogue inhibitors).

S. No	Compound name	IUPAC Name
1	Compound 1	methyl (2S)-2-{[4-(3-hexadecanamidopropanamido)phenyl]formamido}-4-(methylsulfanyl)butanoate
2	Compound 2	methyl (2S)-2-{[4-(3-hexadecanamidopropanamido)benzene]sulfonamido}-4-(methylsulfanyl)butanoate
3	Compound3	methyl (2S)-2-({4-[(3-hexadecanamido-2-oxopropyl)amino]phenyl}formamido)-4-(methylsulfanyl)butanoate
4	Compound4	N-(2,3-dimethylphenyl)-3-(3-hexadecanamidopropanamido)benzamide
5	Compound5	N-[2-({3-[(2,3-dimethylphenyl)sulfamoyl]phenyl}carbamoyl)ethyl]hexadecanamide
6	Compound6	N-[2-({3-[(2,3-dimethylnaphthalen-1-yl)sulfamoyl]phenyl}carbamoyl)ethyl]hexadecanamide
7	Compound7	N-[2-({3-[(naphthalen-1-ylmethyl)sulfamoyl]phenyl}carbamoyl)ethyl]hexadecanamide
8	Compound8	N-{2-[(3-{[2-(1H-indol-3-yl)ethyl]sulfamoyl}phenyl)carbamoyl]ethyl}hexadecanamide
9	Compound9	N-[2-({3-[(2,3-dimethylphenyl)sulfamoyl]phenyl}carbamoyl)ethyl]tetradecanamide
10	Compound10	N-[2-({3-[(2,3-dimethylphenyl)sulfamoyl]phenyl}carbamoyl)ethyl]octadecanamide
11	Compound11	(9Z)-N-[2-({3-[(2,3-dimethylphenyl)sulfamoyl]phenyl}carbamoyl)ethyl]octadec-9-enamide
12	Compound12	(9Z,12Z)-N-[2-({3-[(2,3-dimethylphenyl)sulfamoyl]phenyl}carbamoyl)ethyl]octadeca-9,12-dienamide
13	Compound13	N-[2-({3-[(2,3-dimethylphenyl)sulfamoyl]phenyl}carbamoyl)ethyl]-N-methylhexadecanamide
14	Compound14	N-[({3-[(2,3-dimethylphenyl)sulfamoyl]phenyl}carbamoyl)methyl]heptadecanamide

15	Compound15	N-[3-({3-[(2,3-dimethylphenyl)sulfamoyl]phenyl}carbamoyl)propyl]pentadecanamide
16	Compound16	(2E)-N-[2-({3-[(2,3-dimethylphenyl)sulfamoyl]phenyl}carbamoyl)ethyl]-3-(4-phenylphenyl)prop-2-enamide

Table 5.5: IUPAC name of peptidyl (acyloxy) methyl ketones.

S. No	Compound Name	IUPAC Name
1	(FABK(CH3)3)	(3S)-3-[(2S)-2-{[(benzyloxy)carbonyl]amino}-3-phenylpropanamido] -2-oxobutyl 2,4,6- trimethylbenzoate
2	Y(FGBK(CH3)2	(3S)-3-[(2S)-2-[(2S)-2-acetamido-3-(4-hydroxyphenyl)propanamido]-3-phenylpropanamido]-2-oxobutyl 2,6-dimethylbenzoate
3	(FKBK(CH3)3)	(3S)-7-amino-3-[(2S)-2-{[(benzyloxy)carbonyl]amino}-3-phenylpropanamido]-2-oxoheptyl 2,4,6-trimethylbenzoate

5.4.5 ***Structure based virtual screening*****:** In order to find the new and potent inhibitors against CAAX prenyl protease I and II, structure based virtual screening has been performed based on active site of both proteins. Three databases namely, Asinex, Life chemicals and Maybridge having 55958, 288651 and 93148 structures respectively were used for virtual screening. Initially, we performed docking using HTVS which is helpful in rapid screening of the ligands and is the least computationally intense process. Ligands were selected for further steps on the basis of docking score. These ligands were docked with the same receptor using SP docking protocol. The top 10% compounds from SP docking are selected on the basis of docking score and and carried further for XP docking method. XP docking method is a powerful and discriminative procedure. The total of 52 compounds from Asinex, 206 compounds from Life Chemicals and 66 compounds from Maybridge for CAAX prenyl protease I and II were resulted from XP docking method. Best screened compounds for CAAX prenyl protease I and II are tabulated in Table 5.9 and 5.10 respectively. It is clear from the results that screened compounds have better interaction as well as docking score than the known compounds. The best compounds obtained from screening were further analyzed for their interactions with key amino acid residues in both CAAX prenyl protease I and II.

Table 5.6: Extra precision docking of non-peptidic, non-preylic inhibitors of the prenyl protein-specific protease RCE1 and peptidyl(acyloxy)methyl ketones with CAAX prenyl protease I.

S.No	Compound Name	Docking Score	Glide Energy	Glide Evdw	Glide Ecoul	Glide Emodel	Residues involved	ΔG_{bind}
Non-peptidic, Non-preylic Inhibitors								
1	Compound8	-9.811	-64.295	-54.526	-9.769	-83.731	Asn392,Pro410	-96.525
2	Compound9	-9.151	-54.104	-45.898	-8.205	-70.269	Ala252,Zn	-64.749
3	Compound1	-9.085	-56.050	-47.344	-8.707	-76.340	Ser361,His409,Zn	-86.654
4	Compound10	-8.956	-63.521	-55.168	-8.353	-88.415	Glu287,Zn	-103.842
5	Compound 3	-8.935	-56.479	-43.496	-12.983	-88.104	Glu287,His290, Asn299 Arg415,Zn	-102.629
6	Compound 14	-8.926	-54.613	-49.534	-5.080	-79.721	Arg415,Zn	-83.652
7	Compound 11	-8.889	-54.892	-47.623	-7.269	-77.343	Asn299,Zn	-62.572
8	Compound12	-8.824	-59.629	-51.730	-7.899	-83.824	Arg415,Zn	-85.600
9	Compound2	-8.728	-59.942	-51.693	-8.249	-84.240	Asn299,Arg415,Zn	-78.589
10	Compound16	-8.705	-54.539	-45.001	-9.538	-88.048	Asn392,Arg415,Zn	-71.185
11	Compound13	-8.438	-59.184	-52.328	-6.856	-90.221	Glu287,His290,Zn	-61.249
12	Compound6	-8.396	-56.956	-46.321	-10.635	-80.335	Ala251,Asn299,Zn	-80.530
13	Compound 4	-8.059	-54.332	-46.111	-8.221	-82.312	Asn299,Zn	-83.677
14	Compound5	-7.311	-57.595	-50.915	-6.679	-86.430	Zn	-85.131
15	Compound 15	-6.871	-53.686	-52.379	-1.306	-80.172	Asn392	-102.824
16	Compound7	-5.836	-63.193	-57.616	-5.577	-98.931	Lys62,Tyr407	-66.257
Peptidyl(acyloxy)methyl ketones								
1	Y(FGBK(CH3)2	-10.391	-49.271	-40.245	-9.026	-89.599	His290, Asn392, Tyr407	-86.651
2	(FABK(CH3)3)	-10.339	-62.310	-52.979	-9.331	-86.916	Ala252,His290,His409,Arg415,Zn	-74.479
3	(FKBK(CH3)3	-9.029	-64.245	-53.435	-10.810	-90.956	His286,His290,Tyr407,His409,Zn	-71.446

Table 5.7: Extra precision docking of non-peptidic, non-preylic inhibitors of the prenyl protein-specific protease RCE1 and Peptidyl(acyloxy)methyl ketones with CAAX prenyl protease II.

S. No	Compound NAME	Docking Score	Glide Energy	Glide Evdw	Glide Ecoul	Glide Emodel	Residues involved	ΔG_{bind}
Non-peptidic, Non-preylic Inhibitors								
1	Compound 7	-4.989	-36.600	-36.600	0.030	-51.897	Gln23	-56.783
2	Compound 12	-4.462	-37.103	-31.388	-5.715	-54.363	Arg22, Arg79	-58.465
3	Compound 10	-3.906	-28.007	-21.654	-6.353	-37.712	Arg22	-61.635
4	Compound 16	-3.736	-44.059	-42.325	-1.734	-56.719	Phe12	-64.621
5	Compound 6	-3.369	-41.214	-38.646	-2.568	-48.142	Pro71, Tyr78	-71.251
6	Compound 9	-3.187	-40.120	-32.297	-7.822	-55.964	Phe12, Arg22	-66.653
7	Compound 13	-3.169	-46.300	-35.776	-10.524	-58.598	Phe12, Arg22, Glu75, Arg79	-57.060
8	Compound 15	-3.046	-41.859	-35.062	-6.798	-43.928	Thr8, Phe12	-62.725
9	Compound 14	-2.960	-39.202	-30.870	-8.322	-44.067	Phe12, Arg22, Glu75, Arg79	-49.831
10	Compound 3	-2.940	-37.071	-31.112	-5.958	-41.859	Arg22, Glu75	-44.577
11	Compound 5	-2.934	-39.202	-33.308	-6.330	-49.601	Phe12, Arg22, Gln23	-60.769
12	Compound 8	-2.300	-41.947	-33.586	-8.362	-52.675	Phe12, Arg22, Gln23, Glu75	-49.821
13	Compound 11	-2.088	-41643	-36.645	-4.997	-39.725	Phe12, Glu75, Arg79	-49.425
14	Compound 2	-1.683	-31.135	-23.422	-7.714	-34.295	Thr8, Arg22, Glu75, Arg79	-66.377
15	Compound 4	-0.578	-35.958	-35.087	-0.872	-39.867	Pro71	-58.525
Peptidyl(acyloxy)methyl ketones								
1	(FABK(CH3)3)	-5.499	-44.022	-34.215	-9.807	-58.707	Phe12,Arg22,Glu75	-52.005
2	Y(FGBK(CH3)2	-5.292	-51.013	-38.209	-12.804	-70.299	Thr8,Phe12, Arg22,Glu75,Arg79	-54.533
3	(FKBK(CH3)3)	-4.778	-45.350	-33.393	-11.957	-54.616	Phe12,Arg22,Glu75,Tyr78	-55.040

Table 5.8: Extra precision docking of non-peptidic, non-preylic inhibitorsof the prenyl protein-specific protease RCE1 and peptidyl(acyloxy)methyl ketones with human CAAX prenyl protease I.

S. No	Compound NAME	Docking Score	Glide Energy	Glide Evdw	Glide Ecoul	Glide Emodel	Residues involved	ΔG_{bind}
Non-Peptidic, Non-preylic Inhibitors								
1	Compound6	-8.678	-55.192	-53.695	-1.497	-75.941	----	-86.550
2	Compound7	-8.356	-59.344	-54.432	-4.911	-83.122	Gln393	-97.332
3	Compound8	-8.294	-58.827	-54.648	-4.179	-84.461	Phe133, Ser134	-104.926
4	Compound10	-7.542	-52.975	-52.191	-0.784	-76.209	Ser134, Gln393, Phe394	-93.247
5	Compound4	-7.524	-52.179	-48.648	-3.532	-76.804	Gln393	-107.792
6	Compound12	-7.174	-48.859	-42.751	-6.108	-67.161	Gln393	-77.928
7	Compound1	-7.148	-55.166	-52.529	-2.637	-80.845	Glu88	-110.722
8	Compound2	-7.000	-53.253	-45.648	-7.605	-69.918	Ser27,Ser134, Gln393, Phe394, Ser397	-95.605
9	Compound3	-6.925	-56.861	-53.313	-3.548	-75.998	Ser134	-102.784
10	Compound5	-6.731	-46.607	-43.085	-3.522	-71.185	Phe133, Gln393	-86.552
11	Compound16	-6.672	-52.802	-52.950	0.148	-81.432	Ser134, Phe394,	-68.547
12	Compound14	-6.664	-48.793	-46.097	-2.696	-74.080	Ala130	-105.226
13	Compound13	-6.657	-52.534	-49.824	-2.710	-78.825	Glu88	-89.779
14	Compound9	-6.435	-53.026	-51.454	-1.572	-67.736	Glu88	-94.151
15	Compound11	-6.279	-52.516	-48.827	-3.689	-74.905	Ala130, Phe394, Gln393	-71.412
16	Compound15	-5.962	-52.043	-49.924	-2.119	-78.601	Glu88, Ser134	-81.641
Peptidyl(acyloxy)methyl ketones								
1	(FKBK(CH3)3	-8.625	-60.572	-52.338	-8.234	-87.302	Glu88, Ser134	-97.443
2	(FABK(CH3)3)	-7.090	-52.620	-51.692	-0.928	-70.127	---	-80.749
3	Y(FGBK(CH3)2	-7.005	-54.632	-47.665	-6.967	-79.855	Glu34	-76.961

Table 5.9: Result of best screened compounds for CAAX prenyl protease I through structure based virtual screening.

S. No	Compound ID	Docking score	Glide Energy	Glide Evdw	Glide Ecoul	Glide E model	Residues involved	ΔG bind
1	F0451-4356 [L]	-10.543	-44.397	-28.635	-15.762	-67.034	Phe254, Glu287, Zn	-52.362
2	F0452-3342 [L]	-10.541	-45.419	-28.555	-16.865	-69.268	Phe254, Glu287, Zn	-50.911
3	F0849-2472 [L]	-10.539	-46.024	-30.274	-15.750	-56.846	Phe254, Glu287, Zn	-53.228
4	F02432-0154 [L]	-10.530	-53.319	-43.288	-10.030	-74.076	His290, Pro410, Arg415, Zn	-56.487
5	F04375-4375 [L]	-10.456	-37.978	-25.295	-12.683	-59.316	Ala252, Phe254, Glu287, Zn	-39.712
6	SYN15784346[A]	-10.197	-42.550	-29.022	-13.527	-46.470	Phe254, Glu287, Zn	-52.152
7	KM09023 [M]	-10.025	-47.891	-38.957	-8.934	-56.748	Phe254, Glu287, His290, Zn	-40.284
8	JFD00284 [M]	-9.848	-33.189	-21.583	-11.606	-53.988	Ala252, Glu287, His290, Zn	-58.789
9	KM03692 [M]	-9.747	-41.769	-29.340	-12.429	-60.294	Phe254, His409, Arg415, Zn	-50.571
10	JFD00284 [M]	-9.729	-43.224	-35.527	-7.697	-62.910	Ala252, His290, Glu365, Zn	-56.605
11	KM03725 [M]	-9.658	-40.398	-28.336	-12.062	-49.792	Phe254,His290,Arg415, Zn	-46.360
12	SYN19993980 [A]	-9.577	-48.455	-39.785	-8.670	-59.666	Pro410, Arg415, Zn	-48.113
13	SYN20008993 [A]	-9.285	-47.714	-36.677	-11.036	-70.363	His409, Pro410, Arg415, Zn	-56.874
14	LEG17766749 [A]	-9.142	-46.841	-37.061	-9.780	-62.036	Glu365, Arg415, Zn	-68.098
15	SYN17739355 [A]	-9.124	-41.946	-32.983	-8.964	-53.060	Glu287, Asn392, Pro410, Zn	-55.131

[A]-Asinex,[L]-Life chemicals, [M]-Maybridge

Table 5.10: Result of best screened compounds for CAAX prenyl protease II through structure based virtual screening.

S. No	Compound ID	Docking score	Glide Energy	Glide Evdw	Glide Ecoul	Glide E model	Residues involved	ΔGbind
1	DP01608[M]	-6.870	-30.420	-20.146	-10.274	-36.217	Phe12, Arg22, Glu75, Arg79	-46.146
2	F2721-0700[L]	-6.751	-38.606	-21.112	-17.494	-52.496	Thr8, Phe12, Arg22, Glu75, Arg79	-38.673
3	F2721-0715[L]	-6.615	-41.850	-26.868	-14.982	-54.693	Phe12, Glu75, Arg79	-73.349
4	F72721-0150[L]	-6.429	-35.509	-22.939	-12.570	-52.591	Phe12, Arg22, Glu75	-73.055
5	S15270[M]	-6.221	-28.341	-20.420	-7.921	-27.620	Arg22, Glu75, Arg79	-34.199
6	F1278-0573[L]	-6.218	-44.828	-30.477	-14.351	-52.302	Phe12, Arg22, Glu75, Arg79	-72.264
7	F1386-0017[L]	-6.091	-24.150	-14.142	-10.908	-29.578	Phe12, Arg22, Glu75, Arg79	-35.776
8	HTS02812[M]	-6.020	-37.745	-20.955	-16.790	-53.083	Phe12, Arg22, Glu75	-53.698
9	RH00579[M]	-5.984	-27.084	-14.245	-12.839	-35.062	Thr8, Arg22, Glu75, Arg79	-47.935
10	HTS02812[M]	-5.896	-39.394	-23.860	-15.535	-47.708	Phe12, Arg22, Glu75	-64.526
11	SYN 17737972[A]	-5.765	-34.890	-27.160	-7.720	-33.798	Phe12, Glu75	-30.469
12	SYN 19819113[A]	-5.671	-26.073	-16.190	-9.883	-39.293	Phe12, Arg22, Glu75, Arg79	-53.944
13	SYN 19817855[A]	-5.594	-35.364	-25.637	-9.727	-48.311	Phe12, Arg22, Glu75, Arg79	-50.625
14	SYN 10322709[A]	-5.512	-39.346	-26.531	-12.816	-46.230	Thr8, Phe12, Arg22, Glu75	-57.585
15	SYN 15030991[A]	-5.476	-33.094	-19.324	-14.670	-44.120	Phe12, Arg22, Glu75	-52.903

[A]-Asinex,[L]-Life chemicals, [M]-Maybridge

5.4.6 ***Binding mode analysis of known compounds and screened compounds*****:** The known inhibitors as well as the new inhibitors obtained from the virtual screening are docked in the active site of the both modeled protein. It was found from the docking result that new compounds obtained from screening have lower docking score when compared to the docking score of known compounds. Table 5.6-5.12 shows the compounds interacting with residues of CAAX I and II proteins which clearly exposes the difference in interacting residues between the known and screened compounds and confirm the gain of interactions in case of screened compounds. Best fifteen compounds from screening of both CAAX prenyl protease I and II were carried for further Induced Fit Docking studies.

5.4.7 ***Induced fit docking*****:** The changes at the interaction interface during the recognition of ligand by the protein could be nicely obtained from Induced fit docking (IFD). The results of the IFD for CAAX prenyl protease I and II were tabulated in Table 5.11 & 5.12 respectively. It discloses the predicted docking score, IFD score and interacting residues in protein ligand binding. It also shows the hydrophobic interactions along with hydrogen bond interactions play major role in protein ligand binding. Both CAAX prenyl protease I and II have got new and potent inhibitors through virtual screening as the compounds have lower docking score. The compounds showing best induced fit docking results with CAAX prenyl protease I were SYN20008993 (Asinex), F0451-4356 (Life chemicals) and F02432-0154 (Life chemicals). The compounds showing best induced fit docking with CAAX prenyl protease II were F2721-0700 (Life chemicals), F2721-0150 (Life chemicals) and DP01608 (Maybridge). Two dimensional interaction diagram of compounds SYN20008993 (Asinex), F0451-4356 (Life chemicals) and F02432-0154 (Life chemicals) with CAAX prenyl protease I were shown in Figure 5.5A, Figure 5.5B and Figure 5.5C respectively. The two dimensional interaction diagram of compounds F2721-0700 (Life chemicals), F2721-0150 (Life chemicals) and DP01608 (Maybridge) with CAAX prenyl protease II were shown in Figure 5.6A, Figure 5.6B and Figure 5.6C respectively.

Table 5.11: Induced fit docking studies for screened compounds for CAAX prenyl protease I.

S. No	Compound CODE	Hydrogen bond interaction	Hydrophobic Interaction	Docking score	Glide E model	Glide Energy	IFD Score
1	SYN20008993[A]	Asn251, Gly256, Leu197	----	-10.819	-75.600	-47.062	-917.242
2	F0451-4356[L]	Phe254,Gly256,Leu197	His290	-10.021	-49.290	-41.512	-916.777
3	F02432-0154[L]	Phe254,Leu197	----	-9.914	-67.057	-46.794	-922.198
4	F0849-2472[L]	Leu197, Gly256	---	-9.803	-63.248	-42.480	-917.217
5	SYN15784346[A]	Leu197,Phe254	----	-9.764	-47.238	-45.313	-915.952
6	LEG17766749[A]	Glu365,Arg415	----	-9.522	-58.944	-47.058	-922.020
7	SYN17739355[A]	Leu197,Gly256, Glu365	----	-9.244	-46.987	-34.594	-916.191
8	F0452-3342[L]	Leu197, Gly256, Lys261	---	-9.079	-51.349	-36.175	-916.217
9	KM09023[M]	Phe254	---	-8.913	-69.007	-46.463	-918.675
10	KM03725[M]	Phe254,Gly256	Tyr297	-8.882	-62.814	-39.924	-916.808
11	F04375-4375[L]	Phe254, His286, Glu287, Arg415	---	-8.745	-50.914	-36.377	-916.032
12	SYN19993980[A]	Leu197, Gly256	Tyr 253	-8.705	-78.389	-51.848	-917.174
13	KM03692[M]	Phe254, Gly256	---	-8.615	-53.026	-43.512	-916.708
14	JFD00284[M]	PHE254	Tyr253, His290	-8.604	-56.771	-44.596	-916.669
15	JFD00284[M]	Thr154, Arg158, Phe196	---	-8.381	-55.947	-43.326	-917.054

[A]-Asinex, [L]-Life chemicals, [M]-Maybridge

Table 5.12: Induced fit docking studies for screened compounds for CAAX prenyl protease II.

S. No	Compound CODE	Hydrogen bond interaction	Hydrophobic Interaction	Docking score	Glide E model	Glide Energy	IFD Score
1	F2721-0700[L]	His109,Arg201,Arg88	----	-10.639	-83.614	-54.439	-463.625
2	F72721-0150[L]	Arg119,Ile209,Ser112	----	-9.365	-76.292	-55.366	-460.397
3	DP01608[M]	------	Phe77,Arg88, Arg201	-9.206	-59.199	-39.603	-373.868
4	RH00579[M]	Arg119, Ile209	---	-8.613	-51.805	-38.976	-374.560
5	SYN 15030991[A]	Val204	His109,Trp219	-6.566	-67.470	-44.969	-459.358
6	F2721-0715[L]	Asp116, Ile209	---	-5.723	-66.316	-43.751	-369.517
7	F1386-0017[L]	Arg88	His109	-5.341	-44.730	-34.336	-453.101
8	SYN 19817855[A]	Arg88,Asp116,	Phe77,Arg119	-5.220	-52.549	-46.224	-455.534
9	S15270[M]	His109,Ala208	----	-4.811	-24.859	-34.346	-363.760
10	SYN 10322709[A]	Val204	Arg88	-4.648	-50.363	-48.664	-453.415
11	SYN 19819113[A]	----	Arg88	-4.246	-64.669	-44.000	-453.099
12	SYN 17737972[A]	Arg88, His109	-	-3.950	-78.540	-68.211	-411.256
13	F1278-0573[L]	Ser112, His106, His109	His109	-3.754	-88.300	-58.741	-453.402
14	HTS02812[M]	His106, His109	-	-3.622	-40.363	-47.664	-443.005
15	HTS02812[M]	Arg88	Trp219	-3.252	-69.526	-48.020	-435.086

[A]-Asinex, [L]-Life chemicals, [M]-Maybridge

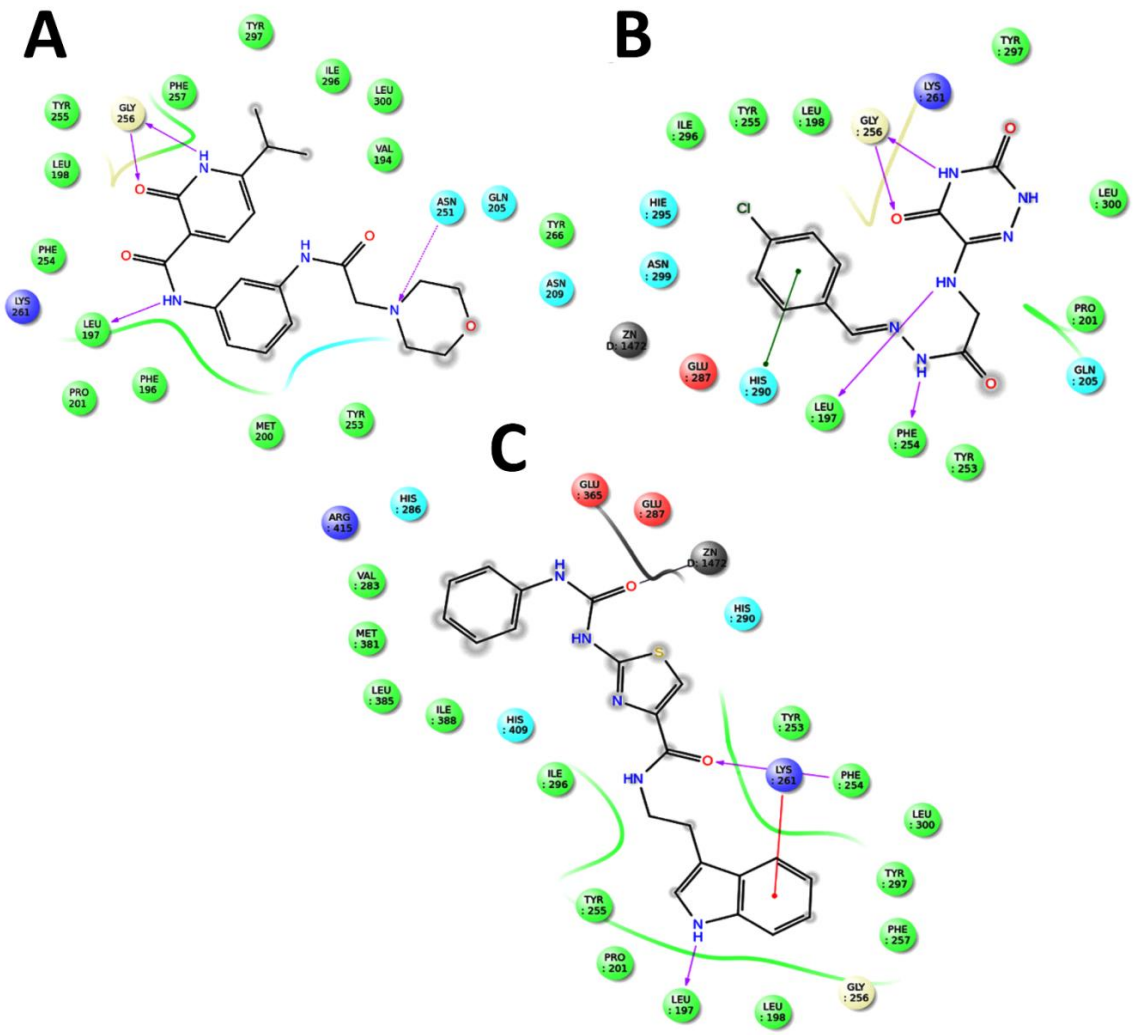

Figure 5.5: 2D Interaction diagram of induced fit docking results of CAAX prenyl protease I with top three compounds from screening namely, (A) Compound SYN20008993, (B) Compound F0451-4356 and(C) Compound F02432-0154**.**

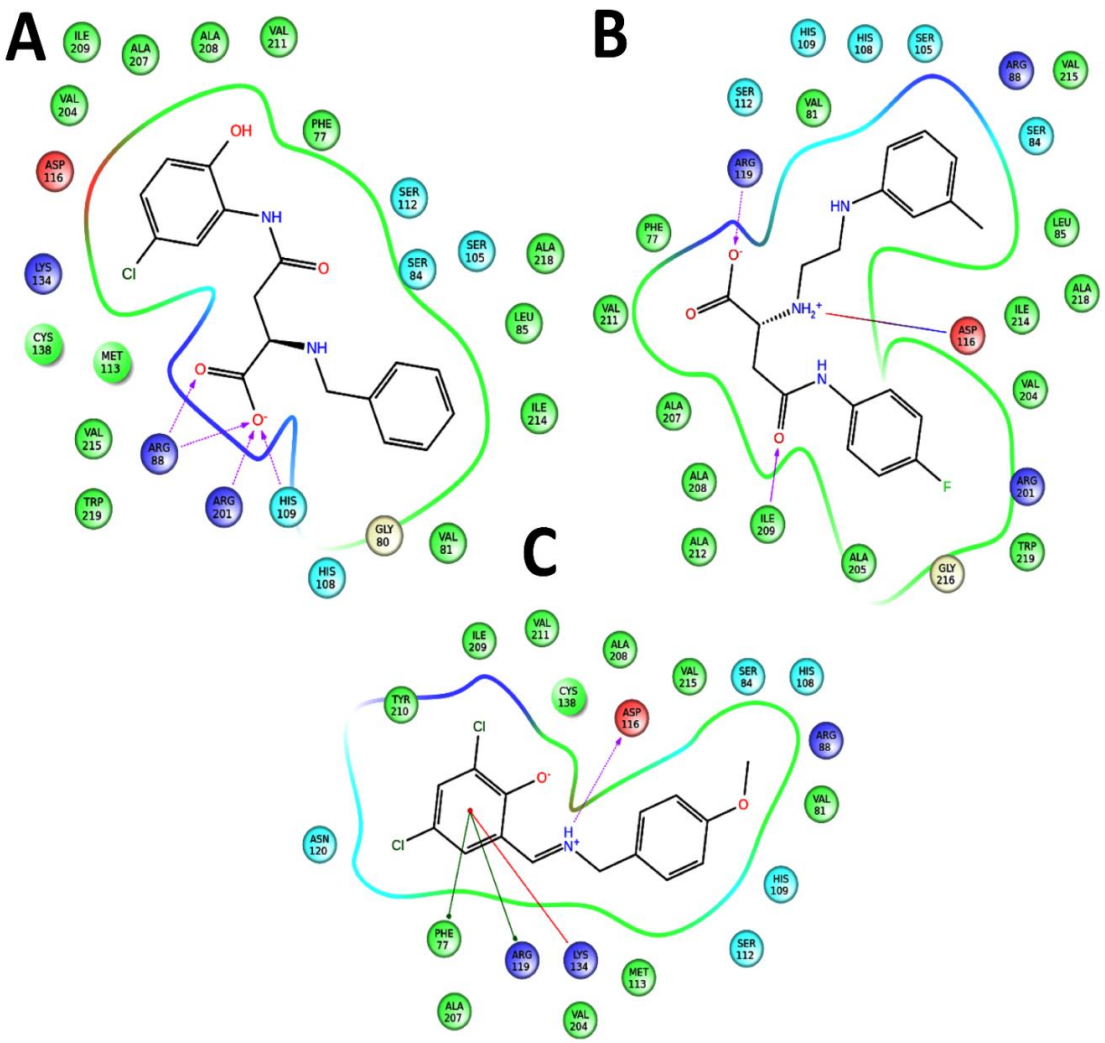

Figure 5.6: 2D Interaction diagram of induced fit docking results of CAAX prenyl protease II with top three compounds from screening namely, (A) Compound F2721-0700, (B) Compound F2721-0150 and (C) Compound DP01608**.**

5.4.8 ***ADME properties*****:** The drug-like properties of the lead compounds was assessed by evaluating their physicochemical properties, the pharmacokinetic parameters, including their absorption, distribution, metabolism and excretion (ADME), were analyzed using QikProp. The partition coefficient (QP logPo/w) which is crucial for estimating the absorption and distribution of drugs within the body, ranges from 0.204 to 4.509 in case of CAAX prenyl protease I and 0.021 to 4.460 in case of CAAX prenyl protease II. These pharmacokinetic parameters are well within the acceptable range defined for human use, thereby indicating their potential as drug-like molecules. The results of QikProp for CAAX prenyl protease I and II are shown in Table 5.15 and Table 5.16 respectively.

The drug like properties of the lead compounds was calculated using DruLiTo tool to avoid the method biasness and the results were appended in Table 5.13 & 5.14. The results reveal that the drug like properties were found to be good in agreement.

5.4.9 ***Molecular dynamics simulations*****: :** In order to check the stability of the modeled protein and three best docked protein ligand complex from screening, Molecular Dynamics Simulation (MDS) for 20 ns has been performed using Desmond module of Schrödinger. Root Mean Square Deviation (RMSD) of both modeled proteins were found to have deviations up to 8 ns of the simulation time period for CAAX prenyl protease I and 12 ns for CAAX prenyl protease II of simulation time period where the initial fluctuations were considered as the time taken for the equilibration. Later both proteins were found to be stable throughout the rest of simulation time period. Backbone RMSD of both CAAX I and II were depicted in Figure 5.7A & 5.7B. RMSD was supported by RMSF graph where the residue fluctuations were shown. The stable and equilibrated structure obtained from the initial MDS were used for further docking studies. RMSF graph for CAAX prenyl protease I is shown in Figure 5.7C and for CAAX prenyl protease II is shown in Figure 5.7D. Binding stability of three best docket complexes of CAAX prenyl protease I and II were analyzed through RMSD, RMSF, Protein ligand contacts over 20ns of simulation time period. RMSD graph shown in Figure 5.8A & 5.8B reveals the stability of both CAAX I and CAAX II proteins with their respective ligands. RMSF graph (Figure 5.8C and 5.8D) shows the residue fluctuations where the regions where residues involved in interaction were found to have lesser fluctuation. RMSF graph (Figure 8C and 8D) shows the residue fluctuations where the

residues involved in interaction were found to have lesser fluctuation. Histogram and Timeline of Protein ligand contacts for CAAX prenyl protease I and II complexes with three best docked complexes over 20ns of simulation time period were shown in Figure 5.9 and 5.10 respectively. Our data clearly shows the contribution of each residue in active site towards interaction with ligand. Both complexes were found to have stable interaction throughout the simulation. It has been concluded that all three complexes of both proteins were found to have good binding stability and these compounds can be carried further for more confirmatory analysis which could provide help in rational drug design of both CAAX I and II.

Table 5.13: Result of drug likeness properties prediction of compounds obtained from virtual screening against CAAX prenyl protease I using DruLiTo. Here HBA and HBD represent hydrogen bond acceptor and hydrogen bond donor respectively.

S.No	Compound Code	MW	logP	Alogp	HBA	HBD	TPSA	AMR	nRB	nAtom	nAcidic	RC	nRingdb	nAromatic	nHB	SAlerts
1	SYN20008993[A]	398.2	-0.19	-0.825	8	3	99.77	112.88	8	55	0	3	23	1	11	1
2	F0451-4356[L]	322.06	0.97	-0.522	9	4	124.05	77.59	6	33	0	2	17	1	13	3
3	F02432-0154[L]	405.13	1.337	-0.522	7	4	119.92	120.42	9	48	0	4	23	4	11	0
4	F0849-2472[L]	362.13	1.46	-1.64	11	4	142.51	120.42	9	44	0	2	18	1	15	3
5	SYN15784346[A]	361.15	1.416	0.164	7	3	85.83	107.83	4	46	0	4	26	2	10	0
6	LEG17766749[A]	400.16	1.411	-0.638	7	2	116.17	109.4	9	52	0	3	21	2	9	1
7	SYN17739355[A]	397.11	-0.797	-0.754	7	2	103.96	112.33	4	47	0	4	27	2	9	0
8	F0452-3342[L]	370.1	1.86	0.26	9	4	124.05	82.79	8	39	0	2	19	1	13	4
9	KM09023[M]	408.05	1.682	1.471	6	4	139.65	115.02	11	43	0	2	16	2	10	2
10	KM03725[M]	355.09	-0.097	0.037	7	4	124.63	100.39	7	41	0	3	20	2	11	1
11	F04375-4375[L]	278.05	0.381	-2.285	10	4	133.28	63.96	6	30	0	2	15	1	14	3
12	SYN19993980[A]	419.16	0.191	-0.134	9	2	103.34	119.84	7	52	0	4	27	3	11	0
13	KM03692[M]	477.06	1.556	2.086	6	3	112.6	107.77	8	45	0	3	26	2	9	2
14	JFD00284[M]	330.11	0.588	1.022	6	2	93.06	93.25	9	42	0	2	16	2	8	2
15	JFD00284[M]	330.11	0.588	1.022	6	2	93.06	93.25	9	42	0	2	16	2	8	2

[A]-Asinex,[L]-Life chemicals, [M]-Maybridge

Table 5.14: Result of drug likeness properties prediction of compounds obtained from virtual screening against CAAX prenyl protease II using DruLiTo.

S.no	Compound_Code	MW	logP	Alogp	HBA	HBD	TPSA	AMR	nRB	nAtom	nAcidic	RC	nRingdb	nAromatic	nHB	SAlerts
1	F2721-0700[L]	348.09	0.972	-1.137	5	3	106.07	91.31	8	41	0	2	17	2	8	1
2	F72721-0150[L]	359.16	0.251	-1.246	5	3	97.87	97.96	10	48	0	2	17	2	8	2
3	DP01608[M]	309.03	2.374	-0.412	2	1	46.26	84.25	4	33	0	2	17	2	3	1
4	RH00579[M]	245.22	1.094	-1.267	3	2	76.97	68.41	4	33	0	2	15	2	5	0
5	SYN 15030991[A]	329.19	0.476	-1.762	4	2	55.49	96.81	8	49	0	3	18	2	6	0
6	F2721-0715[L]	342.16	1.367	-0.804	5	3	106.07	95.33	9	47	0	2	17	2	8	1
7	F1386-0017[L]	274.05	2.405	0.29	3	1	55.6	54.96	3	27	0	2	16	2	4	2
8	SYN 19817855[A]	324.14	0.272	-1.37	4	1	58.4	93.32	5	41	0	3	21	2	5	1
9	S15270[M]	240.12	-1.532	-3875	6	2	83.64	55.67	2	33	0	2	16	0	8	1
10	SYN 10322709[A]	319.16	0.714	-4.142	5	3	69.78	81.0	4	43	0	3	21	2	8	1
11	SYN 19819113[A]	340.23	2.586	-2.625	4	1	58.4	92.27	6	53	0	3	21	1	5	0
12	SYN 17737972[A]	330.12	0.898	-0.359	5	1	72.09	91.68	3	41	0	3	22	1	6	0
13	F1278-0573[L]	390.13	0.57	-0.371	5	2	95.07	105.08	10	50	0	2	18	2	7	0
14	HTS02812[M]	370.21	-0.052	-0.608	5	4	77.24	109.61	9	55	0	3	20	2	9	0
15	HTS02812[M]	370.21	-0.052	-0.608	5	4	77.24	109.61	9	55	0	3	20	2	9	0

[A]-Asinex,[L]-Life chemicals, [M]-Maybridge

Table 5.15: ADME properties of screened compounds of CAAX prenyl protease I.

S. No.	Compound Code	SASA	QP logHERG	QP PMDCK	QP logPC16	QP logPo/w	QP logS	QPPCaco	Human oral Absorption %
1	SYN20008993[A]	734.879	-6.749	43.758	13.017	2.263	-3.780	96.590	75.723
2	F0451-4356[L]	765.306	-7.467	957.823	11.250	1.328	-3.997	31.436	61.524
3	F02432-0154[L]	657.810	-6.820	111.909	15.989	3.186	-5.824	200.184	86.793
4	F0849-2472[L]	739.279	-6.520	2777.298	11.842	1.643	-4.221	41.129	52.497
5	SYN15784346[A]	666.419	-6.398	207.695	12.787	3.286	-5.685	448.003	93.640
6	LEG17766749[A]	714.609	-4.536	333.283	13.371	3.578	-5.113	236.212	90.371
7	SYN17739355[A]	659.462	-5.828	22.856	13.091	1.279	-4.594	56.954	65.857
8	F0452-3342[L]	607.006	-5.906	288.817	10.738	2.319	-4.936	41.159	69.419
9	KM09023[M]	572.308	-5.408	29.025	15.876	3.729	-6.889	280.245	92.587
10	KM03725[M]	507.473	-4.955	10.441	13.566	2.095	-4.692	70.277	72.267
11	F04375-4375[L]	672.082	-5.678	78.653	9.709	0.204	-2.583	28.170	54.086
12	SYN19993980[A]	653.351	-4.075	306.093	13.050	2.313	-3.715	468.074	88.282
13	KM03692[M]	651.751	-5.441	15.718	12.570	4.509	-7.809	219.041	95.240
14	JFD00284[M]	748.019	-6.301	214.552	12.538	3.235	-4.390	252.823	88.890
15	JFD00284[M]	621.628	-5.488	68.634	11.573	3.192	-3427	607.803	95.461

[A]-Asinex,[L]-Life chemicals, [M]-Maybridge

Table 5.16: ADME properties of screened compounds of CAAX prenyl protease II.

S. No.	Compound Code	SASA	QP logHERG	QP PMDCK	QP logPC16	QP logPo/w	QP logS	QPPCaco	Human oral Absorption %
1	F2721-0700[L]	625.893	-5.085	-34.046	12.697	1.087	-3.908	26.582	58.810
2	F72721-0150[L]	702.472	-5.549	23.005	12.997	1.562	-4.846	24.640	60.999
3	DP01608[M]	562.703	-5.069	10000	10.138	4.460	-5.069	3626.530	100.000
4	RH00579[M]	499.558	-3.898	13.925	9.334	0.169	-2.358	26.807	51.521
5	SYN 15030991[A]	577.220	-5.530	288.648	10.592	2.450	-1.721	553.262	90.384
6	F2721-0715[L]	687.255	-5.448	5.919	13.299	1.119	-4.454	12.149	52.906
7	F1386-0017[L]	464.242	-4.680	1074.747	7.455	2.073	-2.502	213.470	80.775
8	SYN 19817855[A]	627.873	-7.234	195.538	11.799	3.083	-3.768	262.529	88.298
9	S15270[M]	472.445	-4.389	58.188	7.087	0.021	-0.993	125.730	64.645
10	SYN 10322709[A]	575.888	-3.997	1406.159	10.257	2.929	-4.236	1178.342	100.000
11	SYN 19819113[A]	668.965	-6.265	140.175	11.845	3.512	-4.170	283.600	91.410
12	SYN 17737972[A]	565.168	-4.563	481.289	10.086	2.244	-3.689	972.752	93.563
13	F1278-0573[L]	719.048	-5.255	49.803	13.555	2.368	-5.406	42.680	69.990
14	HTS02812[M]	658.208	-6.560	30.814	13.604	2.255	-2.545	69.826	73.156
15	HTS02812[M]	600.320	-5.351	334.501	12.558	1.904	-1.638	77.522	71.912

[A]-Asinex, [L]-Life chemicals, [M]-Maybridge

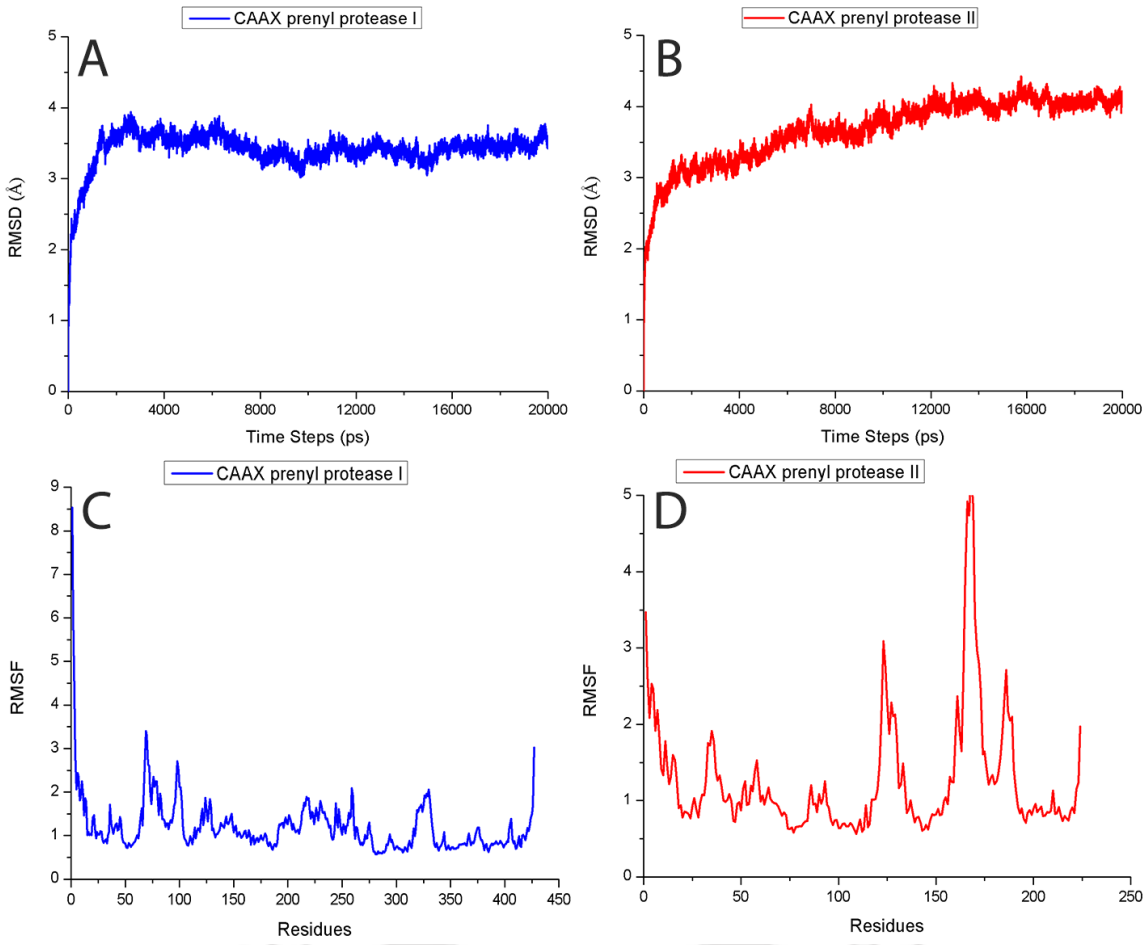

Figure 5.7: (A) Backbone RMSD and (C) RMSF of CAAX prenyl protease I and (B) Backbone RMSD and (D) RMSF of CAAX prenyl protease II over 20ns of simulation time period.

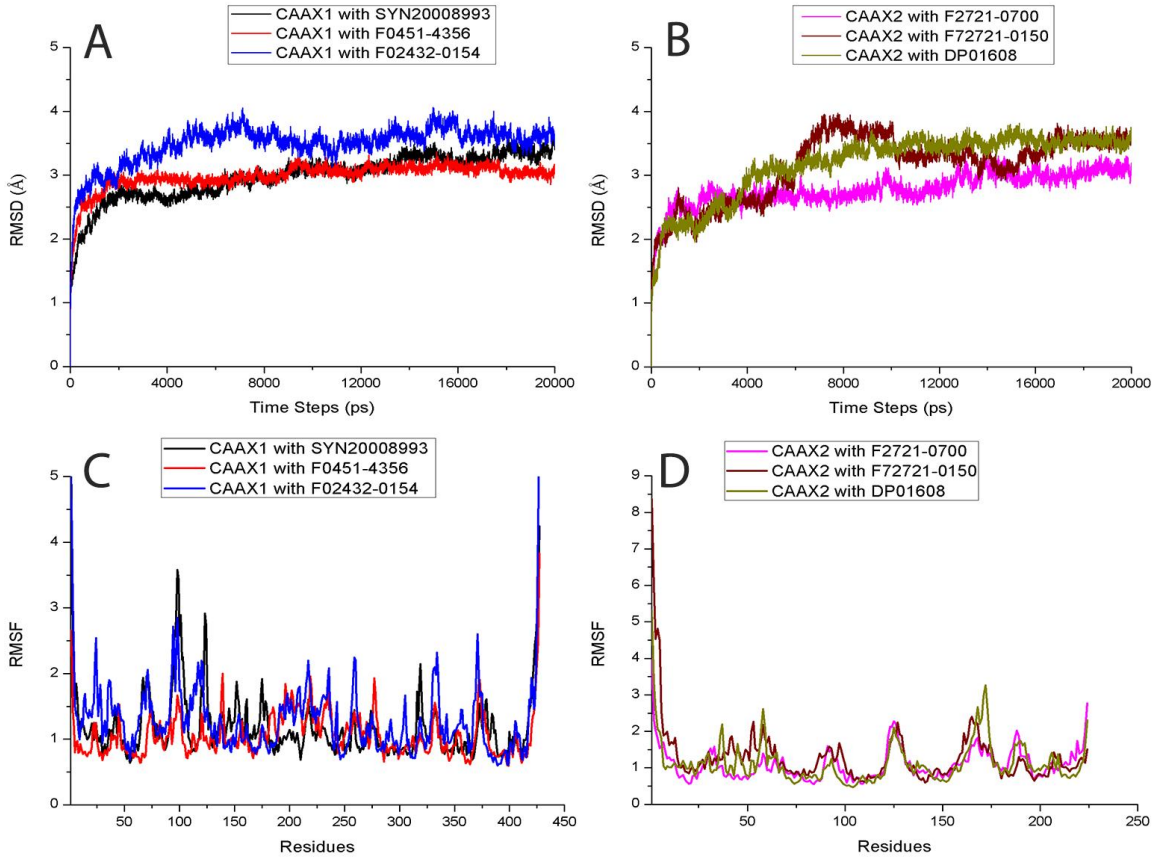

Figure 5.8: (A) Backbone RMSD and (C) RMSF of CAAX prenyl protease I with compounds SYN20008993, F0451-4356 and F02432-0154. (B) Backbone RMSD and (D) RMSF of CAAX prenyl protease II with compounds F2721-0700, F72721-0150 and DP01608.

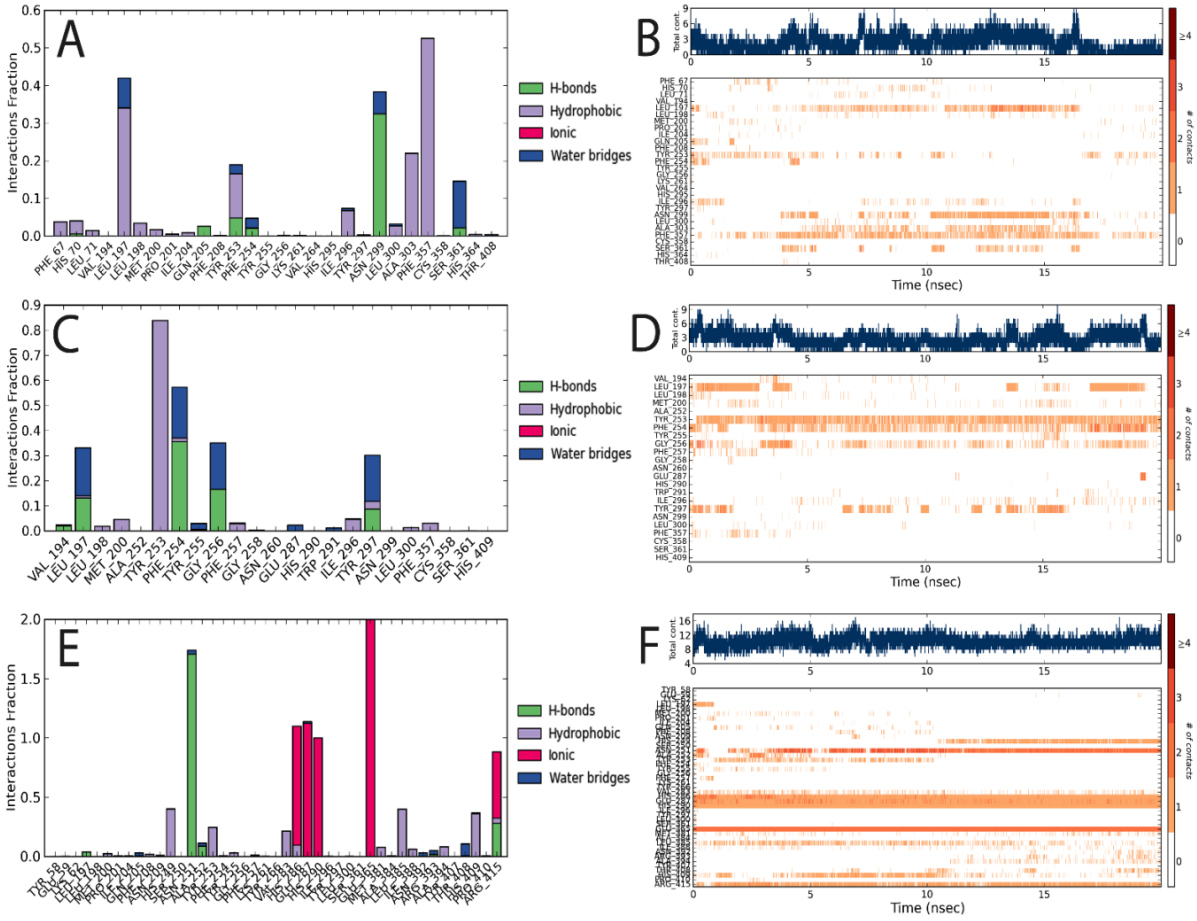

Figure 5.9: Histogram and timeline of protein ligand contacts of CAAX prenyl protease I complexed with SYN20008993 (A & B), F0451-4356 (C & D) and F02432-0154 (D & E) over 20ns of simulation time period.

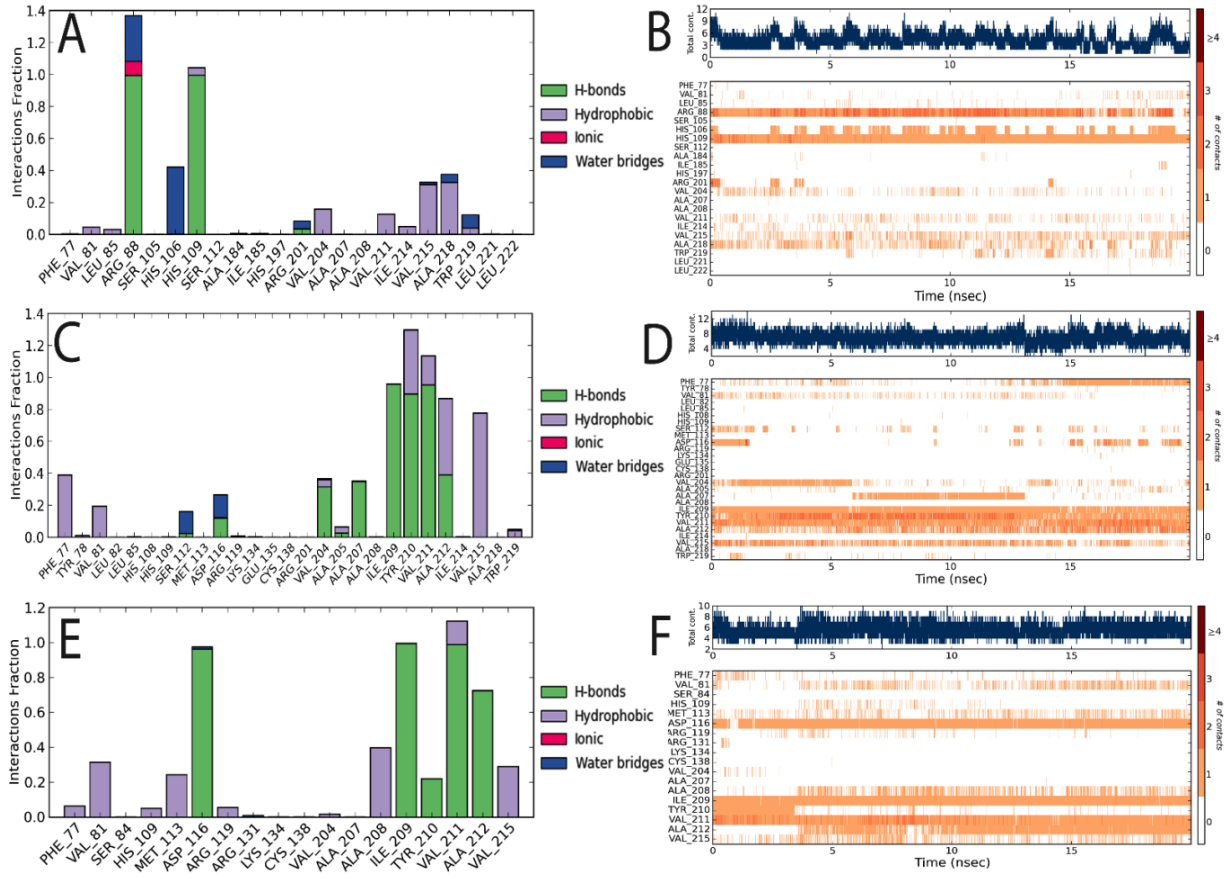

Figure 5.10: Histogram and timeline of protein ligand contacts of CAAX prenyl protease II complexed with F2721-0700 (A & B), F72721-0150 (C & D) and DP01608 (D & E) over 20 ns of simulation time period.

5.5 Discussion:

In this present study we have performed homology modelling for both CAAX prenyl protease I and II and validated by using SAVES and PROSA server. Further, Molecular Dynamics Simulations for 20 ns simulation brought stable structures that were carried for further molecular modelling studies. Active sites for both proteins were predicted using Sitemap which reveals the key interacting residues in the active site. Further molecular docking studies with known compounds provided help in predicting the binding mode with both proteins. Subsequently, structure based virtual screening was carried out to bring new and potent inhibitors for both proteins. It also reveals that the screened compounds were better than known compounds based on the docking score as well as interacting residues. Then the best 15 compounds were carried further for IFD studies which predict accurate binding poses of compounds with both proteins. ADME properties prediction of best compounds from screening was good in agreement and those compounds can be used for Human consumption. Molecular dynamics simulation studies of best complexes of both proteins reveal the binding stability and conformational stability. Finally, the best compounds obtained from screening could be carried for the further rational drug design of CAAX prenyl protease I and II inhibitors.

CHAPTER VI

Summary of Work

6.1 Abstract:

In an attempt to discover novel drug candidates, we have identified hypericin as a potential and novel inhibitor of spermidine synthase of *Leishmania donovani*. Further biochemical studies of *Leishmania* promastigotes after hypericin treatment has revealed generation of ROS and necrotic like death of the parasite. Either trypanothione or spermidine supplementation has shown revival of ROS pool, but only spermidine supplementation was effective in reviving the death of the parasite. This indicates the role of spermidine in pathways other than redox metabolism of the parasite. Further, to identify the putative role of spermidine in pathways other than redox metabolism of *Leishmania donovani*, quantitative mRNA expression of several genes was checked. Hypericin treatment was shown to cause lowered hypusine modification of eIF5A and further translational defect. These effects were reverted back by spermidine supplementation but not by trypanothione supplementation indication the role of spermidine in hypusination. Hypericin treatment has causes generation of certain events like autophagy, ATP surge, NAD^+ surge, increase expression of DNA repair enzymes as a cytoprotective mechanism towards oxidative stress. These cytoprotective events and translational defects were further supported by proteomic analysis of untreated

and hypericin treated *Leishmania* promastigotes. Proteomics analysis has revealed alteration in several proteins involved in protein synthesis, stress related proteins, signalling and transporter protein, proteins of metabolic pathways and ubiquitin proteasome system and several hypothetical proteins. Further, as an approach towards multi target drug discovery, we have also modelled CAAX prenyl protease I & II of *Leishmania donovani* and have identified potential inhibitors against these proteases by using *in silico* analysis. A formulation of inhibitors identified against spermidine synthase and CAAX prenyl protease I and II could be a good strategy to cope up drug resistance problem and to identify a formulation effective against *Leishmania donovani*.

6.2 Introduction of Leishmaniasis:

Leishmaniasis, popularly known as kala azar, is caused by different species of digenetic parasite *Leishmania*. There are several drugs available in the market against Leishmaniasis. However, these available drugs experience many disadvantages. These disadvantages include high cost, development of resistance of different strains of *Leishmania* against drugs, toxicity, difficult route of administration etc. Increasing burden of the disease and the limitations of available drugs, necessitate the requirement for the development of novel and potent drug candidates having specific drug targets.

6.3 Molecular mechanism of hypericin induced parasite death:

In a search for developing new drug candidate, we have identified hypericin as a novel drug candidate specifically targeting spermidine synthase of *Leishmania donovani*. Target specificity of hypericin was confirmed by both computational and biochemical method. Further exploring the mechanism of action of hypericin we have identified that hypericin has caused generation of reactive oxygen species which is reverted back by either trypanothione or spermidine supplementation. Hypericin was found to cause necrosis like death of the parasite. The death of the parasite was reverted back by spermidine but not by trypanothione. This suggests the role of spermidine in processes other than redox metabolism of the parasite.

6.4 Molecular events leading to death of *Leishmania donovani* under spermidine starvation:

To further explore the putative role of spermidine in pathways other than redox metabolism, we have checked the quantitative gene expression of several genes. We have found altered expression of genes involved in autophagy, hypusine modification, DNA repair and redox metabolism of the parasite. Hypericin was found to induce autophagy as a cytoprotective against DNA damage due ROS generation. Autophagy was reverted by either trypanothione or spermidine supplementation. Also, there was increase in ATP production after hypericin treatment which is reverted back either by trypanothione, spermidine or 3-methy adenine. This confirms the cytoprotection response of cell against DNA damage. Defective hypusine modification of eIF5A was found to be the main cause of parasite death after hypericin treatment. This was evident from the altered translation and lowered hypusination which get reverted back by spermidine supplementation but not by trypanothione supplementation. This suggests the role of spermidine in hypusine modification of *Leishmania donovani*.

6.5 Proteome profiling of *Leishmania donovani* under spermidine starvation:

Proteome analysis is considered as an important approach to solve various biological challenges. To know the overall mechanism of hypericin induced parasite death, it is important to overview the global change in proteins of *Leishmania* after hypericin treatment. We have utilized label free quantitation approach for proteome profiling of untreated and hypericin treatment *Leishmania donovani*. In line with our previous studies we have identified change in proteins related to protein synthesis and stress related proteins. This further confirms the occurrence of two major events i.e. DNA damage response and translational defects. This has ultimately led to the altered metabolic and signalling pathways of the parasite. We have also analyzed the relative distribution of total altered protein, up regulated proteins and down regulated proteins. Proteome profiling of *Leishmania donovani* has shown altered levels of proteins involved in signalling, transporters proteins and several membrane proteins. This also suggests the crucial role of these proteins in *Leishmania donovani*.

6.6 Structure based virtual screening studies of CAAX prenyl protease I and II of *Leishmania donovani*:

Multitarget drug discovery is a new approach for targeting several diseases. CAAX prenyl proteases are involved in modification of several proteins involved in signalling pathways. So, targeting CAAX prenyl proteases of *Leishmania donovani* can be a good approach towards developing another drug candidate. We have modelled the structure of CAAX prenyl protease I and II of *Leishmania donovani* using homology modelling approach. The modelled structure was validated and further simulated in DPPC lipid membrane and TIP3P water molecule. Active site of both CAAX prenyl protease I and II was predicted using Schrodinger suite. Using structure based virtual screening, several known and new inhibitors were docked against CAAX prenyl protease I and II to get the best docked compounds. Best docked 15 compounds were subjected to induced fit docking to predict accurate binding poses with CAAX prenyl protease I and II. ADME properties of the best compounds were predicted which confirms that these compounds can be used for Human consumption. Binding and conformational stability of the best protein inhibitor complex was confirmed by using molecular dynamics simulation studies. Overall, we have identified inhibitors against CAAX prenyl protease I and II of *Leishmania donovani* whose potential as drug candidate can be further confirmed by using biochemical and cellular studies.

Overall, we have identified a novel inhibitor of hypericin and we have also elucidated the mechanism of hypercin induced parasite death. Further, the potential of hypericin can be elucidated to check its in vivo effect on the infected animal models. Further, hypericin can be taken up for clinical trials on human. Several strains of *Leishmania* parasite are gaining resistance against the available drugs like sodium stibogluconate, amphotericin B and miltefosine. Hypericin can be a new drug molecule which can be used to treat patients unresponsive towards these drugs. We have also identified potential inhibitors of CAAX prenyl protease I and II of *Leishmania donovani*. The potential of best identified inhibitors to inhibit the recombinant CAAX prenyl protease I and II of *Leishmania donovani* can be validated. The inhibitor showing *in vitro* inhibition can be further taken up to check its potential as antileishmanial agent by monitoring its effects on the promastigotes of *Leishmania donovani*.

Bibliography

Alers S, Löffler AS, Wesselborg S and Stork B. 2012. Role of AMPK-mTOR-Ulk1/2 in the regulation of autophagy: cross talk, shortcuts, and feedbacks. *Mol Cell Biol*. 32 :2-11.

Al-Quadan T, Abu Kwaik Y. 2011. Molecular characterization of exploitation of the polyubiquitination and farnesylation machineries of *Dictyostelium discoideum* by the AnkB F-box effector of *Legionella pneumophila*. *Front. Microbiol*. 2:23.

Azam SS, Abbasi SW, and Batool M. 2014. Structure modelling and docking study of HCV NS5B-3a RNA polymerase for the identification of potent inhibitors. *Medicinal Chemistry Research.* 23: 618-627.

Baglo Y, Gabrielsen M, Sylte I, and Gederaas OA. 2013. Homology modeling of human γ-butyric acid transporters and the binding of pro-drugs 5-aminolevulinic acid and methyl aminolevulinic acid used in photodynamic therapy. *PLoS ONE*, 8: e65200.

Baines CP, Kaiser RA, Purcell NH, Blair NS, Osinska H, et al. 2004. Loss of cyclophilin D reveals a critical role for mitochondrial permeability transition in cell death. *Nature*. 434: 658-662.

Bañuls A, Hide M, and Prugnolle F. 2007. Leishmania and the Leishmaniases: A Parasite Genetic Update and Advances in Taxonomy, Epidemiology and Pathogenicity in Humans. *Advances in Parasitology*. 64:1-109.

Bao K, Bostanci N, Selevsek N, Thurnheer T and Belibasakis GN. 2015. Quantitative proteomics reveal distinct protein regulations caused by Aggregatibacter actinomycetemcomitans within subgingival biofilms. *PLoS One.* 10: e0119222.

Basselin M, Coombs GH, Barrett MP. 2000. Putrescine and spermidine transport in *Leishmania. Mol Biochem Parasitol.*109:37–46.

Bera A, Singh S, Nagaraj R, Vaidya T. 2003. Induction of autophagic cell death in *Leishmania donovani* by antimicrobial peptides. *Mol Biochem Parasitol*. 127: 23-35.

Bhattacharya A, Biswas A, Das PK. 2009. Role of a differentially expressed cAMP phosphodiesterase in regulating the induction of resistance against oxidative damage in *Leishmania donovani. Free Radic. Biol.* Med. 47:1494–1506.

Bjørkøy G, Lamark T, Brech A, Outzen H, Perander M, et al. 2005. p62/SQSTM1 forms protein aggregates degraded by autophagy and has a protective effect on huntingtin-induced cell death. *J Cell Biol*. 171:603–14.

Boyartchuk VL, Ashby MN, and Rine J. 1997. Modulation of Ras and a-factor function by carboxyl-terminal proteolysis. *Science*. 275*:* 1796–800.

Bradford MM. 1976. A rapid and sensitive method for the quantitation of microgram quantities of protein utilizing the principle of protein-dye binding. *Analytical Biochemistry.* 72: 248-254.

Brugarolas J, Lei K, Hurley RL, Manning BD, Reiling JH, Hafen E, Witters LA, Ellisen LW, Kaelin Jr WG. 2004. Regulation of mTOR function in response to hypoxia by REDD1 and the TSC1/TSC2 tumor suppressor complex. *Genes Dev.* 18: 2893–2904.

Byfield MP, Murray JT, and Backer JM. 2005. hVps34 is a nutrient-regulated lipid kinase required for activation of p70 S6 kinase. *J. Biol. Chem.* 280: 33076–33082.

Carter KC, Hutchison S, Henriquez FL, Légaré D et. al. 2006. Resistance of *Leishmania donovani* to sodium stibogluconate is related to the expression of host and parasite γ-glutamylcysteine synthetase. *Antimicrob Agents Chemother*. 50: 88–95.

Casey PJ. 1992. Biochemistry of protein prenylation. *Journal of Lipid Research.* 33:1731-1740.

Catalano-Dupuy DL, Lopez-Rivero A, Soldano and Ceccarelli EA. 2013. Redox Proteins as Targets for Drugs Development Against Pathogens. *Curr Pharm Des*. 19:2594-605.

Chattopadhyay MK, Tabor CL, and Tabor H. 2003. Spermidine but not spermine is essential for hypusine biosynthesis and growth in Saccharomyces cerevisiae: Spermine is converted to spermidine in vivo by the FMS1-amine oxidase. *Proc. Natl. Acad. Sci.* 100: 13869–13874.

Chattopadhyay MK, Park MH, and Tabor H. 2008. Hypusine modification for growth is the major function of spermidine in *Saccharomyces cerevisiae* polyamine auxotrophs grown in limiting spermidine. *Proc. Natl. Acad. Sci.*105: 6554-6559.

Chawla B, Jhingran A, Singh S, Tyagi N, Park MH, Srinivasan N, Roberts SC, Madhubala R. 2010. Identification and characterization of a novel deoxyhypusine synthase in *Leishmania donovani. J Biol Chem.* 285:453–463.

Chawla B, Kumar RR, Tyagi N, Subramanian G, Srinivasan N, Park MH, Madhubala R. A unique modification of the eukaryotic initiation factor 5A shows the presence of the complete hypusine pathway in *Leishmania donovani*. *PLoS ONE*. 7: e33138.

Claborn DM. 2010. The biology and control of leishmaniasis vectors. *Journal of Global Infectious Diseases*. 2:127-134.

Cloutier S, Laverdière M, Chou MN et. al. 2012. Translational Control through eIF2alpha Phosphorylation during the *Leishmania* Differentiation Process. *PLoS ONE*. 7: e35085.

Cooke MS, Evans MD, Dizdaroglu M and Lunec J. 2003. Oxidative DNA damage: mechanisms, mutation, and disease. *The FASEB Journal*. 17: 1195-1214.

Croft SL, Coombs GH. 2003. Leishmaniasis-current chemotherapy and recent advances in the search for novel drugs. *Trends Parasitol*. 19:502–508.

Croft SL, Sundar S, Fairlamb AH. 2006. Drug resistance in leishmaniasis. *Clin Microbiol Rev*. 19:111–126.

Das M, Saudagar P, Sundar S, Dubey VK. 2013. Miltefosine-unresponsive *Leishmania donovani* has a greater ability than miltefosine-responsive *L. donovani* to resist reactive oxygen species. *FEBS J*. 280:4807-4815.

Dever TE, Gutierrez E and Shin BS. 2014. The hypusine-containing translation factor eIF5A. *Critical Reviews in Biochemistry and Molecular Biology*. 49:413-425.

Dolence JM, Steward LE, Dolence EK, Wong DH, and Poulter CD. 2000. Studies with recombinant Saccharomyces cerevisiae CaaX prenyl protease Rce1p. *Biochemistry.* 39: 4096–104.

Eisenberg T, Knauer H, Schauer H et. al. 2009. Induction of autophagy by spermidine promotes longevity. *Nature Cell Bio*. 11: 1305 – 1314.

Enomoto, K, Nagasaki T, Yamauchi A, Onoda J, Sakai K, Yoshida T, Maekawa K, Kinoshita Y, Nishino I, Kikuoka S, Fukunaga T, Kawamoto K, Numata Y, Takemoto H, Nagata K. 2006. Development of high-throughput spermidine synthase activity assay using homogeneous time-resolved fluorescence. *Anal Biochem*. 351:229-240.

Epple UD, Suriapranata I, Eskelinen EL, and Thumm M. 2001. Aut5/Cvt17p, a putative lipase essential for disintegration of autophagic bodies inside the vacuole. *J Bacteriol.* 183:5942-55.

Eskelinen EL. 2005.Maturation of autophagic vacuoles in Mammalian cells. *Autophagy. 1:1-10.*

Feng Z, Zhang H, Levine AJ, and Jin S. 2005. The coordinate regulation of the p53 and mTOR pathways in cells. *Proc. Natl. Acad. Sci. USA*. 102: 8204–8209.

Friesner RA, Banks JL, Murphy RB, Halgren TA, Klicic JJ, Mainz DT, Repasky MP, Knoll, EH, Shelley M, et al. 2004. Glide: a new approach for rapid, accurate docking and scoring. 1. Method and assessment of docking accuracy. *Journal of Medicinal Chemistry.*47: 1739-49.

Friesner RA, Murphy RB, Repasky MP, Frye LL, Greenwood JR, Halgren TA, Sanschagrin, PC, and Mainz DT. 2006. Extra precision glide: docking and scoring incorporating a model of hydrophobic enclosure for protein-ligand complexes. *Journal of Medicinal Chemistry.*49: 6177–6196.

Gao X, Zhang Y, Arrazola P, Hino O, Kobayashi T, Yeung RS, Ru B, and Pan D. 2002. Tsc tumour suppressor proteins antagonize amino-acid-TOR signalling. *Nat. Cell Biol.* 4 :699–704.

Gillespiea JR, Yokoyamab K, Lua K, Eastman RT, Bollinger JG, Van Voorhis WC, Gelb MH, and Buckner FS. 2007. C-terminal proteolysis of prenylated proteins in trypanosomatids and RNA interference of enzymes required for the post-translational processing pathway of farnesylated proteins. *Molecular and Biochemical Parasitology.*153: 115–124.

Gilroy C, Olenyik T, Roberts SC, Ullman B. 2011. Spermidine Synthase is Required for Virulence of *Leishmania donovani*. *Infect Immun*. 79:2764–2769.

Glick D, Barth S, and Macleod KF. 2010. Autophagy: cellular and molecular mechanisms. *J Pathol*. 221: 3–12.

Glide, version 6.2. 2014. Schrodinger, LLC, New York, NY.

Glisovic T, Bachorik JL, Yong J, and Dreyfuss G. 2008. RNA-binding proteins and post-transcriptional gene regulation. *FEBS Lett.* 582: 1977–1986.

Gong F, Miller KM. 2013. Mammalian DNA repair: HATs and HDACs make their mark through histone acetylation. *Mutation Research/Fundamental and Molecular Mechanisms of Mutagenesis*. 750: 23–30.

Guan KL and Xiong Y. 2011. Regulation of intermediary metabolism by protein acetylation. *Trends in Biochemical Sciences*. 36: 109-116.

Gundry RL, White MY, Murray CI, Kane LA, Fu Q, Stanley BA, Van Eyk JE. 2009. Preparation of Proteins and Peptides for Mass Spectrometry Analysis in a Bottom-Up Proteomics Workflow. Current protocols in molecular biology / edited by Frederick M Ausubel. [et al] CHAPTER:Unit10.25.

Guo Z, Mohanty U, Noehre J, Sawyer TK, Sherman W, and Krilov G. 2010. Probing the alpha-helical structural stability of stapled p53 peptides: molecular dynamics simulations and analysis. *Chemical Biology and Drug Design.* 75: 348-59.

Gutierrez E, Shin B-S, Woolstenhulme C J, Kim J-R, Saini P, Buskirk AR, Dever TE. 2013. eIF5A promotes translation of polyproline motifs. *Mol. Cell*. 51:35–45.

Haar EV, Lee SI, Bandhakavi S, Griffin TJ, and Kim DH. 2007. Insulin signalling to mTOR mediated by the Akt/PKB substrate PRAS40. *Nat. Cell Biol.* 9: 316–323.

Hanada T, Noda NN, Satomi Y, Ichimura Y, Fujioka Y, Takao T, Inagaki F, and Ohsumi Y. 2007.The Atg12-Atg5 conjugate has a novel E3-like activity for protein lipidation in autophagy. *J Biol Chem.* 282:37298-302.

Haqqani AS, Kelly JF, Stanimirovic DB. 2008. Quantitative protein profiling by mass spectrometry using label-free proteomics. *Methods Mol Biol*. 439: 241-56.

Hara K, Maruki Y, Long X, Yoshino K, Oshiro N, Hidayat S, Tokunaga C, Avruch J, Yonezawa K. 2002. Raptor, a binding partner of target of rapamycin (TOR), mediates TOR action. *Cell*. 110: 177–189.

Hara K, Yonezawa K, Weng QP, Kozlowski MT, Belham C, and Avruch J. 1998. Amino acid sufficiency and mTOR regulate p70 S6 kinase and eIF-4E BP1 through a common effector mechanism. *J. Biol. Chem*. 273:14484–14494.

He C, and Klionsky DJ. 2009. Regulation Mechanisms and Signaling Pathways of Autophagy. *Annual review of genetics*. 43:67-93.

Heitman J, Movva NR, Hall MN. 1991. Targets for cell cycle arrest by the immunosuppressant rapamycin in yeast. *Science*. 253: 905–909.

Hide M, Bucheton B, Kamhawi S et al. 2007. Understanding Human Leishmaniasis: The need for an Integrated Approach. *Encyclopedia of Infectious Diseases: Modern Methodologies* (ed. by M. Tibayrenc). Wiley-Liss, Hoboken, N.J.

Hu J, Mahmoud MI, el-Fakahany EE. 1994. Polyamines inhibit nitric oxide synthase in rat cerebellum. *Neurosci Lett.* 175:41-45.

. Induced Fit Docking, Schrodinger, LLC, New York, NY, 2014.

Inoki K, Zhu T, Guan KL. 2003. TSC2 mediates cellular energy response to control cell growth and survival. *Cell*. 115: 577–590.

Islam MS, Shahik SM, Sohel M, Patwary NIA, and Hasan MA. 2015. *In Silico* Structural and Functional Annotation of Hypothetical Proteins of *Vibrio cholerae* O139. *Genomics Inform*. 13: 53–59.

Jung CH, Ro S-H, Cao J, Otto NM and Kim D-H. 2010. mTOR regulation of autophagy. *FEBS letters.* 584: 1287-1295.

Jacinto E, Facchinetti V, Liu D, Soto N, Wei S, Jung SY, Huang Q, Qin J, Su B. 2006. SIN1/MIP1 maintains rictor–mTOR complex integrity and regulates Akt phosphorylation and substrate specificity. *Cell*. 127: 125–137.

Jin BF, He K, Wang HX, Wang J, Zhou T, Lan Y, et al. 2003. Proteomic analysis of ubiquitin-proteasome effects: insight into the function of eukaryotic initiation factor 5A. *Oncogene.* 22: 4819-4830.

Kabeya Y, Mizushima N, Ueno T, Yamamoto A, Kirisako T, Noda T, Kominami E, Ohsumi Y, Yoshimori T. 2000. LC3, a mammalian homologue of yeast Apg8p, is localized in autophagosome membranes after processing. *EMBO J.* 19:5720-8.

Kaerberlein M. 2009. Spermidine surprise for a long life. *Nature Cell Biology* 11: 1277 - 1278.

Kamada Y, Funakoshi T, Shintani T, Nagano K, Ohsumi M, and Ohsumi Y. 2000. Tor-mediated induction of autophagy via an Apg1 protein kinase complex. *J Cell Biol.* 150:1507-13.

Katayama M, Kawaguchi T, Berger MS and Pieper RO. 2007. DNA damaging agent-induced autophagy produces a cytoprotective adenosine triphosphate surge in malignant glioma cells. *Cell Death and Differentiation*. 14: 548–558.

Kedzierski L. 2012. Leishmaniasis Vaccine: Where are We Today*?*. *Journal of Global Infectious Diseases*. 2: 177-185.

Kim DE, Chivian D, and Baker D. 2004. Protein structure prediction and analysis using the Robetta server. *Nucleic Acids Research.* 1*:* W526-31.

Kim E, Ambroziak P, and Otto JC. 1999. Disruption of the Mouse Rce1 Gene Results in Defective Ras Processing and Mislocalization of Ras within Cells. *The Journal of Biological Chemistry.* 274: 8383-8390.

Kim J, Huang WP, and Klionsky DJ. 2001. Membrane recruitment of Aut7p in the autophagy and cytoplasm to vacuole targeting pathways requires Aut1p, Aut2p, and autophagy conjugation complex. *J. Cell Biol*. 152: 51–64.

Kim J, Kundu M, Viollet B and Guan KL. 2011. AMPK and mTOR regulate autophagy through direct phosphorylation of Ulk1. *Nature Cell Biology*.13: 132–141.

Kim PK, Hailey DW, Mullen RT, Lippincott-Schwartz J. 2008. Ubiquitin signals autophagic degradation of cytosolic proteins and peroxisomes. *Proc Natl Acad Sci USA*. 105:20567–74.

Kirisako T, Baba M, Ishihara N, Miyazawa K, Ohsumi M, Yoshimori T, Noda T, and Ohsumi Y . 1999. Formation process of autophagosome is traced with Apg8/Aut7p in yeast. *J Cell Biol.* 147:435-46.

Klionsky DJ. 2005. The molecular machinery of autophagy: unanswered questions. *J Cell Sci.* 118:7-18.

Krauth-Siegel RL and Leroux AE. 2012. Low-Molecular-Mass Antioxidants in Parasites. 2012. *Antioxidants & Redox Signalling.* 0:1-25.

Krauth-Siegel RL and Comini MA. 2008. Redox control in trypanosomatids, parasitic protozoa with trypanothione-based thiol metabolism. *Biochim Biophys Acta.* 1780:1236−1248.

Krauth-Siegel RL, Meiering SK, Schmidt H. 2003. The parasite-specific trypanothione metabolism of trypanosoma and leishmania. *Biol Chem*. 384:539-49.

Kubin A, Wierrani F, Burner U, Alth G, Grünberger W. 2005. Hypericin--the facts about a controversial agent. *Curr Pharm Des*. 11:233-253.

Lakhlili W, Chevé G, Yasri A, and Ibrahimi A. 2015. Determination and validation of mTOR kinase-domain 3D structure by homology modeling. *Onco Targets and Therapy*. 30: 1923-30.

Leach, F. 1981. ATP Determination with Firefly Luciferase, *J Appl Biochem 3*, 473, 1981.

Li L, Chen Y and Gibson SB. 2013. Starvation-induced autophagy is regulated by mitochondrial reactive oxygen species leading to AMPK activation. *Cellular Signalling*. 25: 50-60.

Liao J. and Gong Z. 1997. *Biotechniques*. 23:368–370.

LigPrep, version 2.9. 2014. Schrodinger, LLC, New York, NY.

Lin SS, Manchester JK, Gordon JI. 2001. Enhanced gluconeogenesis and increased energy storage as hallmarks of aging in *Saccharomyces cerevisiea*. *J Biol Chem.* 2001 276:36000-7.

Lindoso JALL, Costa JML, Queiroz IT, Goto H. 2012. Review of the current treatments for leishmaniases. *Research and Reports in Tropical Medicine*. 3: 69–77.

Long X, Ortiz-Vega S, Lin Y, and Avruch J. 2005. Rheb binding to mammalian target of rapamycin (mTOR) is regulated by amino acid sufficiency. *J. Biol. Chem.* 280: 23433–23436.

Lu JJ, Pan W, Hu YJ, and Wang YT. 2012. Multi-Target Drugs: The Trend of Drug Research and Development. *PLoS ONE*. *7:*e40262.

Lu SP and Lin SJ. 2010. Regulation of yeast sirtuins by NAD(+) metabolism and calorie restriction. *Biochimica et Biophysica Acta*. 1804: 1567-1575.

Lum JJ, Deberardinis RJ, Thompson CB. 2005b. Autophagy in metazoans: Cell survival in the land of plenty. *Nat. Rev. Mol. Cell Biol.* 6:439–448

Lyne PD, Lamb ML, and Saeh JC. 2006. Accurate prediction of the relative potencies of members of a series of kinase inhibitors using molecular docking and MM-GBSA scoring. *Journal of Medicinal Chemistr.*16: 4805–4808.

Madeo F, Eisenberg T, Büttner S, Ruckenstuhl C, Kroemer G. 2010. Spermidine: a novel autophagy inducer and longevity elixir. *Autophagy*. 6:160-2.

Magdolen V, Klier H, Wohl T, Klink F, Hirt H et al. 1994. The function of the hypusine-containing proteins of yeast and other eukaryotes is well conserved. *Mol Gen Genet*. 244: 646–652

Mahmood T and Yang PC. 2012. Western Blot: Technique, Theory, and Trouble Shooting. N *Am J Med Sci*. 4: 429–434.

Maier B, Tersey SA, and Mirmira RG. 2010. Hypusine: a New Target for Therapeutic Intervention in Diabetic Inflammation. *Discov Med*. 10:18-23.

Mandal S, Mandal A, Johansson HE, Orjalo AV, Park MH. 2013. Depletion of cellular polyamines, spermidine and spermine, causes a total arrest in translation and growth in mammalian cells. *Proc. Nati. Acad. Sci. USA*. 110:2169-2174.

Manning BD. 2004. Balancing Akt with S6K: implications for both metabolic diseases and tumorigenesis. *J. Cell Biol.* 167: 399–403.

McFarland AJ, Anoopkumar-Dukie S, Perkins AV, Davey AK and Grant GD. 2012. Inhibition of autophagy by 3-methyladenine protects 1321N1 astrocytoma cells against pyocyanin- and 1-hydroxyphenazine-induced toxicity. *Archives of Toxicology*. 86: 275-284.

Meissner D, Odman-Naresh J, Vogelpohl I, and Merzendorfer H. 2010. A novel role of the yeast CaaX protease Ste24 in chitin synthesis. *Molecular Biology of the Cell.* 21: 2425-33.

Meléndez A, Tallóczy Z, Seaman M, Eskelinen EL, Hall DH, Levine B. 2003. Autophagy genes are essential for dauer development and life-span extension in C. elegans. *Science.* 301:1387-91.

Michaelson D, Ali W, Chiu VK, Bergo M, Silletti J, Wright L, Young SG, and Philips M. 2005. Postprenylation CAAX Processing Is Required for Proper Localization of Ras but Not Rho GTPases. *Molecular Biology of the Cell*. 16*:* 1606-1616.

Minois N. 2014. Molecular basis of the 'anti-aging' effect of spermidine and other natural polyamines - a mini-review. *Gerontology*. 60:319-26.

Mitropoulos P, Konidas P, Durkin-Konidas M. 2010. New World cutaneous leishmaniasis: Updated review of current and future diagnosis and treatment. *J Am Acad Dermatol.* 63:309-322.

Mizushima N, Kuma A, Kobayashi Y, Yamamoto A, Matsubae M, Takao T, Natsume T, Ohsumi Y, Yoshimori T. 2003. Mouse Apg16L, a novel WD-repeat protein, targets to the autophagic isolation membrane with the Apg12-Apg5 conjugate. *J Cell Sci. 116:1679-88.*

Mizushima N, Noda T, and Ohsumi Y. 1999. Apg16p is required for the function of the Apg12p-Apg5p conjugate in the yeast autophagy pathway. *EMBO J.* 18:3888-96.

Mizushima N. 2007. Autophagy: process and function. *Genes & Dev*. 21:2861-2873.

MacMorris-Adix M. 2008. Leishmaniasis: A review of the disease and the debate over the origin and dispersal of the causaitive parasite Leishmania, *Macalester Reviews in Biogeography.* 1: 1-18.

Monzote L. 2009. Current Treatment of Leishmaniasis: A Review. *The Open Antimicrobial Agents Journal. 1:* 9-19.

Mori Y, and Okumura H. 2013. Pressure-Induced Helical Structure of a Peptide Studied by Simulated Tempering Molecular Dynamics Simulations. *Journal of Physical Chemistry Letters.* 4: 2079–2083.

Morselli E, Galluzzi L, Kepp O, Criollo A, Maiuri MC, Tavernarakis N, Madeo F, Kroemer G. 2009. Autophagy mediates pharmacological lifespan extension by spermidine and resveratrol. *Aging*. 1: 961-70.

Morselli E, Mariño G, Bennetzen MV, Eisenberg T, Megalou E, Schroeder S, Cabrera S, Bénit P, Rustin P, Criollo A, Kepp O, Galluzzi L, Shen S, Malik SA, Maiuri MC, Horio Y, López-Otín C, Andersen JS, Tavernarakis N, Madeo F, Kroemer G. 2011. Spermidine and resveratrol induce autophagy by distinct pathways converging on the acetylproteome. *J Cell Biol*. 192:615-629.

Mortimore GE, Pösö, AR. 1987. Intracellular protein catabolism and its control during nutrient deprivation and supply. *Annu. Rev. Nutr.* 7:539–564.

Mosmann T. 1983. Rapid colorimetric assay for cellular growth and survival: application to proliferation and cytotoxicity assays. *J. Immunol. Methods*. 65:55–63.

Mount DW. 2007. Using the Basic Local Alignment Search Tool (BLAST). *Cold Spring Harbor Protocols.*1: pdb.top17.

Mukhopadhyay R, Dey S, Xut N, Gaget D, Lightbody J, Ouellettet M, Rosen BP. 1996. Trypanothione overproduction and resistance to antimonials and arsenicals in leishmania. *Proc. Natl. Acad. Sci*. 93:10383–10387.

Murray HW, Berman JD, Davies CR, Saravia NG 2005. Advances in leishmaniasis. *Lancet.* 366:1561- 1577.

Nobukuni T, Joaquin M, Roccio M, Dann SG, Kim SY, Gulati P, Byfield MP, Backer JM, Natt F, Bos JL, *et al.* 2005. Amino acids mediate mTOR/raptor signaling through activation of class 3 phosphatidylinositol 3OH-kinase. *Proc. Natl. Acad. Sci. USA*. 102: 14238–14243.

Noda T, Ohsumi Y. 1998. Tor, a phosphatidylinositol kinase homologue, controls autophagy in yeast. *J. Biol. Chem*. 273:3963–3966.

Heby O. 1986. Putrescine, Spermidine, and Spermine. NIPS Volume 1 /February 1986.

Pandey RK., Sharma D, Bhatt TK., Sundar S, & Prajapati VK. 2015. Developing imidazole analogues as potential inhibitor for *Leishmania donovani* trypanothione reductase: virtual screening, molecular docking, dynamics and ADMET approach. *Journal of Biomolecular Structure and Dynamics*. 28:1-13.

Pankiv S, Clausen TH, Lamark T, Brech A, Bruun JA, et al. 2007. p62/SQSTM1 binds directly to Atg8/LC3 to facilitate degradation of ubiquitinated protein aggregates by autophagy. *J Biol Chem*. 282: 24131–45.

Park MH, Cooper HL, and Folk JE. 1981. Identification of hypusine, an unusual amino acid, in a protein from human lymphocytes and of spermidine as its biosynthetic precursor. *Proc. Nati. Acad. Sci. USA*. 78: 2869-2873.

Park MH, Wolff EC, Folk JE. 1993. Hypusine: its post-translational formation in eukaryotic initiation factor 5A and its potential role in cellular regulation. *Biofactors*. 4:95-104.

Pei J, Grishin NV. 2001. Type II CAAX prenyl endopeptidases belong to a novel superfamily of putative membrane-bound metalloproteases. *Trends Biochem Sci*.26:275–277.

Pei J, Mitchell DA, and Grishin NV. 2011. Expansion of type II CAAX proteases reveals evolutionary origin of γ-secretase subunit APH-1. *Journal of molecular biology*. 410: 18-26.

Pichiah PBT, Suriyakalaa U, Kamalakkannan S, Kokilavani P, Kalaiselvi S, SankarGanesh D, Gowri J, Archunan G, Cha YS, Achiraman S. 2011. Spermidine may decrease ER stress in pancreatic beta cells and may reduce apoptosis via activating AMPK dependent autophagy pathway. *Medical Hypotheses*. 77:677-679.

Pohl C, and Jentsch S. 2009. Midbody ring disposal by autophagy is a post-abscission event of cytokinesis. *Nat Cell Biol*.11:65–70.

Porta R, Esposito C, Sellinger OZ. (1981). Rapid assay of spermidine synthase activity by high-performan ce liquid Chromatography. *Journal of Chromatography*. 226:208-212.

Porter SB, Hildebrandt ER, Breevoort SR, Mokry DZ, Dore TM, and Schmidt WK. 2007. Inhibition of the CaaX proteases Rce1p and Ste24p by peptidyl (acyloxy) methyl ketones. *Biochimica et Biophysica Acta.* 1773: 853-62.

Prime, version 3.5. 2014. Schrodinger, LLC, New York, NY.

Progenesis QI for proteomics, Nonlinear dynamics.

Protein preparation wizard, 2014. Schrodinger, LLC, New York, NY.

Proto WR, Coombs GH, Mottram JC (2013) Cell death in parasitic protozoa: regulated or incidental. *Nature* 58: 58-66.

Pryor EE Jr, Horanyi PS, Clark KM, Fedoriw N, Connelly SM, Koszelak-Rosenblum M, Zhu G, Malkowski MG, Wiener MC, Dumont ME. 2013. Structure of the integral membrane protein CAAX protease Ste24p. *Science.* 339: 1600-1604

Ravikumar B, Vacher C, Berger Z, Davies JE, Luo S, Oroz LG, Scaravilli F, Easton DF, Duden R, O'Kane CJ and Rubinsztein DC. 2004. Inhibition of mTOR induces autophagy and reduces toxicity of polyglutamine expansions in fly and mouse models of Huntington disease. *Nat Genet*. 36: 585-95.

Reddy KK, and Singh SK. 2014. Combined ligand and structure-based approaches on HIV-1 integrase strand transfer inhibitors. *Chemico-Biological Interactions.* 218:71-81.

Reddy KK, Singh P, and Singh SK. 2014. Blocking the interaction between HIV-1 integrase and human LEDGF/p75: mutational studies, virtual screening and molecular dynamics simulations. *Molecular Biosystems.* 10: 526-36.

Rio DC, Ares M Jr, Hannon GJ and Nilsen TW. 2010. Purification of RNA using TRIzol (TRI reagent). *Cold Spring Harb Protoc*. 6:pdb.prot5439

Robert F, Brakier-Gingras L. 2001. Ribosomal protein S7 from Escherichia coli uses the same determinants to bind 16S ribosomal RNA and its messenger RNA. *Nucleic Acids Res.* 29:677-82.

Russell RC, Fang C and Guan KL. 2011. An emerging role for TOR signaling in mammalian tissue and stem cell physiology. *Development*. 138: 3343-3356.

Saini P, Eyler DE, Green R and Dever TE. 2009. Hypusine-containing protein eIF5A promotes translation elongation. *Nature.* 459:118-121.

Sahoo GC, Ansari MY, Dikhit MR, Kannan M, Rana S, & Das P. 2013. Structure prediction of gBP21 protein of *L. donovani* and its molecular interaction. *Journal of Biomolecular Structure and Dynamics*. 32: 709-29.

Sanli T, Steinberg GR, Singh G, Tsakiridis T. 2014. AMP-activated protein kinase (AMPK) beyond metabolism: a novel genomic stress sensor participating in the DNA damage response pathway. *Cancer Biol Ther*. 15: 156–169.

Sarbassov DD, Ali SM, Kim DH, Guertin DA, Latek RR, Erdjument-Bromage H, Tempst P, Sabatini DM. 2004. Rictor, a novel binding partner of mTOR, defines a rapamycin-insensitive and raptor-independent pathway that regulates the cytoskeleton. *Curr Biol.* 14:1296–1302.

Sarbassov DD, Guertin DA, Ali SM, Sabatini DM. 2005. Phosphorylation and regulation of Akt/PKB by the rictor–mTOR complex. *Science*. 307:1098–1101.

Sastry GM, Adzhigirey M, Day T, Annabhimoju R, and Sherman W. 2013. Protein and ligand preparation: parameters, protocols, and influence on virtual screening enrichments. *Journal of Computer-Aided Molecular Design.* 27: 221-34.

Saudagar P, Saha P, Saikia AK, Dubey VK. 2013. Molecular mechanism underlying antileishmanial effect of oxabicyclo[3.3.1]nonanones: Inhibition of key redox enzymes of the pathogen. *Eur J Pharm Biopharm*. 85:569-577.

Schlitzer M, Winter-Vann A, and Casey PJ. 2001. Non-peptidic, non-prenylic inhibitors of the prenyl protein-specific protease Rce1. *Bioorganic & Medicinal Chemistry Letters.* 11: 425-7.

Schmidt WK, Tam A, and Michaelis S. 2000. Reconstitution of the Ste24p-dependent N-terminal proteolytic step in yeast a-factor biogenesis. *Journal of Biological Chemistry.* 275: 6227–33.

Schnier J, Schwelberger HG, McBride ZS, Kang HA and Hershey JW. 1991.Translation initiation factor 5A and its hypusine modification are essential for cell viability in the yeast Saccharomyces cerevisiae. *Mol. Cell. Biol.* 11: 6 3105-31.

Scott RC, Schuldiner O, Neufeld TP. 2004. Role and regulation of starvation-induced autophagy in the Drosophila fat body. *Dev Cell.* 7:167-78.

Seabra MC. 1998. Membrane Association and Targeting of Prenylated Ras-like GTPases. *Cellular Signalling*. 10: 167-172.

Seglen PO and Gordon PB. 1982. 3-Methyladenine: Specific inhibitor of autophagic/lysosomal protein degradation in isolated rat hepatocytes. *Proc Natl Acad Sci U S A.* 79:1889-92.

Selvaraj C, Sivakamavalli J, Vaseeharan B, Singh P, and Singh SK. 2014. Structural elucidation of SrtA enzyme in Enterococcus faecalis: an emphasis on screening of potential inhibitors against the biofilm formation. *Molecular Biosystems.* 10: 1775-89.

Sharma K, Vabulas RM, Macek B, Pinkert S, Cox J, Mann M, Hartl FU. 2012. Quantitative proteomics reveals that Hsp90 inhibition preferentially targets kinases and the DNA damage response. *Mol Cell Proteomics.* 11: M111.014654.

Sharma U and Singh S. 2008. Insect vectors of Leishmania: distribution, physiology and their control. *J Vector Borne Dis*. 45: 255–272.

Sherman W, Day T, Jacobson MP, Friesner RA, Farid R. 2006. Novel procedure for modeling ligand/receptor induced fit effects. *Journal of Medicinal Chemistry*. 49: 534-53.

Shukla AK, Patra S, Dubey VK. 2011. Evaluation of selected antitumor agents as subversive substrate and potential inhibitor of trypanothione reductase: an alternative approach for chemotherapy of Leishmaniasis. *Mol. Cell. Biochem*. 352:261–270.

Shukla AK, Patra S, Dubey VK. 2012. Iridoid glucosides from *Nyctanthes arbortristis* result in increased reactive oxygen species and cellular redox homeostasis imbalance in *Leishmania* parasite. *Eur. J. Med. Chem.* 54:49–58.

Shukla AK, Singh BK, Patra S, Dubey VK. 2009. Rational approaches for drug designing against leishmaniasis. *Appl Biochem Biotechnol*.160:2208-2218.

Simon HU, Haj-Yehia A, Levi-Schaffer F. 2000. Role of reactive oxygen species (ROS) in apoptosis induction. *Apoptosis*. 5:415-418.

Sinensky M, Fantle K, Trujillo M, McLain T, Kupfer A, Dalton M. 1994. The processing pathway of prelamin A. *J Cell Sci.* 107:61-7.

Sinensky M, Lutz RJ. 1992. The prenylation of proteins. *Bioessays*. 14:25-31.

Singh BK., Sarkar N, Jagannadham MV & Dubey VK. 2008. Modeled Structure of Trypanothione Reductase of *Leismania infantum*. *BMB Reports*. 41: 444-447.

Singh S, Sarma S, Katiyar SP et. al. 2015. Probing the Molecular Mechanism of Hypericin-Induced Parasite Death Provides Insight into the Role of Spermidine beyond Redox Metabolism in Leishmania donovani. *Antimicrob. Agents Chemother.* 59: 1 15-24.

SiteMap, version 3.0. 2014. Schrodinger, LLC, New York, NY.

Stockdale L, Newton R. 2013. A review of preventative methods against human leishmaniasis infection. *PLoS Negl Trop Dis*. 7:e2278.

Stuart K, Brun R, Croft S, Fairlamb A, Gürtler RE, McKerrow J, Reed S, and Tarleton R. 2008. Kinetoplastids: related protozoan pathogens, different diseases. *The Journal of Clinical Investigation.* 118: 1301–1310.

Suryanarayanan V, and Singh SK. 2014. Assessment of dual inhibition property of newly discovered inhibitors against PCAF and GCN5 through in silico screening, molecular dynamics simulation and DFT approach. *Journal of Receptors and Signal Transduction.* 18: 1-11.

Suzuki K, and Ohsumi Y. 2007. Molecular machinery of autophagosome formation in yeast, Saccharomyces cerevisiae. *FEBS Lett.* 581: 2156–2161.

Suzuki K, Kirisako T, Kamada Y, Mizushima N, Noda T, and Ohsumi Y. 2001. The pre-autophagosomal structure organized by concerted functions of APG genes is essential for autophagosome formation. *EMBO J*. 20: 5971–5981.

Suzuki K, Kubota Y, Sekito T, and Ohsumi Y. 2007. Hierarchy of Atg proteins in pre-autophagosomal structure organization. *Genes Cells.* 12:209-18.

Szklarczyk D, Franceschini A, Kuhn M, Simonovic M, Roth A, Minguez P , Doerks T, Stark M, Muller J, Bork P, Jensen LJ and Mering CV. 2011. The STRING database in 2011: functional interaction networks of proteins, globally integrated and scored. *Nucleic Acids Res*. 39:D561–D568.

Takeshige K, Baba M, Tsuboi S, Noda T, and Ohsumi Y. 1992. Autophagy in yeast demonstrated with proteinase-deficient mutants and conditions for its induction. *J. Cell Biol.* 119: 301–311.

Tam A, Schmidt WK, Michaelis S. 2001. The multispanning membrane protein Ste24p catalyzes CAAX proteolysis and NH2-terminal processing of the yeast a-factor precursor. *J Biol Chem.* 276:46798–806.

Tam A, Schmidt WK, Michaelis S. 2001. The multispanning membrane protein Ste24p catalyzes CAAX proteolysis and NH2-terminal processing of the yeast a-factor precursor. *The Journal of Biological Chemistry*. 276: 46798–806.

Tanida I, Minematsu-Ikeguchi N, Ueno T, and Kominami E. 2005. Lysosomal turnover, but not a cellular level, of endogenous LC3 is a marker for autophagy. *Autophagy.* 1:84-91.

Tavares L, Alves PM, Ferreira RB, and Santos CN. 2011. Comparison of different methods for DNA-free RNA isolation from SK-N-MC neuroblastoma. *BMC Res Notes.* 4:3.

Teter SA, Eggerton KP, Scott SV, Kim J, Fischer AM, Klionsky DJ. 2001. Degradation of lipid vesicles in the yeast vacuole requires function of Cvt17, a putative lipase. *J Biol Chem.* 276:2083-7.

Trachootham D, Lu W, Ogasawara MA, Valle NR-D, Huang P. 2008. Redox Regulation of Cell Survival. *Antioxidants & Redox Signaling*. 10:1343-1374.

Tripathi SK, Singh SK, and Singh P, Chellaperumal P, Reddy KK, and Selvaraj C. 2012. Exploring the selectivity of a ligand complex with CDK2/CDK1: a molecular dynamics simulation approach. *Journal of Molecular Recognition.* 25: 504-12.

Trueblood CE, Boyartchuk VL, Picologlou EA, Rozema D, Poulter CD, and Rine J. 2000. The CaaX Proteases, Afc1p and Rce1p, Have Overlapping but Distinct Substrate Specificities. *Molecular and Cellular Biology.* 20: 4381–4392.

Wan CY, Wilkins TA. 1993. Spermidine facilitates PCR amplification of target DNA. *PCR Methods Appl.* 3: 208-210.

Wang M, Tan W, Zhou J et. al. 2008. A Small Molecule Inhibitor of Isoprenylcysteine Carboxymethyltransferase Induces Autophagic Cell Death in PC3 Prostate Cancer Cells. *J Biol Chem*. 283: 18678-18684.

Wiederstein M, and Sippl M. 2007. ProSA-web: interactive web service for the recognition of errors in three-dimensional structures of proteins. *Nucleic Acids Research.* 35: W407-10.

Williams RAM, Smith TK, Cull B, Mottram JC and Coombs GH. 2012. ATG5 Is Essential for ATG8-Dependent Autophagy and Mitochondrial Homeostasis in *Leishmania major*. *PLoS Pathog*. 8: e1002695.

Wolff EC, Park MH, and Folk JE. 1990. Cleavage of spermidine as the first step in deoxyhypusine synthesis. The role of NAD. *J Biol Chem*. 265:4793-9.

Wong JW, Cagney G. 2010. An overview of label-free quantitation methods in proteomics by mass spectrometry. *Methods Mol Biol*. 604:273-83.

Wright LP and Philips MR. 2006. Thematic review series: lipid posttranslational modifications. CAAX modification and membrane targeting of Ras. *Journal of lipid research*. 2006: 47:883-91.

Wullschleger S, Loewith R, Hall MN. 2006. TOR signaling in growth and metabolism. *Cell*. 124:471–484

Yadav S, Gupta S, Selvaraj C, Doharey PK, Verma A, Singh SK, and Saxena JK. 2014. In silico and in vitro studies on the protein-protein interactions between Brugia malayi immunomodulatory protein calreticulin and human C1q. *PLoS One.* 9: e106413.

Yi C and Yu L. 2012. How does acetylation regulate autophagy? *Autophagy.* 8:1529-1530.

Zanelli CF and Valentini SR. 2007. Is there a role for eIF5A in translation? *Amino Acids.* 33: 351–358.

Zhang FL, and Casey PJ. 1996. Protein Prenylation: Molecular Mechanisms and Functional Consequences. *Annual Reviews Biochemistry.* 65: 241-269.

Zhang Y, Yan L, Zhou Z, Yang P, Tian E, et al. 2009. SEPA-1 mediates the specific recognition and degradation of P granule components by autophagy in *C. elegans*. *Cell*. 136:308–21.

Zhu CT , Rand DM. 2012. A Hydrazine Coupled Cycling Assay Validates the Decrease in Redox Ratio under Starvation in Drosophila. *PLoS ONE.* 7: e47584.

Zhu W, Smith JW, Huang CM. 2010. Mass Spectrometry-Based Label-Free Quantitative Proteomics. *Journal of Biomedicine and Biotechnology*. 2010: 1-6.

Publications

Journal Publications from PhD thesis

1. **Shalini Singh**, Shyamali Sarma, Shashank P. Katiyar, Mousumi Das, Ruchika Bhardwaj, Durai Sundar, Vikash Kumar Dubey. Probing the molecular mechanism of hypericin-induced parasite death provides insight into the role of spermidine beyond redox metabolism in *Leishmania donovani*. **(2015) *Antimicrob Agents Chemother*.** 59: 15 –24.

2. **Shalini Singh**, Sitrarasu Vijaya Prabhu, Venkatesan Suryanarayanan, Ruchika Bhardwaj, Sanjeev Kumar Singh and Vikash Kumar Dubey. Molecular docking and structure based virtual screening studies of CAAX prenyl protease I &II. **(2016) *Journal of Biomolecular Structure and Dynamics.*** 1-20.[Epub ahead of print].

3. **Shalini Singh** and Vikash Kumar Dubey. Proteome analysis of *Leishmania donovani* using label free quantitation by mass spectrometry**. (2016) accepted for publication in *Plos One*,** doi: 10.1371/journal.pone.0154262.

4. **Shalini Singh**, Ekta Kumari, Ruchika Bharadwaj and Vikash Kumar Dubey. Molecular events leading to death of *Leishmania donovani* under spermidine starvation. **(2016) manuscript under communication**.

Journal Publications *from collaborative work:*

1. Mousumi Das, **Shalini Singh** and Vikash Kumar Dubey. Novel inhibitors of ornithine decarboxylase of *Leishmania* parasite (*Ld*ODC): The parasite resists *Ld*ODC inhibition by over-expression of spermidine synthase mRNA. **(2016)** *accepted in* ***Chemical Biology and Drug Design***. 87: 352-360.

Book Chapter:

1. **Shalini Singh*,** Ritesh Kumar*, Vikash Kumar Dubey. Bioinformatics Tools to Analyze Proteome and Genome Data. Advances in the Understanding of Biological Sciences Using Next Generation Sequencing (NGS) Approaches. Springer. ***doi: 10.1007/978-3-319-17157-9_11.*** * Equal contribution.

***Conference publications for* from PhD thesis work**

1. **Shalini Singh**, Mousumi Das, Ruchika Bhardwaj, Vikash Kumar Dubey. Is spermidine synthase only a redox enzyme? 83rd Annual Meeting of Society of Biological Chemists (India), **18th -21st December, 2014,** Odisha, BHUBANESHWAR.

2. **Shalini Singh**, Mousumi Das, Ankur Kumar and Vikash Kumar Dubey. Over-expression, purification and characterization of CAAX prenyl protease I and CAAX prenyl protease II of *Leishmania donovani* . Indraprastha International Conference on Biotechnology (IICB-2013), **October 22-25, 2013**, New Delhi.